22.101 Applied Nuclear Physics (Fall 2004)
Lecture 1 (9/8/04)

Basic Nuclear Concepts

References --
P. Marmier and E. Sheldon, *Physics of Nuclei and Particles* (Academic Press, New York, 1969), vol. 1.

General Remarks:

This subject deals with foundational knowledge for all students in NED.
Emphasis is on nuclear concepts (as opposed to traditional nuclear physics), especially nuclear radiations and their interactions with matter. We will study different types of reactions, single-collision phenomena (cross sections) and leave the effects of many collisions to later subjects (22.105 and 22.106). Quantum mechanics is used at a lower level than in 22.51 and 22.106.

Nomenclature:

$_{z}X^{A}$ denotes a nuclide, a specific nucleus with Z number of protons (Z = *atomic number*) and A number of nucleons (neutrons or protons). Symbol of nucleus is X. There is a one-to-one correspondence between Z and X, thus specifying both is actually redundant (but helpful since one may not remember the atomic number of all the elements. The number of neutrons N of this nucleus is A – Z. Often it is sufficient to specify only X and A, as in U^{235}, if the nucleus is a familiar one (uranium is well known to have Z=92). Symbol A is called the *mass number* since knowing the number of nucleons one has an approximate idea of what is the mass of the particular nucleus. There exist uranium nuclides with different mass numbers, such as U^{233}, U^{235}, and U^{238}; nuclides with the same Z but different A are called *isotopes*. By the same token, nuclides with the same A but different Z are called *isobars*, and nuclides with N but different Z are called *isotones*. *Isomers* are nuclides with the same Z and A in different excited states.

We are, in principle, interested in all the elements up to Z = 94 (plutonium). There are about 20 more elements which are known, most with very short lifetimes; these are of interest mostly to nuclear physicists and chemists, not to nuclear engineers. While each element can have several isotopes of significant abundance, not all the elements are

of equal interest to us in this class. The number of nuclides we might encounter in our studies is probably less than no more than 20.

A great deal is known about the properties of nuclides. It should be appreciated that the great interest in nuclear structure and reactions is not just for scientific knowledge alone, the fact that there are two applications that affects the welfare of our society – nuclear power and nuclear weapons – has everything to do with it.
We begin our studies with a review of the most basic physical attributes of nuclides to provide motivation and a basis to introduce what we want to accomplish in this course (see the Lecture Outline).

Basic Physical Attributes of Nuclides

Nuclear Mass

We adopt the unified scale where the mass of C^{12} is exactly 12. On this scale, one mass unit 1 mu ($C^{12} = 12$) = $M(C^{12})/12 = 1.660420 \times 10^{-24}$ gm (= 931.478 Mev), where $M(C^{12})$ is actual mass of the nuclide C^{12}. Studies of atomic masses by mass spectrograph shows that a nuclide has a mass nearly equal to the mass number A times the proton mass. Three important rest mass values, in mass and energy units, to keep handy are:

	mu [$M(C^{12}) = 12$]	Mev
electron	0.000548597	0.511006
proton	1.0072766	938.256
neutron	1.0086654	939.550

Reason we care about the mass is because it is an indication of the stability of the nuclide. One can see this from $E = Mc^2$. The higher the mass the higher the energy and the less stable is the nuclide (think of nuclide being in an excited state). We will see that if a nuclide can lower its energy by undergoing distintegration, it will do so – this is the simple explanation of radioactivity. Notice the proton is lighter than the neutron, which suggests that the former is more stable than the latter. Indeed, if the neutron is not bound

in a nucleus (that is, it is a free neturon) it will decay into a proton plus an electron (and antineutrino) with a half-life of about 13 min.

Nuclear masses have been determined to quite high accuracy, precision of ~ 1 part in 10^8 by the methods of mass spectrograph and energy measurements in nuclear reactions. Using the mass data alone we can get an idea of the stability of nuclides. Consider the idea of a mass defect by defining the difference between the actual mass of a nuclide and its mass number, $\Delta = M - A$, which we call the "mass decrement". If we plot Δ versus A, we get a curve sketched in Fig. 1. When $\Delta < 0$ it means that taking the individual

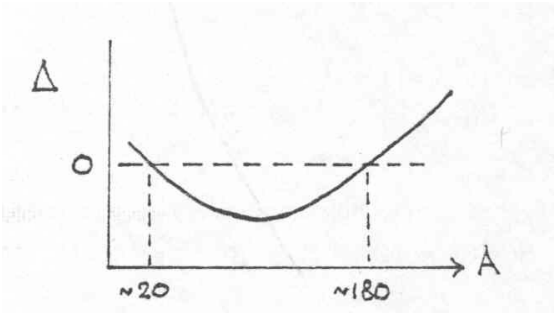

Fig. 1. Variation of mass decrement (M-A) showing that nuclides with mass numbers in the range ~ (20-180) should be stable.

nucleons when they are separated far from each other to make the nucleus in question results in a product that is lighter than the sum of the components. The only way this can happen is for energy to be given off during the formation process. In other words, to reach a final state (the nuclide) with smaller mass than the initial state (collection of individual nucleons) one must take away some energy (mass). This also means that the final state is more stable than the initial state, since energy must be put back in if one wants to reverse the process to go from the nuclide to the individual nucleons. We therefore expect that $\Delta < 0$ means the nuclide is stable. Conversely, when $\Delta > 0$ the nuclide is unstable. Our sketch therefore shows that very light elements ($A < 20$) and heavy elements ($A > 180$) are not stable, and that maximum stability occurs around $A \sim 50$. We will return to discuss this behavior in more detail later.

Nuclear Size

According to Thomson's "electron" model of the nucleus (~ 1900), the size of a nucleus should be about 10^{-8} cm. We now know this is wrong. The correct nuclear size was determined by Rutherford (~ 1911) in his atomic nucleus hypothesis which put the size at about 10^{-12} cm. Nuclear radius is not well defined, strictly speaking, because any measurement result depends on the phenomenon involved (different experiments give different results). On the other hand, all the results agree qualitatively and to some extent also quantitatively. Roughly speaking, we will take the nuclear radius to vary with the 1/3 power of the mass number $R = r_o A^{1/3}$, with $r_o \sim 1.2 - 1.4 \times 10^{-13}$ cm. The lower value comes from electron scattering which probes the charge distribution of the nucleus, while the higher value comes from nuclear scattering which probes the range of nuclear force. Since nuclear radii tend to have magnitude of the order 10^{-13} cm, it is conventional to adopt a length unit called Fermi (F), $F \equiv 10^{-13}$ cm.

Because of particle-wave duality we can associate a wavelength with the momentum of a particle. The corresponding wave is called the deBroglie wave. Before discussing the connection between a wave property, the wavelength, and a particle property, the momentum, let us first set down the relativistic kinematic relations between mass, momentum and energy of a particle with arbitrary velocity. Consider a particle with rest mass m_o moving with velocity v. There are two expressions we can write down for the total energy E of this particle. One is the sum of its kinetic energy E_{kin} and its rest mass energy, $E_o = m_o c^2$,

$$E_{tot} = E_{kin} + E_o = m(v)c^2 \qquad (1.1)$$

The second equality introduces the relativistic mass m(v) which depends on its velocity,

$$m(v) = \gamma m_o, \qquad \gamma = (1 - v^2/c^2)^{-1/2} \qquad (1.2)$$

where γ is the Einstein factor. To understand (1.2) one should look into the Lorentz transformation and the special theory of relativity in any text. Eq.(1.1) is a first-order

relation for the total energy. Another way to express the total energy is a second-order relation

$$E^2 = c^2 p^2 + E_o^2 \tag{1.3}$$

where p = m(v)v is the momentum of the particle. Eqs. (1.1) – (1.3) are the general relations between the total and kinetic energies, mass, and momentum. We now introduce the deBroglie wave by defining its wavelength λ in terms of the momentum of the corresponding particle,

$$\lambda = h / p \tag{1.4}$$

where h is the Planck's constant ($h/2\pi = \hbar = 1.055x10^{-27}$ erg sec). Two limiting cases are worth noting.

Non-relativistic regime:

$$E_o >> E_{kin}, \qquad p = (2m_o E_{kin})^{1/2}, \qquad \lambda = h/\sqrt{2m_o E_{kin}} = h/m_o v \tag{1.5}$$

Extreme relativsitic regime:

$$E_{kin} >> E_o, \qquad p = E_{kin}/c, \qquad \lambda = hc/E \tag{1.6}$$

Eq.(1.6) applies as well to photons and neutrinos which have zero rest mass. The kinematical relations discussed above are general. In practice we can safely apply the non-relativistic expressions to neutrons, protons, and all nuclides, the reason being their rest mass energies are always much greater than any kinetic energies we will encounter. The same cannot be said for electrons, since we will be interested in electrons with energies in the Mev region. Thus, the two extreme regimes do not apply to electrons, and one should use (1.3) for the energy-momentum relation. Since photons have zero rest mass, they are always in the relativistic regime.

Nuclear charge

The charge of a nuclide ${}_z X^A$ is positive and equal to Ze, where e is the magnitude of the electron charge, e = 4.80298 x 10^{-10} esu (= 1.602189 x 10^{-19} Coulomb). We consider

single atoms as exactly neutral, the electron-proton charge difference is < 5 x 10-19 e, and the charge of a neutron is < 2 x 10-15 e.

As to the question of the charge distribution in a nucleus, we can look to high-energy electron scattering experiments to get an idea of how nuclear density and charge density are distributed across the nucleus. Fig. 2 shows two typical nucleon density distributions obtained by high-electron scattering. One can see two basic components in each distribution, a core of constant density and a boundary where the density decreases smoothly to zero. Notice the magnitude of the nuclear density is 10^{38} nucleons per cm^3, whereas the atomic density of solids and liquids is in the range of 10^{24} nuclei per cm^3. What does this say about the packing of nucleons in a nucleus, or the average distance between nucleons versus the separation between nuclei? The shape of the distributions

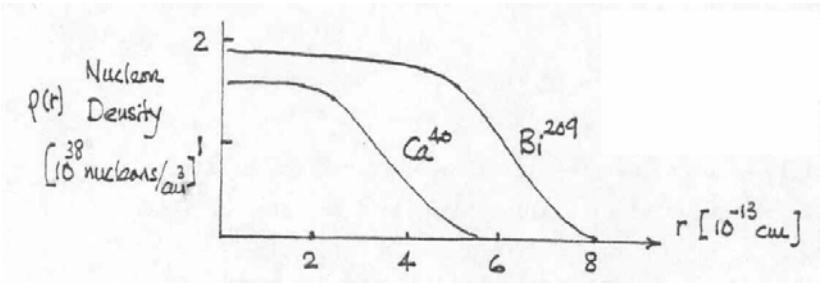

Fig. 2. Nucleon density distributions showing nuclei having no sharp boundary.

shown in Fig. 2 can be fitted to the expression, called the Saxon distribution,

$$\rho(r) = \frac{\rho_o}{1 + \exp[(r - R)/a]} \tag{1.7}$$

where ρ_o = 1.65 x 10^{38} nucleons/cm^3, R ~ 1.07 $A^{1/3}$ F, and a ~ 0.55 F. A sketch of this distribution, given in Fig. 3, shows clearly the core and boundary components of the distribution.

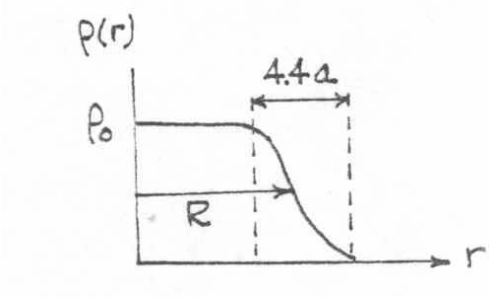

Fig. 3. Schematic of the nuclear density distribution, with R being a measure of the nuclear radius, and the width of the boundary region being given by 4.4a.

Detailed studies based on high-energy electron scattering have also rvealed that even the proton and the neutron have rather complicated structures. This is illustrated in Fig. 4.

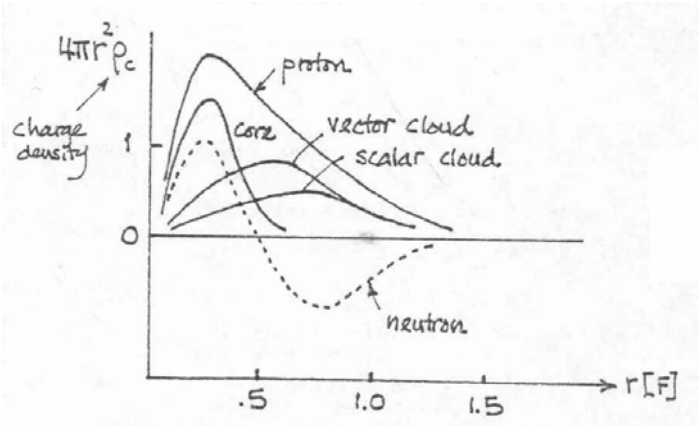

Fig. 4. Charge density distributions of the proton and the neutron showing how each can be decomposed into a core and two meson clouds, inner (vector) and outer (scalar). The core has a positive charge of ~0.35e with probable radius 0.2 F. The vector cloud has a radius 0.85 F, with charge .5e and -.5e for the proton and the neutron respectively, whereas the scalar clouid has radius 1.4 F and charge .15e for both proton and neutron[adopted from Marmier and Sheldon, p. 18].

We note that mesons are unstable particles of mass between the electron and the proton: π-mesons (pions) olay an important role in nuclear forces ($m_\pi \sim 270 m_e$), μ-mesons(muons) are important in cosmic-ray processes ($m_\mu \sim 207 m_e$).

Nuclear Spin and Magnetic Moment

Nuclear angular momentum is often known as nuclear spin $\hbar \underline{I}$; it is made up of two parts, the intrinsic spin of each nucleon and their orbital angular momenta. We call I the spin of the nucleus, which can take on integral or half-integral values. The following is usually accepted as facts. Neutron and proton both have spin 1/2 (in unit of $\hbar$). Nuclei with even mass number A have integer or zero spin, while nuclei of odd A have half-integer spin. Angular momenta are quantized.

Associated with the spin is a magnetic moment $\underline{\mu}_I$, which can take on any value because it is not quantized. The unit of magnetic moment is the magneton

$$\mu_n \equiv \frac{|e|\hbar}{2m_p c} = \frac{\mu_B}{1836.09} = 0.505 \text{ x } 10\text{-}23 \text{ ergs/gauss} \qquad (1.8)$$

where μ_B is the Bohr magneton. The relation between the nuclear magnetic moment and the nuclear spin is

$$\underline{\mu}_I = \gamma \hbar \underline{I} \qquad (1.9)$$

where γ here is the gyromagnetic ratio (no relation to the Einstein factor in special relativity). Experimentally, spin and magnetic moment are measured by hyperfine structure (splitting of atomic lines due to interaction between atomic and nuclear magnetic moments), deflations in molecular beam under a magnetic field (Stern-Gerlach), and nuclear magnetic resonance 9precession of nuclear spin in combined DC and microwave field). We will say more about nmr later.

Electric Quadruple Moment

The electric moments of a nucleus reflect the charge distribution (or shape) of the nucleus. This information is important for developing nuclear models. We consider a classical calculation of the energy due to electric quadruple moment. Suppose the

nuclear charge has a cylindrical symmetry about an axis along the nuclear spin I, see Fig. 5.

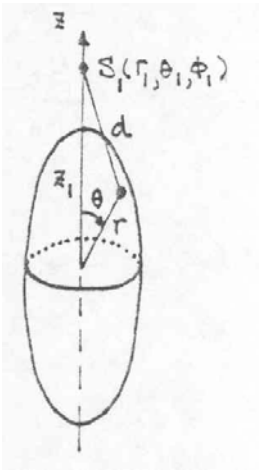

Fig. 5. Geometry for calculating the Coulomb potential energy at the field point S_1 due to a charge distribution $\rho(r)$ on the spheroidal surface as sketched.

The Coulomb energy at the point S_1 is

$$V(r_1,\theta_1) = \int d^3r \frac{\rho(r)}{d} \tag{1.10}$$

where $\rho(r)$ is the charge density, and $d = |\underline{r}_1 - \underline{r}|$. We will expand this integral in a power series in $1/r_1$ by noting the expansion of 1/d in a Legendre polynomial series,

$$\frac{1}{d} = \frac{1}{r_1}\sum_{n=0}^{\infty}\left(\frac{r}{r_1}\right)^n P_n(\cos\theta) \tag{1.11}$$

where $P_0(x) = 1$, $P_1(x) = x$, $P_2(x) = (3x^2 - 1)/2$, …Then (1.10) can be written as

$$V(r_1,\theta_1) = \frac{1}{r_1}\sum_{n=0}^{\infty}\frac{a_n}{r_1^n} \tag{1.12}$$

with $$a_o = \int d^3 r \rho(r) = \text{Ze} \qquad (1.13)$$

$$a_1 = \int d^3 r z \rho(r) = \text{ electric dipole} \qquad (1.14)$$

$$a_2 = \int d^3 r \frac{1}{2}(3z^2 - r^2)\rho(r) \equiv \frac{1}{2}\ \text{eQ} \qquad (1.15)$$

The coefficients in the expansion for the energy, (1.12), are recognized to be the total charge, the dipole (here it is equal to zero), the quadruple, etc. In (1.15) Q is defined to be the quadruole moment (in unit of 10^{-24} cm^2, or barns). Notice that if the charge distribution were spherically symmetric, <x2> = <y2> = <z2> = <r2>/3, then Q = 0. We see also, Q > 0, if $3\langle z^2\rangle > \langle r^2\rangle$ and Q <0, if $3\langle z^2\rangle < \langle r^2\rangle$
The corresponding shape of the nucleus in these two cases would be prolate or oblate spheroid, respectively (see Fig. 6).

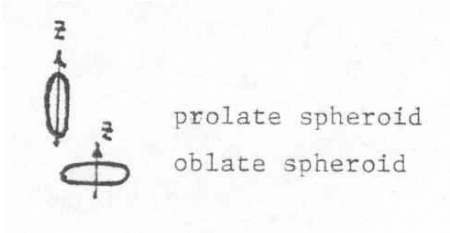

Fig. 6. Prolate and oblate spheroidal shapes of nuclei as indicated by a positive or negative value of the electric quadruple moment Q.

Some values of the spin and quadruple moments are:

Nucleus	I	Q [10^{-24} cm^2]
n	1/2	0
p	1/2	0
H^2	1	0.00274
He^4	0	0
Li^6	1	-0.002
U^{233}	5/2	3.4
U^{235}	7/2	4
Pu^{241}	5/2	4.9

22.101 Applied Nuclear Physics (Fall 2004)
Lecture 2 (9/13/04)

Schrödinger Wave Equation

References --
R. M. Eisberg, *Fundamentals of Modern Physics* (Wiley & Sons, New York, 1961).
R. L. Liboff, *Introductory Quantum Mechanics* (Holden Day, New York, 1980).

With this lecture we begin the discussion of quantum mechanical description of nuclei. There are certain properties of a nucleus which can be described properly only by the use of quantum mechanics. The ones which come to mind immediately are the energy levels of a nucleus and the transitions that can take place from one level to another. Other examples are the various types of nuclear radiation which are sometimes treated as particles and at other times as waves.

It is not our goal in this subject to take up the study of quantum mechanics as a topic by itself. On the other hand, we have no reason to avoid using quantum mechanics if it is the proper way to understand nuclear concepts and radiation interactions. In fact the serious students in 22.101 has little choice in deciding whether or not to learn quantum mechanics. This is because the concepts and terminologies in quantum mechanics are such integral parts of nuclear physics that some knowledge of quantum mechanics is *essential* to having full command of the language of nuclear physics. The position we adopt throughout the term is to learn enough quantum mechanics to appreciate the fundamental concepts of nuclear physics, and let each student go beyond this level if he/she is interested. What this means is that we will not always derive the basic equations and expressions that we will use; the student is expected to work with them as postulates when this happens (as always, with the privilege of reading up on the background material on his own).

Waves and Particles

We will review some basic properties of waves and the concept of wave-particle duality. In classical mechanics the equation for a one-dimensional periodic disturbance $\xi(x,t)$ is

$$\frac{\partial^2 \xi}{\partial t^2} = c^2 \frac{\partial^2 \xi}{\partial x^2} \tag{2.1}$$

which has as a general solution,

$$\xi(x,t) = \xi_o e^{i(kx-\omega t)} \tag{2.2}$$

where $\omega = 2\pi\nu$ is the circular frequency, ν the linear frequency, and k is the wavenumber related to the wavelength λ by $k = 2\pi\lambda$. If (2.2) is to be a solution of (2.1), then k and ω must satisfy the relation

$$\omega = ck \tag{2.3}$$

So our solution has the form of a traveling wave with phase velocity equal to c, which we denote by v_{ph}. In general the relation between frequency and wavenumber is called the dispersion relation. We will see that different kinds of particles can be represented as waves which are characterized by different dispersion relations.

The solution (2.2) is called a plane wave. In three dimensions a plane wave is of the form $\exp(i\underline{k} \cdot \underline{r})$. It is a wave in space we can visualize as a series of planes perpendicular to the wavevector $\underline{k}$; at any spatial point on a given plane the phase of the wave is the same. That is to say, the planes are planes of constant phase. When we include the time variation $\exp(-i\omega t)$, then $\exp[i(\underline{k} \cdot \underline{r} - \omega t)]$ becomes a traveling plane wave, meaning that the planes of constant phase are now moving in the direction along $\underline{k}$ at a speed of ω / k, the phase velocity of the wave.

The wave equation (2.1) also admits solutions of the form

$$\xi(x,t) = a_o \sin kx \cos \omega t \tag{2.4}$$

These are standing wave solutions. One can tell a standing wave from a traveling wave by the behavior of the nodes, the spatial positions where the wave function is zero. For a

standing wave the zeroes do not change with time, whereas for a traveling wave, (2.2), the nodes are $x_n = (n\pi + \omega t)/k$, which clearly are positions moving in the +x direction with velocity $dx/dt = \omega/k$. We will see below that the choice between traveling and standing wave solutions depends on the physical solution of interest (which kind of problem one is solving). For the calculation of energy levels of a nucleus, the bound state problem, we will be concerned with standing wave solutions, while for the discussion of scattering problem (see the lecture on neutron-proton scattering) it will be more appropriate to consider traveling wave solutions.

Our interest in the properties of waves lies in the fact that the quantum mechanical description of a nucleus is based on the wave representation of the nucleus. It was first postulated by deBroglie (1924) that one can associate a particle of momentum p and total relativistic energy E with a group of waves (wave packet) which are characterized by a wavelength λ and a frequency ν, with the relation

$$\lambda = h/p \tag{2.5}$$

$$\nu = E/h \tag{2.6}$$

and that, moreover, the motion of the particle is governed by the wave propagation of the wave packet. This statement is the essence of particle-wave duality, a concept which we will adopt throughout our study of nuclear physics [see, for example, Eisberg, chap 6].

It is important to distinguish between a single wave and a group of waves. This distinction is seen most simply by considering a group of two waves of slightly different wavelengths and frequencies. Suppose we take as the wave packet

$$\Psi(x,t) = \Psi_1(x,t) + \Psi_2(x,t) \tag{2.7}$$

with

$$\Psi_1(x,t) = \sin(kx - \omega t) \tag{2.8}$$

$$\Psi_2(x,t) = \sin[k(k+dk)x - (\omega + d\omega)t] \tag{2.9}$$

Using the identity

$$\sin A + \sin B = 2\cos[(A-B)/2]\sin[(A+B)/2] \tag{2.10}$$

we rewrite $\Psi(x,t)$ as

$$\Psi(x,t) = 2\cos[(dks - d\omega t)/2]\sin\{[(2k+dk)x - (2\omega + d\omega)]t/2\}$$

$$\approx 2\cos[(dkx - d\omega t)/2]\sin(kx - \omega t) \tag{2.11}$$

In this approximation, terms of higher order in dk/k or $d\omega/\omega$ are dropped. Eq. (2.11) shows the wave packet oscillates in space with a period of $2\pi/k$, while its amplitude oscillates with a period of $2\pi/dk$ (see Fig. 1). Notice that the latter oscillation has its

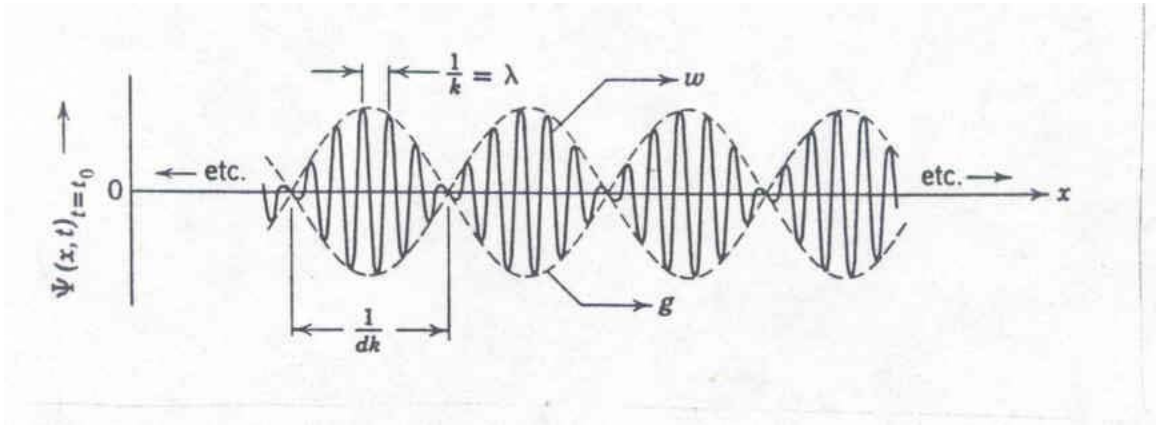

Fig. 1. Spatial variation of a sum of two waves of slightly different frequencies and wavenumbers showing the wave packet moves with velocity g which is distinct from the propagation (phase) velocity w [from Eisberg, p. 144].

own propagation velocity, $d\omega/dk$. This velocity is in fact the speed with which the associated particle is moving. Thus we identify

$$g = d\omega / dk \tag{2.12}$$

as the group velocity. This velocity should not be confused with the propagation velocity of the wave packet, which we can calculate from

$$w = \nu\lambda = E / p = c\sqrt{1 + (m_o c / p)^2} \tag{2.13}$$

Here m_o is the rest mass of the particle and c the speed of light. Thus we see the wave packet moves with a velocity that is greater then c, whereas the associated particle speed is necessarily less than c. There is no contradiction here because the former is the phase velocity while the latter is the group velocity.

In this class we will be dealing with three kinds of particles whose wave representations will be of interest. These are nucleons or nuclides which can be treated as non-relativistic particles for our purposes, electrons and positrons which usually should be treated as relativistic particles since their energies tend to be comparable or greater than the rest-mass energy, and finally photons which are fully relativistic since they have zero rest-mass energy. For a non-relativistic particle of mass m moving with momentum p, the associated wavevector $\underline{k}$ is $\underline{p} = \hbar\underline{k}$. Its kinetic energy is $p^2 / 2m = \hbar^2 k^2 / 2m$. The wavevector, or its magnitude, the wavenumber k, is a useful variable for the discussion of particle scattering since in a beam of such particles the only energies are kinetic, and both momentum and energy can be specified by giving $\underline{k}$. For electromagnetic waves, the associated particle, the photon, has momentum $\underline{p}$, which is also given by $\hbar\underline{k}$, but its energy is $E = \hbar ck = \hbar p$. Comparing these two cases we see that the dispersion relation is $\omega = \hbar k^2 / 2m$ for a non-relativistic particle, and $\omega = ck$ for a photon. The group velocity, according to9 (2.12), IS $v_g = \hbar k / m = p / m$ and $v_g = c$, respectively. This is consistent with our intuitive notion about particle speeds.

The Schrödinger Wave Equation

The Schrödinger equation is the fundamental equation governing the deBroglie wave with which we associate a particle. The wave will be called the wave function, and it will be denoted as a space- and time-dependent quantity, $\Psi(\underline{r},t)$. One does not derive the Schrödinger equation in the same sense that one also does not derive Newton's equation of motion, $\underline{F} = m\underline{a}$. The equation is a postulate which one can simply accept. Of course one can give systematic motivations to suggest why such an equation is valid [see Eisberg, chap 7 for a development]. We will write down the Schrödinger equation in its time-dependent form for a particle in a potential field V(r),

$$i\hbar\frac{\partial\Psi(\underline{r},t)}{\partial t} = \left[-\frac{\hbar^2}{2m}\nabla^2 + V(r)\right]\Psi(\underline{r},t) \tag{2.14}$$

Notice that the quantity in the bracket is the Hamiltonian H of the system. Its physical meaning is the total energy, which consists of the kinetic part $p^2/2m$ and the potential part V(r). Appearance of the Laplacian operator ∇^2 is to be expected, since the particle momentum $\underline{p}$ is an operator in configuration space, and it is represented as $\underline{p} = -i\hbar\underline{\nabla}$. For the same reason, H is an operator having the representation

$$H = -\frac{\hbar^2}{2m}\nabla^2 + V(r) \tag{2.15}$$

so another form of the Schrödinger equation is

$$i\hbar\frac{\partial\Psi(\underline{r},t)}{\partial t} = H\Psi(\underline{r},t) \tag{2.16}$$

As a side remark we note that (2.14) is valid only for a non-relativistic particle, whereas (2.16) is more general if H is left unspecified. This means that one can use a relativistic expression for H, then (2.16) would lead to the Dirac equation, which is what one should consider if the particle were an electron. Compared to the classical wave equation, (2.1), which relates the second spatial derivative of the wave function to the second-order time

derivative, the time-dependent Schrödinger wave equation, (2.14) or (2.16), is seen to relate the spatial derivative of the wave function to the *first-order* time derivative. This is a significant distinction which we do not go into in this class. Among other implications is the fact that the classical wave is real and messurable (elastic strings and electromagnetic waves) whereas the Schrödinger wave function is *complex (therefore not measurable)*. To ascribe physical meaning to the wave function one needs to consider the probability density defined as $\Psi^*(\underline{r},t)\Psi(\underline{r},t)$, where $\Psi^*(\underline{r},t)$ is the complex conjugate of the wave function.

For almost all our discussions the time-independent form of the Schrödinger equation is needed. This is obtained by considering a periodic solution to (2.16) of the form

$$\Psi(\underline{r},t) = \psi(\underline{r})e^{iEt/\hbar} \tag{2.17}$$

where E is a constant (soon to be identified as the total energy). Inserting this solution into (2.16)gives the time-independent Schrödinger equation,

$$H\psi(\underline{r}) = E\psi(\underline{r}) \tag{2.18}$$

We see that (2.18) has the form of an eigenvalue problem with H being the operator, E the eigenvalue, and $\psi(\underline{r})$ the eigenfunction.

It is instructive to recognize a certain similarity between the Schrödinger equation and the classical wave equation when the latter incorporates the concept of deBroglie waves. To show this we first write the three-dimensional generalization (2.1) as

$$\frac{\partial^2 \xi(\underline{r},t)}{\partial t^2} = v_{ph}^2 \nabla^2 \xi(\underline{r},t) \tag{2.19}$$

and use (2.13),

$$v_{ph} = \frac{E}{p} = \frac{E}{\sqrt{2m(E-V)}} \tag{2.20}$$

For periodic solutions, $\xi(\underline{r},t) = \varsigma(\underline{r})e^{iEt/\hbar}$, we see that one is led immediately to (2.19). Notice that the connection between the classical wave equation and the Schrödinger equation is possible only in terms of the time-independent form of the equations. As mentioned above, the two equations, in their time-dependent forms, differ in important ways, consequently different properties have to be ascribed to the classical wave function and the Schrödinger wave function.

Following our previous statement about the different types of wave solutions, we can ask what types of solutions to the Schrödinger equation are of interest. To answer this question we will consider (2.18) in one dimension for the sake of illustration. Writing out the equation explicitly, we have

$$\frac{d^2\psi(x)}{dx^2} = -k^2\psi(x) \tag{2.21}$$

where $k^2 = 2m[E-V(x)]/\hbar^2$. In general k^2 is a function of x because of the potential energy V9x), but for piecewise constant potential functions such as a rectangular well or barrier, we can write a separate equation for each region where V(x0 is constant, and thereby treat k^2 as a constant in (2.21). A general solution (2.21) is then

$$\psi(x) = Ae^{ikx} + Be^{-ikx} \tag{2.22}$$

where A and B are constants to be determined by appropriate boundary conditions. Now suppose we are dealing with finite-range potentials so that $V(x) \to 0$ as $x \to \infty$, then k becomes $(2mE/\hbar^2)^{1/2}$. For E > 0, k is real and Ψ, as given by (2.17), is seen to have the form of traveling plane waves. On the other hand, if E < 0, $k = i\kappa$ is imaginary, then $\Psi \approx e^{-\kappa x}e^{-i\omega t}$, and the solution has the form of a standing wave. What this means is that for the description of scattering problems one should use *positive-energy* solutions (these

are called scattering states), while for bound-state calculations one should work with *negative-energy* solutions. Fig. 2 illustrates the behavior of the two types of solutions. The condition at infinity, $x \to \pm\infty$, is that ψ is a plane wave in the scattering problem, and an exponentially decaying function in the bound-state problem. In other words, outside the potential (the exterior region) the scattering state should be a plane wave representing the presence of an incoming or outgoing particle, while the bound state should be represented by an exponentially damped wave signifying the localization of the particle inside the potential well. Inside the potential (the interior region) both solutions are seen to be oscillatory, with the shorter period corresponding to higher kinetic energy T = E – V.

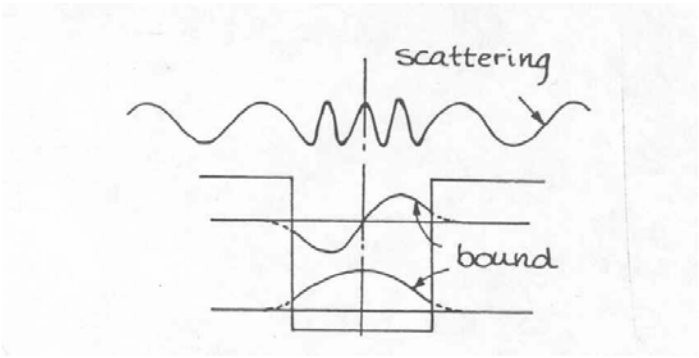

Fig. 2. Traveling and standing wave functions as solutions to scattering and bound-state problems respectively.

There are general properties of Ψ which we require for either problem. These arise from the fact that we are seeking physical solutions to the wave equation, and that $|\psi(\underline{r})|^2 d^3r$ has the interpretation of being the probability of finding the particle in an element of volume d3r about r. In view of (2.17) we see that $|\Psi(\underline{r},t)|^2 = |\psi(\underline{r})|^2$, which means that we are dealing with stationary solutions. Since a time-independent potential cannot create or destroy particles, the normalization condition

$$\int d^3r |\psi(\underline{r})|^2 = 1 \qquad (2.23)$$

cannot be applied to the bound-state solutions with integration limits extending to infinity. However, for scattering solutions one needs to specify an arbitrary volume Ω for the normalization of a plane wave. This poses no difficulty since in any calculation all physical results will be found to be independent of Ω. Other properties of Ψ, or ψ, which can be invoked as conditions for the solutions to be physically meaningful are:

(i) finite everywhere

(ii) single-valued and continuous everywhere

(iii) first derivative continuous

(iv) $\Psi \to 0$ when $V \to \infty$

Condition (iii) is equivalent to the statement that the particle current must be continuous everywhere. The current is related to the wave function by the expression

$$\underline{j}(\underline{r}) = \frac{\hbar}{2mi}[\psi^{+}(\underline{r})\underline{\nabla}\psi(\underline{r}) - \psi(\underline{r})\underline{\nabla}\psi^{+}(\underline{r})] \tag{2.24}$$

which can be derived directly from (2.18).

22.101 Applied Nuclear Physics (Fall 2004)
Lecture 3 (9/15/04)

Bound States in One Dimensional Systems – Particle in a Square Well

---

References --
R. L. Liboff, *Introductory Quantum Mechanics* (Holden Day, New York, 1980).

We will solve the Schrödinger wave equation in the simplest problem in quantum mechanics, a particle in a potential well. The student will see from this calculation how the problem is solved by dividing the system into two regions, the interior where the potential energy is nonzero, and the exterior where the potential is zero. The solution to the wave equation is different in these two regions because of the physical nature of the problem. The interior wave function is oscillatory in the interior and exponential (non-oscillatory) in the exterior. Matching these two solutions at the potential boundary gives a condition on the wavenumber (or wavelength), which turns out to be quantization condition. That is, solutions only exist if the wavenumbers take on certain discrete values which then translate into discrete energy levels for the particle. For a given potential well of certain depth and width, only a discrete set of wave functions can exist in the potential well. These wave functions are the eigenfunctions of the Hamiltonian (energy) operator, with corresponding energy levels as the eigenvalues. Finding the wavefunctions and the spectrum of eigenvalues is what we mean by solving the Schrödinger wave equation for the particle in a potential well. Changing the shape of the potential means a different set of eigenfunctions and the eigenvalues. The procedure to find them, however, is the same.

For a one-dimensional system the time-independent wave equation is

$$-\frac{\hbar^2}{2m}\frac{d^2\psi(x)}{dx^2}+V(x)\psi(x)=E\psi(x) \qquad (3.1)$$

We will use this equation to investigate the bound-states of a particle in a square well potential, depth V_o and width L. The physical meaning of (3.1) is essentially the statement of energy conservation, the total energy E, a negative and constant quantity, is the sum of kinetic and potential energies. Since (3.1) holds at every point in space, the

fact that the potential energy V(x) varies in space means the kinetic energy of the particle also will vary in space. For a square well potential, V(x) has the form

$$V(x) = -V_o \qquad -L/2 \le x \ge L/2$$

$$= \ 0 \qquad \text{elsewhere} \qquad (3.2)$$

as shown in Fig. 1. Taking advantage of the piecewise constant behavior of the potnetial,

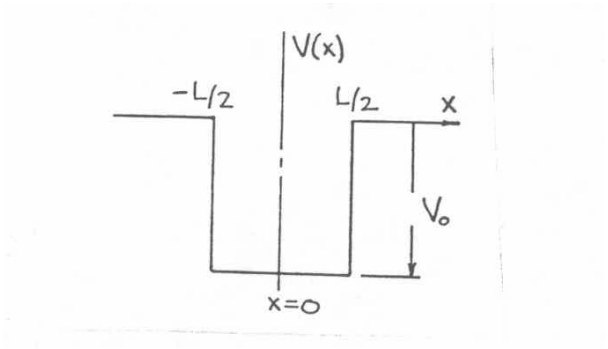

Fig. 1. The square well potential centered at the origin with depth V_o and width L.

we divide the configuration space into an interior region, where the potential is constant and negative, and an exterior region where the potential vanishes. For the interior region the wave equation can be put into the standard form of a second-order differential equation with constant coefficient,

$$\frac{d^2\psi(x)}{dx^2} + k^2\psi(x) = 0 \qquad |x| \le L/2 \qquad (3.3)$$

where we have introduced the wavenumber k such that $k^2 = 2m(E + V_o)/\hbar^2$ is always positive, and therefore k is always real. For this to be true we are excluding solutions where $-E > V_o$. For the exterior region, the wave equation similarly can be put into the form

$$\frac{d^2\psi(x)}{dx^2} - \kappa^2\psi(x) = 0 \qquad |x| \geq L/2 \qquad (3.4)$$

where $\kappa^2 = -2mE/\hbar^2$. To obtain the solutions of physical interest to (3.3) and (3.4), we keep in mind that the solutions should have certain symmetry properties, in this case they should have definite parity, or inversion symmetry (see below). This means when x $\rightarrow$ -x, $\psi(x)$ must be either invariant or it must change sign. The reason for this requirement is that the Hamiltonian H is symmetric under inversion (potential is symmetric with our choice of coordinate system (see Fig. 1). Thus we take for our solutions

$$\psi(x) = A\sin kx \qquad |x| \leq L/2$$

$$= Be^{-\kappa x} \qquad x > L/2 \qquad (3.5)$$

$$= Ce^{\kappa x} \qquad x < -L/2$$

We have used the condition of definite parity in choosing the interior solution. While we happen to have chosen a solution with odd parity, the even-parity solution, coskx, would be just as acceptable. On the other hand, one cannot choose the sum of the two, Asinkx + Bcoskx, since this does not have definite parity. For the exterior region we have applied condition (i) in Lec2 to discard the exponentially growing solution. This is physically intuitive since for a bound state the particle should be mostly inside the potential well, and away from the well the wave function should be decaying rather than growing.

In the solutions we have chosen there are three constants of integration, A, B, and C. These are to be determined by applying boundary conditions at the interface between the interior and exterior regions, plus a normalization condition (2.23). Notice there is another constant in the problem which has not been specified, the energy eigenvalue E. All we have said thus far is that E is negative. We have already utilized the boundary condition at infinity and the inversion symmetry condition of definite parity. The

condition which we can now apply at the continuity conditions (ii) and (iii) in Lec2. At the interface, $x_o = \pm L/2$, the boundary conditions are

$$\psi_{\text{int}}(x_o) = \psi_{ext}(x_o) \tag{3.6}$$

$$\left.\frac{d\psi_{\text{int}}(x)}{dx}\right|_{x_o} = \left.\frac{d\psi_{ext}(x)}{dx}\right|_{x_o} \tag{3.7}$$

with subscripts int and ext denoting the interior and exterior solutions respectively.

The four conditions at the interface do not allow us to determine the four constants because our system of equations is homogeneous. As in situations of this kind, the proportionality constant is fixed by the normalization condition (2.23). We therefore obtain C = -B, $B = A\sin(kL/2)\exp(\kappa L/2)$, and

$$\cot(kL/2) = -\kappa/k \tag{3.8}$$

with the constant A determined by (2.23). The most important result of this calculation is (3.8), sometimes also called a dispersion relation. It is a relation which determines the allowed values of E, a quantity that appears in both k and κ. These are then the discrete (quantized) energy levels which the particle can have in the particular potential well given, namely, a square well of width L and depth V_o. Eq.(3.8) is the consequence of choosing the odd-parity solution for the interior wave. For the even-parity solution, $\psi_{\text{int}}(x) = A'\cos kx$, the corresponding dispersion relation is

$$\tan(kL/2) = \kappa/k \tag{3.9}$$

Since both solutions are equally acceptable, one has two distinct sets of energy levels, given (3.8) and (3.9).

We now carry out an analysis of (3.8) and (3.9). First we put the two equations into dimensionless form,

$$\xi \cot \xi = -\eta \qquad \text{(odd-parity)} \qquad (3.10)$$

$$\xi \tan \xi = \eta \qquad \text{(even-parity)} \qquad (3.11)$$

where $\xi = kL/2$, $\eta = \kappa L/2$, and

$$\xi^2 + \eta^2 = 2mL^2|V_o|/4\hbar^2 \equiv \Lambda \qquad (3.12)$$

is a constant for fixed values of V_o and L. In Fig. 4 we plot the left- and right-hand sides of (3.10) and (3.11), and obtain from their intersections the allowed energy levels. The graphical method of obtaining solutions to the dispersion relations reveals the following

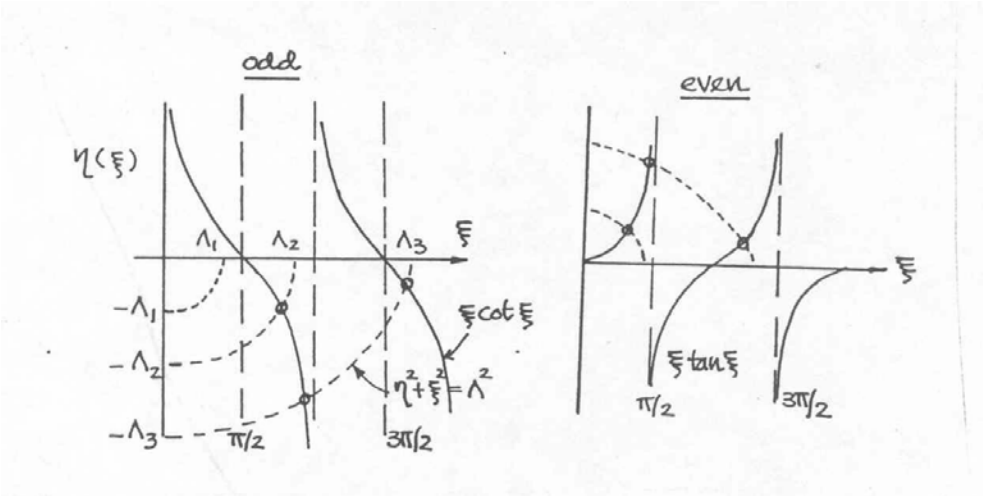

Fig. 4. Graphical solutions of (3.10) and (3.11) showing that there could be no odd-parity solutions if Λ is not large enough (the potential is not deep enough or not wide enough), while there is at least one even-parity solution no matter what values are the well depth and width.

features. There exists a minimum value of Λ below which no odd-parity solutions are allowed. On the other hand, there is always at least one even-parity solution. The first even-parity energy level occurs at $\xi < \pi/2$, whereas the first odd-parity level occurs at

$\pi/2 < \xi < \pi$. Thus, the even- and odd-parity levels alternate in magnitudes, with the lowest level being even in parity. We should also note that the solutions depend on the potential function parameters only through the variable Λ, or the combination V_oL^2, so that changes in well depth have the same effect as changes in the square of the well width.

At this point it is well to keep in mind that when we consider problems in three dimensions (next chapter), the cosine solution to the wave function has to be discarded because of the condition of regularity (wave function must be finite) at the origin. This means that there will be a minimum value of Λ or V_oL^2 below which no bound states can exist.

We now summarize our results for the allowed energy levels of a particle in a square well potential and the corresponding wave functions.

$$\psi_{\text{int}}(x) = A\sin kx \quad \text{or} \quad A'\cos kx \qquad |x| < L/2 \tag{3.13}$$

$$\psi_{ext}(x) = Be^{-\kappa x} \qquad x > L/2$$

$$= Ce^{\kappa x} \qquad x < -L/2 \tag{3.14}$$

where the energy levels are

$$E = -|V_o| + \frac{\hbar^2 k^2}{2m} = -\frac{\hbar^2 \kappa^2}{2m} \tag{3.15}$$

The constants B and C are determined from the continuity conditions at the interface, while A and A' are to be fixed by the normalization condition. The discrete values of the bound-state energies, k or κ, are obtained (3.8) and (3.9). In Fig. 5 we show a sketch of the two lowest-level solutions, the ground state with even-pairty and the first excited state with odd parity. Notice that the number of excited states that one can have depends on

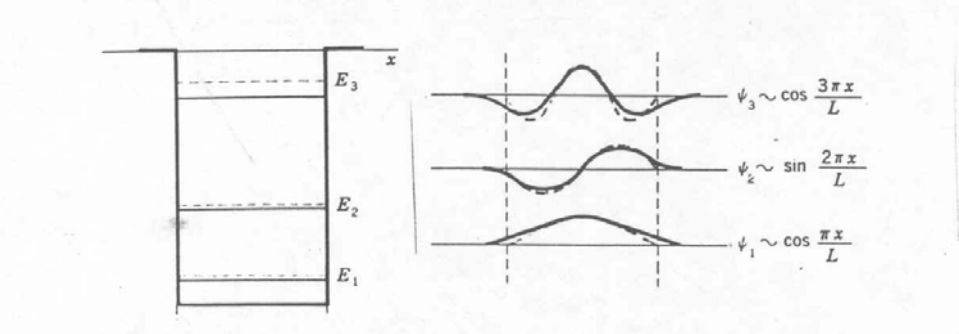

Fig. 5. Ground-state and first two excited-state solutions [from Cohen, p. 16]

the value of Vo because our solution is valid only for negative E. This means that for a potential of a given depth, the particle can be bound only in a finite number of states.

To obtain more explicit results it is worthwhile to consider an approximation to the boundary condition at the interface. Instead of the continuity of ψ and its derivative at the interface, one might assume that the penetration of the wave function into the external region can be neglected and require that ψ vanishes at $x = \pm L/2$. Applying this condition to (3.13) gives $kL = n\pi$, where n is any integer, or equivalently,

$$E_n = -|V_o| + \frac{n^2\pi^2\hbar^2}{2mL^2}, \qquad \text{n = 1, 2, …} \tag{3.16}$$

This shows explicitly how the energy eigenvalue En varies with the level index n, which is the quantum number. The corresponding wave functions are

$$\psi_n(x) = A_n \cos(n\pi x/L), \qquad \text{n = 1, 3, …}$$

$$= A_n' \sin(n\pi x/L) \qquad \text{n = 2, 4, …} \tag{3.17}$$

The first solutions in this approximate calculation are also shown in Fig. 5. We see that requiring the wave function to vanish at the interface is tantamount to assuming that the particle is confined in a well of width L and infinitely steep walls (the infinite well

potential or limit of $V_o \to \infty$). It is therefore to be expected that the problem becomes independent of V_o and there is no limit on the number of excited states. Clearly, the approximate solutions become the more useful the greater is the well depth, and the error is always a higher energy level as a result of squeezing of the wave function (physically, the wave has a shorter period or a larger wavenumber).

22.101 Applied Nuclear Physics (Fall 2004)
Lecture 4 (9/20/04)

Bound States in Three Dimensions – Orbital Angular Momentum

References --
R. L. Liboff, *Introductory Quantum Mechanics* (Holden Day, New York, 1980).
L. I. Schiff, *Quantum Mechanics*, McGraw-Hill, New York, 1955).
P. M. Morse and H. Feshbach, *Methods of Theoretical Physics* (McGraw-Hill, New York, 1953).

We will now extend the bound-state calculation to three-dimensional systems. The problem we want to solve is the same as before, namely, to determine the bound-state energy levels and corresponding wave functions for a particle in a *spherical* well potential. Although this is a three-dimensional potential, its symmetry makes the potential well a function of only one variable, the distance between the particle position and the origin. In other words, the potential is of the form

$$\begin{aligned} V(r) &= -V_o \qquad r < r_o \\ &= 0 \qquad \text{otherwise} \end{aligned} \tag{4.1}$$

Here r is the radial position of the particle relative to the origin. Any potential that is a function only of r, the magnitude of the position $\underline{r}$ and not the position vector itself, is called the central-force potential. As we will see, this form of the potential makes the solution of the Schrödinger wave equation particularly simple. For a system where the potential or interaction energy has no angular dependence, one can reformulate the problem by factorizing the wave function into a component that involves only the radial coordinate and another component that involves only the angular coordinates. The wave equation is then reduced to a system of uncoupled one-dimensional equations, each describing a radial component of the wave function. As to the justification for using a central-force potential for our discussion, this will depend on which properties of the nucleus we wish to study.

We again begin with the time-independent wave equation

$$\left[-\frac{\hbar^2}{2m}\nabla^2 + V(r)\right]\psi(\underline{r}) = E\psi(\underline{r}) \tag{4.2}$$

Since the potential function has spherical symmetry, it is natural for us to carry out the analysis in the spherical coordinate system rather than the Cartesian system. A position vector $\underline{r}$ then is specified by the radial coordinate r and two angular coordinates, θ and φ, the polar and azimuthal angles respectively, see Fig. 1. In this coordinate system

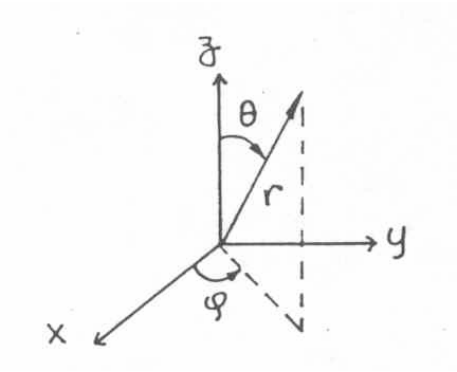

Fig. 1. The spherical coordinate system. A point in space is located by the radial coordinate r, and polar and azimuthal angles θ and φ.

the Laplacian operator ∇^2 is of the form

$$\nabla^2 = D_r^2 + \frac{1}{r^2}\left[\frac{-L^2}{\hbar^2}\right] \tag{4.3}$$

where D_r^2 is an operator involving the radial coordinate,

$$D_r^2 = \frac{1}{r^2}\frac{\partial}{\partial r}\left[r^2\frac{\partial}{\partial r}\right] \tag{4.4}$$

and the operator L^2 involves only the angular coordinates,

$$-\frac{L^2}{\hbar^2}=\frac{1}{\sin\theta}\frac{\partial}{\partial\theta}\left[\sin\theta\frac{\partial}{\partial\theta}\right]+\frac{1}{\sin^2\theta}\frac{\partial^2}{\partial\varphi^2} \tag{4.5}$$

In terms of these operators the wave equation (4.2) becomes

$$\left[-\frac{\hbar^2}{2m}D_r^2+\frac{L^2}{2mr^2}+V(r)\right]\psi(r\theta\varphi)=E\psi(r\theta\varphi) \tag{4.6}$$

For any potential V(r) the angular variation of ψ is always determined by the operator $L^2/2mr^2$. Therefore one can study the operator L^2 separately and then use its properties to simplify the solution of (4.6). This needs to be done only once, since the angular variation is independent of whatever form one takes for V(r). It turns out that L^2 is very well known (it is the square of L which is the angular momentum operator); it is the operator that describes the angular motion of a free particle in three-dimensional space.

We first summarize the basic properties of L^2 before discussing any physical interpretation. It can be shown that the eigenfunction of L^2 are the spherical harmonics functions, $Y_\ell^m(\theta,\varphi)$,

$$L^2Y_\ell^m(\theta,\varphi)=\hbar^2\ell(\ell+1)Y_\ell^m(\theta,\varphi) \tag{4.7}$$

where

$$Y_\ell^m(\theta,\varphi)=\left[\frac{2\ell+1}{4\pi}\frac{(\ell-|m|)!}{(\ell+|m|)!}\right]^{1/2}P_\ell^m(\cos\theta)e^{im\varphi} \tag{4.8}$$

and

$$P_\ell^m(\mu)=\frac{(1-\mu^2)^{m/2}}{2^\ell\ell!}\frac{d^{\ell+m}}{d\mu^{\ell+m}}(\mu^2-1)^\ell \tag{4.9}$$

with $\mu=\cos\theta$. The function $P_\ell^m(\mu)$ is called the associated Legendre polynomials, which are in turn expressible in terms of Legendre polynomials $P_\ell(\mu)$,

$$P_\ell^m(\mu) = (1-\mu)^{|m|/2} \frac{d^{|m|}}{d\mu^{|m|}} P_\ell(\mu) \qquad (4.10)$$

with $P_o(x) = 1$, $P_1(x) = x$, $P_2(x) = (3X^2 - 1)/2$, $P_3(x) = (5x^3\text{-}3x)/2$, etc. Special functions like Y_ℓ^m and P_ℓ^m are quite extensively discussed in standard texts [see, for example, Schiff, p.70] and reference books on mathematical functions [More and Feshbach, p. 1264]. For our purposes it is sufficient to regard them as well known and tabulated quantities like sines and cosines, and whenever the need arises we will invoke their special properties as given in the mathematical handbooks.

It is clear from (4.7) that $Y_\ell^m(\theta,\varphi)$ is an eigenfunction of L^2 with corresponding eigenvalue $\ell(\ell+1)\hbar^2$. Since the angular momentum of the particle, like its energy, is quantized, the index ℓ can take on only positive integral values or zero,

$$\ell = 0, 1, 2, 3, \ldots$$

Similarly, the index m can have integral values from $-\ell$ to ℓ,

$$m = -\ell, -\ell+1, \ldots, -1, 0, 1, \ldots, \ell-1, \ell$$

For a given ℓ, there can be $2\ell+1$ values of m. The significance of m can be seen from the property of L_z, the projection of the orbital angular momentum vector $\underline{L}$ along a certain direction in space (in the absence of any external field, this choice is up to the observer). Following convention we will choose this direction to be along the z-axis of our coordinate system, in which case the operator Lz has the representation, $L_z = -i\hbar\partial/\partial\varphi$, and its eignefunctions are also $Y_\ell^m(\theta,\varphi)$, with eigenvalues $m\hbar$. The indices ℓ and m are called quantum numbers. Since the angular space is two-dimensional (corresponding to two degrees of freedom), it is to be expected that there will be two quantum numbers in our analysis. By the same token we should expect three quantum numbers in our description of three-dimensional systems. We should regard the particle as existing in various states which are specified by a unique set of quantum numbers,

each one is associated with a certain orbital angular momentum which has a definite magnitude and orientation with respect to our chosen direction along the z-axis. The particular angular momentum state is described by the function $Y_\ell^m(\theta,\varphi)$ with ℓ known as the orbital angular momentum quantum number, and m the magnetic quantum number. It is useful to keep in mind that $Y_\ell^m(\theta,\varphi)$ is actually a rather simple function for low order indices. For example, the first four spherical harmonics are:

$$Y_0^0 = 1/\sqrt{4\pi}\,, \quad Y_1^{-1} = \sqrt{3/8\pi}e^{-i\varphi}\sin\theta\,, \quad Y_1^0 = \sqrt{3/4\pi}\cos\theta\,, \quad Y_1^1 = \sqrt{3/8\pi}e^{i\varphi}\sin\theta$$

Two other properties of the spherical harmonics are worth mentioning. First is that $\{Y_\ell^m(\theta,\varphi)\}$, with ℓ = 0, 1, 2, … and $-\ell \le m \le \ell$, is a *complete set* of functions in the space of $0 \le \theta \le \pi$ and $0 \le \varphi \le 2\pi$ in the sense that any arbitrary function of θ and φ can be represented by an expansion in these functions. Another property is orthonormality,

$$\int_0^\pi \sin\theta d\theta \int_0^{2\pi} d\varphi Y_\ell^{m*}(\theta,\varphi) Y_{\ell'}^{m'}(\theta,\varphi) = \delta_{\ell\ell'}\delta_{mm'} \tag{4.11}$$

where $\delta_{\ell\ell'}$ denotes the Kronecker delta function; it is unity when the two subscripts are equal, otherwise the function is zero.

Returning to the wave equation (4.6) we look for a solution as an expansion of the wave function in spherical harmonics series,

$$\psi(r\theta\varphi) = \sum_{\ell,m} R_\ell(r) Y_\ell^m(\theta,\varphi) \tag{4.12}$$

Because of (4.7) the L^2 operator in (4.6) can be replaced by the factor $\ell(\ell+1)\hbar^2$. In view of (4.11) we can eliminate the angular part of the problem by multiplying the wave

equation by the complex conjugate of a spherical harmonic and integrating over all solid angles (recall an element of solid angle is $\sin\theta d\theta d\varphi$), obtaining

$$\left[-\frac{\hbar^2}{2m}D_r^2+\frac{\ell(\ell+1)\hbar^2}{2mr^2}+V(r)\right]R_\ell(r)=ER_\ell(r) \tag{4.13}$$

This is an equation in one variable, the radial coordinate r, although we are treating a three-dimensional problem. We can make this equation look like a one-dimensional problem by transforming the dependent variable R_ℓ. Define the radial function

$$u_\ell(r)=rR_\ell(r) \tag{4.14}$$

Inserting this into (4.13) we get

$$-\frac{\hbar^2}{2m}\frac{d^2u_\ell(r)}{dr^2}+\left[\frac{\ell(\ell+1)\hbar^2}{2mr^2}+V(r)\right]u_\ell(r)=Eu_\ell(r) \tag{4.15}$$

We will call (4.15) *the radial wave equation*. It is the basic starting point of three-dimensional problems involving a particle interacting with a central potential field.

We observe that (4.15) is actually a system of uncoupled equations, one for each fixed value of the orbital angular momentum quantum number ℓ. With reference to the wave equation in one dimension, the extra term involving $\ell(\ell+1)$ in (4.15) represents the contribution to the potential field due to the centrifugal motion motions of the particle. The 1/r2 dependence makes the effect particularly important near the origin; in other words, centrigfugal motion gives rise to a barrier which tends to keep the particle away from the origin. This effect is of course absent in the case of ℓ = 0, a state of zero orbital angular momentum, as one would expect. The first few ℓ states usually are the only ones of interest in our discussion (because they tend to have the lowest energies); they are given special spectroscopic designations with the following equivalence,

notation: **s, p, d, f, g, h**, …

ℓ = **0, 1, 2, 3, 4, 5**, …

where the first four letters stand for ‘sharp’, ‘principal’, ‘diffuse’, and ‘fundamental’ respectively. After f the letters are asigned in alphabetical order, as in h, i, j, … The wave function describing the state of orbital angular momentum ℓ is often called the ℓ th partial wave,

$$\psi_\ell(r\theta\varphi) = R_\ell(r)Y_\ell^m(\theta\varphi) \tag{4.16}$$

notice that in the case of s-wave the wave function is spherically symmetric since Y_0^0 is independent of θ and φ.

Interpretation of Orbital Angular Momentum

In classical mechanics, the angular momentum of a particle in motion is defined as the vector product, $\underline{L} = \underline{r} \times \underline{p}$, where r is the particle position and p its linear momentum. L is directed along the axis of rotation (right-hand rule), as shown in Fig. 2.

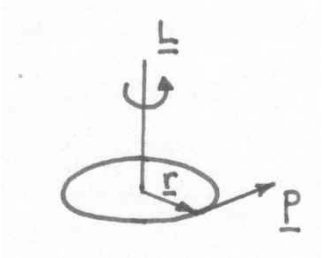

Fig. 2. Angular momentum of a particle at position r moving with linear momentum p (classical definition).

L is called an axial or pseudovector in contrast to r and p, which are polar vectors. Under inversion, $\underline{r} \to -\underline{r}$, and $\underline{p} \to -\underline{p}$, but $\underline{L} \to \underline{L}$. Quantum mechanically, L^2 is an operator with eigenvalues and eigenfunctions given in (4.7). Thus the magnitude of L is $\hbar\sqrt{\ell(\ell+1)}$, with ℓ = 0, 1, 2, …being the orbital angular momentum quantum number. We can specify the magnitude and one Cartesian component (usually called the z-component) of L by specifying ℓ and m, an example is shown in Fig. 3. What about the x- and y-components? They are undetermined, in that they cannot be observed

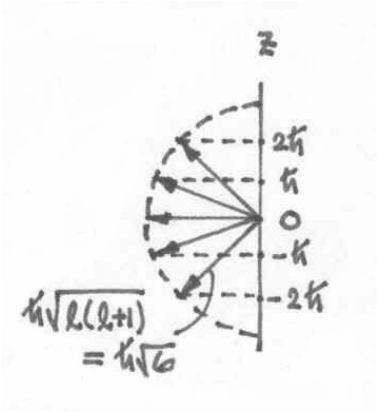

Fig. 3. The $\ell(\ell+1) = 5$ projections along the z-axis of an orbital angular momentum with $\ell = 2$. Magnitude of L is $\sqrt{6}\hbar$.

simultaneously with the observation of L^2 and L_z. Another useful interpretation is to look at the energy conservation equation in terms of radial and tangential motions. By this we mean that the total energy can be written as

$$E = \frac{1}{2}m(v_r^2 + v_t^2) + V = \frac{1}{2}mv_r^2 + \frac{L^2}{2mr^2} + V \qquad (4.17)$$

where the decomposition into radial and tangential velocities is depicted in Fig. 4. Eq.(4.17) can be compared with the radial wave equation (4.15).

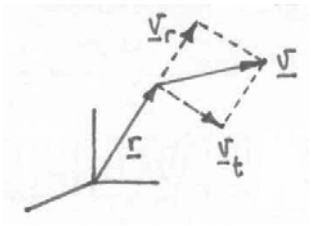

Fig. 4. Decomposing the velocity vector of a particle at position r into radial and tangential components.

Thus far we have confined our discussions of the wave equation to its solution in spherical coordinates. There are situations where it will be more appropriate to work in another coordinate system. As a simple example of a bound-state problem, we can

consider the system of a free particle contained in a cubical box of dimension L along each side. In this case it is clearly more convenient to write the wave equation in Cartesian coordinates,

$$-\frac{\hbar^2}{2m}\left[\frac{\partial^2}{\partial x^2}+\frac{\partial^2}{\partial y^2}+\frac{\partial^2}{\partial z^2}\right]\psi(xyz)=E\psi(xyz) \tag{4.17}$$

$0 < x, y, z < L$. The boundary conditions are $\psi = 0$ whenever x, y, or z is 0 or L. Since both the equation and the boundary conditions are separable in the three coordinates, the solution is of the product form,

$$\psi(xyz)=\psi_{n_x}(x)\psi_{n_y}(y)\psi_{n_z}(z)$$

$$= (2/L)^{3/2}\sin(n_x\pi x/L)\sin(n_y\pi y/L)\sin(n_z\pi z/L) \tag{4.18}$$

where n_x, n_y, n_z are positive integers (excluding zero), and the energy becomes a sum of three contributions,

$$E_{n_xn_yn_z}=E_{n_x}+E_{n_y}+E_{n_z}$$

$$=\frac{(\hbar\pi)^2}{2mL^2}\left[n_x^2+n_y^2+n_z^2\right] \tag{4.19}$$

We see that the wave functions and corresponding energy levels are specified by the set of three quantum numbers (n_x, n_x, n_z). While each state of the system is described by a unique set of quantum numbers, there can be more than one state at a particular energy level. Whenever this happens, the level is said to be *degenerate*. For example, (112), (121), and (211) are three different states, but they are all at the same energy, so the level at $6(\hbar\pi)^2/2mL^2$ is triply degenerate. The concept of degeneracy is useful in our later discussion of the nuclear shell model where one has to determine how many nucleons can

be put into a certain energy level. In Fig. 6 we show the energy level diagram for a particle in a cubical box. Another way to display the information is through a table, such as Table I.

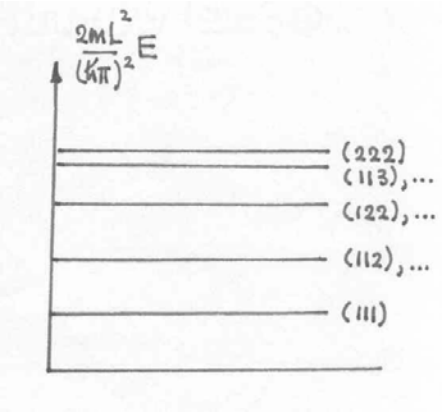

Fig. 6. Bound states of a particle in a cubical box of width L.

Table I. The first few energy levels of a particle in a cubical box which correspond to Fig. 6.

n_x	n_y	n_z	$\frac{2mL^2}{(\hbar\pi)^2}E$	degeneracy
1	1	1	3	1
1	1	2	6	3
1	2	1		
2	1	1		
1	2	2, …	9	3
1	1	3, …	11	3
2	2	2	12	1

The energy unit is seen to be $\Delta E = (\hbar\pi)^2 / 2mL^2$. We can use this expression to estimate the magnitude of the energy levels for electrons in an atom, for which m = 9.1 x10^{-28} gm and L ~ 3 x 10^{-8}cm, and for nucleons in a nucleus, for which m = 1.6x10^{-24} gm and L ~ 5F. The energies come out to be ~30 ev and 6 Mev respectively, values which are typical

in atomic and nuclear physics. Notice that if an electron were in a nucleus, then it would have energies of the order 10^{10} ev !

In closing this section we note that Bohr had put forth the "correspondence principle" which states that quantum mechanical results will approach the classical results when the quantum numbers are large. Thus we have

$$|\psi_n|^2 = \frac{2}{L}\sin^2(n\pi x/L) \to \frac{1}{L} \qquad (4.20)$$
$$n \to \infty$$

What this means is that the probability of finding a particle anywhere in the box is 1/L, i.e., one has a uniform distribution, see Fig. 7.

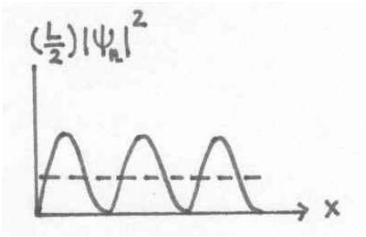

Fig. 7. The behavior of $\sin^2 nx$ in the limit of large n.

Parity

Parity is a symmetry property of the wave function associated with the inversion operation. This operation is one where the position vector $\underline{r}$ is reflected through the origin (see Fig. 1), so $\underline{r} \to -\underline{r}$. For physical systems which are not subjected to an external vector field, we expect these systems will remain the same under an inversion operation, or the Hamiltonian is invariant under inversion. If $\psi(\underline{r})$ is a solution to the wave equation, then applying the inversion operation we get

$$H\psi(-\underline{r}) = E\psi(-\underline{r}) \qquad (4.21)$$

which shows that $\psi(-\underline{r})$ is also a solution. A general solution is therefore obtained by adding or subtracting the two solutions,

$$H\left[\psi(\underline{r}) \pm \psi(-\underline{r})\right] = E\left[\psi(\underline{r}) \pm \psi(-\underline{r})\right] \tag{4.22}$$

Since the function $\psi_+(\underline{r}) = \psi(\underline{r}) + \psi(-\underline{r})$ is manifestly invariant under inversion, it is said to have positive parity, or its parity, denoted by the symbol π, is +1. Similarly, $\psi_-(\underline{r}) = \psi(\underline{r}) - \psi(-\underline{r})$ changes sign under inversion, so it has negative parity, or π = -1. The significance of (4.22) is that a physical solution of our quantum mechanical description should have definite parity, and this is the condition we have previously imposed on our solutions in solving the wave equation (see Lec3). Notice that there are functions who do not have definite parity, for example, Asinkx + Bcoskx. This is the reason that we take either the sine function or the cosine function for the interior solution in Lec3. In general, one can accept a solution as a linear combination of individual solutions all having the same parity. A linear combination of solutions with different parities has no definite parity, and is therefore unacceptable.

In spherical coordinates, the inversion operation of changing $\underline{r}$ to $-\underline{r}$ is equivalent to changing the polar angle θ to $\pi - \theta$, and the azimuthal angle φ to $\varphi + \pi$. The effect of the transformation on the spherical harmonic function $Y_\ell^m(\theta,\varphi) \sim e^{im\varphi} P_\ell^m(\theta)$ is

$$e^{im\varphi} \to e^{im\varphi} e^{im\pi} = (-1)^m e^{im\varphi}$$

$$P_\ell^m(\theta) \to (-1)^{\ell-m} P_\ell^m(\theta)$$

so the parity of $Y_\ell^m(\theta,\varphi)$ is $(-1)^\ell$. In other words, the parity of a state with a definite orbital angula momentum is even if ℓ is even, and odd if ℓ is odd. All eigenfunctions of the Hamiltonian with a spherically symmetric potential are therefore either even or odd in parity.

22.101 Applied Nuclear Physics (Fall 2004)
Lecture 5 (9/22/04)

Barrier Penetration

References --
R. D. Evans, *The Atomic Nucleus*, McGraw-Hill, New York, 1955), pp. 60, pp.852.

We have previously observed that one can look for different types of solutions to the wave equation. An application which will turn out to be useful for later discussion of nuclear decay by α -particle emission is the problem of barrier penetration. In this case one looks for positive-energy solutions as in a scattering problem. We consider a one-dimensional system where a particle with mass m and energy E is incident on a potential barrier with width L and height V_o that is greater than E. Fig. 1 shows that with the particle approaching from the left, the problem separates into three regions, left of the barrier (region I), inside the barrier (region II), and right of the barrier (region III).

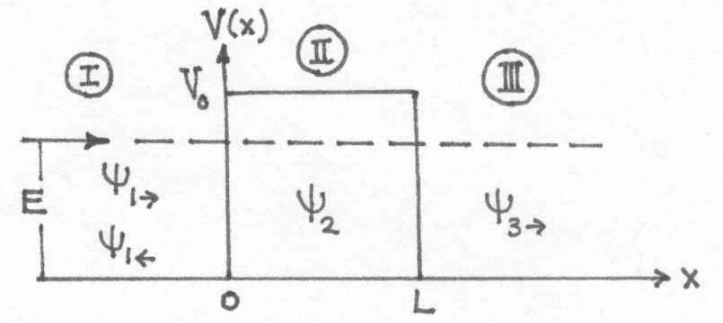

Fig. 1. Particle with energy E penetrating a square barrier of height V_o ($V_o > E$) and width L.

In regions I and III the potential is zero, so the wave equation (3.1) is of the form

$$\frac{d^2\psi(x)}{dx^2} + k^2\psi(x) = 0\,, \qquad k^2 = 2mE/\hbar^2 \tag{5.1}$$

where k^2 is positive. The wave functions in these two regions are therefore

$$\psi_1 = a_1 e^{ikx} + b_1 e^{-ikx} \equiv \psi_{1\rightarrow} + \psi_{1\leftarrow} \tag{5.2}$$

$$\psi_3 = a_3 e^{ikx} + b_3 e^{-ikx} \equiv \psi_{3\rightarrow} \tag{5.3}$$

where we have set $b_3 = 0$ by imposing the boundary condition that there is no particle in region III traveling to the left (since there is nothing in this region that can reflect the particle). By contrast, in region I we allow for reflection of the incident particle by the barrier which means that b_1 will be nonzero. The subscripts $\rightarrow$ and $\leftarrow$ denote the wave functions traveling to the right and to the left respectively.

In region II, the wave equation is

$$\frac{d^2\psi(x)}{dx^2} - \kappa^2\psi(x) = 0, \qquad \kappa^2 = 2m(|V_o| - E)/\hbar^2 \tag{5.4}$$

So we write the solution in the form

$$\psi_2 = a_2 e^{\kappa x} + b_2 e^{-\kappa x} \tag{5.5}$$

Notice that in region II the kinetic energy, $E - V_o$, is negative, so the wavenumber is imaginary in a propagating wave (another way of saying the wave function is monotonically decaying rather than oscillatory). What this means is that there is no wave-like solution in this region. By introducing κ we can think of it as the wavenumber of a hypothetical particle whose kinetic energy is positive, $V_o - E$.

Having obtained the wave function in all three regions we proceed to discuss how to organize this information into a useful form, namely, the transmission and reflection coefficients. We recall that given the wave function ψ, we know immediately the particle density (number of particles per unit volume, or the probability of the finding the particle in an element of volume d^3r about $\underline{r}$), $|\psi(\underline{r})|^2$, and the net current, given by (2.24),

$$\underline{j} = \frac{\hbar}{2mi}\left(\psi^* \underline{\nabla}\psi - \psi \underline{\nabla}\psi^*\right) \tag{5.6}$$

Using the wave functions in regions I and III we obtain

$$j_1(x) = v\left[|a_1|^2 - |b_1|^2\right] \tag{5.7}$$

$$j_3(x) = v|a_3|^2 \tag{5.8}$$

where $v = \hbar k / m$ is the particle speed. We see from (5.7) that j_1 is the net current in region I, the difference between the current going to the right and that going to the left. Also, in region III there is only the current going to the right. Notice that current is like the flux in that it has the dimension of number of particles per unit area per second. This is consistent with (5.7) and (5.8) since $|a|^2$ and $|b|^2$ are particle densities with the dimension of number of particles per unit volume. From here on we can regard a_1, b_1, and a_3 as the amplitudes of the incident, reflected, and transmitted waves, respectively. With this interpretation we define

$$T = \left|\frac{a_3}{a_1}\right|^2, \qquad R = \left|\frac{b_1}{a_1}\right|^2 \tag{5.9}$$

Since particles cannot absorbed or created in region II and there is no reflection in region III, the net current in region I must be equal to the net current in region III, or $j_1 = j_3$. This means that the condition

$$T + R = 1 \tag{5.10}$$

is always satisfied (as one would expect). The transmission coefficient is sometimes also called the Penetration Factor and denoted as P.

To calculate a_1 and a_3, we apply the boundary conditions at the interfaces, x = 0 and x = L,

$$\psi_1 = \psi_2, \qquad \frac{d\psi_1}{dx} = \frac{d\psi_2}{dx} \qquad \text{x = 0} \tag{5.11}$$

$$\psi_2 = \psi_3 \ , \qquad \frac{d\psi_2}{dx} = \frac{d\psi_3}{dx} \qquad \text{x = L} \tag{5.12}$$

These 4 conditions allow us to eliminate 3 of the 5 integration constants. For the purpose of calculating the transmission coefficient we need to keep a_1 and a_3. Thus we will eliminate b_1, a_2, and b_2 and in the process arrive at the ratio of a_1 to a_3 (after about a page of algebra),

$$\frac{a_1}{a_3} = e^{(ik-\kappa)L}\left[\frac{1}{2} - \frac{i}{4}\left(\frac{\kappa}{k} - \frac{k}{\kappa}\right)\right] + e^{(ik+\kappa)L}\left[\frac{1}{2} + \frac{i}{4}\left(\frac{\kappa}{k} - \frac{k}{\kappa}\right)\right] \tag{5.13}$$

This result then leads to (after another half-page of algebra)

$$\frac{|a_3|^2}{|a_1|^2} = \left|\frac{a_3}{a_1}\right|^2 = \frac{1}{1 + \dfrac{V_o^2}{4E(V_o - E)}\sinh^2 \kappa L} \equiv P \tag{5.14}$$

with $\sinh x = (e^x - e^{-x})/2$. A sketch of the variation of P with κL is shown in Fig. 2.

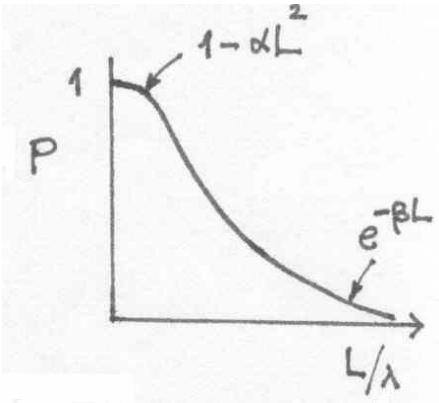

Fig. 2. Variation of transmission coefficient (Penetration Factor) with ratio of barrier width L to λ, the effective wavelength of the incident particle.

Using the leading expression of sinh(x) for small and large arguments, one can readily obtain simpler expressions for P in the limit of thin and thick barriers,

$$P \sim 1 - \frac{V_o^2}{4E(V_o - E)}(\kappa L)^2 = 1 - \frac{(V_o L)^2}{4E}\frac{2m}{\hbar^2} \qquad \kappa L << 1 \qquad (5.15)$$

$$P \sim \frac{16E}{V_o}\left(1 - \frac{E}{V_o}\right)e^{-2\kappa L} \qquad \kappa L >> 1 \qquad (5.16)$$

Thus the transmission coefficient decreases monotonically with increasing V_o or L, relatively slowly for thin barriers and more rapidly for thick barriers.

Which limit is more appropriate for our interest? Consider a 5 Mev proton incident upon a barrier of height 10 Mev and width 10 F. This gives $\kappa \sim 5 \times 10^{12}$ cm^{-1}, or $\kappa L \sim 5$. Using (5.16) we find

$$P \sim 16x\frac{1}{2}x\frac{1}{2}xe^{-10} \sim 2x10^{-4}$$

As a further simplification, one sometimes even ignores the prefactor in (5.16) and takes

$$P \sim e^{-\gamma} \qquad (5.17)$$

with

$$\gamma = 2\kappa L = \frac{2L}{\hbar}\sqrt{2m(V_o - E)} \qquad (5.18)$$

We show in Fig. 3 a schematic of the wave function in each region. In regions I and III, ψ is complex, so we plot its real or imaginary part. In region II ψ is not oscillatory. Although the wave function in region II is nonzero, it does not appear in either the transmission or the reflection coefficient.

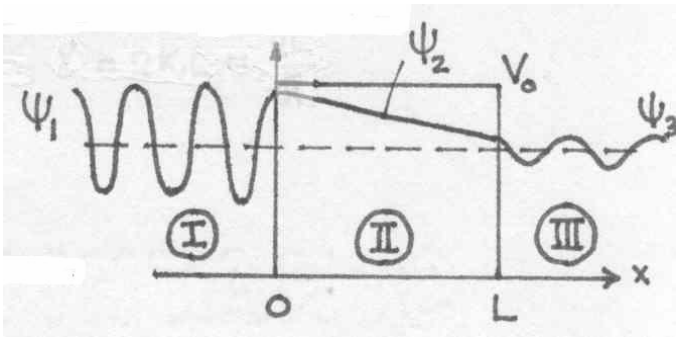

Fig. 3. Particle penetration through a square barrier of height V_o and width L at energy E ($E < V_o$), schematic behavior of wave functions in the three regions.

When the potential varies continuously in space, one can show that the attenuation coefficient γ is given approximately by the expression

$$\gamma \cong \frac{2}{\hbar}\int_{x_1}^{x_2} dx\left[2m\{V(x)-E\}\right]^{1/2} \tag{5.19}$$

where the limits of integration are indicated in Fig. 4; they are known as the 'classical turning points'. This result is for 1D. For a spherical barrier ($\ell = 0$ or s-wave solution),

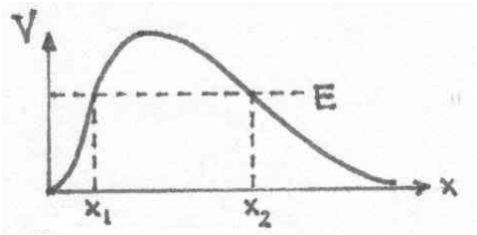

Fig. 4. Region of integration in (5.19) for a variable potential barrier.

one has

$$\gamma \approx \frac{2}{\hbar}\int_{r_1}^{r^2} dr\left[2m\{V(r)-E\}\right]^{1/2} \tag{5.20}$$

We will use this expression in the discussion of α-decay.

22.101 Applied Nuclear Physics (Fall 2004)
Lecture 6 (9/27/04)

The Neutron-Proton System -- Bound State of the Deuteron

References –
W. E. Meyerhof, *Elements of Nuclear Physics* (McGraw-Hill, New York, 1967), App. A.
B. L. Cohen, *Concepts of Nuclear Physics* (McGraw-Hill, New. York, 1971), chap. 3.

"The investigation of this nuclear force has turned out to be a truly monumental task: Perhaps more man-hours of work have been devoted to it than any other scientific question in the history of mankind" – B. L. Cohen, *Concepts of Nuclear Physics*, p. 32.

A direct way to study nuclear forces is to consider the simplest possible nucleus, which is a two-nucleon system – the deuteron H^2 nucleus composed of a neturon and a proton. We will discuss two properties of this system using elementary quantum mechanics, the bound state of the nucleus (this lecture) and the scattering of a neutron by a proton (next lecture). The former problem is an application of our study of bound states in three-dimensions, while the latter is a new application of solving the time-independent Schrödinger wave equation. From these two problems a number of fundamental features of the nuclear potential will emerge.

Bound State of the Deuteron

The deuteron is the only stable bound system of two nucleons – neither the di-neutron nor the di-proton are stable. Experimentally it is known that the deuteron exists in a bound state of energy 2.23 Mev. This energy is the energy of a gamma ray given off in the reaction where a thermal neutron is absorbed by a hydrogen nucleus,

$$n + H^1 \rightarrow H^2 + \gamma \ \text{(2.23 Mev)}$$

The inverse reaction of using electrons of known energy to produce external *bremsstrahlung* for (γ, n) reaction on H^2 also has been studied. Besides the ground state

no stable excited states of H^2 have been found; however, there is a virtual state at ~ 2.30 Mev.

Suppose we combine the information on the bound-state energy of the deuteron with the bound-state solutions to the wave equation to see what we can learn about the potential well for neutron-proton interaction. Again we will assume the interaction between the two nucleons is of the form of a spherical well,

$$V(r) = -V_o \qquad r < r_o$$

$$= \ 0 \qquad r > r_o$$

We ask what is the energy level structure and what values should V_o and r_o take in order to be consistent with a bound state at energy E_B = 2.23 Mev.

There is good reason to believe that the deuteron ground state is primarily 1s (n=1, ℓ =0). First, the lowest energy state in practically all the model potentials is an s-state. Secondly, the magnetic moment of H^2 is approximately the sum of the proton and the neturon moments, indicating that $\underline{s}_n$ and $\underline{s}_p$ are parallel and no orbital motion of the proton relative to the neutron. This is also consistent with the total angular momentum of the ground state being I = 1.

We therefore proceed by considering only the ℓ = 0 radial wave equation,

$$-\frac{\hbar}{m}\frac{d^2u(r)}{dr^2} + V(r)u(r) = Eu(r) \qquad (6.1)$$

where E = - E_B, and m is the neutron (or proton) mass. In view of our previous discussions of bound-state calculations we can readily write down the interior and exterior solutions,

$$u(r) = A\sin Kr \qquad K = [m(V_o - E_B)]^{1/2}/\hbar \qquad r < r_o \qquad (6.2)$$

$$u(r) = Be^{-\kappa r} \qquad \kappa = \sqrt{mE_B}/\hbar \qquad r > r_o \qquad (6.3)$$

Applying the boundary condition at the interface, we obtain the relation between the potential well parameters, depth and width, and the bound-state energy E_B,

$$K \cot Kr_o = -\kappa, \quad \text{or} \quad \tan Kr_o = -\left(\frac{V_o - E_B}{E_B}\right)^{1/2} \qquad (6.4)$$

To go further we can consider either numerical or graphical solutions as discussed before, or approximations based on some special properties of the nuclear potential. Let us consider the latter option.

Suppose we take the potential well to be deep, that is, Vo >> E_B, then the RHS (right hand side) of (6.4) is large and we get an approximate value for the argument of the tangent,

$$Kr_o \sim \pi/2 \qquad (6.5)$$

Then,

$$K \sim \sqrt{mV_o}/\hbar \sim \pi/2r_o$$

or
$$V_o r_o^2 \sim \left(\frac{\pi}{2}\right)^2 \frac{\hbar^2}{m} \sim \text{ 1 Mev-barn} \qquad (6.6)$$

We see that a knowledge of E_B allows us to determine the product of $V_o r_o^2$, and not V_o and r_o separately. From a study of neutron scattering by a proton which we will discuss in the next chapter, we will find that $r_o \sim 2F$. Putting this into (6.6) we get $V_o \sim 36$ Mev, which justifies our taking V_o to be large compared to E_B. A sketch of the nuclear potential deduced from our calculation is shown in Fig. 1.

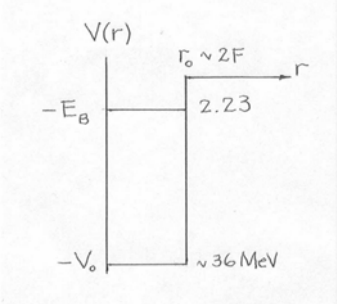

Fig. 1. The nuclear potential for the neutron-proton system in the form of a spherical well of depth V_o and width r_o. E_B is the bound-state energy of the deuteron.

We notice that since the interior wave function, sinKr, must match the exterior wave function, $\exp(-\kappa r)$, at the interface, the quantity Kr_o must be slightly greater than $\pi/2$ (a more accurate estimate gives 116^o instead of 90^o). If we write

$$K = 2\pi/\lambda \sim \pi/2r_o$$

then the 'effective wavelength' λ is approximately 4F, which suggests that much of the wave function is not in the interior region. The relaxation constant, or decay length, in the interior region can be estimated as

$$\frac{1}{\kappa} = \frac{\hbar}{\sqrt{mE_B}} \sim 4.3 \text{ F}$$

This means that the two nucleons in H^2 spend a large fraction of their time at $r > r_o$, the region of negative kinetic energy that is classically forbidden. We can calculate the root-mean-square radius of the deuteron wave function,

$$R_{rms}^2 = \frac{\int d^3 r r^2 R^2(r)}{\int d^3 r R^2(r)} = \frac{\int_0^\infty r^2 dr r^2 R^2(r)}{\int_0^\infty r^2 dr R^2(r)} \qquad (6.7)$$

If we take $R(r) \sim e^{-\kappa r}$ for all r (this should result in an overestimate), we would obtain

$$R_{rms}^2 = \frac{\hbar}{\sqrt{2mE_B}} = 3F$$

This value can be compared with the estimate of nuclear radius based on the mass number,

$$(\text{radius})^2 \sim (1.4 \text{x} A^{1/3})^2 \sim 3.1 \text{ F}, \quad \text{or} \quad (1.2 \text{x} A^{1/3})^2 \sim 2.3 \text{ F}$$

22.101 Applied Nuclear Physics (Fall 2004)
Lecture 7 (9/27/04)

Overview of Cross Section Calculation

References –
Appendix A: Concepts of Cross Sections
Appendix B: Cross Section Calculation: Method of Phase Shifts

---

The method of phase shifts has been discussed in Appendix B. Here we will summarize the key steps in this method, going from the introduction of the scattering amplitude $f(\theta)$ to the expression for the angular differential cross section $\sigma(\theta)$.

Expressing $\sigma(\theta)$ in terms of the Scattering Amplitude $f(\theta)$

We consider a scattering scenario sketched in Fig.B.1.

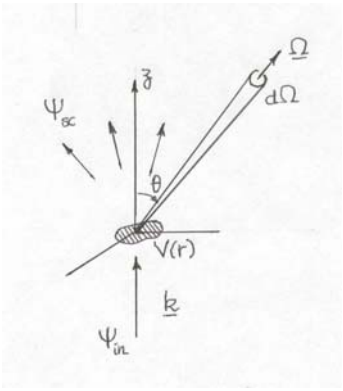

Fig.B.1. Scattering of an incoming plane wave by a potential field V(r), resulting in spherical outgoing wave. The scattered current crossing an element of surface area $d\Omega$ about the direction $\underline{\Omega}$ is used to define the angular differential cross section $d\sigma / d\Omega \equiv \sigma(\theta)$, where the scattering angle θ is the angle between the direction of incidence and direction of scattering.

We write the incident plane wave as

$$\Psi_{in} = be^{i(\underline{k}\cdot\underline{r}-\omega t)} \qquad \text{(B.1)}$$

where the wavenumber k is set by the energy of the incoming effective particle E, and the scattered spherical outgoing wave as

$$\Psi_{sc} = f(\theta) b \frac{e^{i(kr-\omega t)}}{r} \tag{B.2}$$

where $f(\theta)$ is the scattering amplitude. The angular differential cross section for scattering through $d\Omega$ about $\underline{\Omega}$ is

$$\sigma(\theta) = \frac{\underline{J}_{sc} \cdot \underline{\Omega}}{J_{in}} = \left| f(\theta) \right|^2 \tag{B.5}$$

where we have used the expression

$$\underline{J} = \frac{\hbar}{2\mu i}\left[\Psi^*(\underline{\nabla}\Psi) - \Psi(\underline{\nabla}\Psi^*) \right] \tag{B.3}$$

Calculating $f(\theta)$ from the *Schrödinger* wave equation

The *Schrödinger* equation to be solved is of the form

$$\left(-\frac{\hbar^2}{2\mu}\nabla^2 + V(r) \right)\psi(\underline{r}) = E\psi(\underline{r}) \tag{B.6}$$

where $\mu = m_1 m_2 / (m_1 + m_2)$ is the reduced mass, and $E = \mu v^2 / 2$, with v being the relative speed, is positive. To obtain a solution to our particular scattering set-up, we impose the boundary condition

$$\psi_k(\underline{r}) \rightarrow_{r>>r_o} e^{ikz} + f(\theta)\frac{e^{ikr}}{r} \tag{B.7}$$

where r_o is the range of force, V(r) = 0 for r > r_o. In the region beyond the force range the wave equation describes a free particle, so the free-particle solution to is what we want to match up with the RHS of (B.7). The most convenient form of the free-particle is an expansion in terms of partial waves,

$$\psi(r,\theta) = \sum_{\ell=0}^{\infty} R_\ell(r) P_\ell(\cos\theta) \tag{B.8}$$

where $P_\ell(\cos\theta)$ is the Legendre polynomial of order ℓ. Inserting (B.8) into (B.6), and setting $u_\ell(r) = rR_\ell(r)$, we obtain

$$\left(\frac{d^2}{dr^2} + k^2 - \frac{2\mu}{\hbar^2}V(r) - \frac{\ell(\ell+1)}{r^2}\right)u_\ell(r) = 0\,, \tag{B.10}$$

Eq.(B.10) describes the wave function everywhere. Its solution clearly depends on the form of V(r). Outside of the interaction region, r > r_o, Eq.(B.10) reduces to the radial wave equation for a free particle,

$$\left(\frac{d^2}{dr^2} + k^2 - \frac{\ell(\ell+1)}{r^2}\right)u_\ell(r) = 0 \tag{B.11}$$

with general solution

$$u_\ell(r) = B_\ell r j_\ell(kr) + C_\ell r n_\ell(kr) \tag{B.12}$$

where B_ℓ and C_ℓ are integration constants, and j_ℓ and n_ℓ are spherical Bessel and Neumann functions respectively (see Appendix B for their properties).

Introduction of the Phase Shift δ_ℓ

We rewrite the general solution (B.12) as

$$u_\ell(r) \to_{kr>>1} (B_\ell / k)\sin(kr - \ell\pi/2) - (C_\ell / k)\cos(kr - \ell\pi/2)$$

$$= (a_\ell / k)\sin[kr - (\ell\pi/2) + \delta_\ell] \qquad \text{(B.14)}$$

where we have replaced B and C by two other constants, a and δ, the latter is seen to be a *phase shift*. Combining (B.14) with (B.8) the partial-wave expansion of the free-particle wave function in the asymptotic region becomes

$$\psi(r,\theta) \to_{kr>>1} \sum_\ell a_\ell \frac{\sin[kr - (\ell\pi/2) + \delta_\ell]}{kr} P_\ell(\cos\theta) \qquad \text{(B.15)}$$

This is the LHS of (B.7). Now we prepare the RHS of (B.7) to have the same form of partial wave expansion by writing

$$f(\theta) = \sum_\ell f_\ell P_\ell(\cos\theta) \qquad \text{(B.16)}$$

and

$$e^{ikr\cos\theta} = \sum_\ell i^\ell (2\ell+1) j_\ell(kr) P_\ell(\cos\theta)$$

$$\to_{kr>>1} \sum_\ell i^\ell (2\ell+1) \frac{\sin(kr - \ell\pi/2)}{kr} P_\ell(\cos\theta) \qquad \text{(B.17)}$$

Inserting both (B.16) and (B.17) into the RHS of (B.7), we match the coefficients of exp(ikr) and exp(-ikr) to obtain

$$f_\ell = \frac{1}{2ik}(-i)^\ell [a_\ell e^{i\delta_\ell} - i^\ell (2\ell+1)] \qquad \text{(B.18)}$$

$$a_\ell = i^\ell (2\ell + 1) e^{i\delta_\ell} \tag{B.19}$$

Combing (B.18) and (B.16) we obtain

$$f(\theta) = (1/k) \sum_{\ell=0}^{\infty} (2\ell + 1) e^{i\delta_\ell} \sin\delta_\ell P_\ell(\cos\theta) \tag{B.20}$$

Final Expressions for $\sigma(\theta)$ and σ

In view of (B.20) (B.5), becomes

$$\sigma(\theta) = \lambda\!\!\!^{-2} \left| \sum_{\ell=0}^{\infty} (2\ell + 1) e^{i\delta_\ell} \sin\delta_\ell P_\ell(\cos\theta) \right|^2 \tag{B.21}$$

where $\lambda\!\!\!^{-} = 1/k$ is the reduced wavelength. Correspondingly,

$$\sigma = \int d\Omega \sigma(\theta) = 4\pi \lambda\!\!\!^{-2} \sum_{\ell=0}^{\infty} (2\ell + 1) \sin^2 \delta_\ell \tag{B.22}$$

S-wave scattering

We have seen that if kr_o is appreciably less than unity, then only the ℓ = 0 term contributes in (B.21) and (B.22). The differential and total cross sections for s-wave scattering are therefore

$$\sigma(\theta) = \lambda\!\!\!^{-2} \sin^2 \delta_o(k) \tag{B.23}$$

$$\sigma = 4\pi \lambda\!\!\!^{-2} \sin^2 \delta_o(k) \tag{B.24}$$

Notice that s-wave scattering is spherically symmetric, or $\sigma(\theta)$ is independent of the scattering angle. This is true in CMCS, but not in LCS. From (B.18) we see

$f_o = (e^{i\delta_o} \sin\delta_o)/k$. Since the cross section must be finite at low energies, as k $\to 0$ f_o has to remain finite, or $\delta_o(k) \to 0$. We can set

$$\lim_{k\to 0}[e^{i\delta_o(k)} \sin\delta_o(k)] = \delta_o(k) = -ak \tag{B.25}$$

where the constant *a* is called the scattering length. Thus for low-energy scattering, the differential and total cross sections depend only on knowing the scattering length of the target nucleus,

$$\sigma(\theta) = a^2 \tag{B.26}$$

$$\sigma = 4\pi a^2 \tag{B.27}$$

Physical significance of sign of scattering length

Fig. B.2 shows two sine waves, one is the reference wave $\sin kr$ which has not had

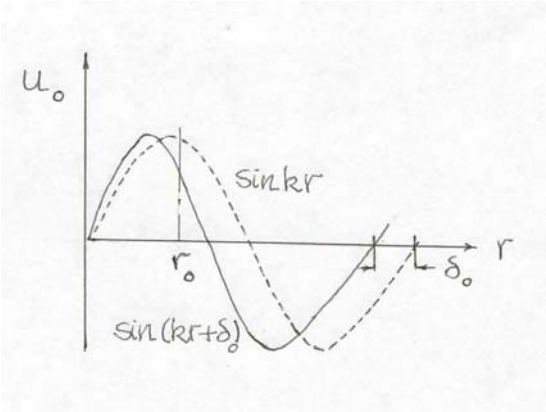

Fig. B.2. Comparison of unscattered and scattered waves showing a phase shift δ_o in the asymptotic region as a result of the scattering.

any interaction (unscattered) and the other one is the wave $\sin(kr + \delta_o)$ which has suffered a phase shift by virtue of the scattering. The entire effect of the scattering is seen to be represented by the phase shift δ_o , or equivalently the scattering length through (B.25). In the vicinity of the potential, we take kr_o to be small (this is again the condition of low-

energy scattering), so that $u_o \sim k(r-a)$, in which case *a becomes the distance at which the wave function extrapolates to zero* from its value and slope at $r = r_o$. There are two ways in which this extrapolation can take place, depending on the value of kr_o. As shown in Fig. B.3, when $kr_o > \pi/2$, the wave function has reached more than a quarter of its wavelength at $r = r_o$. So its slope is downward and the extrapolation gives a distance a which is positive. If on the other hand, $kr_o < \pi/2$, then the extrapolation gives a distance a which is negative. The significance is that $a > 0$ means the potential is such that it can have a bound state, whereas $a < 0$ means that the potential can only give rise to a virtual state.

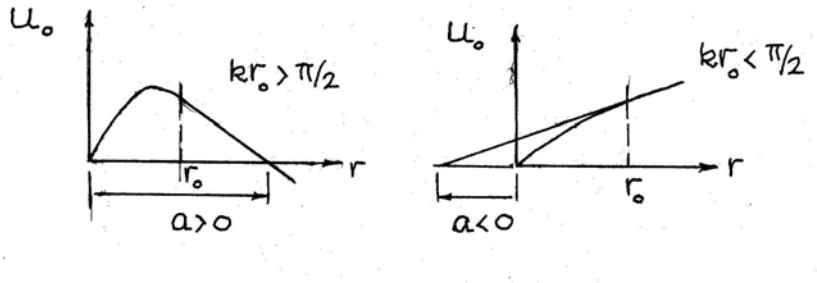

Fig. B.3. Geometric interpretation of positive and negative scattering lengths as the distance of extrapolation of the wave function at the interface between interior and exterior solutions, for potentials which can have a bound state and which can only virtual state respectively.

22.101 Applied Nuclear Physics (Fall 2004)

Lecture 8 (10/4/04)

Neutron-Proton Scattering

References:

M. A. Preston, *Physics of the Nucleus* (Addison-Wesley, Reading, 1962).

E. Segre, *Nuclei and Particles* (W. A. Benjamin, New York, 1965), Chap. X.

We continue the study of the neutron-proton system by taking up the well-known problem of neutron scattering in hydrogen. The scattering cross section has been carefully measured to be 20.4 barns over a wide energy range. Our intent is to apply the method of phase shifts summarized in the preceding lecture to this problem. We see very quickly that the s-wave approximation (the condition of interaction at low energy) is very well justified in the neutron energy range of 1 - 1000 eV. The scattering-state solution, with E > 0, gives us the phase shift or equivalently the scattering length. This calculation yields a cross section of 2.3 barns which is considerably different from the experimental value. The reason for the discrepancy lies in the fact that we have not taken into account the spin-dependent nature of the n-p interaction. The neutron and proton spins can form two distinct spin configurations, the two spins being parallel (triplet state) or anti-parallel (singlet), each giving rise to a scattering length. When this is taken into account, the new estimate is quite close to the experimental value. The conclusion is therefore that n-p interaction is spin-dependent and that the anomalously large value of the hydrogen scattering cross section for neutrons is really due to this aspect of the nuclear force.

For the scattering problem our task is to solve the radial wave equation for s-wave for solutions with E > 0. The interior and exterior solutions have the form

$$u(r) = B\sin(K'r) \ , \qquad r < r_o \tag{8.1}$$

and

$$u(r) = C\sin(kr + \delta_o) \ , \quad r > r_o \tag{8.2}$$

where $K' = \sqrt{m(V_o + E)}/\hbar$ and $k = \sqrt{mE}/\hbar$. Applying the interface condition we obtain

$$K'\cot(K'r_o) = k\cot(kr_o + \delta_o) \tag{8.3)}$$

which is the relation that allows the phase shift to be determined in terms of the potential parameters and the incoming energy E. We can simplify the task of estimating the phase shift by recalling that it is simply related to the scattering length by $\delta_o = -ak$ (cf. (B.25)). Assuming the scattering length a is larger than r_o, we see the RHS of (8.3) is approximately $k\cot(\delta_o)$. For the LHS, we will ignore E relative to V_o in K', and at the same time ignore E_B relative to V_o in K. Then K' ~ K and the LHS can be set equal to $-\kappa$ by virtue of (6.4). Notice that this series of approximations has enabled us to make use of the dispersion relation in the bound-state problem, (6.4), for the scattering calculation. As a result, (8.3) becomes

$$k\cot(\delta_o) = -\kappa \tag{8.4}$$

which is a relation between the phase shift and the binding energy.

Once the phase shift δ_o is known, the differential scattering cross section is then given by (B.23),

$$\sigma(\theta) = (1/k^2)\sin^2\delta_o \tag{8.5}$$

A simple way to make use of (8.4) is to note the trigonometric relation $\sin^2 x = 1/(1+\cot^2 x)$, or

$$\sin^2\delta_o = \frac{1}{1+\cot^2\delta_o} = \frac{1}{1+\kappa^2/k^2} \tag{8.6}$$

Thus,

$$\sigma(\theta) \approx \frac{1}{k^2 + \kappa^2} = \frac{\hbar^2}{m} \frac{1}{E + E_B} \approx \frac{\hbar^2}{m E_B} \tag{8.7}$$

The last step follows because we are mostly interested in estimating the scattering cross section in the energy range 1 - 100 eV. Putting in the numerical values of the constants, $\hbar = 1.055$ x 10^{-27} erg sec, m = 1.67 x 10^{-24} g, and and E_B = 2.23 x 10^6 x 1.6 x 10^{-12} ergs, we get

$$\sigma = 4\pi\hbar^2 / mE_B \sim 2.3 \text{ barns} \tag{8.8}$$

This value is considerably lower than the experimental value of the scattering cross section of H^1, 20.4 barns, as shown in Fig. 8.1.

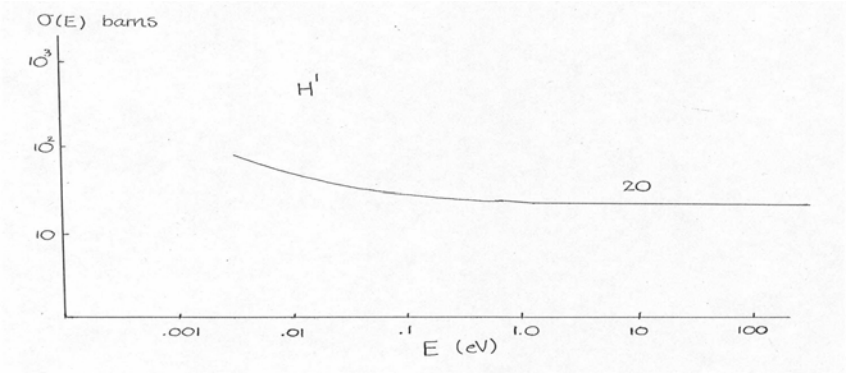

Fig. 8.1. Experimental neutron scattering cross section of hydrogen, showing a constant value of 20.4 barns over a wide range of neutron energy. The rise in the cross section at energies below ~ 0.1 eV can be explained in terms of chemical binding effects in the scattering sample.

The explanation of this well-known discrepancy lies in the neglect of spin-dependent effects. It was suggested by E. P. Wigner in 1933 that neutron-proton scattering should depend on whether the neutron and proton spins are oriented in a parallel configuration (the triplet state, total spin angular momentum equal to $\hbar$) or in an anti-parallel configuration (singlet state, total spin is zero). In each case the interaction

potential is different, and therefore the phase shifts also would be different. Following this idea, one can write instead of (8.7),

$$\sigma(\theta) = \frac{1}{k^2}\left(\frac{1}{4}\sin^2\delta_{os} + \frac{3}{4}\sin^2\delta_{ot}\right) \tag{8.9}$$

We have already mentioned that the ground state of the deuteron is a triplet state at E = -E_B. If the singlet state produces a virtual state of energy E = E*, then (8.8) would become

$$\sigma \approx \frac{\pi\hbar^2}{m}\left(\frac{3}{E_B} + \frac{1}{E^*}\right) \tag{8.10}$$

Taking a value of E* ~ 70 keV, we find from (8.10) a value of 20.4 barns, thus bringing the theory into agreement with experiment.

In summary, experimental measurements have given the following scattering lengths for the two types of n-p interactions, triplet and singlet configurations, and their corresponding potential range and well depth.

Interaction	Scattering length a [F]	r_o [F]	V_o [MeV}
n-p (triplet)	5.4	2	36
n-p (singlet)	-23.7	~ 2.5	18

Notice that the scattering length for the triplet state is positive, while that for the singlet state is negative. This illustrates the point of Fig. 7.3.

As a final remark, we note that experiments have shown that the total angular momentum (nuclear spin) of the deuteron ground state is I = 1, where $\underline{I} = \underline{L} + \underline{S}$, with $\underline{L}$ being the orbital angular momentum, and $\underline{S}$ the intrinsic spin, $\underline{S} = \underline{s}_n + \underline{s}_p$. It is also known that the ground state is mostly 1s (ℓ =0), therefore for this state we have S = 1

(neutron and proton spins are parallel). We have seen from Lec 6 that the deuteron ground state is barely bound at E_B = 2.23 Mev, so all the higher energy states are not bound. The 1s state with S = 0 (neutron and proton spins antiparallel), is a virtual state; it is unbound by ~ 60 Kev. An important implication is that nuclear interaction varies with S, or, *nuclear forces are spin-dependent*.

Effects of Pauli Exclusion Principle

One might ask why are the di-neutron and the di-proton unstable. The answer lies in the indistinguishability of particles and the Exclusion Principle (no two fermions can occupy the same state). Consider the two electrons in a helium atom. Their wave function may be written as

$$\psi(1,2) = \psi_1(\underline{r}_1)\psi(\underline{r}_2)$$

$$= A\frac{\sin k_1 r_1}{r_1}\frac{\sin k_2 r_2}{r_2} \qquad (8.11)$$

where $\psi_1(\underline{r})$ is the wave functrion of electron 1 at $\underline{r}$. But since we cannot distinguish between electrons 1 and 2, we must get the same probability of finding these electrons if we exchange their positions (or exchange the particles),

$$|\psi(1,2)|^2 = |\psi(2,1)|^2 \quad \Rightarrow \quad \psi(1,2) = \pm\psi(2,1)$$

For fermions (electrons, neutrons, protons) we must choose the (-) sign; because of Fermi-Dirac statistics the wave function must be anti-symmetric under exchange. Thus we should modify (8.11) and write

$$\psi(1,2) = \psi_1(\underline{r}_1)\psi_2(\underline{r}_2) \; - \; \psi_2(\underline{r}_1)\psi_1(\underline{r}_2) \; \equiv \; \psi_-$$

$$+ \qquad\qquad \psi_+$$

If we now include the spin, then an acceptable anti-symmetric wave function is

$$\Psi(1,2) = \psi_{-}\chi_1(\uparrow)\chi_2(\uparrow)$$

so that under an interchange of particles, $1 \leftrightarrow 2$, $\psi(1,2) = -\psi(2,1)$. This corresponds to S = 1, symmetric state in spin space. But another acceptable anti-symmetric wave function is

$$\Psi_{-}(1,2) = \psi_{+}[\chi_1(\uparrow)\chi_2(\downarrow) - \chi_1(\downarrow)\chi_2(\uparrow)]$$

which corresponds to S = 0, anti-symmetric state in spin.

For the symmetry of the wave function in configurational space we recall that we have

$$\psi(\underline{r}) \sim \frac{u_\ell(r)}{r} P_\ell^m(\cos\theta) e^{im\varphi}$$

which is even (odd) if ℓ is even (odd). Thus, since Ψ has to be anti-symmetric, one can have two possibilities,

ℓ even, S = 0 (space symmetric, spin anti-symmetric)

ℓ odd, S = 1 (space anti-symmetric, spin symmetric)

These are called T = 1 states (T is isobaric spin), available to the n-p, n-n, p-p systems. By contrast, states which are symmetric (T = 0) are

ℓ even, S = 1

ℓ odd, S = 0

These are available only to the n-p system for which there is no Pauli Exclusion Principle.

The ground state of the deuteron is therefore a T = 0 state. The lowest T = 1 state is ℓ = 0, S =0. As mentioned above, this is known to be unbound (E ~ 60 Kev). We should therefore expect that the lowest T = 1 state in n-n and p-p to be also unbound, i.e., there is no stable di-neutron or di-proton.

Essential Features of Nuclear Forces

In closing we summarize a number of important features of the nucleon-nucleon interaction potential, several of which are basic to the studies in this class [Meyerhof, Chap. 6].

1. There is a dominant short-range part, which is central and which provides the overall shell-model potential.
2. There is a part whose range is much smaller than the nuclear radius, which tends to make the nucleus spherical and to pair up nucleons.
3. There is a part whose range is of the order of the nuclear radius, which tends to distort the nucleus.
4. There is a spin-orbit interaction.
5. There is a spin-spin interaction.
6. The force is charge independent (Coulomb interaction excluded).
7. The force saturates.

22.101 Applied Nuclear Physics (Fall 2004)

Lecture 10 (10/18/04)

Nuclear Shell Model

References:

W. E. Meyerhof, *Elements of Nuclear Physics* (McGraw-Hill, New York, 1967), Chap.2.

P. Marmier and E. Sheldon, *Physics of Nuclei and Particles* (Academic Press, New York, 1969), vol. II, Chap.15.2.

Bernard L. Cohen, *Concepts of Nuclear Physics* (McGraw-Hill, New York, 1971).

There are similarities between the electronic structure of atoms and nuclear structure. Atomic electrons are arranged in orbits (energy states) subject to the laws of quantum mechanics. The distribution of electrons in these states follows the Pauli exclusion principle. Atomic electrons can be excited up to normally unoccupied states, or they can be removed completely from the atom. From such phenomena one can deduce the structure of atoms. In nuclei there are two groups of like particles, protons and neutrons. Each group is separately distributed over certain energy states subject also to the Pauli exclusion principle. Nuclei have excited states, and nucleons can be added to or removed from a nucleus.

Electrons and nucleons have intrinsic angular momenta called intrinsic spins. The total angular momentum of a system of interacting particles reflects the details of the forces between particles. For example, from the coupling of electron angular momentum in atoms we infer an interaction between the spin and the orbital motion of an electron in the field of the nucleus (the spin-orbit coupling). In nuclei there is also a coupling between the orbital motion of a nucleon and its intrinsic spin (but of different origin). In addition, nuclear forces between two nucleons depend strongly on the relative orientation of their spins.

The structure of nuclei is more complex than that of atoms. In an atom the nucleus provides a common center of attraction for all the electrons and inter-electronic forces generally play a small role. The predominant force (Coulomb) is well understood.

Nuclei, on the other hand, have no center of attraction; the nucleons are held together by their mutual interactions which are much more complicated than Coulomb interactions.

All atomic electrons are alike, whereas there are two kinds of nucleons. This allows a richer variety of structures. Notice that there are ~ 100 types of atoms, but more than 1000 different nuclides. Neither atomic nor nuclear structures can be understood without quantum mechanics.

Experimental Basis

There exists considerable experimental evidence pointing to the shell-like structure of nuclei, each nucleus being an assembly of nucleons. Each shell can be filled with a given number of nucleons of each kind. These numbers are called magic numbers; they are **2, 8, 20, 28, 50, 82, and 126**. (For the as yet undiscovered superheavy nuclei the magic numbers are expected to be N = 184, 196, (272), 318, and Z = 114, (126), 164 [Marmier and Sheldon, p. 1262].) Nuclei with magic number of neutrons or protons, or both, are found to be particularly stable, as can be seen from the following data.

(i) Fig. 9.1 shows the abundance of stable isotones (same N) is particularly large for nuclei with magic neutron numbers.

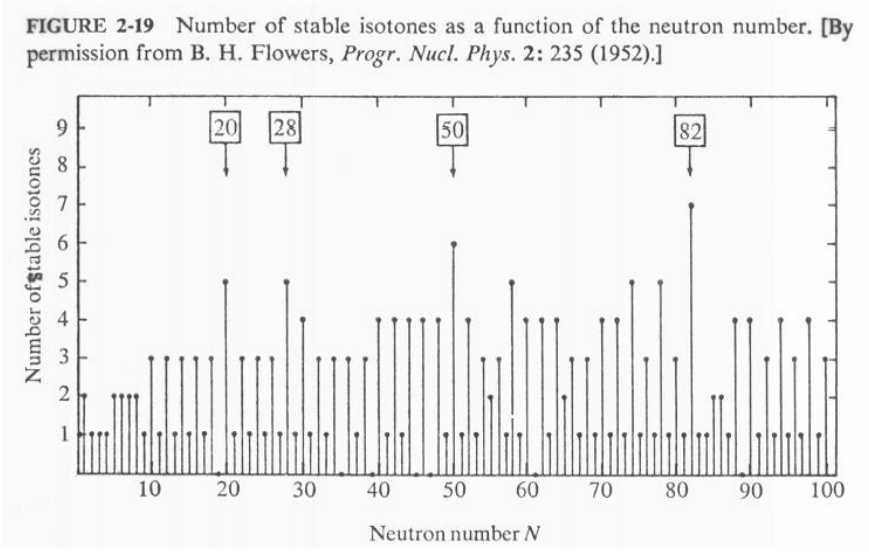

Fig. 9.1. Histogram of stable isotones showing nuclides with neutron numbers 20, 28, 50, and 82 are more abundant by 5 to 7 times than those with non-magic neutron numbers [from Meyerhof].

(ii) Fig. 9.2 shows that the neutron separation energy S_n is particularly low for nuclei with one more neutron than the magic numbers, where

$$S_n = [M(A-1,Z) + M_n - M(A,Z)]c^2 \qquad (9.1)$$

This means that nuclei with magic neutron numbers are more tightly bound.

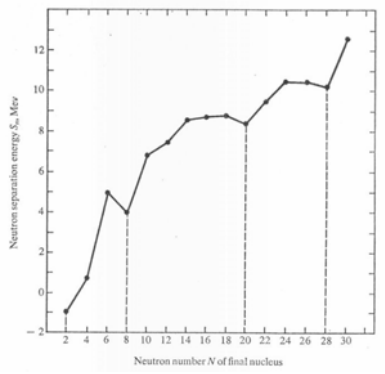

Fig. 9.2. Variation of neutron separation energy with neutron number of the final nucleus M(A,Z) [from Meyerhof].

(iii) The first excited states of even-even nuclei have higher than usual energies at the magic numbers, indicating that the magic nuclei are more tightly bound (see Fig. 9.3).

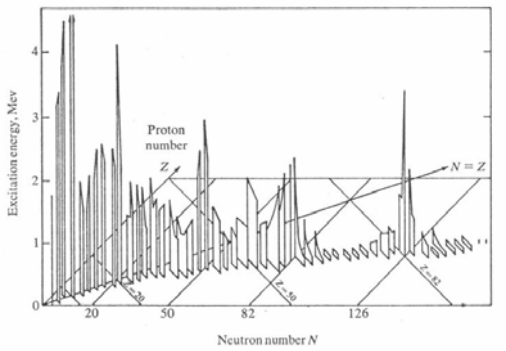

Fig. 9.3. First excited state energies of even-even nuclei [from Meyerhof].

(iv) The neutron capture cross sections for magic nuclei are small, indicating a wider spacing of the energy levels just beyond a closed shell, as shown in Fig. 9.4.

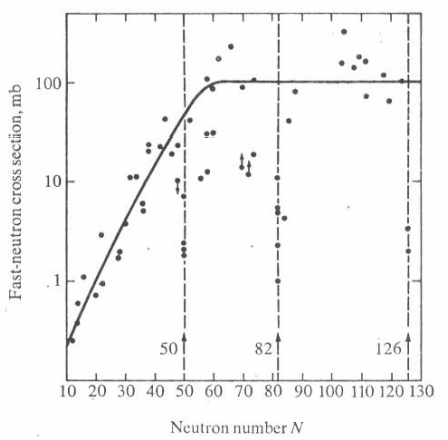

Fig. 9.4. Cross sections for capture at 1 Mev [from Meyerhof].

Simple Shell Model

The basic assumption of the shell model is that the effects of internuclear interactions can be represented by a single-particle potential. One might think that with very high density and strong forces, the nucleons would be colliding all the time and therefore cannot maintain a single-particle orbit. But, because of Pauli exclusion the nucleons are restricted to only a limited number of allowed orbits. A typical shell-model potential is

$$V(r) = -\frac{V_o}{1+\exp[(r-R)/a]} \qquad (9.1)$$

where typical values for the parameters are $V_o \sim 57$ Mev, $R \sim 1.25A^{1/3}$ F, a ~ 0.65 F. In addition one can consider corrections to the well depth arising from (i) symmetry energy from an unequal number of neutrons and protons, with a neutron being able to interact with a proton in more ways than n-n or p-p (therefore n-p force is stronger than n-n and p-p), and (ii) Coulomb repulsion. For a given spherically symmetric potential V(r), one

can examine the bound-state energy levels that can be calculated from radial wave equation for a particular orbital angular momentum ℓ,

$$-\frac{\hbar}{2m}\frac{d^2u_\ell}{dr^2}+\left[\frac{\ell(\ell+1)\hbar^2}{2mr^2}+V(r)\right]u_\ell(r)=Eu_\ell(r) \qquad (9.2)$$

Fig. 9.5 shows the energy levels of the nucleons for an infinite spherical well and a harmonic oscillator potential, $V(r)=m\omega^2r^2/2$. While no simple formulas can be given for the former, for the latter one has the expression

$$E_\nu=\hbar\omega(\nu+3/2)=\hbar\omega(n_x+n_y+n_z+3/2) \qquad (9.3)$$

where ν = 0, 1, 2, …, and n_x, n_y, n_z = 0, 1, 2, … are quantum numbers. One should notice the degeneracy in the oscillator energy levels. The quantum number ν can be divided into *radial* quantum number n (1, 2, …) and *orbital* quantum numbers ℓ (0, 1, …) as shown in Fig. 9.5. One can see from these results that a central force potential is able to account for the first three magic numbers, 2, 8, 20, but not the remaining four, 28, 50, 82, 126. This situation does not change when more rounded potential forms are used. The implication is that something very fundamental about the single-particle interaction picture is missing in the description.

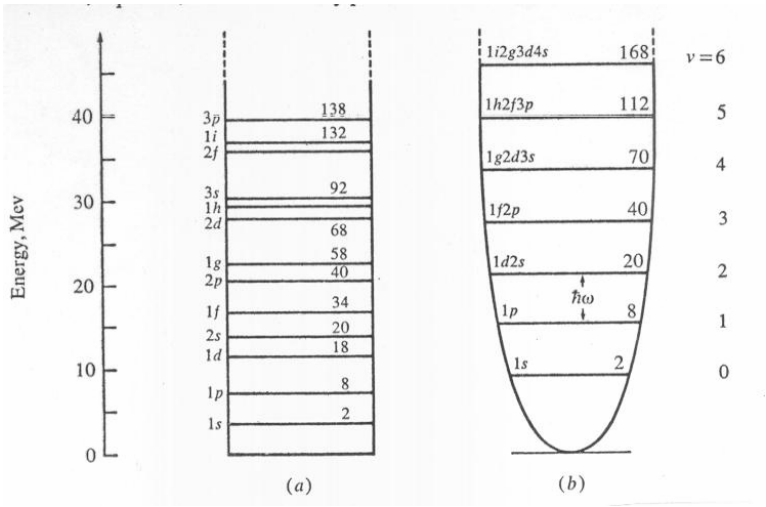

Fig. 9.5. Energy levels of nucleons in (a) infinite spherical well (range R = 8F) and (b) a parabolic potential well. In the spectroscopic notation (n, ℓ), n refers to the number of times the orbital angular momentum state ℓ has appeared. Also shown at certain levels are the cumulative number of nucleons that can be put into all the levels up to the indicated level [from Meyerhof].

Shell Model with Spin-Orbit Coupling

It remains for M. G. Mayer and independently Haxel, Jensen, and Suess to show (1949) that an essential missing piece is an attractive interaction between the orbital angular momentum and the intrinsic spin angular momentum of the nucleon. To take into account this interaction we add a term to the Hamiltonian H,

$$H = \frac{p^2}{2m} + V(r) + V_{so}(r)\underline{s}\cdot\underline{L} \qquad (9.4)$$

where V_{so} is another central potential (known to be attractive). This modification means that the interaction is no longer spherically symmetric; the Hamiltonian now depends on the relative orientation of the spin and orbital angular momenta. It is beyond the scope of this class to go into the bound-state calculations for this Hamiltonian. In order to understand the meaning of the results of such calculations (eigenvalues and eigenfunctions) we need to digress somewhat to discuss the addition of two angular momentum operators.

The presence of the spin-orbit coupling term in (9.4) means that we will have a different set of eigenfunctions and eigenvalues for the new description. What are these new quantities relative to the eigenfunctions and eigenvalues we had for the problem without the spin-orbit coupling interaction? We first observe that in labeling the energy levels in Fig. 9.5 we had already taken into account the fact that the nucleon has an orbital angular momentum (it is in a state with a specified ℓ), and that it has an intrinsic spin of ½ (in unit of $\hbar$). For this reason the number of nucleons that we can put into each level has been counted correctly. For example, in the 1s ground state one can put two

nucleons, for zero orbital angular momentum and two spin orientations (up and down). The student can verify that for a state of given ℓ, the number of nucleons that can go into that state is $2(2\ell+1)$. This comes about because the eigenfunctions we are using to describe the system is a representation that *diagonalizes* the orbital angular momentum operator L^2, its z-component, L_z, the intrinsic spin angular momentum operator S^2, and its z-component S_z. Let us use the following notation to label these eigenfunctions (or representation),

$$\left|\ell, m_\ell, s, m_s\right\rangle \equiv Y_\ell^{m_\ell}\chi_s^{m_s} \tag{9.5}$$

where $Y_\ell^{m_\ell}$ is the spherical harmonic we encountered in Lec4, and we know it is the eigenfunction of the orbital angular momentum operator L^2 (it is also the eigenfunction of L_z). The function $\chi_s^{m_s}$ is the spin eigenfunction with the expected properties,

$$S^2\chi_s^{m_s} = s(s+1)\hbar^2\chi_s^{m_s}, \qquad \text{s=1/2} \tag{9.6}$$

$$S_z\chi_s^{m_s} = m_s\hbar\chi_s^{m_s}, \qquad -s \le m_s \le s \tag{9.7}$$

The properties of $\chi_s^{m_s}$ with respect to operations by S^2 and S_z completely mirror the properties of $Y_\ell^{m_\ell}$ with respect to L^2 and L_z. Going back to our representation (9.5) we see that the eigenfunction is a "ket" with indices which are the good quantum numbers for the problem, namely, the orbital angular momentum and its projection (sometimes called the magnetic quantum number m, but here we use a subscript to denote that it goes with the orbital angular momentum), the spin (which has the fixed value of ½) and its projection (which can be +1/2 or -1/2).

The representation given in (9.5) is no longer a good representation when the spin-orbit coupling term is added to the Hamiltonian. It turns out that the good representation is just a linear combination of the old representation. It is sufficient for our purpose to just know this, without going into the details of how to construct the linear

combination. To understand the properties of the new representation we now discuss angular momentum addition.

The two angular momenta we want to add are obviously the orbital angular momentum operator $\underline{L}$ and the intrinsic spin angular momentum operator $\underline{S}$, since they are the only angular momentum operators in our problem. Why do we want to add them? The reason lies in (9.4). Notice that if we define the total angular momentum as

$$\underline{j} = \underline{S} + \underline{L} \tag{9.8}$$

we can then write

$$\underline{S} \cdot \underline{L} = (j^2 - S^2 - L^2)/2 \tag{9.9}$$

so the problem of diagonalizing (9.4) is the same as diagonalizing j^2, S^2, and L^2. This is then the basis for choosing our new representation. In analogy to (9.5) we will denote the new eigenfunctions by $\left| jm_j \ell s \right\rangle$, which has the properties

$$j^2 \left| jm_j \ell s \right\rangle = j(j+1)\hbar^2 \left| jm_j \ell s \right\rangle, \qquad |\ell - s| \le j \le \ell + s \tag{9.10}$$

$$j_z \left| jm_j \ell s \right\rangle = m_j \hbar \left| jm_j \ell s \right\rangle, \qquad -j \le m_j \le j \tag{9.11}$$

$$L^2 \left| jm_j \ell s \right\rangle = \ell(\ell+1)\hbar^2 \left| jm_j \ell s \right\rangle, \qquad \ell = 0, 1, 2, \ldots \tag{9.12}$$

$$S^2 \left| jm_j \ell s \right\rangle = s(s+1)\hbar^2 \left| jm_j \ell s \right\rangle, \qquad s = ½ \tag{9.13}$$

In (9.10) we indicate the values that j can take for given ℓ and s (=1/2 in our discussion), the lower (upper) limit corresponds to when $\underline{S}$ and $\underline{L}$ are antiparallel (parallel) as shown in the sketch.

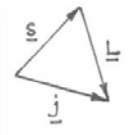

Returning now to the energy levels of the nucleons in the shell model with spin-orbit coupling we can understand the conventional spectroscopic notation where the value of j is shown as a subscript.

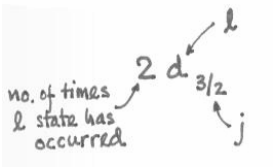

This is then the notation in which the shell-model energy levels are displayed in Fig. 9.6.

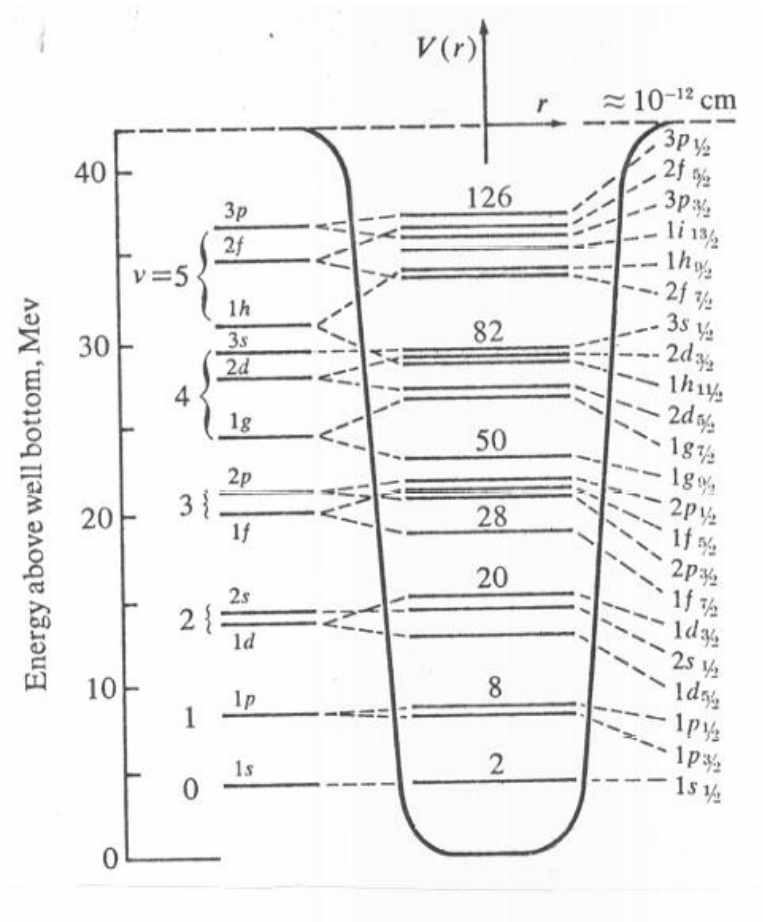

Fig. 9.6. Energy levels of nucleons in a smoothly varying potential well with a strong spin-orbit coupling term [from Meyerhof].

For a given (n, ℓ, j) level, the nucleon occupation number is 2j+1. It would appear that having 2j+1 identical nucleons occupying the same level would violate the Pauli exclusion principle. But this is not the case since each nucleon would have a distinct value of m_j (this is why there are 2j+1 values of m_j for a given j).

We see in Fig. 9.6 the shell model with spin-orbit coupling gives a set of energy levels having breaks at the seven magic numbers. This is considered a major triumph of the model, for which Mayer and Jensen were awarded the Noble prize in physics. For our purpose we will use the results of the shell model to predict the ground-state spin and parity of nuclei. Before going into this discussion we leave the student with the following comments.

1. The shell model is most useful when applied to closed-shell or near closed-shell nuclei.
2. Away from closed-shell nuclei collective models taking into account the rotation and vibration of the nucleus are more appropriate.
3. Simple versions of the shell model do not take into account pairing forces, the effects of which are to make two like-nucleons combine to give zero orbital angula momentum.
4. Shell model does not treat distortion effects (deformed nuclei) due to the attraction between one or more outer nucleons and the closed-shell core. When the nuclear core is not spherical, it can exhibit “rotational” spectrum.

Prediction of Ground-State Spin and Parity

There are three general rules for using the shell model to predict the total angular momentum (spin) and parity of a nucleus in the ground state. These do not always work, especially away from the major shell breaks.

1. Angular momentum of odd-A nuclei is determined by the angular momentum of the last nucleon in the species (neutron or proton) that is odd.
2. Even-even nuclei have zero ground-state spin, because the net angular momentum associated with even N and even Z is zero, and even parity.

3. In odd-odd nuclei the last neutron couples to the last proton with their intrinsic spins in parallel orientation.

To illustrate how these rules work, we consider an example for each case. Consider the odd-A nuclide Be^9 which has 4 protons and 5 neutrons. Since the last nucleon is the fifth neutron, we see in Fig. 9.6 that this nucleon goes into the state $1p_{3/2}$ (ℓ=1, j=3/2). Thus we would predict the spin and parity of this nuclide to be $3/2^-$. For an even-even nuclide we can take A^{36}, with 18 protons and neutrons, or Ca^{40}, with 20 protons and neutrons. For both cases we would predict spin and parity of 0^+. For an odd-odd nuclide we take Cl^{38}, which has 17 protons and 21 neutrons. In Fig. 9.6 we see that the 17^{th} proton goes into the state $1d_{3/2}$ (ℓ=2, j=3/2), while the 21^{st} neutron goes into the state $1f_{7/2}$ (ℓ=3, j=7/2). From the ℓ and j values we know that for the last proton the orbital and spin angular momenta are pointing in opposite direction (because j is equal to ℓ-1/2). For the last neutron the two momenta are point in the same direction (j = ℓ +1/2). Now the rule tells us that the two spin momenta are parallel, therefore the orbital angular momentum of proton is pointing in the opposite direction from the orbital angular momentum of the neutron, with the latter in the same direction as the two spins. Adding up the four angular momenta, we have +3+1/2+1/2-2 = 2. Thus the total angular momentum (nuclear spin) is 2. What about the parity? The parity of the nuclide is the product of the two parities, one for the last proton and the other for the last neutron. Recall that the parity of a state is determined by the orbital angular momentum quantum number ℓ, $\pi = (-1)^\ell$. So with proton in a state with ℓ = 2, its parity is even, while the neutron in a state with ℓ = 3 has odd parity. The parity of the nucleus is therefore odd. Our prediction for Cl^{38} is then 2^-. The student can verify, using for example the Nuclide Chart, the foregoing predictions are in agreement with experiment.

Potential Wells for Neutrons and Protons

We summarize the qualitative features of the potential wells for neutrons and protons. If we exclude the Coulomb interaction for the moment, then the well for a proton is known to be deeper than that for a neutron. The reason is that in a given nucleus

usually there are more neutrons than protons, especially for the heavy nuclei, and the n-p interactions can occur in more ways than either the n-n or p-p interactions on account of the Puali exclusion principle. The difference in well depth ΔV_s is called the symmetry energy; it is approximately given by

$$\Delta V_s = \pm 27 \frac{(N-Z)}{A} \text{ Mev} \qquad (9.14)$$

where the (+) and (-) signs are for protons and neutrons respectively. If we now consider the Coulomb repulsion between protons, its effect is to raise the potential for a proton. In other words, the Coulomb effect is a positive contribution to the nuclear potential which is larger at the center than at the surface.

Combining the symmetry and the Coulomb effects we have a sketch of the potential for a neutron and a proton as indicated in Fig. 9.7. One can also estimate the

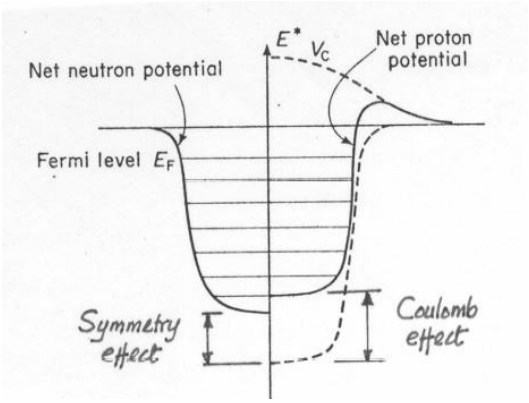

Fig. 9.7. Schematic showing the effects of symmetry and Coulomb interactions on the potential for a neutron and a proton [from Marmier and Sheldon].

Well depth in each case using the Fermi Gas model. One assumes the nucleons of a fixed kind behave like a fully degeneragte gas of fermions (degeneracy here means that the states are filled continuously starting from the lowest energy state and there are no unoccupied states below the occupied ones), so that the number of states occupied is equal to the number of nucleons in the particular nucleus. This calculation is carried out

separately for neutrons and protons. The highest energy state that is occupied is called the *Fermi level*, and the magnitude of the difference between this state and the ground state is called the *Fermi energy* E_F. It turns out that E_F is proportional to $n^{2/3}$, where n is the number of nucleons of a given kind, therefore E_F (neutron) > E_F (proton). The sum of E_F and the separation energy of the last nucleon provides an estimate of the well depth. (The separation energy for a neutron or proton is about 8 Mev for many nuclei.) Based on these considerations one obtains the results shown in Fig. 9.8.

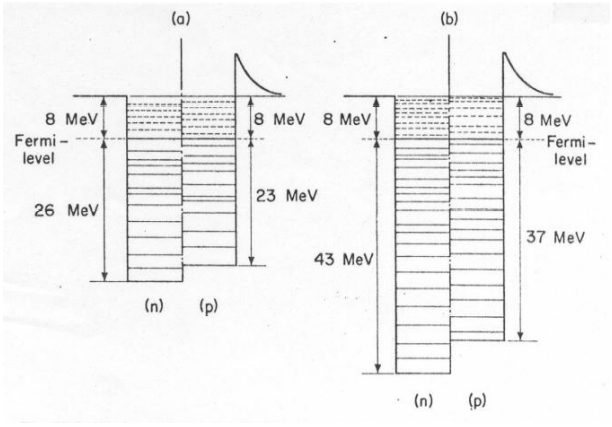

Fig. 9.8. Nuclear potential wells for neutrons and protons according to the Fermi-gas model, assuming the mean binding energy per nucleon to be 8 Mev, the mean relative nucleon admixture to be N/A ~ 1/1.8m Z/A ~ 1/2.2, and a range of 1.4 F (a) and 1.1 F (b) [from Marmier and Sheldon].

We have so far considered only a spherically symmetric nuclear potential well. We know there is in addition a centrifugal contribution of the form $\ell(\ell+1)\hbar^2/2mr^2$ and a spin-orbit contribution. As a result of the former the well becomes narrower and shallower for the higher orbital angular momentum states. Since the spin-orbit coupling is attractive, its effect depends on whether $\underline{S}$ is parallel or anti-parallel to $\underline{L}$. The effects are illustrated in Figs. 9.9 and 9.10. Notice that for ℓ = 0 both are absent.

We conclude this chapter with the remark that in addition to the bound states in the nuclear potential well there exist also virtual states (levels) which are not positive energy states in which the wave function is large within the potential well. This can

happen if the deBroglie wavelength is such that approximately standing waves are formed within the well. (Correspondingly, the reflection coefficient at the edge of the potential is large.) A virtual level is therefore not a bound state; on the other hand, there is a non-negligible probability that inside the nucleus a nucleon can be found in such a state. See Fig. 9.11.

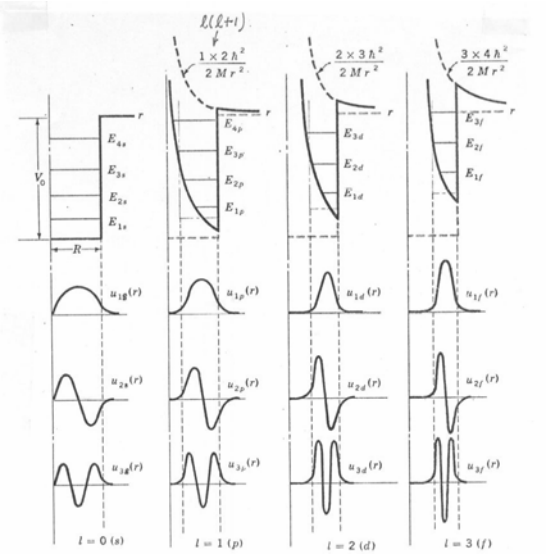

Fig. 9.9. Energy levels and wave functions for a square well for ℓ = 0, 1, 2, and 3 [from Cohen]..

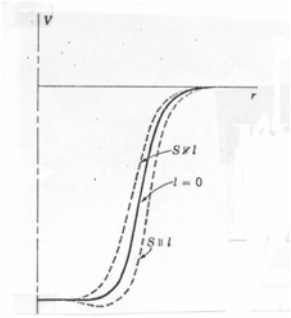

Fig. 9.10. The effect of spin-orbit interaction on the shell-model potential [from Cohen].

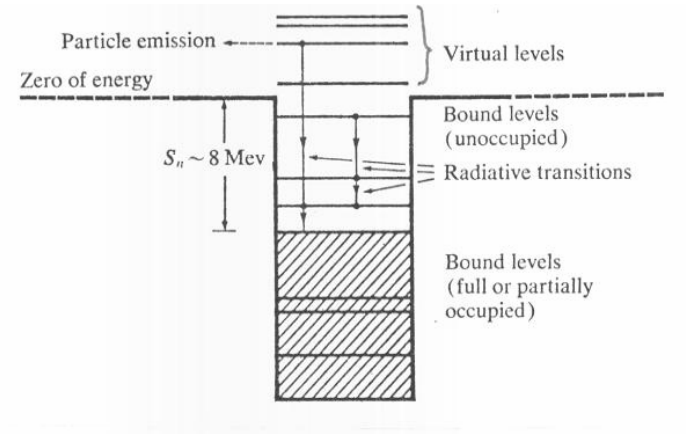

Fig. 9.11. Schematic representation of nuclear levels [from Meyerhof].

22.101 Applied Nuclear Physics (Fall 2004)

Lecture 11 (10/20/04)

Nuclear Binding Energy and Stability

References:

W. E. Meyerhof, *Elements of Nuclear Physics* (McGraw-Hill, New York, 1967), Chap.2.

The stability of nuclei is of great interest because unstable nuclei undergo transitions that result in the emission of particles and/or electromagnetic radiation (gammas). If the transition is spontaneous, it is called a radioactive decay. If the transition is induced by the bombardment of particles or radiation, then it is called a nuclear reaction.

The mass of a nucleus is the decisive factor governing its stability. Knowing the mass of a particular nucleus and those of the neighboring nuclei, one can tell whether or not the nucleus is stable. Yet the relation between mass and stability is complicated. Increasing the mass of a stable nucleus by adding a nucleon can make the resulting nucleus unstable, but this is not always true. Starting with the simplest nucleus, the proton, we can add one neutron after another. This would generate the series,

$$H + n \rightarrow H^2(stable) + n \rightarrow H^3(unstable) \xrightarrow{\beta^-} He^3(stable) + n \rightarrow He^4(stable)$$

Because He^4 is a double-magic nucleus, it is particularly stable. If we continue to add a nucleon we find the resulting nucleus is unstable,

$$He^4 + n \rightarrow He^5 \rightarrow He^4, \text{ with } t_{1/2} \sim 3 \times 10^{-21} \text{ s}$$

$$He^4 + H \rightarrow Li^5 \rightarrow He^4, \text{ with } t_{1/2} \sim 10^{-22} \text{ s}$$

One may ask: With He^4 so stable how is it possible to build up the heavier elements starting with neutrons and protons? (This question arises in the study of the origin of

elements. See, for example, the Nobel lecture of A. Penzias in *Reviews of Modern Physics*, **51**, 425 (1979).) The answer is that the following reactions can occur

$$He^4 + He^4 \rightarrow Be^8$$

$$He^4 + Be^8 \rightarrow C^{12}(stable)$$

Although Be^8 is unstable, its lifetime of ~ 3 x 10^{-16} s is apparently long enough to enable the next reaction to proceed. Once C^{12} is formed, it can react with another He^4 to give O^{16}, and in this way the heavy elements can be formed.

Instead of the mass of a nucleus one can use the binding energy to express the same information. The binding energy concept is useful for discussing the calculation of nuclear masses and of energy released or absorbed in nuclear reactions.

Binding Energy and Separation Energy

We define the binding energy of a nucleus with mass M(A,Z) as

$$B(A,Z) \equiv [ZM_H + NM_n - M(A,Z)]c^2 \qquad (10.1)$$

where M_H is the hydrogen mass and M(A,Z) is the atomic mass. Strictly speaking one should subtract out the binding energy of the electrons; however, the error in not doing so is quite small, so we will just ignore it. According to (10.1) the nuclear binding energy B(A,Z) is the difference between the mass of the constituent nucleons, when they are far separated from each other, and the mass of the nucleus, when they are brought together to form the nucleus. Therefore, one can interpret B(A,Z) as the *work required* to separate the nucleus into the individual nucleons (far separated from each other), or equivalently, as the *energy released* during the assembly of the nucleus from the constituents.

Taking the actual data on nuclear mass for various A and Z, one can calculate B(A,Z) and plot the results in the form shown in Fig. 10.1.

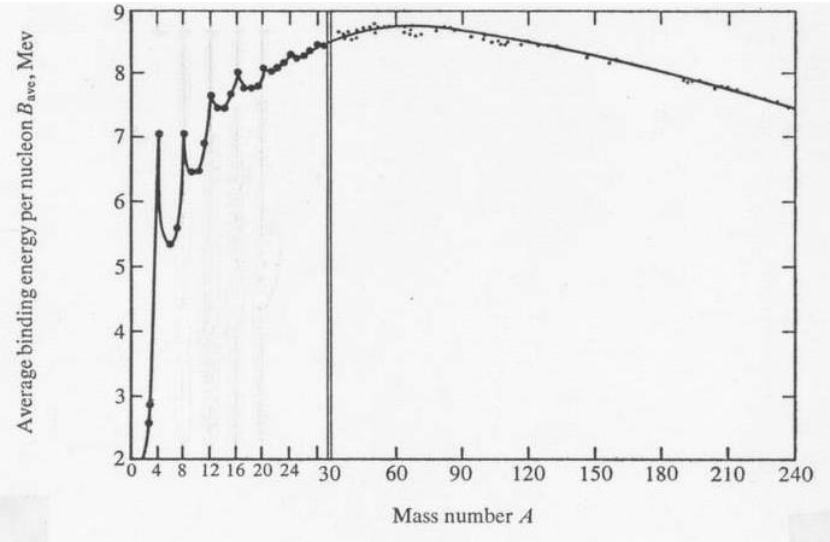

Fig. 10.1. Variation of average binding energy per nucleon with mass number for naturally occurring nuclides (and Be8). Note scale change at A = 30. [from Meyerhof]

The most striking feature of the B/A curve is the approximate constancy at ~ 8 Mev per nucleon, except for the very light nuclei. It is instructive to see what this behavior implies. If the binding energy of a pair of nucleons is a constant, say C, then for a nucleus with A nucleons, in which there are A(A-1)/2 distinct pairs of nucleons, the B/A would be ~ C(A-1)/2. Since this is not what one sees in Fig. 10.1, one can surmise that a given nucleon is not bound equally to all the other nucleons; in other words, nuclear forces, being short-ranged, extend over only a few neighbors. The constancy of B/A implies a saturation effect in nuclear forces, the interaction energy of a nucleon does not increase any further once it has acquired a certain number of neighbors. This number seems to be about 4 or 5.

One can understand the initial rapid increase of B/A for the very light nuclei as the result of the competition between volume effects, which make B increase with A like A, and surface effects, which make B decrease (in the sense of a correction) with A like $A^{2/3}$. The latter should be less important as A becomes large, hence B/A increases (see the discussion of the semi-empiricial mass formula in the next chapter). At the other end of the curve, the gradual decrease of B/A for A > 100 can be understood as the effect of

Coulomb repulsion which becomes more important as the number of protons in the nucleus increases.

As a quick application of the B/A curve we make a rough estimate of the energies release in fission and fusion reactions. Suppose we have symmetric fission of a nucleus with A ~ 240 producing two fragments, each A/2. The reaction gives a final state with B/A of about 8.5 Mev, which is about 1 Mev greater than the B/A of the initial state. Thus the energy released per fission reaction is about 240 Mev. (A more accurate estimate gives 200 Mev.) For fusion reaction we take $H^2 + H^2 \rightarrow He^4$. The B/A values of H^2 and He^4 are 1.1 and 7.1 Mev/nucleon respectively. The gain in B/A is 6 Mev/nucleon, so the energy released per fusion event is ~ 24 Mev.

Binding Energy in Nuclear Reactions

The binding energy concept is also applicable to a binary reaction where the initial state consists of a particle i incident upon a target nucleus I and the final state consists of an outgoing particle f and a residual nucleus F, as indicated in the sketch,

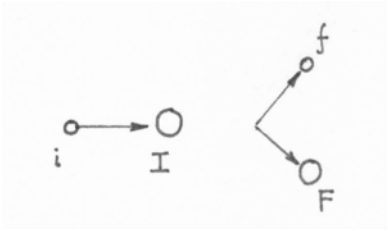

We write the reaction in the form

$$i + I \rightarrow f + F + Q \qquad (10.2)$$

where Q is an energy called the 'Q-value of the reaction'. Corresponding to (10.2) we have the definition

$$Q \equiv [(M_i + M_I) - (M_f + M_F)]c^2 \qquad (10.3)$$

where the masses are understood to be atomic masses. Every nuclear reaction has a characteristic Q-value; the reaction is called exothermic (endothermic) for Q > 0 (<0) where energy is given off (absorbed). Thus an endothermic reaction cannot take place unless additional energy, called the threshold, is supplied. Often the source of this energy is the kinetic energy of the incident particle. One can also express Q in terms of the kinetic energies of the reactants and products of the reaction by invoking the conservation of *total* energy, which must hold for any reaction,

$$T_i + M_i c^2 + T_I + M_I c^2 \rightarrow T_f + M_f c^2 + T_F + M_F c^2 \qquad (10.4)$$

Combining this with (10.3) gives

$$Q = T_f + T_F - (T_i + T_I) \qquad (10.5)$$

Usually T_I is negligible compared to T_i because the target nucleus follows a Maxwellian distribution at the temperature of the target sample (typically room temperature), while for nuclear reactions the incident particle would have a kinetic energy in the Mev range. Since the rest masses can be expressed in terms of binding energies, another expression for Q is

$$Q = B(f) + B(F) - B(i) - B(I) \qquad (10.6)$$

As an example, the nuclear medicine technique called boron neutron capture therapy (BNCT) is based on the reaction

$$_5B^{10} + n \rightarrow _3Li^7 + He^4 + Q \qquad (10.7)$$

In the case, Q = B(Li)+B(α)-B(B) = 39.245+28.296-64.750 = 2.791 Mev. The reaction is exothermic, therefore it can be induced by a thermal neturon. In practice, the simplest way of calculating Q values is to use the rest masses of the reactants and products. For

many reactions of interest Q values are in the range 1 – 5 Mev. An important exception is fission, where Q ~ 170 – 210 Mev depending on what one considers to be the fission products. Notice that if one defines Q in terms of the kinetic energies, as in (10.5), it may appear that the value of Q would depend on whether one is in laboratory or center-of-mass coordinate system. This is illusory because the equivalent definition, (10.3), is clearly frame independent.

Separation Energy

Recall the definition of binding energy, (10.1), involves an initial state where all the nucleons are removed far from each other. One can define another binding energy where the initial state is one where only one nucleon is separated off. The energy required to separate particle *a* from a nucleus is called the separation energy S_a. This is also the energy released, or energy available for reaction, when particle *a* is captured. This concept is usually applied to a neutron, proton, deuteron, or α -particle. The energy balance in general is

$$S_a = [M_a(A', Z') + M(A - A', Z - Z') - M(A, Z)]c^2 \qquad (10.8)$$

where particle *a* is treated as a 'nucleus' with atomic number Z' and mass number A'. For a neutron,

$$S_n = [M_n + M(A-1, Z) - M(A, Z)]c^2$$

$$= \text{B(A,Z)} - \text{B (A-1, Z)} \qquad (10.9)$$

S_n is sometimes called the binding energy of the *last neutron*.

Clearly S_n will vary from one nucleus to another. In the range of A where B/A is roughly constant we can estimate from the B/A curve that $S_n \sim S_p \sim 8$ Mev. This is a rough figure, for the heavy nuclei S_n is more like 5 – 6 Mev. It turns out that when a nucleus M(A-1,Z) absorbs a neutron, there is ~ 1 Mev (or more, can be up to 4 Mev) difference between the neutron absorbed being an even neutron or an odd neutron (see

Fig. 10.2). This difference is the reason that U^{235} can undergo fission with thermal neutrons, whereas U^{238} can fission only with fast neutrons (E > 1 Mev).

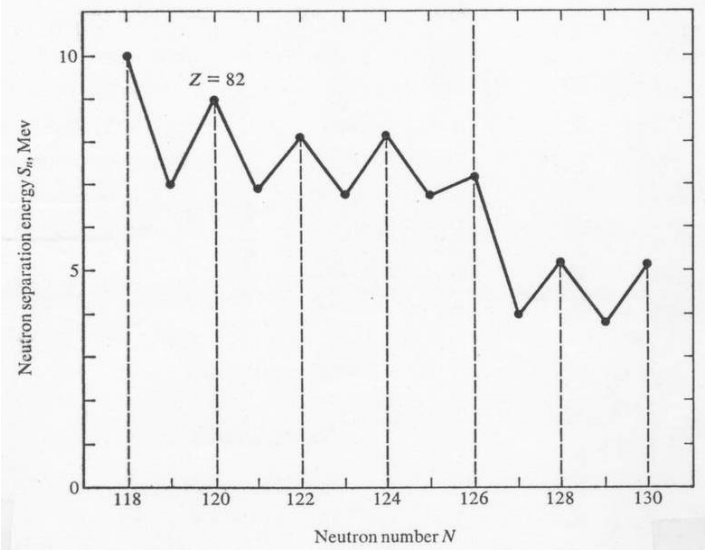

Fig. 10.2. Variation of the neutron separation energies of lead isotopes with neutron number of the absorbing nucleus. [from Meyerhof]

Generally speaking the following systematic behavior is observed in neutron and proton separation energies,

S_n(even N) > S_n(odd N) for a given Z

S_p(even Z) > S_p(odd Z) for a given N

This effect is attributed to the pairing property of nuclear forces – the existence of extra binding between pair of identical nucleons in the same state which have total angular momenta pointing in opposite directions. This is also the reason for the exceptional stability of the α-particle. Because of pairing the even-even (even Z, even N) nuclei are more stable than the even-odd and odd-even nuclei, which in turn are more stable then the odd-odd nuclei.

Abundance Systemtics of Stable Nuclides

One can construct a stability chart by plotting the neutron number N versus the atomic number Z of all the stable nuclides. The results, shown in Fig. 10.3, show that N ~ Z for low A, but N > Z at high A.

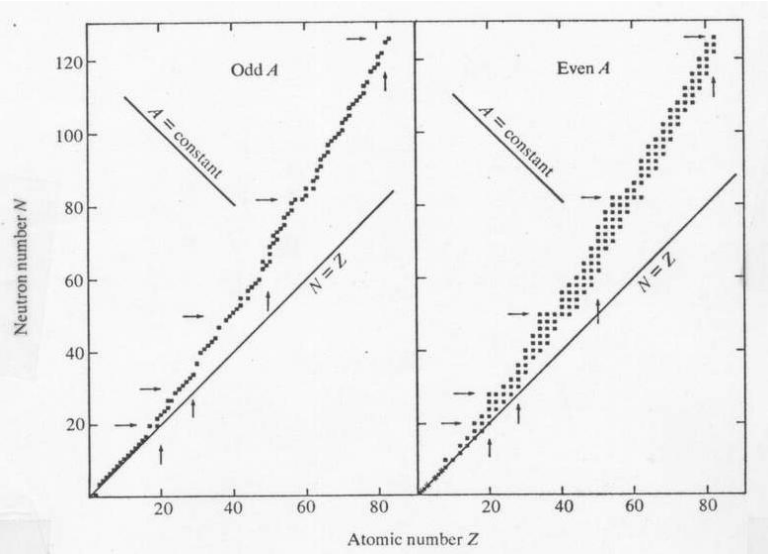

Fig. 10.3. Neutron and proton numbers of stable nuclides which are odd (left) and even isobars (right). Arrows indicate the magic numbers of 20, 28, 50, 82, and 126. Also shown are odd-odd isobars with A = 2, 6, 10, and 14. [from Meyerhof]

Again, one can readily understand that in heavy nuclei the Coulomb repulsion will favor a neutron-proton distribution with more neutrons than protons. It is a little more involved to explain why there should be an equal distribution for the light nuclides (see the following discussion on the semi-empirical mass formula). We will simply note that to have more neutrons than protons means that the nucleus has to be in a higher energy state, and is therefore less stable. This symmetry effect is most pronounced at low A and becomes less important at high A. In connection with Fig. 10.3 we note:

(i) In the case of odd A, only one stable isobar exists, except A = 113, 123.

(ii) In the case of even A, only even-even nuclides exist, except A = 2, 6, 10, 14.

Still another way to summarize the trend of stable nuclides is shown in the following table [from Meyerhof]

Table 2-2. SYSTEMATICS OF STABILITY TRENDS IN NUCLEI

A	*Z*	*N*	Type	Alternative designation	Number of stable + long-lived nuclides	Degree of stability	Usual number of stable isotopes per element
Even	Even	Even	e-e	Even mass, even *N*	166 + 11 = 177	Very pronounced	Several (2 and 3)
Odd	Even	Odd	e-o	Odd mass, odd *N*	55 + 3 = 58	Fair	1
Odd	Odd	Even	o-e	Odd mass, even *N*	51 + 3 = 54	Fair	1
Even	Odd	Odd	o-o	Even mass, odd *N*	6 + 4 = 10	Low	0
					278 + 21 = 299		

22.101 Applied Nuclear Physics (Fall 2004)

Lecture 12 (10/25/04)

Empirical Binding Energy Formula and Mass Parabolas

References:

W. E. Meyerhof, *Elements of Nuclear Physics* (McGraw-Hill, New York, 1967), Chap. 2.

P. Marmier and E. Sheldon, *Physics of Nuclei and Particles* (Academic Press, New York, 1969), Vol. I, Chap. 2.

R. D. Evan, *The Atomic Nucleus* (McGraw-Hill, New York, 1955).

The binding energy curve we have discussed in the last chapter is an overall representation of how the stability of nuclides varies across the entire range of mass number A. The curve shown in Fig. 10.1 was based on experimental data on atomic masses. One way to analyze this curve is to decompose the binding energy into various contributions from the interactions among the nucleons. An empirical formula for the binding energy consisting of contributions representing volume, surface, Coulomb and other effects was first proposed by von Weizsäcker in 1935. Such a formula is useful because it not only allows one to calculate the mass of a nucleus, thereby eliminating the need for table of mass data, but also it leads to qualitative understanding of the essential features of nuclear binding. More detailed theories exist, for example Bruecker et al., Physical Review **121**, 255 (1961), but they are beyond the scope of our study.

The empirical mass formula we consider here was derived on the basis of the liquid crop model of the nucleus. The essential assumptions are:

1. The nucleus is composed of incompressible matter, thus $R \sim A^{1/3}$.
2. The nuclear force is the same among neutrons and protons (excluding Coulomb interactions).
3. The nuclear force saturates (meaning it is very short ranged).

The empirical mass formula is usually given in terms of the binding energy,

$$B(A,Z) = a_v A - a_s A^{2/3} - a_c \frac{Z(Z-1)}{A^{1/3}} - a_a \frac{(N-Z)^2}{A} + \delta \qquad (11.1)$$

where the coefficients *a* are to be determined (by fitting the mass data), with subscripts v, s, c, and a referring to volume, surface, Coulomb, and asymmetry respectively. The last term in (11.1) represents the pairing effects,

$\delta = a_p / \sqrt{A}$ even-even nuclei

$= 0$ even-odd, odd-even nuclei

$= -a_p / \sqrt{A}$ odd-odd nuclei

where coefficient a_p is also a fitting parameter. A set of values for the five coefficients in (11.1) is:

a_v	a_s	a_c	a_a	a_p	
16	18	0.72	23.5	11	Mev

Since the fitting to experimental data is not perfect one can find several slightly different coefficients in the literature. The average accuracy of (11.1) is about 2 Mev except where strong shell effects are present. One can add a term, ~ 1 to 2 Mev, to (11.1) to represent the shell effects, extra binding for nuclei with closed shells of neutrons or protons.

A simple way to interpret (11.1) is to regard the first term as a first approximation to the binding energy. That is to say, the binding energy is proportional to the volume of the nucleus or the mass number A. This assumes every nucleon is like every other nucleon. Of course this is an oversimplification, and the remaining terms can be regarded as corrections to this first approximation. That is why the terms representing surface, Coulomb and asymmetry come in with negative signs, each one subtracting from the

volume effect. It is quite understandable that the surface term should vary with $A^{2/3}$, or R^2. The Coulomb term is also quite self-evident considering that Z(Z-1)/2 is the number of pairs that one can form from Z protons, and the $1/A^{1/3}$ factor comes from the 1/R. The asummetry term in (11.1) is less obvious, so we digress to derive it.

What we would like to estimate is the energy difference between an actual nucleus where N > Z and an ideal nucleus where N = Z = A/2. This is then the energy to transform a symmetric nucleus, in the sense of N = Z, to an asymmetric one, N > Z. For fixed N and Z, the number of protons that we need to transform into neutrons is ν, with N=(A/2) + ν and Z = (A/2) - ν. Thus, ν = (N – Z)/2. Now consider a set of energy levels for the neutrons and another set for the protons, each one filled to a certain level. To transform ν protons into neutrons the protons in question have to go into unoccupied energy levels above the last neutron. What this means is that the amount of energy involved is ν (the number of nucleons that have to be transformed) times $\nu\Delta$ (energy change for each nucleon to be transformed) = $\nu^2\Delta = (N-Z)^2\Delta/4$, where Δ is the spacing between energy levels (assumed to be the same for all the levels) . To estimate Δ, we note that $\Delta \sim E_F/A$, where E_F is the Fermi energy (see Figs. 9.7 and 9.8) which is known to be independent of A. Thus $\Delta \sim 1/A$, and we have the expression for the asymmetry term in (11.1).

The magnitudes of the various contributions to the binding energy curve are depicted in Fig. 11.1. The initial rise of B/A with A is seen to be due to the decreasing importance of the surface contribution as A increases. The Coulomb repulsion effect grows in importance with A, causing a maximum in B/A at A ~ 60, and a subsequent decrease of B/A at larger A. Except for the extreme ends of the mass number range the semi-empirical mass formula generally can give binding energies accurate to within 1%

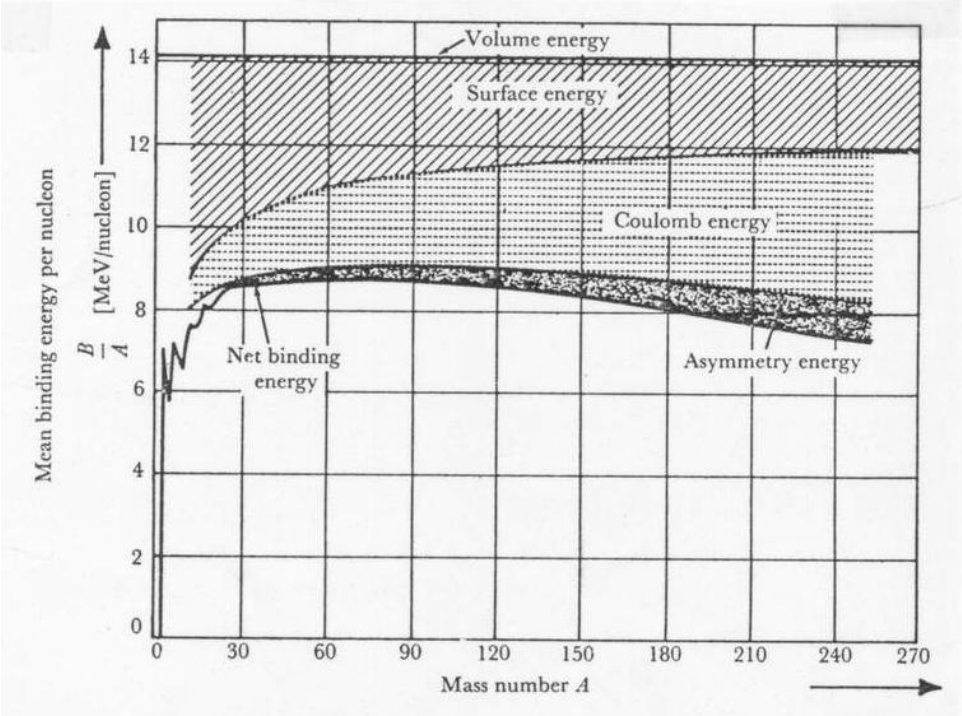

Fig. 11.1. Relative contributions to the binding energy per nucleon showing the importance of the various terms in the semi-empirical Weizsäcker formula. [from Evans]

of the experimental values [Evans, p. 382]. This means that atomic masses can be calculated correctly to roughly 1 part in 10^4. However, there are conspicuous discrepancies in the neighborhood of magic nuclei. Attempts have been made to take into account the nuclear shell effects by generalizing the mass formula. In addition to what we have already mentioned, one can consider another term representing nuclear deformation [see Marmier and Sheldon, pp. 39, for references].

One can use the mass formula to determine the constant r_o in the expression for the nuclear radius, $R = r_o A^{1/3}$. The radius appears in the coefficients a_v and a_s. In this way one obtains $r_o = 1.24 \times 10^{-13}$ cm.

Mass Parabolas and Stability Line

The mass formula can be rearranged to give the mass M(A,Z),

$$M(A,Z)c^2 \cong A\left[M_n c^2 - a_v + a_a + a_s / A^{1/3}\right] + xZ + yZ^2 - \delta \qquad (11.2)$$

where

$$x = -4a_a - \left(M_n - M_H\right)c^2 \cong -4a_a \tag{11.3}$$

$$y = \frac{4a_a}{A} + \frac{a_c}{A^{1/3}} \tag{11.4}$$

Notice that (11.2) is not exact rearrangement of (11.1), certain small terms having been neglected. What is important of about (11.2) is that it shows that with A held constant the variation of M(A,Z) with Z is given by a parabola, as sketch below. The minimum of

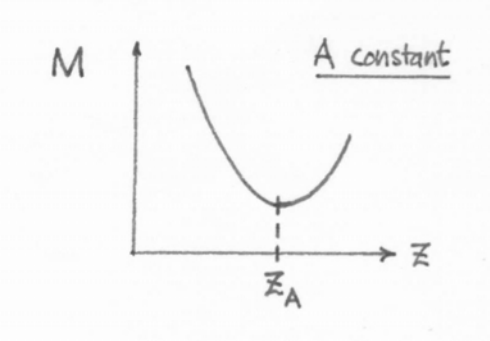

this parabola occurs at an atomic number, which we label as Z_A, of the stable nucleus for the given A. This therefore represents a way of determining the stable nuclides.

We can analyze (11.2) further by considering $\partial M / \partial Z\big|_{Z_A} = 0$. This gives

$$Z_A = -x/2y \approx \frac{A/2}{1 + \frac{1}{4}\left(\frac{a_c}{a_a}\right)A^{2/3}} \tag{11.5}$$

Notice that if we had considered only the volume, surface and Coulomb terms in B(A,Z), then we would have found instead of (11.5) the expression

$$Z_A \approx \frac{(M_n - M_H)c^2 A^{1/3}}{2a_c} \sim 0.9A^{1/3} \qquad (11.6)$$

This is a very different result because for a stable nucleus with $Z_A = 20$ the corresponding mass number given by (11.6) would be ~ 9,000, which is clearly unrealistic. Fitting (11.5) to the experimental data gives $a_c / 4a_a = 0.0078$, or $a_a \sim 20 - 23$ Mev. We see therefore the deviation of the stability line from N = Z = A/2 is the result of Coulomb effects, which favor $Z_A < A/2$, becoming relatively more important than the asymmetry effects, which favor $Z_A = A/2$.

We can ask what happens when a nuclide is unstable because it is proton-rich. The answer is that a nucleus with too many protons for stability can emit a positron (positive electron e^+ or β^+) and thus convert a proton into a neutron. In this process a neutrino (ν) is also emitted. An example of a positron decay is

$$_9F^{16} \rightarrow _8O^{16} + \beta^+ + \nu \qquad (11.7)$$

By the same token if a nucleus has too many neutrons, then it can emit an electron (e^- or β^-) and an antineutrino $\bar{\nu}$, converting a neutron into a proton. An electron decay for the isobar A = 16 is

$$_7N^{16} \rightarrow _8O^{16} + \beta^- + \bar{\nu} \qquad (11.8)$$

A competing process with positron decay is electron capture (EC). In this process an inner shell atomic electron is captured by the nucleus so the nuclear charge is reduced from Z to Z – 1. (Note: Orbital electrons can spend a fraction of their time inside the nucleus.) The atom as a whole would remain neutral but it is left in an excited state because a vacancy has been created in one of its inner shells.

As far as atomic mass balance is concerned, the requirement for each process to be energetically allowed is:

$$M(A, Z+1) > M(A,Z) + 2\, m_e \qquad \beta^+ \text{- decay} \qquad (11.9)$$

$$M(A,Z) > M(A, Z+1) \qquad \beta^- \text{ - decay} \qquad (11.10)$$

$$M(A, Z+1) > M(A,Z) \qquad \text{EC} \qquad (11.11)$$

where M(A,Z) is atomic mass. Notice that EC is a less stringent condition for the nucleus to decrease its atomic number. If the energy difference between initial and final states is less than twice the electron rest mass (1.02 Mev), the transition can take place via EC whereas it would be energetically forbidden via positron decay. The reason for the appearance of the electron rest mass in (11.9) may be explained by looking at an energy balance in terms of nuclear mass M'(A,Z), which is related to the atomic mass by M(A,Z) = Zm_e + M'(A,Z) if we ignore the binding energy of the electrons in the atom. For β^+ - decay the energy balance is

$$M'(A,Z) = M'(A,Z-1) + m_e + \nu \qquad (11.12)$$

which we can rewrite as

$$Zm_e + M'(A,Z) = (Z-1)m_e + M'(A,Z-1) + 2m_e + \nu \qquad (11.13)$$

The LHS is just M(A,Z) while the RHS is at least M(A,Z-1) + 2me with the neutrino having a variable energy. Thus one obtains (11.9). Another way to look at this condition is that is that in addition to the positron emitted the daughter nuclide also has to eject an electron (from an outer shell) in order to preserve charge neutrality.

Having discussed how a nucleus can change its atomic number Z while preserving its mass number A, we can predict what transitions will occaur as an unstable nuclide moves along the mass parabola toward the point of stability. Since the pairing term δ vanishes for odd-A isobars, one has single mass parabola in this case in contrast to two mass parabolas for the even-A isobars. One might then expect that when A is odd there

can be only one stable isobar. This is generally true with two exceptions, at A = 113 and 123. In these two cases the discrepancies arise from small mass differences which cause one of the isobars in each case to have exceptionally long half life. In the case of even A there can be stable even-even isobars (three is the largest number found). Since the odd-odd isobars lie on the upper mass parabola, oue would expect there should be no stable odd-odd nuclides. Yet there are several exceptions, H^2, Li^6, B^{10} and N^{14}. One explanation is that there are rrapid variations of the binding energy for the very light nuclides due to nuclear structure effects that are not taken into account in the sem-empirical mass formula. For certain odd-odd nuclides both conditions for β^+ and β^- decays are satisfied, and indeed both decays do occur in the same nucleus. Examples of odd- and even-A mass parabolas are shown in Fig. 11.2.

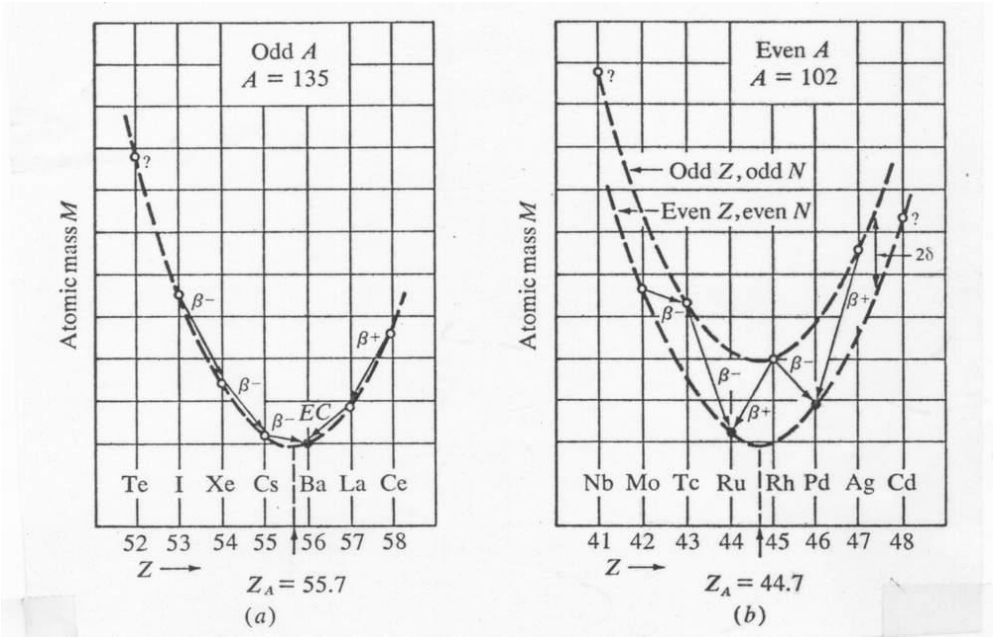

Fig. 11.2. Mass parabolas for odd and even isobars. Stable and radioactive nuclides are denoted by closed and open circles respectively. [from Meyerhof]

22.101 Applied Nuclear Physics (Fall 2004)

Lecture 13 (10/27/04)

Radioactive-Series Decay

References:

R. D. Evan, *The Atomic Nucleus* (McGraw-Hill, New York, 1955).

W. E. Meyerhof, *Elements of Nuclear Physics* (McGraw-Hill, New York, 1967).

We begin with an experimental observation that in radioactive decay that the probability of a decay during a small time interval Δt, which we will denote as P(Δt), is proportional to Δt. Given this as a fact one can write

$$P(\Delta t) = \lambda \Delta t \qquad (12.1)$$

where λ is the proportionality constant which we will call the *decay constant.* Notice that this expression is meaningful only when $\lambda \Delta t < 1$, a condition which defines what we mean by a small time interval. In other words, $\Delta t < 1/\lambda$, which will turn out to be the mean life time of the radioisotope.

Suppose we are interested in the survival probability S(t), the probability that the radioisotope does not decay during an arbitrary time interval t. To calculate S(t) using (12.1) we can take the time interval t and divide it into equal small segments, each one of magnitude Δt. For a given t the number of such segments will be $t / \Delta t = n$. To survive the entire time interval t, we need to first survive the first segment $(\Delta t)_1$, then the next segment $(\Delta t)_2$, …, all the way up to the nth segment $(\Delta t)_n$. Thus we can write

$$S(t) = \prod_{i=1}^{n} \left[1 - P((\Delta t)_i)\right]$$

$$= \left[1 - \lambda(t/n)\right]^n \rightarrow e^{-\lambda t} \qquad (12.2)$$

where the arrow indicated the limit of $n \to \infty$, $\Delta t \to 0$. Unlike (12.1) (12.2) is valid for any t, and when λt is sufficiently small compared to unity, it reduces to (12.1) as expected. Stated another way, (12.2) is extension of 1 – P(t) for arbitrary t. One should also notice a close similarity between (12.2) and the probability that a particle will go a distance x without collision, $e^{-\Sigma x}$, where Σ is the macroscopic collision cross section (recall Lec1). The role of the decay constant λ in the probability of no decay in a time t is the same as the macroscopic cross section Σ in the probability of no collision in a distance x. The exponential attenuation in time or space is quite a general result (one encounters it frequently). There is another way to derive it. Suppose the radioisotope has not decayed up to a time interval of t1, for it to survive the next small segment Δt the probability is just 1 - P(Δt) = 1 - λ Δt. Then we have

$$S(t_1 + \Delta t) = S(t_1)\left[1 - \lambda \Delta t\right] \tag{12.3}$$

which we can rearrange to read

$$\frac{S(t + \Delta t) - S(t)}{\Delta t} = -\lambda S(t) \tag{12.4}$$

Taking the limit of small Δt, we get

$$\frac{dS(t)}{dt} = -\lambda \tag{12.5}$$

which we can readily integrate to give (12.2), since the initial condition in this case is S(t=0) = 1.

The decay of a single radioisotope is described by S(t) which depends on a single physical constant λ. Instead of λ one can speak of two equivalent quantities, the half life $t_{1/2}$ and the mean life τ. They are defined as

$$S(t_{1/2}) = 1/2 \quad \to \quad t_{1/2} = \ell n 2 / \lambda = 0.693 / \lambda \tag{12.6}$$

and $$\tau = \frac{\int_0^\infty dt' t' S(t')}{\int_0^\infty dt' S(t')} = \frac{1}{\lambda} \qquad (12.7)$$

Fig. 12.1 shows the relationship between these quantities and S(t).

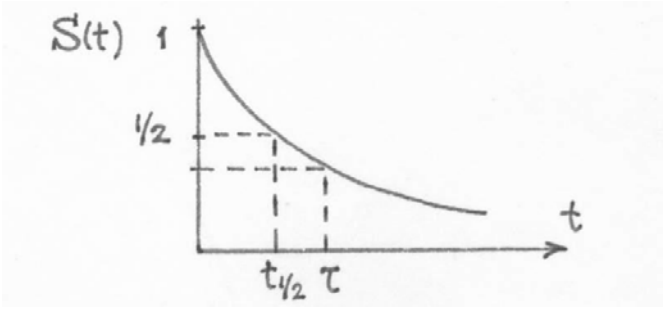

Fig. 12.1. The half life and mean life of a survival probability S(t).

Radioactivity is measured in terms of the rate of radioactive decay. The quantity λ N(t), where N is the number of radioisotope atoms at time t, is called *activity*. A standard unit of radioactivity has been the *curie*, 1 Ci = 3.7 x 10^{10} disintegrations/sec, which is roughly the activity of 1 gram of Ra^{226}. Now it is replaced by the *becquerel* (Bq), 1 Bq = 2.7 x 10^{-11} Ci. An old unit which is not often used is the *rutherford* (10^6 disintegrations/sec).

Radioisotope Production by Bombardment

There are two general ways of producing radioisotopes, activation by particle or radiation bombardment such as in a nuclear reactor or an accelerator, and the decay of a radioactive series. Both methods can be discussed in terms of a differential equation that governs the number of radioisotopes at time N(t). This is a first-order linear differential equation with constant coefficients, to which the solution can be readily obtained. Although there are different situations to which one can apply this equation, the analysis

is fundamentally quite straightforward. We will treat the activation problem first. Let Q(t), the rate of production of the radioisotope, have the form shown in the sketch below.

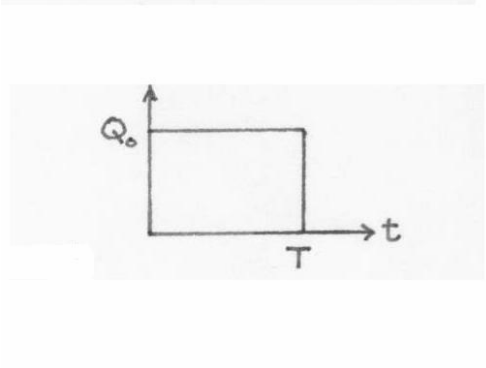

This means the production takes place at a constant Q_o for a time interval (0, T), after which production ceases. During production, t < T, the equation governing N(t) is

$$\frac{dN(t)}{dt} = Q_o - \lambda N(t) \tag{12.8}$$

Because we have an external source term, the equation is seen to be inhomogeneous. The solution to (12.8) with the initial condition that there is no radioisotope prior to production, N(t = 0) = 0, is

$$N(t) = \frac{Q_o}{\lambda}\left(1 - e^{-\lambda t}\right), \quad t < T \tag{12.9}$$

For t > T, the governing equation is (12.8) without the source term. The solution is

$$N(t) = \frac{Q_o}{\lambda}(1 - e^{-\lambda T})e^{-\lambda(t-T)} \tag{12.10}$$

A sketch of the solutions (12.9) and (12.10) is shown in Fig. 12.2. One sees a build up of N(t) during production which approaches the asymptotic value of Q_o / λ, and after production is stopped N(t) undergoes an exponential decay, so that if $\lambda T >> 1$,

$$N(t) \approx \frac{Q_o}{\lambda} e^{-\lambda(t-T)} \tag{12.11}$$

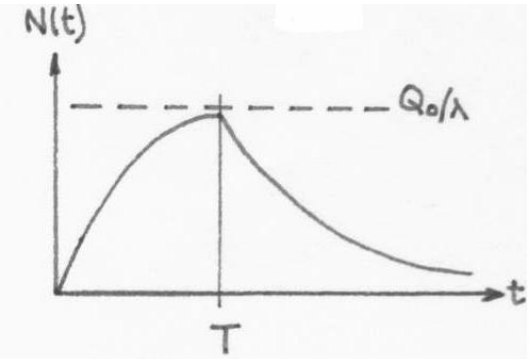

Fig. 12.2. Time variation of number of radioisotope atoms produced at a constant rate Qo for a time interval of T after which the system is left to decay.

Radioisotope Production in Series Decay

Radioisotopes also are produced as the product(s) of a series of sequential decays. Consider the case of a three-member chain,

$$N_1 \xrightarrow{\lambda_1} N_2 \xrightarrow{\lambda_2} N_3 \text{ (stable)}$$

where λ_1 and λ_2 are the decay constants of the parent (N_1) and the daughter (N_2) respectively. The governing equations are

$$\frac{dN_1(t)}{dt} = -\lambda_1 N_1(t) \tag{12.12}$$

$$\frac{dN_2(t)}{dt} = \lambda_1 N_1(t) - \lambda_2 N_2(t) \tag{12.13}$$

$$\frac{dN_3(t)}{dt} = \lambda_2 N_2(t) \tag{12.14}$$

For the initial conditions we assume there are N_{10} nuclides of spcies 1 and no nuclides of species 2 and 3. The solutions to (12.12) – (12.14) then become

$$N_1(t) = N_{10} e^{-\lambda_1 t} \tag{12.15}$$

$$N_2(t) = N_{10} \frac{\lambda_1}{\lambda_2 - \lambda_1} \left(e^{-\lambda_1 t} - e^{-\lambda_2 t} \right) \tag{12.16}$$

$$N_3(t) = N_{10} \frac{\lambda_1 \lambda_2}{\lambda_2 - \lambda_1} \left(\frac{1 - e^{-\lambda_1 t}}{\lambda_1} - \frac{1 - e^{-\lambda_2 t}}{\lambda_2} \right) \tag{12.17}$$

Eqs.(12.15) through (12.17) are known as the Bateman equations. One can use them to analyze situations when the decay constants λ_1 and λ_2 take on different relative values. We consider two such scenarios, the case where the parent is short-lived, $\lambda_1 >> \lambda_2$, and the opposite case where the parent is long- lived, $\lambda_2 >> \lambda_1$.

One should notice from (12.12) – (12.14) that the sum of these three differential equations is zero. This means that $N_1(t) + N_2(t) + N_3(t)$ = constant for any t. We also know from our initial conditions that this constant must be N_{10}. One can use this information to find $N_3(t)$ given $N_1(t)$ and $N_2(t)$, or use this as a check that the solutions given by (12.15) – (12.17) are indeed correct.

Series Decay with Short-Lived Parent

In this case one expects the parent to decay quickly which means the daughter will build up quickly. The daughter then decays more slowly which means that the grand daughter will build up slowly, eventually approaching the initial number of the parent. Fig. 12.3 shows schematically the behavior of the three isotopes. The initial values of N2(t) and N3(t) can be readily deduced from an examination of (12.16) and (12.17).

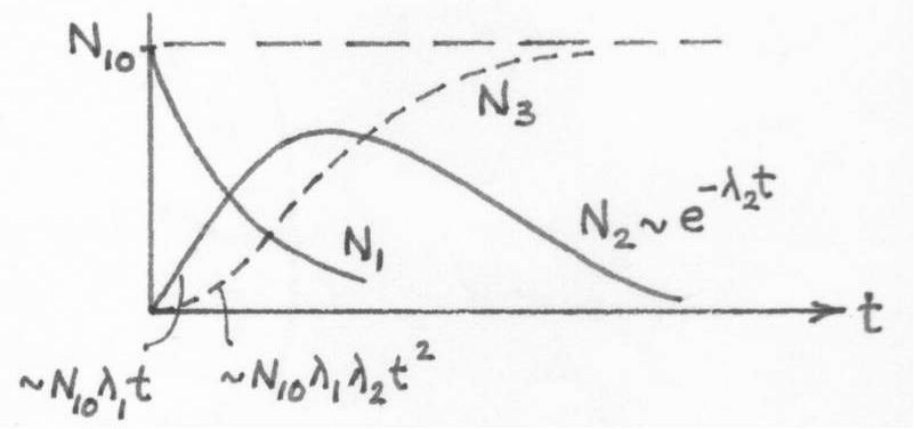

Fig. 12.3. Time variation of a three-member decay chain for the case $\lambda_1 >> \lambda_2$.

Series Decay with Long-Lived Parent

When $\lambda_1 << \lambda_2$, we expect the parent to decay slowly so that the daughter and grand daughter build up slowly. Since the daughter decays quickly the long-time behavior of the daughter follows that of the parent. Fig. 12.4 shows the general behavior

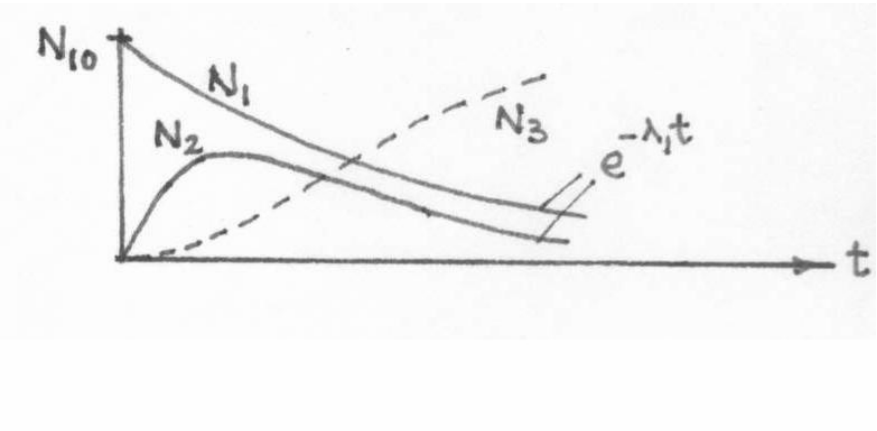

Fig. 12.4. Time variation of a three-member chain with a long-lived parent.

(admittedly the N_2 behavior is not sketched accurately). In this case we find

$$N_2(t) \approx N_{10} \frac{\lambda_1}{\lambda_2} e^{-\lambda t} \qquad (12.18)$$

or $$\lambda_2 N_2(t) \approx \lambda_1 N_1(t) \qquad (12.19)$$

The condition of approximately equal activities is called secular equilibrium. Generalizing this to arbitrary chain, we can say for the series

$$N_1 \rightarrow N_2 \rightarrow N_3 \rightarrow ...$$

if $$\lambda_2 >> \lambda_1,\ \lambda_3 >> \lambda_1, \ldots$$

then $$\lambda_1 N_1 \approx \lambda_2 N_2 \approx \lambda_3 N_3 \approx ... \qquad (12.20)$$

This condition can be used to estimate the half life of a very long-lived radioisotope. An example is U^{238} whose half life is so long that it is difficult to determine by directly measuring its decay. However, it is known that $U^{238} \rightarrow Th^{234} \rightarrow \ldots \rightarrow Ra^{226} \rightarrow \ldots$, and in uranium mineral the ratio of $N(U^{238})/N(Ra^{226}) = 2.8 \times 10^6$ has been measured, with $t_{1/2}(Ra^{226}) = 1620$ yr. Using these data we can write

$$\frac{N(U^{238})}{t_{1/2}(U^{238})} = \frac{N(Ra^{226})}{t_{1/2}(Ra^{226})} \quad \text{or} \quad t_{1/2}(U^{238}) = 2.8 \times 10^6 \times 1620 = 4.5 \times 10^9 \text{ yr.}$$

In so doing we assume that all the intermediate decay constants are larger than that of U^{238}. It turns out that this is indeed true, and that the above estimate is a good result. For an extensive treatment of radioactive series decay, the student should consult Evans.

22.101 Applied Nuclear Physics (Fall 2004)

Lecture 14 (11/1/04)

Charged-Particle Interactions: Stopping Power, Collisions and Ionization

---

References:

R. D. Evan, *The Atomic Nucleus* (McGraw-Hill, New York, 1955), Chaps 18-22.

W. E. Meyerhof, *Elements of Nuclear Physics* (McGraw-Hill, New York, 1967).

When a swift charged particle enters a materials medium it will interact with the electrons and nuclei in the medium and begins to lose energy as it penetrates into the medium. The interaction can be generally thought of as *collisions* between the charged particle and either the atomic electron or the nucleus (considered separately). The energy given off will result in *ionization*, production of ion-electron pairs, in the medium; also it can appear in the form of *electromagnetic radiation*, a process known as *bremsstrahlung* (braking radiation). We are interested in describing the energy loss per unit distance traveled by the charged particle, and the range of the particle in various materials, the latter being defined as the distance traveled from the point of entry to the point of being essentially rest.

A charged particleis called 'heavy' if its rest mass is large compared to the rest mass of the electron. Thus mesons, protons, α -particles, and of course fission fragments are all heavy charged particles. By the same token, electrons and positrons are 'light' particles.

If we ignore nuclear forces and consider only the interactions arising from Coulomb forces, then we can speak of four principal types of charged-particle interactions:

(i) Inelastic Collision with Atomic Electrons. This is the principal process of energy transfer, particularly if the particle velocity is below the level where bremsstrahlung is significant, it leads to excitation of the atomic electrons (still bound to the nucleus) and to ionization (electron stripped off the nucleus). Inelastic here refers to electronic levels.

(ii) Inelastic Collision with a Nucleus. This process can leave the nucleus in an excited state or the particle can radiate (bremsstrahlung).

(iii) Elastic Collision with a Nucleus. This process is known as Rutherford scattering. There is no excitation of the nucleus, nor radiation. The particle loses energy only through the recoil of the nucleus.

(iv) Elastic Collision with Atomic Electrons. The process is elastic defection which results in a small amount of energy transfer. It is significant only for charged particles that are low-energy electrons.

In general interaction of type (i), which is sometimes simply called collision, is the dominant process of energy loss, unless the charged particle has a kinetic energy exceeding its rest mass energy in which case the radiation process, type (ii), becomes important. For heavy particles, radiation occurs only at such kinetic energies, ~ 10^3 Mev, that it is of no practical interest. The characteristic behavior of electron and proton energy loss in a high-Z medium like lead is shown in Fig. 13.1 [Meyerhof Fig. 3.7].

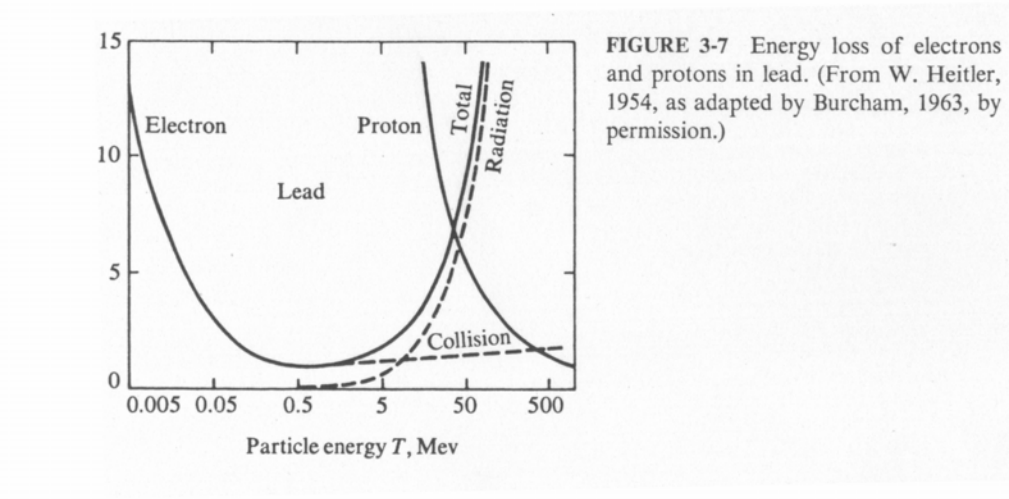

FIGURE 3-7 Energy loss of electrons and protons in lead. (From W. Heitler, 1954, as adapted by Burcham, 1963, by permission.)

Stopping Power: Energy Loss of Charged Particles in Matter

The kinetic energy loss per unit distance suffered by a charged particle, to be denoted as –dT/dx, is conventionally known as the *stopping powe*. This is a positive quantity since dT/dx is <0. There are quantum mechanical as well as classical theories for calculating this basic quantity. One wants to express –dT/dx in terms of the properties specifying the incident charged particle, such as it velocity v and charge ze,

and the properties pertaining to the atomic medium, the charge of the atomic nucleus Ze, the density of atoms n, and the average ionization potential $\bar{I}$.

We consider only a crude, approximate derivation of the formula for –dT/dx. We begin with an estimate of the energy loss suffered by an indicend charged particle when it interacts with a free and initially stationary electron. Referring to the collision cylinder whose radius is the impact parameter b and whose length is the small distance traveled dx shown in Fig. 13.2 [Meyerhof Fig. 3-1], we see that the net momentum transferred to the

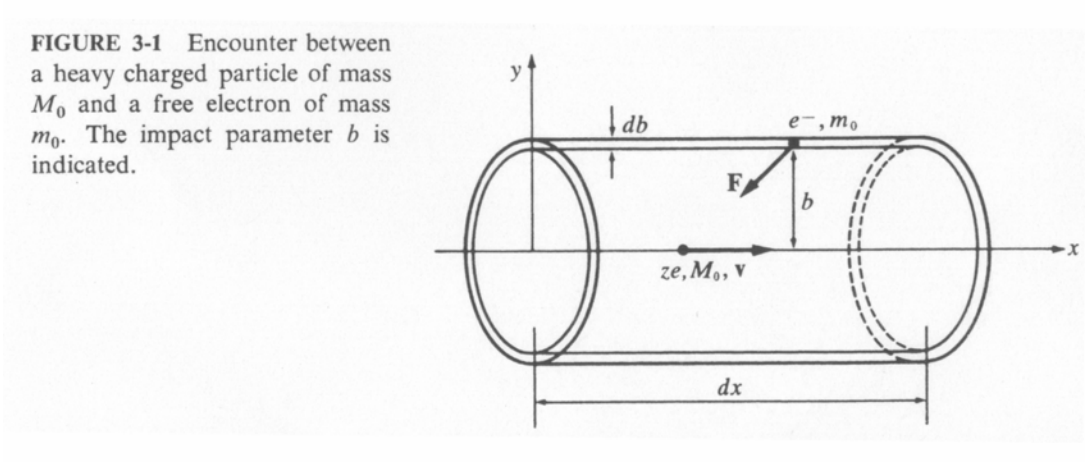

FIGURE 3-1 Encounter between a heavy charged particle of mass M_0 and a free electron of mass m_0. The impact parameter b is indicated.

electron as the particle moves from one end of the cylinder to the other end is essentially entirely directed in the perpendicular direction (because F_x changes sign so the net momentum along the horizontal direction vanishes) along the negative y-axis. So we write

$$\int dtF_x(t) \approx 0 \qquad (13.1)$$

$$p_e = \int dtF_y(t)$$

$$= \int \frac{ze^2}{x^2 + b^2} \frac{b}{\left(x^2 + b^2\right)^{1/2}} \frac{dx}{v}$$

$$\cong \frac{ze^2 b}{v}\int_{-\infty}^{\infty}\frac{dx}{\left(x^2+b^2\right)^{3/2}} = \frac{2ze^2}{vb} \tag{13.2}$$

The kinetic energy transferred to the electron is therefore

$$\frac{p_e^2}{2m_e} = \frac{2(ze^2)^2}{m_e b^2 v^2} \tag{13.3}$$

If we assume this is equal to the energy loss of the charged particle, then multiplying by $nZ(2\pi bdbdx)$, the number of electrons in the collision cylinder, we obtain

$$-\frac{dT}{dx} = \int_{b_{\min}}^{b_{\max}} nZ\,2\pi b db\,\frac{2}{m_e}\left(\frac{ze^2}{vb}\right)^2$$

$$= \frac{4\pi(ze^2)^2 nZ}{m_e v^2}\,\ell n\left(\frac{b_{\max}}{b_{\min}}\right) \tag{13.4}$$

where b_{max} and b_{min} are the maximum and minimum impact parameters which one should specify according to the physical description he wishes to treat.

In reality the atomic electrons are of course not free electrons, so the charged particle must transfer at least an amount of energy equal to the first excited state of the atom. If we take the time interval of energy transfer to be $\Delta t \approx b/v$, then $(\Delta t)_{\max} \sim 1/v$, where $h\nu \approx \bar{I}$ is the mean ionization potential. Then

$$b_{\max} \approx h\nu / \bar{I} \tag{13.5}$$

An empirical expression for $\bar{I}$ is $\bar{I} \approx kZ$, with k ~ 19 ev for H and ~ 10 ev for Pb. We estimate bmin by using the uncertainty principle to say that the electron position cannot be specified more precisely than it de Broglie wavelength in the relative coordinate

system of the electron and the charged particle. Since electron momentum in the relative coordinate system is $m_e v$, we find

$$b_{\min} \approx h / m_e v \tag{13.6}$$

Combining these two estimates we obtain

$$-\frac{dT}{dx} = \frac{4\pi z^2 e^4 nZ}{m_e v^2} \ell n\left(\frac{2m_e v^2}{\bar{I}}\right) \tag{13.7}$$

In (13.7) we have inserted a factor of 2 in the argument of the logarithm, this is to make our formula agree with the result of quantum mechanical calculation which was first carried out by H. Bethe using the Born approximation.

Eq.(13.7) describes the energy loss due to particle collisions in the nonrelativistic regime. One can include relativistic effects by replacing the logarithm by

$$\ell n\left(\frac{2m_e v^2}{\bar{I}}\right) - \ell n\left(1 - \frac{v^2}{c^2}\right) - \frac{v^2}{c^2}$$

This correction can be important in the case of electrons and positrons.

Eq.(13.7) is a relatively simple expression, yet one can gain much insight into the factors that govern the energy loss of a charged particle by collisions with the atomic electrons. We can see why one can usually neglect the contributions due to collisions with nuclei. In a collision with a nucleus the stopping power would increase by a factor Z, because of the charge of the target with which the incident charged particle is colliding, and decrease by a factor of $m_e/M(Z)$, where M(Z) is the mass of the atomic nucleus. The decrease is a result of the larger mass of the recoiling target. Since Z is always less than 10^2 whereas M(Z) is at least a factor 2×10^3 greater than m_e, the mass factor always dominates over the charge factor. Another useful observation is that (13.7) is independent of the mass of the incident charged particle. This means that

nonrelativistic electrons and protons of the same velocity would lose energy at the same rate, or equivalently the stopper power of a proton at energy T is about the same as that of an electron at energy ~ T/2000. This scaling is more or less correct as seen in Fig. 13.1.

Fig. 13.2 shows an experimentally determined energy loss curve (stopping power) for a heavy charged particle (proton), on two energy scales, an expanded low-energy region where the stopping power decreases smoothly with increasing kinetic energy of the charged particle T below a certain peak centered about 0.1 Mev, and a more compressed high-energy region where the stopping power reaches a broad minimum around 10^3 Mev. Notice also a slight upturn as one goes to higher energies past the broad minimum which we expect is associated with relativistic corrections. One should regard Fig. 13.2 as the extension at both ends of the energy of the curve for proton in Fig. 13.1.

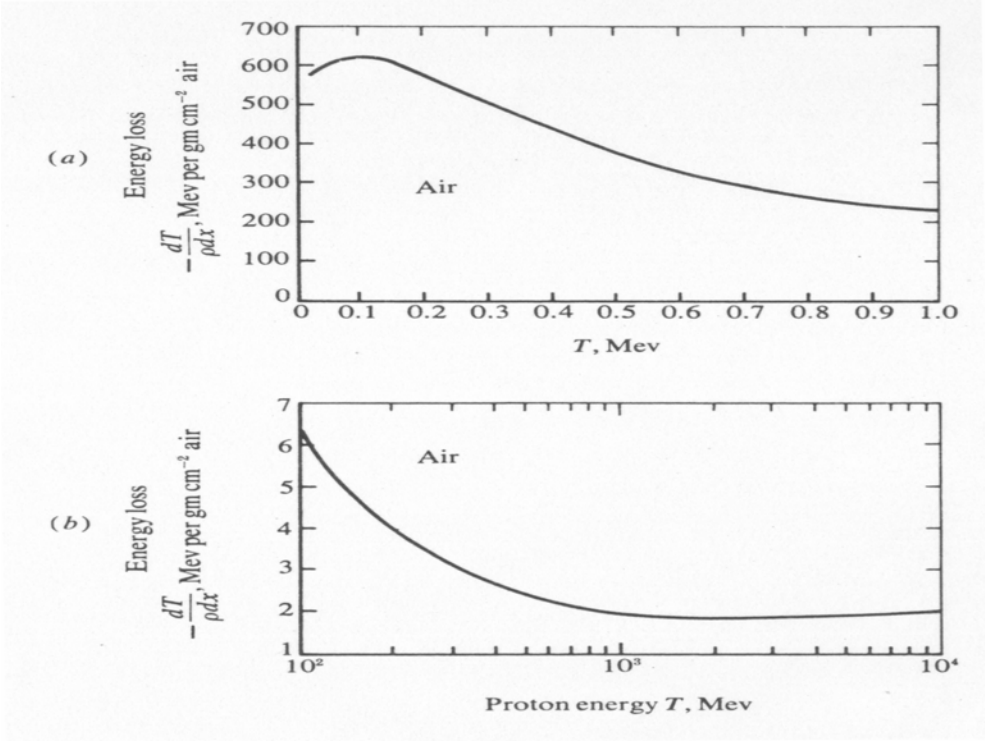

Fig. 13.2. The experimentally determined stopping power, (-dT/dx), for protons in air, (a) low-energy region where the Bethe formula applies down to T ~ 0.3 Mev with $\bar{I}$ ~ 80 ev. Below this range charge loss due to electron capture causes the stopper power to

reach a peak and start to decrease (see Fig. 13.3), (b) high-energy region where a broad minimum occurs at T ~ 1500 Mev. [from Meyerhof]

Experimentally, collisional energy loss is measured through the number of ion pairs formed along the trajectory path of the charged particle. Suppose a heavy charged particle loses on the average an amount of energy w in producing an ion pair, an electron and an ion, the residual nucleus which is now charged. Then the number of ion pairs produced per unit path is

$$i = \frac{1}{w}\left(-\frac{dT}{dx}\right) \tag{13.8}$$

Eq.(13.7) is valid only in a certain energy range because of the assumptions we have made in its derivation. We have seen from Figs. 13.1 and 13.2 that the atomic stopping power varies with energy in the manner sketched below. In the intermediate

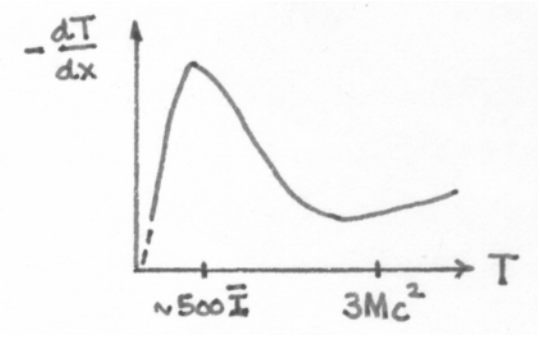

energy region, $500\bar{I} < T \leq Mc^2$, where M is the mass of the charged particle, the stopping power behaves like 1/T, which is roughly what is predicted by (13.7). In this region the relativistic correction is small and the logarithm factor varies slowly. At higher energies the logarithm factor along with the relativistic correction terms give rise to a gradual increase so that a broad minimum is set up in the neighborhood of ~ 3 Mc2. At energies below the maximum in the stopping power, $T < 500\bar{I}$, Eq.(13.7) is not valid

because the charged particle is moving slow enough to capture electrons and begin to lose its charge. Fig. 13.3 [Meyerhof Fig. 3-3] shows the correlation between the mean charge

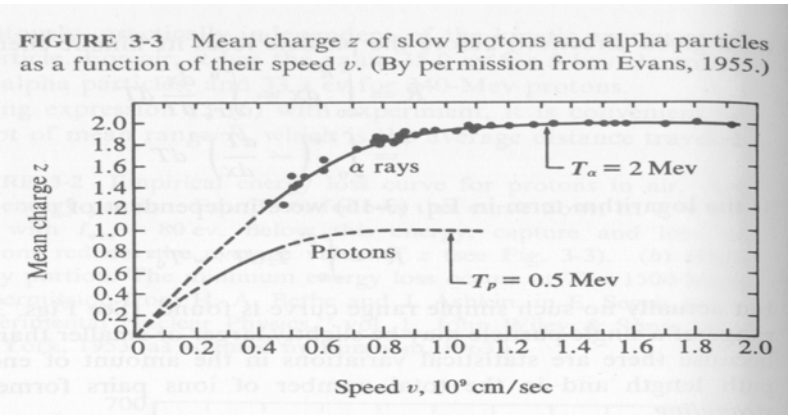

of a charged particle and its velocity. This is a difficult region to analyze theoretically. For α -particles and protons the range begins at ~ 1 Mev and 0.1 Mev respectively [H. A. Bethe and J. Ashkin, "Passage of Radiation Through Matter", in *Experimental Nuclear Physics*, E. Segrè, ed (Wiley, New York, 1953), Vol. I, p.166].

Eq.(13.7) is generally known as the Bethe formula. It is a quantum mechanical result derived on the basis of the Born approximation which is essentially an assumption of weak scattering [E. J. Williams, Rev. Mod. Phys. **17**, 217 (1945)]. The result is valid provided

$$\frac{ze^2}{\hbar v} = \left(\frac{e^2}{\hbar c}\right)\frac{z}{v/c} = \frac{z}{137(v/c)} << 1 \qquad (13.9)$$

On the other hand, Bohr has used classical theory to derive an expression for the stopping power,

$$-\left(\frac{dT}{dx}\right)_{class} = \frac{4\pi z^2 e^4 nZ}{m_e v^2}\ell n\left[\frac{M\hbar v}{2ze^2(m_e+M)}\frac{2m_e v^2}{\bar{I}}\right] \qquad (13.10)$$

which holds if

$$\frac{ze^2}{\hbar v} >> 1 \qquad (13.11)$$

Thus (13.7) and the classical formula apply to opposite conditions. Notice that the two expressions agree when the arguments of the logarithms are equal, that is, $2ze^2/\hbar v = 1$, which is another way of saying that their regions of validity do not overlap. According to Evans (p. 584), the error tends to be an overestimate, so the expression that gives the smaller energy loss is likely to be the more correct. This turns out to be the classical expression when z > 137(v/c), and (13.7) when 2z < 137(v/c). Knowing the charge of the incident particle and its velocity, one can use this criterion to choose the appropriate stopper power formula. In the case of fission fragments (high Z nuclides) the classical result should be used. Also, it should be noted that a quantum mechanical theory has been developed by Bloch that gives the Bohr and Bethe results as appropriate limiting cases.

The Bethe formula,(13.7), is appropriate for heavy charged particles. For fast electrons (relativistic) one should use

$$-\frac{dT}{dx} = \frac{2\pi e^4 nZ}{m_e v^2}\left[\ell n\left(\frac{m_e v^2 T}{\bar{I}^2(1-\beta^2)}\right) - \beta^2\right] \qquad (13.12)$$

where $\beta = v/c$. For further discussions see Evans.

22.101 Applied Nuclear Physics (Fall 2004)

Lecture 15 (11/3/04)

Charged-Particle Interactions: Radiation Loss, Range

References:

R. D. Evan, *The Atomic Nucleus* (McGraw-Hill, New York, 1955), Chaps 18-22.

W. E. Meyerhof, *Elements of Nuclear Physics* (McGraw-Hill, New York, 1967).

The sudden deflection of an electron by the Coulomb field of the nuclei can cause the electron to radiate, producing a continuous spectrum of x-rays called *bremsstrahlung*. The fraction of electron energy converted into bremsstrahlung increases with increasing electron energy and is largest for media of high atomic number. (This process is important in the production of x-rays in conventional x-ray tubes.)

According to the classical theory of electrodynamics [J. D. Jackson, *Classical Electrodynamics* (Wiley, New York, 1962), p. 509], the acceleration produced by a nucleus of charge Ze on an incident particle of charge ze and mass M is proportional to Zze^2/M. The intensity of radiation emitted is proportional to (ze x acceleration)^2 ~ $(Zz2e^3/M)^2$. Notice the $(Z/M)^2$ dependence; this shows that bremsstrahlung is more important in a high-Z medium and is more important for electrons and positrons than for protons and α -particles. Another way to understand the $(Z/M)^2$ dependence is to recall the derivation of stopping power in Lec13 where the momentum change due to a collision between the incident particle and a target nucleus is (2ze2/vb) x Z. The factor Z represents the Coulomb field of the nucleus (in Lec13 this was unity since we had an atomic electron as the target). The recoil velocity of the target nucleus is therefore proportional to Z/M, and the recoil energy, which is the intensity of the radiation emitted, is therefore proportional to $(Z/M)^2$.

In an individual deflection by a nucleus, the electron can radiate any amount of energy up to its kinetic energy T. The specgtrum of bremsstrahlung wavelength for a thick target is of the form sketched below, with $\lambda_{\min} = hc/T$. This converts to a frequency spectrum which is a constant up the maximum frequency of $\nu_{\max} = T/h$. The

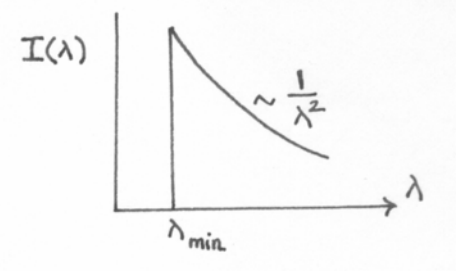

shape of the spectrum is independent of Z, and the intensity varies with electron energy like 1/T.

In the quantum mechanical theory of bremsstrahlung a plane wave representing the electron enters the nuclear field and is scattered. There is a small but finite chance that a photon will be emitted in the process. The theory is intimately related to the theory of pair production where an electron-positron pair is produced by a photon in the field of a nucleus. Because a radiative process involves the coupling of the electron with the electromagnetic field of the emitted photon, the cross sections for radiation are of the order of the fine-structure constant [Dicke and Wittke, p. 11], $e^2/\hbar c$ (= 1/137), times the cross section for elastic scattering. This means that most of the deflections of electrons by atomic nuclei result in elastic scattering, only in a small number of instances is a photon emitted. Since the classical theory of bremsstrahlung predicts the emission of radiation in every collision in which the electron is deflected, it is incorrect. However, when averaged over all collisions the classical and quantum mechanical cross sections are of the same order of magnitude,

$$\sigma_{rad} \sim \frac{Z^2}{137}\left(\frac{e^2}{m_e c^2}\right)^2 \quad \text{cm}^2/\text{nucleus} \qquad (14.1)$$

where $e^2/m_e c^2$ = r_e = 2.818 x 10^{-13} cm is the classical radius of electron. In the few collisions where photons are emitted a relatively large amount of energy is radiated. In this way the quantum theory replaces the multitude of small-energy losses predicted by the classical theory by a much smaller number of larger-energy losses. The spectral

distributions are therefore different in the two theories, with the quantum description being in better agreement with experiments.

Given a nucleus of charge Ze and an incident electron of kinetic energy T, the quantum mechanical differential cross section for the emission of a photon with energy in $d(h\nu)$ about $h\nu$ is

$$\left[\frac{d\sigma}{d(h\nu)}\right]_{rad} = \sigma_o B Z^2 \frac{T + m_e c^2}{T}\frac{1}{h\nu} \qquad (14.2)$$

where $\sigma_o = \left(e^2 / m_e c^2\right)^2 / 137$ = 0.580 x 10^{-3} barns and B ~ 10 is a very slowly varying dimensionless function of Z and T. A general relation between the energy differential cross section, such as (14.2), and the energy loss per unit path length is

$$-\frac{dT}{dx} = n\int_0^T dE E\frac{d\sigma}{dE} \qquad (14.3)$$

where $d\sigma / dE$ is the differential cross section for energy loss E. Applying this to (14.2) we have

$$-\left(\frac{dT}{dx}\right)_{rad} = n\int_0^T d(h\nu)h\nu\left[\frac{d\sigma}{d(h\nu)}\right]_{rad}$$

$$= n(T + m_e c^2)\sigma_{rad} \qquad \text{ergs/cm} \qquad (14.4)$$

where $$\sigma_{rad} = \sigma_o Z^2 \int_0^1 d\left(\frac{h\nu}{T}\right) B \equiv \sigma_o Z^2 \overline{B} \qquad (14/5)$$

is the total bremsstrahlung cross section. The variation of $\overline{B}$, the bremmstrahlung cross section in units of $\sigma_o Z^2$, with the kinetic energy of an incident electron is shown in the sketch for media of various Z [Evans, p. 605].

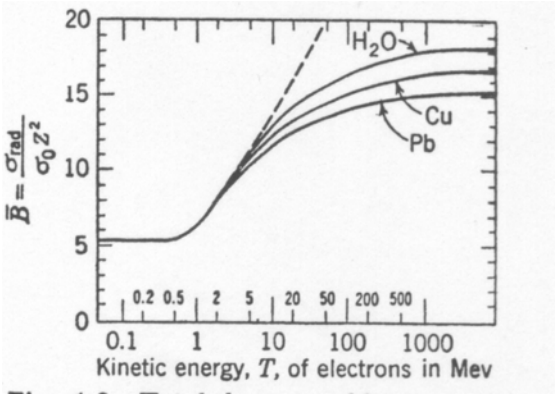

Comparison of Various Cross Sections

It is instructive to compare the cross sections describing the interactions that we have considered between an incident electron and the atoms in the medium. For nonrelativistic electrons, T $\leq$ 0.1 Mev and $\beta = v/c \leq 0.5$, we have the following cross sections (all in barns/atom) [Evans, p. 607],

$$\sigma_{ion} = \frac{2\alpha Z}{\beta^4} \ell n\left(\frac{\sqrt{2}T}{\bar{I}}\right) \qquad \text{ionization} \qquad (14.6)$$

$$\sigma_{nuc} = \frac{\alpha Z^2}{4\beta^4} \qquad \text{backscattering by nuclei} \qquad (14.7)$$

$$\sigma_{el} = \frac{2\alpha Z}{\beta^4} \qquad \text{elastic scattering by atomic electrons} \qquad (14.8)$$

$$\sigma'_{rad} = \frac{8\alpha}{3\pi}\frac{1}{137}\frac{Z^2}{\beta^2} \qquad \text{bremsstrahlung} \qquad (14.9)$$

where $\alpha = 4\pi(e^2/m_e c^2)^2$ = 1.00 barn. The values of these cross sections in the case of 0.1 Mev electrons in air (Z = 7.22, $\bar{I}$ ~ 100 ev) and in Pb (Z = 82, $\bar{I}$ ~ 800 ev) are given in the following table [from Evans, p.608]. The difference between σ_{rad} and σ'_{rad} is that the former corresponds to fractional of *total* energy, $dT/(T + m_e c^2)$, while the latter corresponds to fractional loss of *kinetic* energy, dT/T.

TABLE 2.1. APPROXIMATE CROSS SECTIONS IN BARNS PER ATOM OF Pb, AND OF AIR, FOR INCIDENT 0.1-MEV ELECTRONS, EQS. (2.2) TO (2.6)

	Ionization	Nuclear elastic backward scattering $\vartheta \geq 90°$	Electronic (inelastic) scattering $\vartheta \geq 45°$	Bremsstrahlung	
				σ_{rad}	σ'_{rad}
Approximate variation with Z and β	Z/β^4	Z^2/β^4	Z/β^4	Z^2	Z^2/β^2
Air	1,200	150	160	0.16	1.0
Pb	9,400	19,000	1,800	21	130

Mass Absorption

Ionization losses per unit distance are proportional to nZ, the number of atomic electrons per cm^3 in the absorber (medium). We can express nZ as

$$nZ = (\rho N_o / A)Z = \rho N_o (Z/A) \qquad (14.10)$$

where ρ is the mass density, g/cm^3, and No the Avogadro's number. Since the ratio (Z/A) is nearly a constant for all elements, it means that nZ/ρ is also approximately constant (except for hydrogen). Therefore, if the distance along the path of the charged particle is measured in units of $\rho dx \equiv dw$ (in g/cm^2), then the ionization losses, -dT/dw (in ergs cm^2/g) become more or less independent of the material. We see in Fig. 14.1, the expected behavior of energy loss being material independent holds only approximately,

as -dT/dw actually decreases as Z increases. This is due to two reasons, Z/A descresing slightly as Z increases and $\bar{I}$ increasingly linearly with Z.

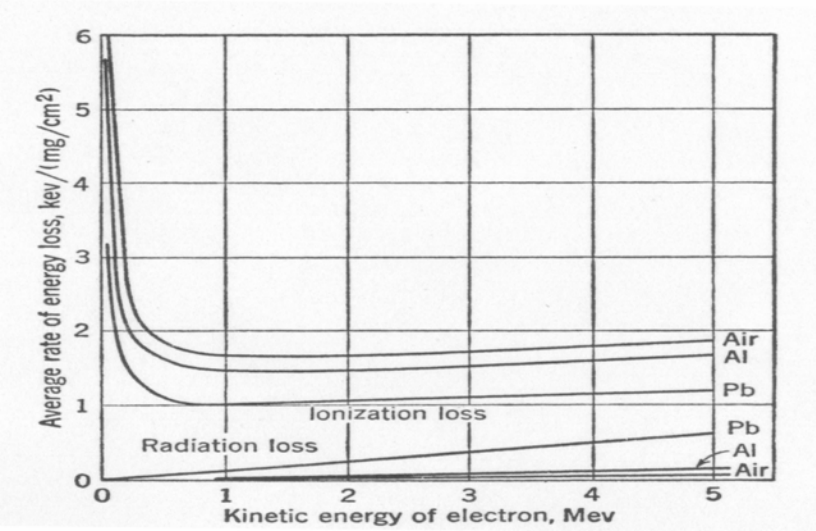

Fig. 14.1. Mass absorption energy losses, -dT/dw, for electrons in air, Al, and Pb, ionization losses (upper curves) versus bremsstrahlung (lower curves). All curves refer to energy losses along the actual path of the electron. [Evans, p.609]

We have seen that ionization losses per path length vary mainly as $1/v^2$ while radiative losses increase with increasing energy. The two become roughly comparable when $T >> Mc^2$, or $T >> m_e c^2$ in the case of electrons. The ratio can be approximately expressed as

$$\frac{(dT/dx)_{rad}}{(dT/dx)_{ion}} \approx Z\left(\frac{m_e}{M}\right)^2\left(\frac{T}{1400 m_e c^2}\right) \qquad (14.11)$$

where for electrons, $M \rightarrow m_e$. The two losses are therefore equal in the case of electrons for $T = 18\, m_e c^2 = 9$ Mev in Pb and T ~ 100 Mev in water or air.

Range, Range-Energy Relations, and Track Patterns

When a charged particle enters an absorbing medium it immediately interacts with the many electrons in the medium. For a heavy charged particle the deflection from

any individual encounter is small, so the track of the heavy charged particle tends to be quite straight except at the very end of its travel when it has lost practically all its kinetic energy. In this case we can estimate the range of the particle, the distance beyond which cannot penetrate, by integrating the stopping power,

$$R = \int_0^R dx = \int_{T_o}^0 \left(\frac{dx}{dT}\right) dT = \int_0^T \left(-\frac{dT}{dx}\right)^{-1} dT \tag{14.12}$$

where To is the initial kinetic energy of the particle. An estimate of R is given by taking the Bethe formula, (13.7), for the stopping power and ignoring the v-dependence in the logarithm. Then one finds

$$R \propto \int_0^{T_o} T dT \;=\; T_o^2 \tag{14.13}$$

This is an example of range-energy relation. Given what we have said about the range of applicability of (13.7) one might expect this behavior to hold at low energies. At high energies it is more reasonable to take the stopping power to be a constant, in which case

$$R \propto \int_0^{T_o} dT \;=\; T_o \tag{14.14}$$

We will return to see whether such behavior are seen in experiments..

Experimentally one can determine the energy loss by the number of ion pairs, positive and negative constituents which result from an ionization event, produced. The amount of energy W required for a particle of certain energy to produce an ion pair is known. The number of ion pairs, i, produced per unit path length (*specific ionization*) of the charged particle is then

$$i = \frac{1}{W}\left(-\frac{dT}{dx}\right) \tag{14.15}$$

The quantity W depends on complicated processes such as atomic excitation and secondary ionization in addition to primary ionization. On the other hand, for a given material it is approximately independent of the nature of the particle or its kinetic energy. For example, in air the values of W are 35.0, 35.2, and 33.3 ev for 5 kev electrons, 5.3 Mev alphas, and 340 Mev protons respectively.

The specific ionization is an appropriate measure of the ionization processes taking place along the path (track length) of the charged particle. It is useful to regard (14.15) as a function of the distance traveled by the particle. Such results can be seen in Fig. 14.2, where one sees a characteristic shape of the ionization curve for a heavy charged particle. Ionization is constant or increasing slowly during the early to mid stages of the total travel, then it rises more quickly and reaches a peak value at the end of the range before dropping sharply to zero.

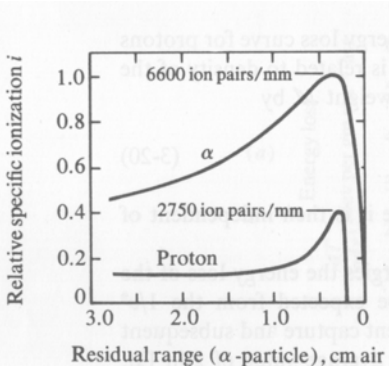

FIGURE 3-4 Number of ion pairs per unit path for a single proton and a single alpha particle as a function of residual range. The residual range is the distance left to travel until the particle comes to rest. The horizontal scale is such that on the left part of the diagram both particles have similar speeds. The proton range then is 0.2 air-cm shorter than the alpha-particle range. (By permission from Evans, 1955.)

Fig. 14.2. Specific ionization of heavy particles in air. Residual range refers to the distance still to travel before coming to rest. Proton range is 0.2 cm shorter than that of the α -particle [Meyerhof, p.80].

We have already mentioned that as the charged particle loses energy and slows down, the probability of capturing electron increases. So the mean charge of a beam of particles will decrease with the decrease in their speed (cf. Fig. 13.3). This is the reason why the specific ionization shows a sharp drop. The value of –dT/dx along a particle track is also called specific energy loss. A plot of –dT/dx along the track of a charged particle is known as a Bragg curve. It should be emphasized that a Bragg curve differs

from a plot of –dT/dx for an individual particle in that the former is an average over a large number of particles. Hence the Bragg curve includes the effects of straggling (statistical distribution of range values for particles having the same initial velocity) and has a pronounced tail beyond the extrapolated range as can be seen in Fig. 14.3.

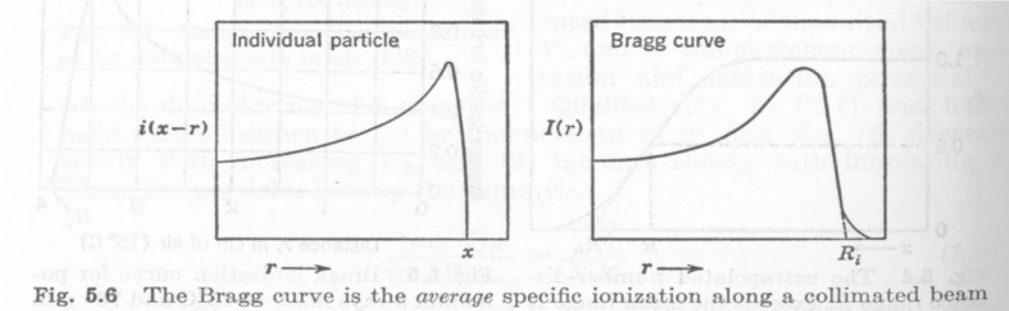

Fig. 5.6 The Bragg curve is the *average* specific ionization along a collimated beam of heavy particles. Extrapolation of the slope of the final portion of the Bragg curve leads to the "extrapolated ionization range" R_i.

Fig. 14.3. Specific ionization for an individual particle versus Bragg curve [Evans, p. 666].

A typical experimental arrangement for determining the range of charged particles is shown in Fig. 14.4. The mean range $\overline{R}$ is defined as the absorber thickness at which the intensity is reduced to one-half of the initial value. The extrapolated range R_o is obtained by linear extrapolation at the inflection point of the transmission curve. This is an example that I/Io is not always an exponential. In charged particle interactions it is not sufficient to think of $I / I_o = e^{-\mu x}$, one should be thinking about the range R.

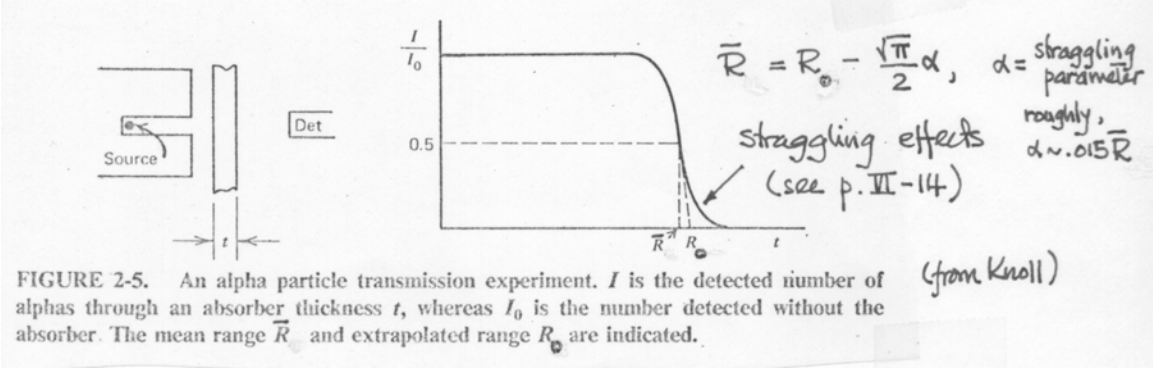

FIGURE 2-5. An alpha particle transmission experiment. I is the detected number of alphas through an absorber thickness t, whereas I_0 is the number detected without the absorber. The mean range $\overline{R}$ and extrapolated range R_o are indicated.

Fig. 14.4. Determination of range by transmission experiment [from Knoll].

In practice one uses range-energy relations that are mostly empirically determined. For a rough estimate of the range one can use the Bragg-Kleeman rule,

$$\frac{R}{R_1} = \frac{\rho_1 \sqrt{A}}{\rho \sqrt{A_1}} \tag{14.16}$$

where the subscript 1 denotes the reference medium which is conventionally taken to be air at 15°C, 760 mm Hg ($\sqrt{A_1}$ = 3.81, ρ_1 = 1.226 x 10^{-3} g/cm^3). Then

$$R = 3.2x10^{-4} \frac{\sqrt{A}}{\rho} \text{ x } R_{air} \tag{14.17}$$

with ρ in g/cm^3. In general such an estimate is good to within about $\pm$ 15 percent. Figs. 14.5 and 14.6 show the range-energy relations for protons and α-particles in air respectively. Notice that at low energy the variation is quadratic, as predicted by (14.13), and at high energy the relation is more or less linear, as given by (14.14). The same trend is also seen in the results for electrons, as shown in Fig. 14.7.

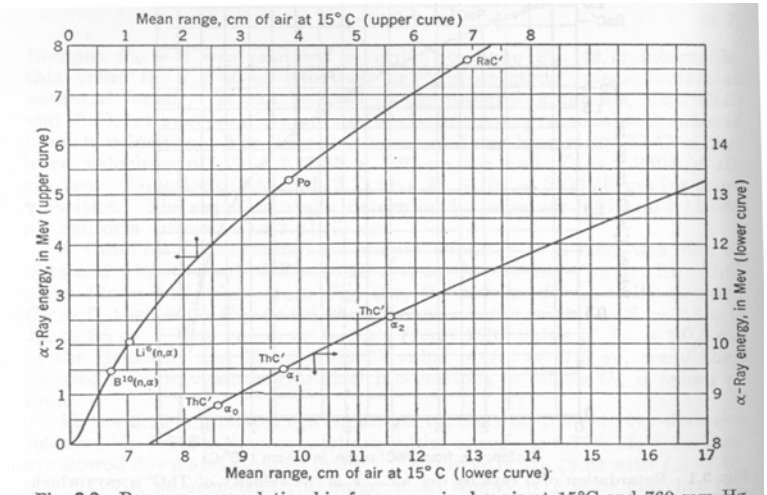

Fig. 3.2 Range-energy relationship for α rays in dry air at 15°C and 760 mm Hg. The curves agree with those of Bethe (B44) and with the tables by Jesse and Sadauskis (J12). Two low-energy calibration points (J12) are provided by the α rays emitted in the thermal neutron reactions $B^{10}(n,\alpha)Li^7$ and $Li^6(n,\alpha)H^3$.

Fig. 14.5. Range-energy relations of α-particles in air [Evans, p. 650].

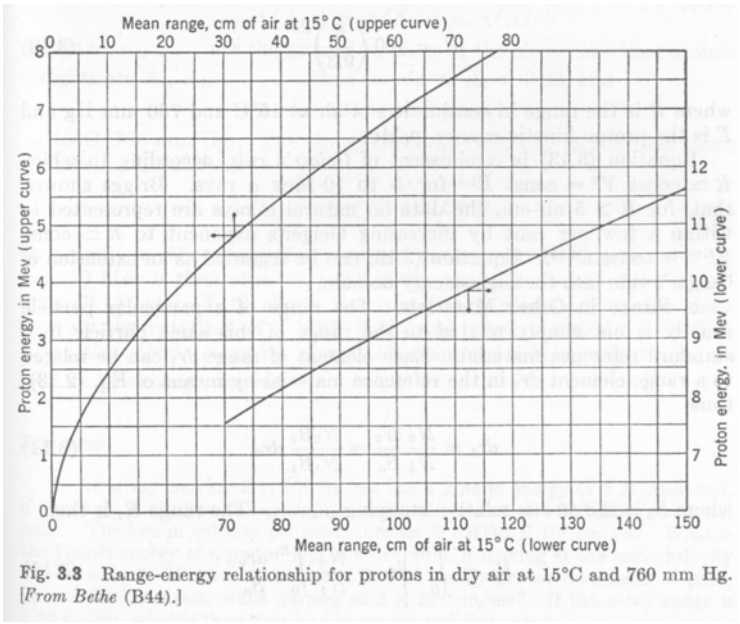

Fig. 3.3 Range-energy relationship for protons in dry air at 15°C and 760 mm Hg. [*From Bethe* (B44).]

Fig. 14.6. Range-energy relation for protons in air [Evans, p. 651].

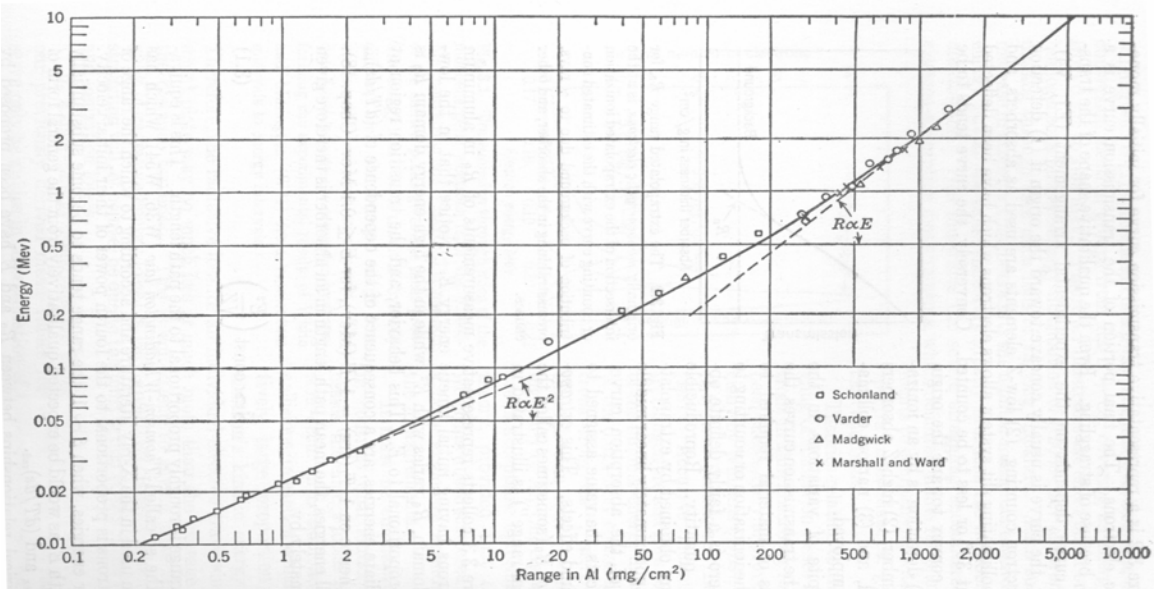

Fig. 3.3 Empirical range-energy relationship for electrons absorbed in aluminum. Experimental values by several observers (S16, V4, M4, M17) on monoenergetic electrons are shown. For *monoenergetic electrons*, the range coordinate refers to the *extrapolated range* R_0 of Fig. 3.2. For *continuous β-ray spectra* the energy coordinate refers to the end-point energy E_{max}, and the range coordinate becomes the *maximum range* R_m of Fig. 3.4. The smooth curve represents the empirical relationship, Eqs. (3.3) and (3.4), developed by Katz and Penfold (K7).

Fig. 14.7. Range-energy relation for electrons in aluminum [Evans, p. 624].

We have mentioned that heavy charged particles traverse essentially in a straight line until reaching the end of its range where straggling effects manifest. In the case of

electrons large deflections are quite likely during its traversal, so the trajectory of electron in a thick absorber is a series of zigzag paths. While one can still speak of the range R, the concept of path length is now of little value. This is illustrated in Figs. 14.8 and 14.9. The total path length S is appreciably greater than the range R

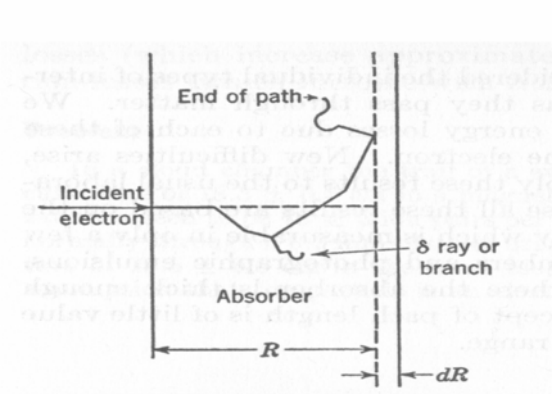

Fig. 1.1 Schematic diagram of the path of an electron which is multiply scattered while traversing an absorber of thickness $R + dR$ and which does not emerge from the absorber. If the absorber had been of thickness R, the electron would have just penetrated it and would be said to have a *range* R. The total *path length* S is measured along the actual path of the electron and is always considerably greater than R.

Fig. 14.8. Distinction between total path length S and range R [Evans, p. 612]

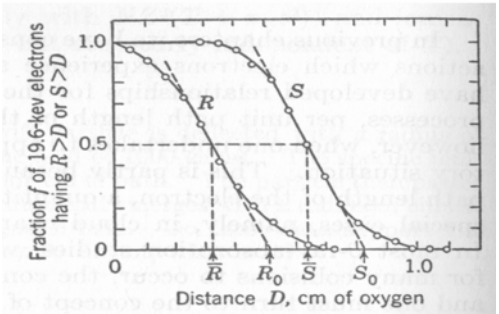

Fig. 1.2 The distribution of path lengths (S) and of range (R) (Fig. 1.1) for 19.6-kev electrons in oxygen at 0°C and 1-atm pressure:
$\bar{R} = 0.32$ cm = mean range
$R_0 = 0.52$ cm = extrapolated range
$\bar{S} = 0.64$ cm = mean path length
$S_0 = 0.82$ cm = extrapolated path length
$\sqrt{2/\pi}(S_0 - \bar{S}) = 0.14$ cm $= 0.22\bar{S}$
= standard deviation of S about $\bar{S}$
The mean path length is 1.24 times the extrapolated range, under these conditions. [*From Williams* (W54).]

Fig. 14.9. Comparing distributions of total path length and range for electrons in oxygen [Evans, p. 612].

The transmission curve I/I_o for a heavy charged particle was shown in Fig. 14.4. The curve has a different characteristic shape for monoenergetic electrons, as indicated in Fig. 14.10, and a still different shape for β-rays (electrons with a distribution of energies), seen in Fig. 14.11. Although the curve for monoenergetic electrons depends to some extent on experimental arrangement, one may regard it as roughly a linear variation which is characteristic of single interaction event in removing the electron. That is, the fraction of electrons getting through is proportional to 1 – P, where P is the interaction probability which is in turn proportional to the thickness. For the β-ray transmission curve which essentially has the form of an exponential, the shape is an accidental consequence of the β-ray spectrum and of the differences between the scattering and absorption of electrons which have various initial energies [cf. Evans, p. 625]. It is found empirically that R_m is the same as R_o if the monoenergetic electrons are given the energy $E = E_{max}$, the maximum energy of the β-ray spectrum (the end-point energy).

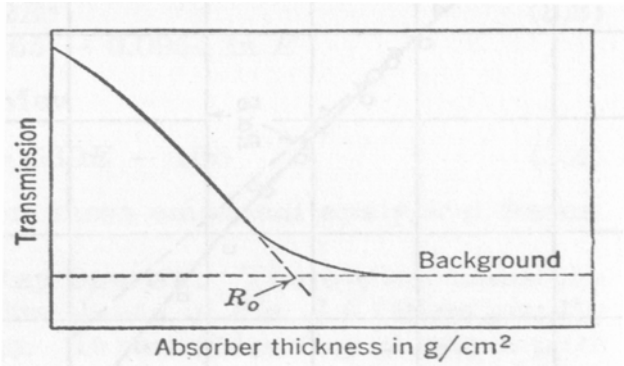

Fig. 3.2 The extrapolated range R_0, for originally *monoenergetic electrons*, is at the intersection of the extrapolated ionization or counting curve with the estimated contribution of background due to γ rays, bremsstrahlung in the absorber, and other causes.

Fig. 14. 10. Transmission curve of monoenergetic electrons (sensitive to experimental arrangement) [Evans, p. 623].

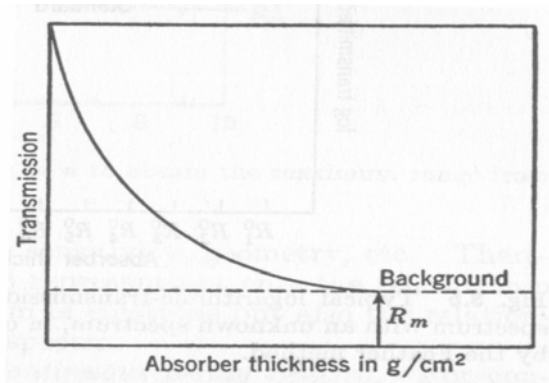

Fig. 3.4 A typical plot of the approximately exponential transmission of a continuous β-ray spectrum through absorbers of various thicknesses. R_m is called the *maximum range.*

Fig. 14.11. Transmission curve for β-rays [Evans, p.625].

Cerenkov Radiation

Electromagnetic radiation is emitted when a charged particle passes through a medium under the condition

$$v_{group} \equiv \beta c > v_{phase} \equiv c / n \qquad (14.15)$$

where n is the index of refraction of the medium. When βn >1, there is an angle (a direction) where constructive interference occurs. This radiation is a particular form of energy loss, due to soft collisions, and is not an additional amount of energy loss. Soft collisions involve small energy transfers from charged particles to distant atoms which become excited and subsequently emit coherent radiation (see Evans, p. 589).

22.101 Applied Nuclear Physics (Fall 2004)

Lecture 16 (11/12/04)

Neutron Interactions: Q-Equation, Elastic Scattering

References:

R. D. Evan, Atomic Nucleus (McGraw-Hill New York, 1955), Chap. 12.

W. E. Meyerhof, *Elements of Nuclear Physics* (McGraw-Hill, New York, 1967), Sec. 3.3.

Since a neutron has no charge it can easily enter into a nucleus and cause reaction. Neutrons interact primarily with the nucleus of an atom, except in the special case of magnetic scattering where the interaction involves the neutron spin and the magnetic moment of the atomic. Since we will not consider magnetic scattering in this class we can neglect the interaction between neutrons and electrons and think of atoms and nuclei interchangeably. Neutron reactions can take place at any energy, so one has to pay particular attention to the energy dependence of the interaction cross section. In a nuclear reactor neutrons with energies from 10^{-3} ev (1 mev) to 10^{7} ev (10 Mev) are of interest, this means we will be covering an energy of 10^{10}.

For a given energy region – thermal, epithermal, resonance, fast – not all the possible reactions are equally important. What reaction is important depends on the target nucleus and the neutron energy. Generally speaking the important types of interactions, in the order of increasing complexity from the standpoint of theoretical understanding, are:

(n,n) – elastic scattering. There are two processes, potential scattering which is neutron interaction at the surface of the nucleus (no penetration) as in billiard ball-like collision, and resonance scattering which involves the format and decay of a compound nucleus.

(n, γ) -- radiative capture.

(n,n') -- inelastic scattering. This reaction involves the excitation of nuclear levels.

(n,p), (n, α), … -- charged particle emission.

(n,f) -- fission.

If we were interested in fission reactors, the reactions in the order of importance would be fission, capture (in fuel and other reactor materials), scattering (elastic and inelastic), fission product decay by β-emission as in decay neutrons and heat production. In this chapter we will mostly study elastic (or potential) scattering. The other reactions all involve compound nucleus formation, a process we will discuss briefly around the end of the semester.

The Q-Equation

Consider the reaction, sketched in Fig. 15.1, where an incoming particle (labeled 1) collides with a target nucleus (2), resulting in the emission of an outgoing particle (3), with the residual nucleus (4) recoiling. For simplicity we assume the target nucleus to be

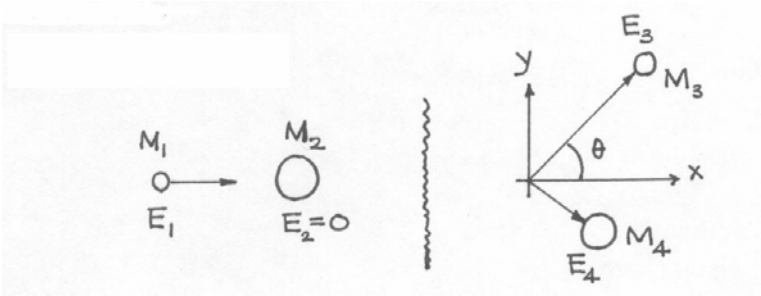

Fig. 15.1. A two-body collision between incident particle 1 and target particle 2, which is at rest, leading to the emission of particle 3 at an angle θ and a recoiling residual particle 4.

at rest, $E_2 = 0$. This is often a good approximation because the target is at room temperature, which means E_2 is 0.025 ev, and unless the incoming neutron is in the thermal energy region, E_1 typically will be much greater than E_2. We will derive an equation relating the outgoing energy E_3 to the outgoing angle θ using the conservation of total energy and linear momentum, and non-relativistic kinematics,

$$(E_1 + M_1c^2) + M_2c^2 = (E_3 + M_3c^2) + (E_4 + M_4c^2) \qquad (15.1)$$

$$\underline{p}_1 = \underline{p}_3 + \underline{p}_4 \tag{15.2}$$

Rewriting the momentum equation as

$$p_4^2 = (\underline{p}_1 - \underline{p}_3)^2$$

$$= \; p_1^2 + p_3^2 - 2p_1 p_3 \cos\theta \; = 2M_4 E_4 \tag{15.3}$$

and recalling

$$Q = (M_1 + M_2 - M_3 - M_4)c^2$$

$$= E_3 + E_4 - E_1 \tag{15.4}$$

we obtain

$$Q = E_3\left(1 + \frac{M_3}{M_4}\right) - E_1\left(1 - \frac{M_1}{M_4}\right) - \frac{2}{M_4}\sqrt{M_1 M_3 E_1 E_3}\cos\theta \tag{15.5}$$

which is known as the Q-equation. Notice that the energies E_i and angle θ are in the laboratory coordinate system (LCS), while Q is independent of coordinate system (since Q can be expressed in terms of masses which of course do not depend on coordinate system). A typical situation is when the incident energy E_1, the masses (and therefore Q-value) are all known, and one is interested in solving (15.5) for E_3 in terms of $\cos\theta$, or vice versa.

Eq. (15.5) is actually not an equation for determining the Q-value, since this is already known in the sense that all four particles in the reaction and their rest masses are prescribed beforehand. This being the case, what then is the quantity that one would solve (15.5) to obtain? We can think of the Q-equation as a relation connecting the 12 degrees of freedom in any two-body collision problem, where two particles collide (as

reactants) to give rise to two other particles (as products). The problem is said to be completely specified when the velocities of the fours particles, or 12 degrees of freedom (each velocity has 3 degrees of freedom), are determined. Clearly not every single degree of freedom is a variable in the situations of interest to us. First of all the direction of travel and energy of the incoming particle are always given, thus eliminating 3 degrees of freedom. Secondly it is customary to take the target nucleus to be stationary, so another 3 degrees of freedom are removed. Since conservation of energy and momentum must hold in any collision (three conditions since momentum and energy are related), this leaves three degrees of freedom in the problem. If we further assume the emission of the outgoing particle (particle 3) is azimuthally symmetric (that is, emission is equally probably into a cone subtended by the angle θ), only two degree of freedom are left. What this means is that the outcome of the collision is completely determined if we just specify another degree of freedom. What variable should we take? Because we are often interested in knowing the energy or direction of travel of the outgoing particle, we can choose this last variable to be either E_3 or the scattering angle θ. In other words, if we know either E_3 or θ, then everything else (energy and direction) about the collision is determined. Keeping this in mind, it should come as no surprise that what we will do with (15.5) is to turn it into a relation between E_3 and θ.

Thus far we have used non-relativistic expressions for the kinematics. To turn (15.5) into the relativistic Q-equation we can simply replace the rest mass M_i by an effective mass, $M_i^{eff} = M_i + T_i / 2c^2$, and use the expression $p^2 = 2MT + T^2 / c^2$ instead of $p^2 = 2ME$. For photons, we take $M^{eff} = h\nu / 2c^2$.

Inspection of (15.5) shows that it is a quadratic equation in the variable x = $\sqrt{E_3}$. An equation of the form $ax^2 + bx + c = 0$ has two roots,

$$x_{\pm} = \left[-b \pm \sqrt{b^2 4ac} \right] / 2a \qquad (15.6)$$

which means there are in general two possible solutions to the Q-equation, $\pm\sqrt{E_3}$. For a solution to be physically acceptable, it must be real and positive. Thus there are

situations where the Q-equation gives one, two, or no physical solutions [cf. Evans, pp. 413-415, Meyerhof, p. 178]. For our purposes we will focus on neutron collisions, in particular the case of elastic (Q = 0) and inelastic (Q < 0) neutron scattering. We will examine these two processes briefly and then return to a more detailed discussion of elastic scattering in the laboratory and center-of-mass coordinate systems.

Elastic vs. Inelastic Scattering

Elastic scattering is the simplest process in neutron interactions; it can be analyzed in complete detail. This is an important process because it is the primary mechanism by which neutrons lose energy in a reactor, from the instant they are emitted as fast neutrons as a result of a fission event to when they appear as thermal neutrons. In this case, there is no excitation of the nucleus, Q = 0, whatever energy is lost by the neutron is gained by the recoiling target nucleus. Let $M_1 = M_3 = m$ (M_n), and $M_2 = M_4 = M = Am$. Then (15.5) becomes

$$E_3\left(1+\frac{1}{A}\right)-E_1\left(1-\frac{1}{A}\right)-\frac{2}{A}\sqrt{E_1E_3}\cos\theta=0 \qquad (15.7)$$

Suppose we ask under what condition is $E_3 = E_1$? We see that this can occur only when $\theta = 0$, which corresponds to forward scattering (no interaction). For all finite θ, E_3 has to be less than E_1. One can show that maximum energy loss by the neutron occurs at $\theta = \pi$, which corresponds to backward scattering,

$$E_3 = \alpha E_1, \qquad \alpha=\left(\frac{A-1}{A+1}\right)^2 \qquad (15.8)$$

Eq.(15.7) is the starting point for the analysis of neutron slowing down in a moderator medium. We will return to it later in this chapter.

Inelastic scattering is the process by which the incoming neutron excites the target nucleus so it leaves the ground state and goes to an excited state at an energy E* above the ground state. Thus Q = -E* (E* > 0). We again let the neutron mass be m and

the target nucleus mass be M (ground state) or M* (excited state), with $M^* = M + E^*/c^2$. Since this is a reaction with negative Q, it is an endothermic process requiring energy to be supplied before the reaction can take place. In the case of scattering the only way energy can be supplied is through the kinetic energy of the incoming particle (neutron). Suppose we ask what is minimum energy required for the reaction, the threshold energy? To find this, we look at the situation where no energy is given to the outgoing particle, E_3 ~0 and $\theta \sim 0$. Then (15.5) gives

$$-E^* = -E_{th}\left(\frac{M_4 - M_1}{M_4}\right), \qquad \text{or } E_{th} \sim E^*(1+1/A) \tag{15.9}$$

where we have denoted the minimum value of E_1 as E_{th}. Thus we see the minimum kinetic energy required for reaction is always greater than the excitation energy of the nucleus. Where does the difference between E_{th} and E* go? The answer is that it goes into the center-of-mass energy, the fraction of the kinetic energy of the incoming neutron (in the laboratory coordinate) that is not available for reaction.

Relations between Outgoing Energy and Scattering Angle

We return to the Q-equation for elastic scattering to obtain a relation between the energy of the outgoing neutron, E_3, and the angle of scattering, θ. Again regarding (15.5) as a quadratic equation for the variable $\sqrt{E_3}$, we have

$$E_3 - \frac{2}{A+1}\sqrt{E_1 E_3}\cos\theta - \frac{A-1}{A+1}E_1 = 0 \tag{15.10}$$

with solution in the form,

$$\sqrt{E_3} = \frac{1}{A+1}\sqrt{E_1}\left(\cos\theta + \left[A^2 - \sin^2\theta\right]^{1/2}\right) \tag{15.11}$$

This is a perfectly good relation between E_3 and θ (with E_1 fixed), although it is not a simple one. Nonetheless, it shows a one-to-one correspondence between these two

variables. This is what we meant when we said that the problem is reduced to only degree of freedom. Whenever we are given either E_3 or θ we can immediately determine the other variable. The reason we said that (15.11) is not a simple relation is that we can obtain another relation between energy and scattering angle, except in this case the scattering angle is the angle in the center-of-mass coordinate system (CMCS), whereas θ is the scattering angle in the laboratory coordinate system (LCS). To find this simpler relation we first review the connection the two coordinate systems.

Relation between LCS and CMCS

Suppose we start with the velocities of the incoming neutron and target nucleus, and those of the outgoing neutron and recoiling nucleus as shown in the Fig. 15.2.

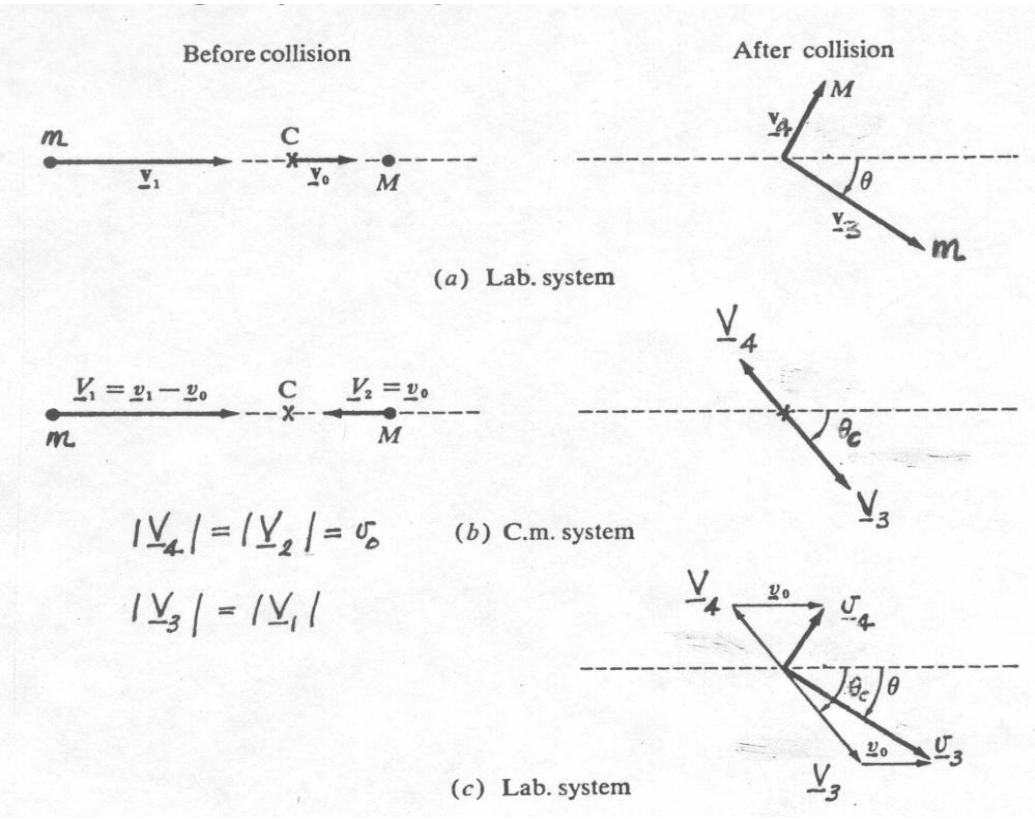

Fig. 15.2. Elastic scattering in LCS (a) and CMCS (b), and the geometric relation between LCS and CMCS post-collision velocity vectors (c).

In this diagram we denote the LCS and CMCS velocities by lower and upper cases respectively, so $\underline{V}_i = \underline{v}_i - \underline{v}_o$, where $\underline{v}_o = [1/(A+1)]\underline{v}_1$ is the velocity of the center-of-mass. Notice that the scattering angle in CMCS is labeled as θ_c. We see that in LCS the center-of-mass moves in the direction of the incoming neutron (with target nucleus at rest), whereas in CMCS the target nucleus moves toward the center-of-mass which is stationary by definition. One can show (in a problem set) that in CMCS the post-collision velocities have the same magnitude as the pre-collision velocities, the only effect of the collision being a rotation, from $\underline{V}_1$ to $\underline{V}_3$, and $\underline{V}_2$ to $\underline{V}_4$.

Part (c) of Fig. 15.1 is particularly useful for deriving relations between LCS and CMCS velocities and angles. Perhaps the most important relation is that between the outgoing speed v_3 and the scattering angle in CMCS , θ_c. We can write

$$\frac{1}{2}mv_3^2 = \frac{1}{2}m(\underline{V}_3 + \underline{v}_o)^2$$

$$= \frac{1}{2}m\left(V_3^2 + v_o^2 + 2V_3 v_o \cos\theta_c\right) \qquad (15.12)$$

or

$$E_3 = \frac{1}{2}E_1\left[(1+\alpha) + (1-\alpha)\cos\theta_c\right] \qquad (15.13)$$

where $\alpha = \left[(A-1)/(A+1)\right]^2$. Compared to (15.11), (15.13) is clearly simpler to manipulate. The two relations must be equivalent since no approximations have been made in either derivation. Taking the square of (15.11) gives

$$E_3 = \frac{1}{(A+1)^2}E_1\left(\cos^2\theta + A^2 - \sin^2\theta + 2\cos\theta\left[A^2 - \sin^2\theta\right]^{1/2}\right) \qquad (15.14)$$

To demonstrate the equivalence of (15.13) and (15.14) one needs a relation between the two scattering angles, θ and θ_c. This can be obtained from Fig. 15.1(c) by writing

$$\cos\theta = \left(v_o + V_3 \cos\theta_c\right)/v_3$$

$$= \frac{1 + A\cos\theta_c}{\sqrt{A^2 + 1 + 2A\cos\theta_c}} \qquad (15.15)$$

The relations (15.13), (15.14), and (15.15) all demonstrate a one-to-one correspondence between energy and angle or angle and angle. They can be used to transform distributions from one variable to another, as we will demonstrate in the discussion of energy and angular distribution of elastically scattered neutrons in the following chapter.

22.101 Applied Nuclear Physics (Fall 2004)

Lecture 18 (11/17/04)

Neutron Interactions: Energy and Angular Distributions, Thermal Motions

---

References:

R. D. Evan, Atomic Nucleus (McGraw-Hill New York, 1955), Chap. 12.

W. E. Meyerhof, *Elements of Nuclear Physics* (McGraw-Hill, New York, 1967), Sec. 3.3.

John R. Lamarsh, *Nuclear Reactor Theory* (Addison-Wesley, Reading, 1966), Chap 2.

We will use the expressions relating energy and scattering angles derived in the previous chapter to determine the energy and angular distributions of an elastically scattered neutron. The energy distribution, in particular, is widely used in the analysis of neutron energy moderation in systems where neutrons are produced at high energies (Mev) by nuclear reactions and slow down to thermal energies. This is the problem of neutron slowing down, where the assumption of the target nucleus being initially at rest is justified. When the neutron energy approaches the thermal region (~ 0.025 ev), the stationary target assumption is no longer valid. One can relax this assumption and derive a more general distribution which holds for neutron elastic scattering at any energy. This then is the result that should be used for the analysis of the spectrum (energy distribution) of thermal neutrons, a problem known as neutron thermalization. As part of this discussion we will have an opportunity to study the energy dependence of the elastic scattering cross section.

We have seen from our study of cross section calculation using the method of phase shift that for low-energy scattering ($kr_o << 1$, which is equivalent to neutron energies below about 10-100 kev) only s-wave contribution to the cross section is important, and moreover, the angular distribution of the scattered neutron is spherically symmetric in CMCS. This is the result that we will make use of in deriving the energy distribution of the elastically scattered neutron.

Energy Distribution of Elastically Scattered Neutrons

We define $P(\underline{\Omega}_c)$ as the probability that the scattered neutron will be going in the direction of the unit vector $\underline{\Omega}_c$ (recall this is a unit vector in angular space). We should also understand that a more physical way of defining P is to say that

$P(\underline{\Omega}_c)d\Omega_c$ = the probability that the neutron will be scattered into an element of solid angle $d\Omega_c$ about $\underline{\Omega}_c$

For s-wave scattering one has therefore

$$P(\underline{\Omega}_c)d\Omega_c = \frac{d\Omega_c}{4\pi} \tag{16.1}$$

Notice that $P(\underline{\Omega}_c)$ is a probability distribution in the two angular variables, φ_c and θ_c, and is properly normalized,

$$\int_0^{2\pi} d\varphi_c \int_0^{\pi} \cos\theta_c d\theta_c P(\underline{\Omega}_c) = 1 \tag{16.2}$$

Since there is a one-to-one relation between θ_c and E_3 (cf. (15.13)), we can transform (16.1) to obtain a probability distribution in the outgoing energy, E_3. To do this we first need to reduce (16.1) from a distribution in two variables to a distribution in the variable θ_c. Let us define $G(\theta_c)$ as the probability of the scattering angle being θ_c. This quantity can be obtained from (16.1) by simply integrating (16.1) over all values of the azimuthal angle φ_c,

$$G(\theta_c)d\theta_c = \int_0^{2\pi} d\varphi P(\underline{\Omega}_c)\sin\theta_c d\theta_c \tag{16.3}$$

$$= \frac{1}{2}\sin\theta_c d\theta_c \tag{16.4}$$

Now we can write down the transformation from G(θ_c) to the energy distribution in the outgoing energy. For the purpose of general discussion our notation system of labeling particles as 1 through 4 is not a good choice. It is more conventional to label the energy of the neutron before and after the collision as either E and E', or vice versa. We will therefore switch notation at this point and let E_1 = E and E_3 = E', and denote the probability distribution for E' as $F(E \to E')$. The transformation between G(θ_c) and $F(E \to E')$ is the same as that for any distribution function,

$$F(E \to E')dE' = G(\theta_c)d\theta_c \tag{16.5}$$

With G(θ_c) given by (16.4) we obtain

$$F(E \to E') = G(\theta_c)\left|\frac{d\theta_c}{dE'}\right| \tag{16.6}$$

The Jacobian of transformation can be readily evaluated from (15.13) after relabeling E_1 and E_3 as E and E'. Thus,

$$F(E \to E') = \frac{1}{E(1-\alpha)} \qquad \alpha E \le E' \le E$$

$$= 0 \qquad \text{otherwise} \tag{16.7}$$

The distribution, which is sketched in Fig. 16.1, is so simple that one can understand completely all its features. The distribution is uniform in the interval (α E, E) because the scattering is spherically symmetric (independence of scattering angle translates into independence of outgoing energy because of the one-to-one correspondence). The fact that the outgoing energy can only lie in a particular interval follows from the range of scattering angle (0, π). Since α depends on the mass of the target, being zero for hydrogen and approaching unity as M >> m, the interval can vary from (0, E) for hydrogen to a vanishing value as A >> 1. In other words, the neutron can lose all its energy in one collision with hydrogen, and loses practically no energy if it collides with a

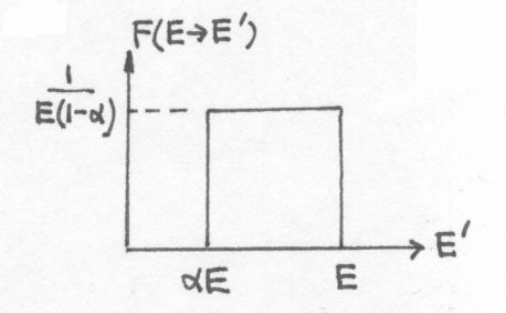

Fig. 16.1. Scattering frequency giving the probability that a neutron elastic scattered at energy E will have an energy in dE' about E'.

very heavy target nucleus. Although simple, the distribution is quite useful for the analysis of neutron energy moderation in the slowing down regime. It also represents a reference behavior for discussing conditions when it is no longer valid to assume the scattering is spherically symmetric in CMCS, or to assume the target nucleus is at rest. We will come back to these two situations later.

Notice that F is a distribution, so its dimension is the reciprocal of its argument, an energy. F is also properly normalized, its integral over the range of the outgoing energy is necessarily unity as required by particle conservation. Knowing the probability distribution F one can construct the energy differential cross section

$$\frac{d\sigma_s}{dE'} = \sigma_s(E)F(E \to E') \tag{16.7}$$

such that

$$\int dE' \frac{d\sigma_s}{dE'} = \sigma_s(E) \tag{16.8}$$

which is the 'total' (in the sense that it is the integral of a differential) scattering cross section. It is important to keep in mind that $\sigma_s(E)$ is a function of the initial (incoming)

neutron energy, whereas the integration in (16.8) is over the final (outgoing) neutron energy. The quantity $F(E \to E')$ is a distribution in the variable E' and also a function of E. We can multiply (16.7) by the number density of the target nuclei N to obtain

$$N\sigma_s(E)F(E \to E') \equiv \Sigma_s(E \to E') \tag{16.9}$$

which is sometimes known as the scattering kernel. As its name suggests, this is the quantity that appears in the neutron balance equation for neutron slowing down in an absorbing medium,

$$\left[\Sigma_s(E) + \Sigma_a(E)\right]\phi(E) = \int_E^{E/\alpha} dE'\,\Sigma_s(E' \to E)\phi(E') \tag{16.10}$$

where $\phi(E) = vn(E)$ is the neutron flux and n(E) is the neutron number density. Eq.(16.10) is an example of the usefulness of the energy differential scattering cross section (16.7).

The scattering distribution $F(E \to E')$ can be used to calculate various energy-averaged quantities pertaining to elastic scattering. For example, the average loss for a collision at energy E is

$$\int_{\alpha E}^{E} dE'(E - E')F(E \to E') = \frac{E}{2}(1 - \alpha) \tag{16.11}$$

For hydrogen the energy loss in a collision is one-half its energy before the collision, whereas for a heavy nucleus it is ~ 2E/A.

Angular Distribution of Elastically Scattered Neutrons

We have already made use of the fact that for s-wave scattering the angular distribution is spherically symmetric in CMCS. This means that the angular differential scattering cross section in CMCS if of the form

$$\frac{d\sigma_s}{d\Omega_c} = \sigma_s(\theta_c) \equiv \sigma_s(E)\frac{1}{4\pi} \tag{16.12}$$

One can ask what is the angular differential scattering cross section in LCS? The answer can be obtained by transforming the results (16.12) from a distribution in the unit vector $\underline{\Omega}_c$ to a distribution in $\underline{\Omega}$. As before (cf. (16.5)) we write

$$\sigma_s(\theta)d\Omega = \sigma_s(\theta_c)d\Omega_c \tag{16.13}$$

or

$$\sigma_s(\theta) = \sigma_s(\theta_c)\frac{\sin\theta_c}{\sin\theta}\frac{d\theta_c}{d\theta} \tag{16.14}$$

From the relation between $\cos\theta$ and $\cos\theta_c$, (15.15), we can calculate

$$\frac{d(\cos\theta)}{d(\cos\theta_c)} = \frac{\sin\theta_c d\theta_c}{\sin\theta d\theta}$$

Thus

$$\sigma_s(\theta) = \frac{\sigma_s(E)}{4\pi}\frac{\left(\gamma^2 + 2\gamma\cos\theta_c + 1\right)^{3/2}}{1+\gamma\cos\theta_c} \tag{16.15}$$

with γ = 1/A. Since (16.15) is a function of θ, the factor $\cos\theta_c$ on the right hand side should be expressed in terms of $\cos\theta$ in accordance with (15.15). The angular distribution in LCS, as given by (16.15), is somewhat too complicated to sketch simply. From the relation between LCS and CMCS indicated in Fig. 15.2, we can expect that if the distribution is isotropic in LCS, then the distribution in CMCS should be peaked in the forward direction (simply because the scattering angle in LCS is always than the angle in CMCS). One way to demonstrate that this is indeed the case is to calculate the average value of $\mu = \cos\theta$,

$$\bar{\mu} = \frac{\int d\Omega \cos\theta \sigma_s(\theta)}{\int d\Omega \sigma_s(\theta)} = \frac{\int_{-1}^{1} d\mu \mu \sigma_s(\mu)}{\int_{-1}^{1} d\mu \sigma_s(\mu)} = \frac{\int_{-1}^{1} d\mu_c \mu(\mu_c) \sigma_s(\mu_c)}{\int_{-1}^{1} d\mu_c \sigma_s(\mu_c)} = \frac{2}{3A} \qquad (16.16)$$

The fact that $\bar{\mu} > 0$ means that the angular distribution is peaked in the forward direction. This bias becomes less pronounced the heavier the target mass; for A >> 1 the distinction between LCS and CMCS vanishes.

Assumptions in Deriving $F(E \to E')$

In arriving at the scattering distribution (also sometimes called the scattering frequency), (16.7), we have made use of three assumptions, namely,

(i) elastic scattering

(ii) target nucleus at rest

(iii) scattering is isotropic in CMCS (s-wave)

These assumptions imply certain restrictions pertaining to the energy of incoming neutron E and the temperature of the scattering medium. Assumption (i) is valid provided the neutron energy is not high enough to excite the nuclear levels of the compound nucleus formed by the target nucleus plus the incoming neutron. On the other hand, if the neutron energy is high to excite the first nuclear energy level above the ground state, then inelastic scattering becomes energetically possible, Inelastic scattering is a threshold reaction (Q < 0), it can occur in heavy nuclei at E ~ 0.05 – 0.1 Mev, or in medium nuclei at ~ 0.1 – 0.2 Mev. Typically the cross section for inelastic scattering, $\sigma(n,n')$, is of the order of 1 barn or less. In comparison elastic scattering, which is always present no matter what other reactions can take place, is of order 5 – 10 barns except in the case of hydrogen where it is 20 barns as we have previously discussed.

Assumption (ii) is valid when the neutron energy is large compared to the kinetic energy of the target nucleus, typically taken to $k_B T$ assuming the medium is in equilibrium at temperature T. This would be the case for neutron energies ~ 0.1 ev and above. When the incident neutron energy is comparable to the energy of the target

nucleus, the assumption of stationary target is clearly invalid. To take into account the thermal motions of the target, one should know what is the state of the target since the nuclear (atomic) motions in solids are different from those in liquids, vibrations in the former and diffusion in the latter. If we assume the scattering medium can be treated as a gas at temperature T, then the target nucleus moves in a straight line with a speed that is given by the Maxwellian distribution. In this case one can derive the scattering distribution which is an extension of (16.7) [see, for example, G. I. Bell and S. Glasstone, *Nuclear Reactor Theory* (Van Nostrand reinhold, New York 1970), p. 336]. We do not go into the details here except to show the qualitative behavior in Fig. 16.2. From the way the scattering distribution changes with incoming energy E one can get a good intuitive feeling for how the more general $F(E \to E')$ evolves from a spread-out distribution (the curves for E = k_BT) to the more restricted form given by (16.7).

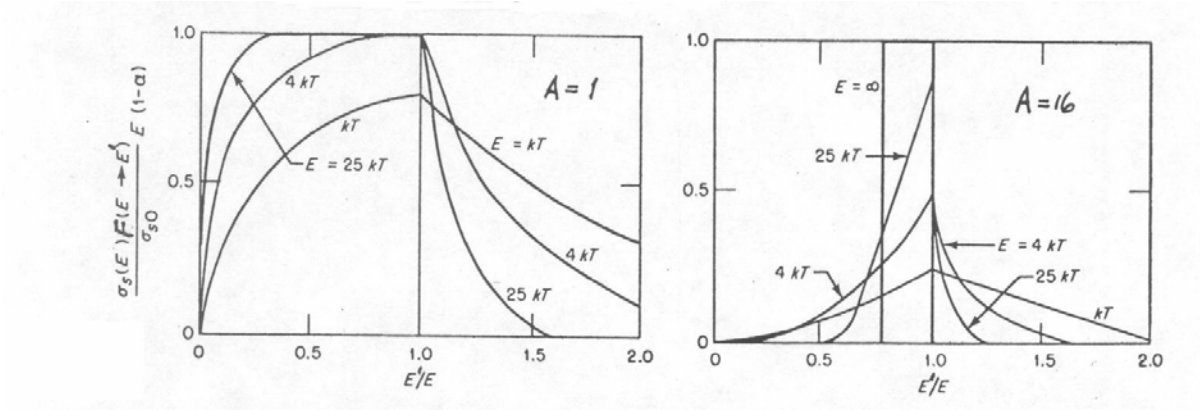

Fig. 16.2. Energy distribution of elastically scattered neutrons in a gas of nuclei with mass A = M/m at temperature T. (from Bell and Glasstone)

Notice that for E ~ k_BT there can be appreciable upscattering which is not possible when assumption (ii) is invoked. As E becomes larger compared to k_BT, upscattering becomes less important. The condition of stationary nucleus also means that E >> k_BT.

When thermal motions have to be taken into account, the scattering cross section $\sigma_s(E)$ is also changed; it is no longer a constant, $4\pi a^2$, where a is the scattering length. This occurs in the energy region of neutron thermalization; it covers the range (0, 0.1 -

0.5 ev). We will now discuss the energy dependence of $\sigma_s(E)$. For the case of the scattering medium being a gas of atoms with mass A and at temperature T, it is still relatively straightforward to work out the expression for $\sigma_s(E)$. We will give the essential steps to give the student some feeling for the kind of analysis that one can carry out even for more complicated situations such as neutron elastically in solids and liquids.

Energy Dependence of Scattering Cross Section $\sigma_s(E)$

When the target nucleus is not at rest, one can write down the expression for the elastic scattering cross section measured in the laboratory (we will call it the measured cross section),

$$v\sigma_{meas}(v) = \int d^3V |\underline{v} - \underline{V}| \sigma_{theo}(|\underline{v} - \underline{V}|) P(\underline{V}, T) \tag{16.17}$$

where v is the neutron speed in LCS, $\underline{V}$ is the target nucleus velocity in LCS, σ_{theo} is the scattering cross section we calculate theoretically, such as what we had previously studied using the phase-shift method and solving the wave equation for an effective one-body problem (notice that the result is a function of the relative speed between neutron and target nucleus), and P is the thermal distribution of the target nucleus velocity which depends on the temperature of the medium. Eq.(16.17) is a general relation between what is calculated theoretically, in solving the effective one-body problem, and what is measured in the laboratory where one necessarily has only an average over all possible target nucleus velocities. What we call the scattering cross section $\sigma_s(E)$ we mean σ_{meas}. It turns out that we can reduce (16.17) further by using for P the Maxwellian distribution and obtain the result

$$\sigma_s(v) = \frac{\sigma_{so}}{\beta^2}\left[\left(\beta^2 + \frac{1}{2}\right) erf(\beta) + \frac{1}{\sqrt{\pi}}\beta e^{-\beta^2}\right] \tag{16.18}$$

where $erf(x)$ is the error function integral

$$erf(x) = \frac{2}{\sqrt{\pi}} \int_0^x dt e^{-t^2} \tag{16.19}$$

and $\beta^2 = AE / k_B T$, and $E = mv^2 / 2$. Given that the error function has the limiting behavior for small and large arguments,

$$erf(x) \sim \frac{2}{\sqrt{\pi}} \left(x - \frac{x^3}{3} + ...\right) \qquad \text{x << 1}$$

$$1 - \frac{e^{-x^2}}{x\sqrt{\pi}} \left(1 - \frac{1}{2x^2} + ...\right) \qquad \text{x >> 1} \tag{16.20}$$

we obtain

$$\sigma_s(v) \sim \sigma_{so} / v \qquad \beta << 1 \tag{16.21}$$

$$\sigma_s(v) \sim \sigma_{so} \qquad \beta >> 1 \tag{16.22}$$

The physical significance of this calculation is that one sees two limiting behavior for the elastic scattering cross section, a 1/v behavior at low energy (or how temperature) and a constant behavior at high energy. The expression (16.18) is therefore a useful expression giving the energy variation of the scattering cross section over the entire energy range from thermal to Mev, so far as elastic scattering is concerned. On the other hand, this result has been obtained by assuming the target nuclei move as in a gas of noninteracting atoms. This assumption is not realistic when the scattering medium is a solid or a liquid. For these situations one can also work out the expressions for the cross section, but the results are more complicated (and beyond the scope of this course). We will therefore settle for a brief, qualitative look at what new features can be seen in the energy dependence of the elastic scattering cross sections of typical solids (crystals) and liquids.

Fig. 16.3 shows the total and elastic scattering cross sections of graphite (C^{12}) over the entire energy range of interest to this class. At the very low-energy end we see a number of features we have not discussed previously. These all have to do with the fact that the target nucleus (atom) is bound to a crystal lattice and therefore the positions of the nuclei are fixed to well-defined lattice sites and their motions are small-amplitude vibrations about these sites. There is a sharp drop of the cross section below an energy marked Bragg cutoff. Cutoff here refers to Bragg reflection which occurs when the condition for constructive interference (reflection) is satisfied, a condition that depends on the wavelength of the neutron (hence its energy) and the spacing between the lattice planes in the crystal. When the wavelength is too long (energies below the cutoff) for Bragg condition to be satisfied, the cross section drops sharply. What is then left is the interaction between the neutron and the vibrational motions of the nuclei, this process involves the transfer of energy from the vibrations to the neutron which has much lower energy. Since there is more excitation of the vibrational modes at higher temperatures, this is reason why the cross section below the Bragg cutoff is very sensitive to temperature, increasing with increasing T.

Above the Bragg cutoff the cross section shows some oscillations. These correspond to the onset of additional reflections by planes which have smaller spacings. At energies around kBT the cross section smooths out to a constant and remains constant up to ~ 0.3 Mev. This is the region where our previous calculation of cross section would apply. Between 0.3 and 1 Mev the scattering cross section decreases gradually, a behavior which we can still understand using simple theory (beyond what we had discussed). Above 1 Mev one sees scattering resonances, a form which we have not yet discussed, and also there is now a difference between total and scattering cross sections (which should be attributed to absorption).

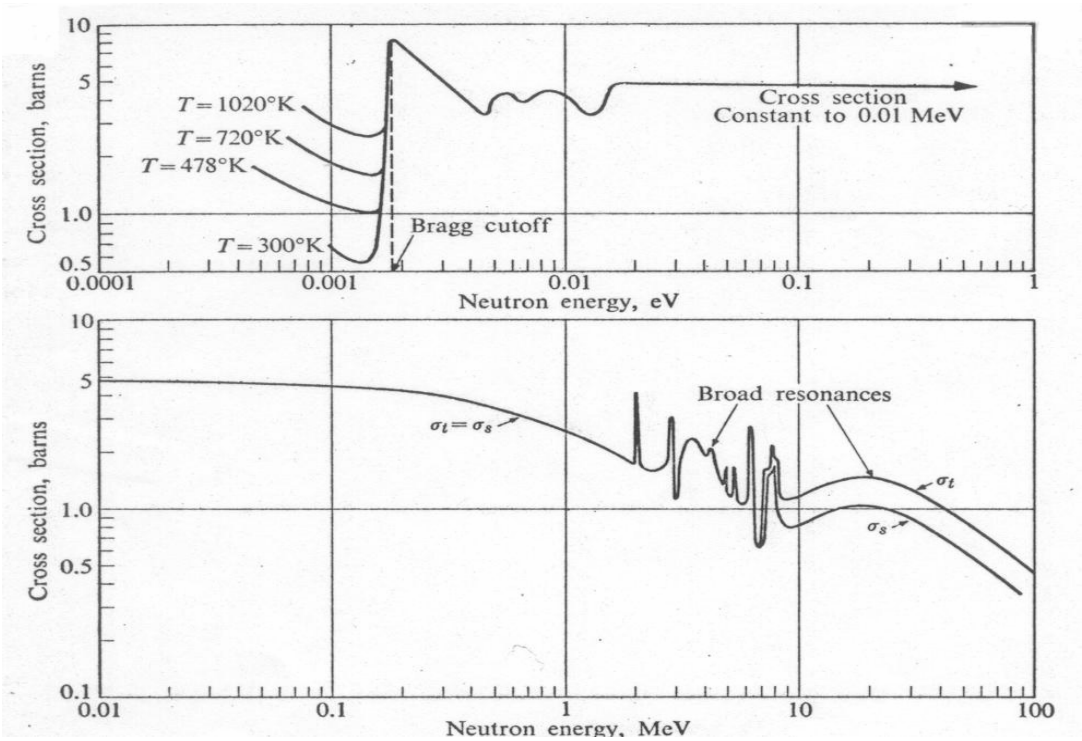

Fig. 16.3. Total and elastic scattering cross sections of C^{12} in the form of graphite. (from Lamarsh).

Fig. 16.4 shows the measured total cross section of H_2O in the form of water. The cross section is therefore the sum of contributions from two hydrogen and an oxygen. Compared to Fig. 16.3 the low-energy behavior is quite different. This is not unexpected since a crystal and a liquid are really very different with regard to their atomic structure and atomic motions. In this case the cross section rises from a constant value at energies above 1 ev in a manner like the 1/v behavior given by (16.21). Notice that the constant value of about 45 barns is just what we know from the hydrogen cross section σ_{so} of 20 barns per hydrogen and a cross section of about 5 barns for oxygen.

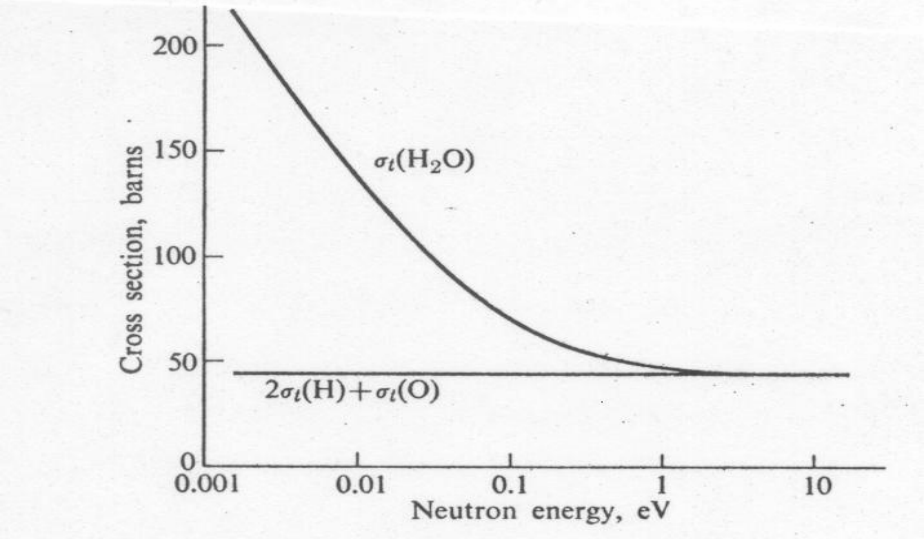

Fig. 16.4. Total cross section of water. (from Lamarsh)

The importance of hydrogen (water) in neutron scattering has led to another interpretation of the rise of the cross section with decreasing neutron energy, one which focuses on the effect of chemical binding. The idea is that at high energies (relative to thermal) the neutron does not see the water molecule. Instead it sees only the individual nuclei as targets which are free-standing and essentially at rest. In this energy range (1 ev and above) the interaction is the same as that between a neutron and free protons and oxygen nuclei. This is why the cross section is just the sum of the individual contributions. When the cross section starts to rise as the energy decreases, this is an indication that the chemical binding of the protons and oxygen in a water molecule becomes to have an effect, to the extent that when the neutron energy is at k_BT the neutron now sees the entire water molecule rather than the individual nuclei. In that case the scattering is effectively between a neutron and a water molecule. What this amounts to is that as the neutron energy decreases the target changes from individual nuclei with their individual mass to a water molecule with mass 18. Now one can show that the scattering cross section is actually proportional to the square of the reduced mass of the scatterer μ,

$$\sigma_s \propto \mu^2 = \left(\frac{mM}{m+M}\right)^2 = \left(\frac{A}{A+1}\right)^2 \qquad (16.23)$$

Thus one can define a *free-atom* cross section appropriate for the energy range where the cross section is a constant, and a *bound-atom* cross section for the energy range where the cross section is rising, with the relation

$$\sigma_{free} = \sigma_{bound}\left(\frac{A}{A+1}\right)^2 \tag{16.24}$$

For hydrogen these two cross sections would have the values of 20 barns and 80 barns respectively.

We will end this chapter with a brief consideration of assumption (iii) used in deriving (16.7). When the neutron energy is in the 10 Kev range and higher, the contributions from the higher angular momentum (p-wave and above) scattering may become significant. In that case we know the angular distribution will be more forward peaked. This means one should replace (16.1) by a different form of $P(\underline{\Omega}_c)$. Without going through any more details, we show in Fig. 16.5 the general behavior that one can expect in the scattering distribution F when scattering in CMCS is no longer isotropic.

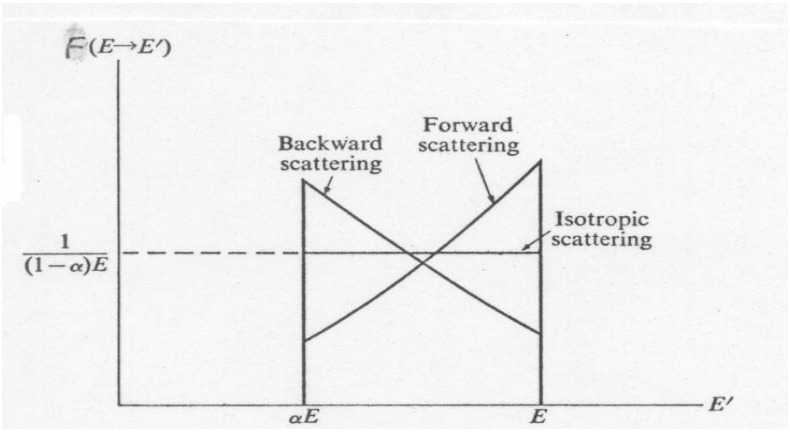

Fig. 16.5. Energy distribution of elastically scattered neutrons by a stationary nucleus. (from Lamarsh)

22.101 Applied Nuclear Physics (Fall 2004)

Lecture 19 (11/22/04)

Gamma Interactions: Compton Scattering

References:

R. D. Evan, Atomic Nucleus (McGraw-Hill New York, 1955), Chaps 23 – 25..

W. E. Meyerhof, *Elements of Nuclear Physics* (McGraw-Hill, New York, 1967), pp. 91-108.

W. Heitler, *Quantum Theory of Radiation* (Oxford, 1955), Sec. 26.

We are interested in the interactions of gamma rays, electromagnetic radiations produced by nuclear transitions. These are typically photons with energies in the range of ~ 0.1 – 10 Mev. The attenuation of the intensity of a beam of gamma rays in an absorber, sketched in Fig. 17.1, follows a true exponential variation with the distance of penetration, which is unlike that of charged particles,

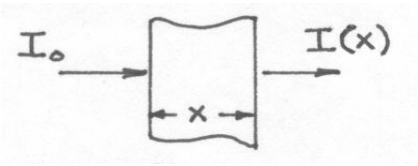

Fig. 17.1. Attenuation of a beam of gamma radiation through an absorber of thickness x.

$$I(x) = I_o e^{-\mu x} \tag{17.1}$$

The interaction is expressed through the linear attenuation coefficient μ which does not depend on x but does depend on the energy of the incident gamma. By attenuation one means either scattering or absorption. Since either process will remove the gamma from the beam, the probability of penetrating a distance x is the same as the probability of traveling a distance x without any interaction, exp(- μ x). The attenuation coefficient is

therefore the *probability per unit path* of interaction; it is what we would call the macroscopic cross section Σ in the case of neutron interaction.

There are several different processes of gamma interaction. Each process can be treated as occurring independently of each other; for this reason μ is the sum of the individual contributions. These contributions, of course, are not equally important at any given energy. Each process has its own energy variation as well as dependence on the atomic number of the absorber . We will focus our discussions on the three most important processes of gamma interaction, Compton scattering, photoelectric effect, and pair production. These can be classified by object with which the photon interacts and the type of process (absorption or scattering). As shown in the matrix below, photoelectric is the absorption of a photon followed by the ejection of an atomic electron. Compton scattering is inelastic (photon loses energy) relativistic scattering by a free electron. Implication here is that the photon energy is at least comparable to the rest mass energy of the electron. When the photon energy is much lower than the rest mass energy, the scattering by a free electron becomes elastic (no energy loss). This is the low-energy limit of Compton scattering, a process known as Thomson scattering. When the photon energy is greater than twice the rest mass energy of electron, the photon can absorbed and an electron-positron pair is emitted. This process is called pair production. Other combinations of interaction and process in the matrix (marked x) could be discussed, but they are of no interest to this class.

Interaction with \	absorption	elastic scattering	inelastic scattering
atomic electron	*photoelectric*	*Thomson*	*Compton*
nucleus	x	x	x
electric field around the nucleus	*pair production*	x	x

Given what we have just said, the attenuation coefficient becomes

$$\mu = \mu_C + \mu_\tau + \mu_\kappa \qquad (17.1)$$

where the subscripts C, τ, and κ denote Compton scattering, photoelectric effect, and pair production respectively.

Compton Scattering

The treatment of Compton scattering is similar to our analysis of neutron scattering in several ways. This analogy should be noted by the student as the discussion unfolds here. The phenomenon is the scattering of a photon with incoming momentum $\hbar\underline{k}$ by a free, stationary electron, which is treated relativistically. After scattering at angle θ, the photon has momentum $\hbar\underline{k}'$, while the electron moves off at an angle φ with momentum $\underline{p}$ and kinetic energy T, as shown in Fig. 17.1.

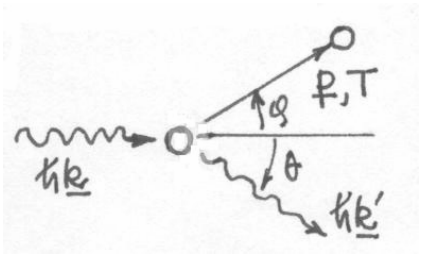

Fig. 17.1. Schematic of Compton scattering at angle θ with momentum and energy transferred to the free electron.

To analyze the kinematics we write the momentum and energy conservation equations,

$$\hbar\underline{k} = \hbar\underline{k}' + \underline{p} \tag{17.2}$$

$$\hbar ck = \hbar ck' + T \tag{17.3}$$

where the relativistic energy-momentum relation for the electron is

$$cp = \sqrt{T\left(T = 2m_e c^2\right)} \tag{17.4}$$

with c being the speed of light. One should also recall the relations, $\omega = ck$ and $\lambda\nu = c$, with ω and ν being the circular and linear frequency, respectively ($\omega = 2\pi\nu$), and λ the wavelength of the photon. By algebraic manipulations one can obtain the following results.

$$\lambda' - \lambda = \frac{c}{\nu'} - \frac{c}{\nu} = \frac{h}{m_e c}(1 - \cos\theta) \tag{17.5}$$

$$\frac{\omega'}{\omega} = \frac{1}{1 + \alpha(1 - \cos\theta)} \tag{17.6}$$

$$T = \hbar\omega - \hbar\omega' = \hbar\omega \frac{\alpha(1 - \cos\theta)}{1 + \alpha(1 - \cos\theta)} \tag{17.7}$$

$$\cot\varphi = (1 + \alpha)\tan\frac{\theta}{2} \tag{17.8}$$

In (17.5) the factor $h/m_e c = 2.426 \times 10^{-10}$ cm is called the Compton wavelength. The gain in wavelength after scattering at an agle of θ is known as the Compton shift. This shift in wavelength is independent of the incoming photon energy, whereas the shift in energy (17.7) is dependent on energy. In (17.6) the parameter $\alpha = \hbar\omega / m_e c^2$ is a measure of the photon energy in units of the electron rest mass energy (0.511 Mev). As $\alpha \to 1$, $\omega' \to \omega$ and the process goes from inelastic to elastic. Low-energy photons are scattered with only a moderate energy change, while high-energy photons suffer large energy change. For example, at $\theta = \pi/2$, if $\hbar\omega$ = 10 kev, then $\hbar\omega'$ = 9.8 kev (2% change), but if $\hbar\omega$ = 10 Mev, then $\hbar\omega'$ = 0.49 Mev (20-fold change).

Eq.(17.7) gives the energy of the recoiling electron which is of interest because it is often the quantity that is measured in Compton scattering. In the limit of energetic gammas, α >> 1, the scattered gamma energy becomes only a function of the scattering

angle; it is a minimum for backward scattering ($\theta = \pi$), $\hbar\omega' = m_e c^2 / 2$, while for 90o scattering $\hbar\omega' = m_e c^2$. The maximum energy transfer is given (17.7) with $\theta = \pi$,

$$T_{\max} = \frac{\hbar\omega}{1 + \frac{1}{2\alpha}} \tag{17.9}$$

Klein-Nishina Cross Section

The proper derivation of the angular differential cross section for Compton scattering requires a quantum mechanical calculation using the Dirac's relativistic theory of the electron. This was first published in 1928 by Klein and Nishina [for details, see W. Heitler]. We will simply quote the formula and discuss some of its implications. The cross section is

$$\frac{d\sigma_C}{d\Omega} = \frac{r_e^2}{4}\left(\frac{\omega'}{\omega}\right)^2\left[\frac{\omega}{\omega'} + \frac{\omega'}{\omega} - 2 + 4\cos^2\Theta\right] \tag{17.10}$$

where Θ is the angle between the electric vector $\underline{\varepsilon}$ (polarization) of the incident photon and that of the scattered photon, $\underline{\varepsilon}'$. The diagrams shown in Fig. 17.2 are helpful in visualizing the various vectors involved. Recall that a photon is an electromagnetic wave

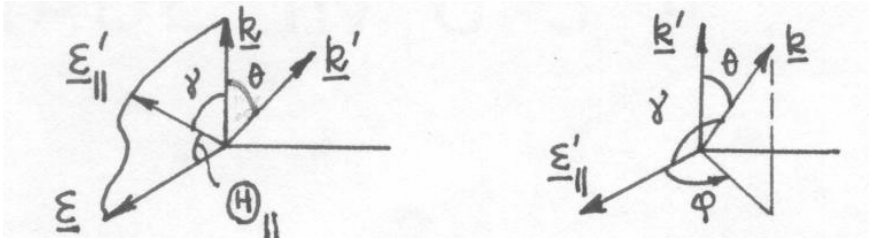

Fig. 17.2. Angular relations among incoming and outgoing wave vectors, $\underline{k}$ and $\underline{k}'$, of the scattered photon, and the electric vectors, $\underline{\varepsilon}$ and $\underline{\varepsilon}'$, which are transverse to the corresponding wave vectors.

characterized by a wave vector $\underline{k}$ and an electric vector $\underline{\varepsilon}$ which is perpendicular to $\underline{k}$. For a given incident photon with $(\underline{k}, \underline{\varepsilon})$, shown above, we can decompose the scattered photon electric vector $\underline{\varepsilon}'$ into a component $\underline{\varepsilon}'_{\perp}$ perpendicular to the plane containing $\underline{k}$ and $\underline{\varepsilon}$, and a parallel component $\underline{\varepsilon}'_{\text{II}}$ which lies in this plane. For the perpendicular component $\cos\Theta_{\perp} = 0$, and for the parallel component we notice that

$$\cos\gamma = \cos\left(\frac{\pi}{2} - \Theta_{\text{II}}\right) = \sin\Theta_{\text{II}} = \sin\theta\cos\varphi \tag{17.11}$$

Therefore,

$$\cos^2\Theta = 1 - \sin^2\theta\cos^2\varphi \tag{17.12}$$

The decomposition of the scattered photon electric vector means that the angular differential cross section can be written as

$$\frac{d\sigma_C}{d\Omega} = \left(\frac{d\sigma_C}{d\Omega}\right)_{\perp} + \left(\frac{d\sigma_C}{d\Omega}\right)_{\text{II}}$$

$$= \frac{r_e^2}{2}\left(\frac{\omega'}{\omega}\right)^2\left[\frac{\omega}{\omega'} + \frac{\omega'}{\omega} - 2\sin^2\theta\cos^2\varphi\right] \tag{17.14}$$

This is because the cross section is proportional to the total scattered intensity which in turn is proportional to $(\underline{\varepsilon}')^2$. Since $\underline{\varepsilon}'_{\perp}$ and $\underline{\varepsilon}'_{\text{II}}$ are orthogonal, $(\underline{\varepsilon}')^2 = (\underline{\varepsilon}'_{\perp})^2 + (\underline{\varepsilon}'_{\text{II}})^2$ and the cross section is the sum of the contributions from each of the components.

In the low-energy (non-relativistic) limit, $\hbar\omega << m_e c^2$, we have $\omega' \approx \omega$, then

$$\left(\frac{d\sigma_C}{d\Omega}\right)_{\perp} \sim 0, \qquad \left(\frac{d\sigma_C}{d\Omega}\right)_{\text{II}} \sim r_e^2\left(1 - \sin^2\theta\cos^2\varphi\right) \tag{17.15}$$

This means that if the incident radiation is polarized (photons have a specific polarization vector), then the scattered radiation is also polarized. But if the incident radiation is unplolarized, then we have to average $d\sigma_C / d\Omega$ over all the allowed directions of $\underline{\varepsilon}$ (remember $\underline{\varepsilon}$ is perpendicular to $\underline{k}$). Since $d\sigma_C / d\Omega$ depends only on angles θ and φ, we can obtain the result for *unpolarized* radiation by averaging over φ. Thus,

$$\left(\frac{d\sigma_C}{d\Omega}\right)_{unpol} = \frac{1}{2\pi}\int_0^{2\pi} d\varphi \left(\frac{d\sigma_C}{d\Omega}\right)_{\text{II}}$$

$$= \frac{r_e^2}{2}\left(1+\cos^2\theta\right) \tag{17.16}$$

with $r_e \equiv e^2/m_e c^2$ = 2.818 x 10^{-13} cm, the classical radius of the electron (cf. (14.1)). This is a well-known expression for the angular differential cross section for Thomson scattering. Integrating this over all solid angles gives

$$\sigma_C = \int d\Omega \left(\frac{d\sigma_C}{d\Omega}\right)_{unpol} = \frac{8\pi}{3} r_e^2 \equiv \sigma^o \tag{17.17}$$

which is known as the Thomson cross section.

Returning to the general result (17.14) we have in the case of unpolarized radiation,

$$\frac{d\sigma_C}{d\Omega} = \frac{r_e^2}{2}\left(\frac{\omega'}{\omega}\right)^2\left(\frac{\omega}{\omega'}+\frac{\omega'}{\omega}-\sin^2\theta\right) \tag{17.18}$$

We can rewrite this result in terms of α and $\cos\theta$ by using (17.6),

$$\frac{d\sigma_C}{d\Omega} = \frac{r_e^2}{2}\left(1+\cos^2\theta\right)\left(\frac{1}{1+\alpha(1-\cos\theta)}\right)^2\left[1+\frac{\alpha^2(1-\cos\theta)^2}{(1+\cos^2\theta)\left[1+\alpha(1-\cos\theta)\right]}\right] \tag{17.19}$$

The behavior of $d\sigma_C / d\Omega$ is shown in Fig. 17.3. Notice that at any given α the angular distribution is peaked in the forward direction. As α increases, the forward peaking becomes more pronounced. The deviation from Thomson scattering is largest at large scattering angles; even at $\hbar\omega \sim$ 0.1 Mev the assumption of Thomson scattering is not

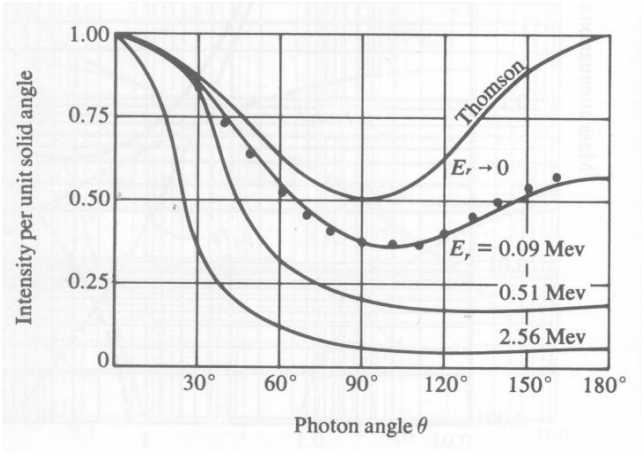

Fig. 17.3. Angular distribution of Compton scattering at various incident energies E_r. All curves are normalized at 0^o. Note the low-energy limit of Thomson scattering. (from Heitler)

valid. In practice the Klein-Nishina cross section has been found to be in excellent agreement with experiments at least out to $\hbar\omega = 10 m_e c^2$.

To find the total cross section per electron for Compton scattering, one can integrate (17.19) over solid angles. The analytical result is given in Evans, p. 684. We will note only the two limiting cases,

$$\frac{\sigma_C}{\sigma^o} = 1 - 2\alpha + \frac{26}{5}\alpha^2 - \ldots \qquad \alpha << 1$$

$$= \frac{3}{8}\frac{m_e c^2}{\hbar\omega}\left[\ell n \frac{2\hbar\omega}{m_e c^2} + \frac{1}{2}\right] \qquad \alpha >> 1 \tag{17.20}$$

We see that at high energies ($\geq$ 1 Mev) the Compton cross section decreases with energy like $1/\hbar\omega$.

Collision, Scattering and Absorption Cross Sections

In discussing the Compton effect a distinction should be made between collision and scattering. Here collision refers to ordinary scattering in the sense of removal of the photon from the beam. This is what we have been discussing above. Since the electron recoils, not all the original energy $\hbar\omega$ is scattered, only a fraction ω'/ω is. Thus one can define a *scattering* cross section,

$$\frac{d\sigma_{sc}}{d\Omega} = \frac{\omega'}{\omega}\frac{d\sigma_C}{d\Omega} \tag{17.21}$$

This leads to a slightly different total cross section,

$$\frac{\sigma_{sc}}{\sigma^o} \sim 1 - 3\alpha + 9.4\alpha^2 - \ldots \qquad \alpha << 1 \tag{17.22}$$

Notice that in the case of Thomson scattering all the energy is scattered and none are absorbed. The difference between σ_C and σ_{sc} is called the Compton *absorption* cross section.

Energy Distribution of Compton Electrons and Photons

We have been discussing the angular distribution of the Compton scattered photons in terms of $\frac{d\sigma_C}{d\Omega}$. To transform the angular distribution to an energy distribution we need first to reduce the angular distribution of two angle variables, θ and φ, to a distribution in θ (in the same way as we had done in Chapter 15). We therefore define

$$\frac{d\sigma_C}{d\theta} = \int_0^{2\pi} d\varphi \frac{d\sigma_C}{d\Omega}\sin\theta = \frac{d\sigma_C}{d\Omega} 2\pi \sin\theta \tag{17.23}$$

and write

$$\frac{d\sigma_C}{d\omega'} = \frac{d\sigma_C}{d\theta}\left|\frac{d\theta}{d\omega'}\right| \tag{17.24}$$

with ω' and θ being related through (17.6). Since we can also relate the scattering angle θ to the angle of electron recoil ϕ through (17.8), we can obtain the distribution of electron energy by performing two transformations, from θ to ϕ first, then from ϕ to T by using the relation

$$T = \hbar\omega \frac{2\alpha \cos^2\phi}{(1+\alpha)^2 - \alpha^2 \cos^2\phi} \tag{12.24}$$

as found by combining (17.7) and (17.8). Thus,

$$\frac{d\sigma_C}{d\Omega_e} 2\pi \sin\phi d\phi = \frac{d\sigma_C}{d\Omega} 2\pi \sin\theta d\theta \tag{12.25}$$

$$\frac{d\sigma_C}{d\phi} = \frac{d\sigma_C}{d\Omega_e} 2\pi \sin\phi \tag{12.26}$$

$$\frac{d\sigma_C}{dT} = \frac{d\sigma_C}{d\phi}\left|\frac{d\phi}{dT}\right| \tag{12.27}$$

These results show that all the distributions are related to one another. In Fig. 17.4 we show several calculated electron recoil energy distributions which can be compared with the experimental data shown in Fig. 17.5.

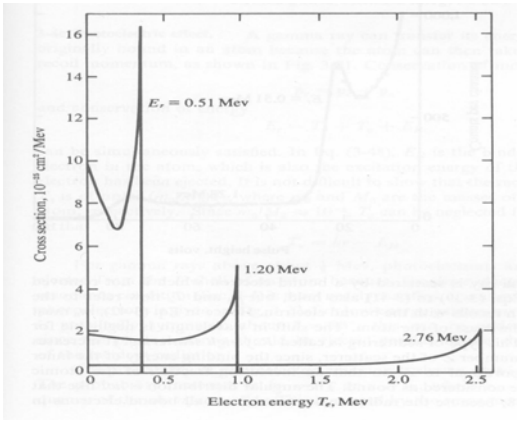

Fig. 17.4. Energy distribution of Compton electrons for several incident gamma-ray energies. (from Meyerhof)

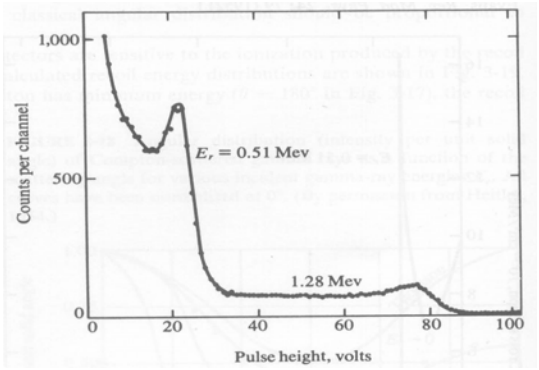

Fig. 17.5. Pulse-height spectra of Compton electrons produced by 0.51- and 1.28-Mev gamma rays. (from Meyerhof)

For a given incident gamma energy the recoil energy is maximum at $\theta = \pi$, where $\hbar\omega'$ is smallest. We had seen previously that if the photon energy is high enough, the outgoing photon energy is a constant at ~0.255 Mev. In Fig. 17.4 we see that for incident photon energy of 2.76 Mev the maximum electron recoil energy is approximately 2.53 Mev, which is close to the value of (2.76 – 0.255). This correspondence should hold even better at higher energies, and not as well at lower energies, such as 1.20 and 0.51 Mev.

We can also see by comparing Figs. 17.4 and 17.5 that the relative magnitudes of the distributions at the two lower incident energies match quite well between calculation and experiment. The distribution peaks near the cutoff T_{max} because there is an appreciable range of θ near $\theta = \pi$, where $\cos\theta \sim 1$ (cosine changes slowly in this region) and so $\hbar\omega'$ remains close to $m_e c^2/2$. This feature is reminiscent of the Bragg curve depicting the specific ionization of a charged particle (Fig. (14.3)).

From the electron energy distribution $\frac{d\sigma_C}{dT}$ we can deduce directly the photon energy distribution $\frac{d\sigma_C}{d\omega'}$ from

$$\frac{d\sigma_C}{d\omega'} = \frac{d\sigma_C}{dT}\left|\frac{dT}{d\omega'}\right| = \hbar\frac{d\sigma_C}{dT} \tag{12.28}$$

since $\hbar\omega' = \hbar\omega - T$.

22.101 Applied Nuclear Physics (Fall 2004)

Lecture 21 (11/29/04)

Gamma Interactions: Photoelectric Effect and Pair Production

References:

R. D. Evan, Atomic Nucleus (McGraw-Hill New York, 1955), Chaps 24, 25.

W. E. Meyerhof, *Elements of Nuclear Physics* (McGraw-Hill, New York, 1967), pp. 91-108.

W. Heitler, *Quantum Theory of Radiation* (Oxford, 1955), Sec. 26.

Photoelectric Effect

This is the predominant mode of γ - interaction in all medium, especially high-Z absorbers, at energies less than ~ 0.1 Mev. The process, sketched in Fig. 18. 1, is the interaction between the gamma and the entire atom (atomic electron cloud) that results in the absorption of the gamma and the ejection of an electron with kinetic energy

$$T \sim \hbar\omega - B_e \tag{18.1}$$

where B_e is the electron binding energy. The recoiling atom is left in an excited state at an excitation energy of B_e; it can de-excite by emitting x-rays or Auger electrons.

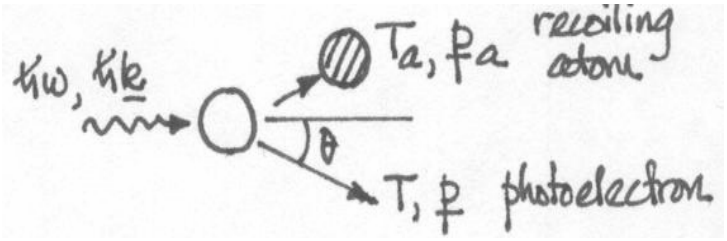

Fig. 18.1. Schematic of photoelectric effect, absorption of an incident gamma ray which results in the ejection of an atomic electron and excitation of the recoiling atom.

Notice this is atomic and not nuclear excitation. One can show that the incident γ cannot be totally absorbed by a free electron because momentum and energy conservations cannot be satisfied simultaneously, but total absorption can occur if the electron is initially bound in an atom. The most tightly bound electrons have the greatest probability of absorbing the γ. It is known theoretically and experimentally that ~ 80% of the absorption occurs in the K (innermost) shell, so long as $\hbar\omega > B_e(K-shell)$. Typical ionization potentials of K electrons are 2.3 kev ($A\ell$), 10 kev (Cu), and ~ 100 kev (Pb).

The conservations equations for photoelectric effect are

$$\hbar\underline{k} = \underline{p} + \underline{p}_a \tag{18.2}$$

$$\hbar\omega = T + T_a + B_e \tag{18.3}$$

where $\underline{p}_a$ is the momentum of the recoiling atom whose kinetic energy is T_a. Since T_a ~ $T(m_e/M)$, where M is the mass of the atom, one can usually ignore T_a.

The theory describing the photoelectric effect is essentially a first-order perturbation theory calculation (cf. Heitler, Sec. 21). In this case the transition taking place is between an initial state consisting of two particles, a bound electron, wave function ~ $e^{-r/a}$, with $a = a_o/Z$, a_o being the Bohr radius (= $\hbar^2/m_e e^2$ = 0.529 x 10^{-8} cm), and an incident photon, wave function $e^{i\underline{k}\cdot\underline{r}}$, and a final state consisting of a free electron whose wave function is $e^{i\underline{p}\cdot\underline{r}/\hbar}$. The interaction potential is of the form $\underline{A}\cdot\underline{p}$, where A is the vector potential of the electromagnetic radiation and $\underline{p}$ is the electron momentum. The result of this calculation is

$$\frac{d\sigma_\tau}{d\Omega} = 4\sqrt{2}\,\frac{r_e^2 Z^5}{(137)^4}\left(\frac{m_e c^2}{\hbar\omega}\right)^{7/2}\frac{\sin^2\theta\cos^2\varphi}{\left(1-\frac{v}{c}\cos\theta\right)^4} \tag{18.4}$$

where v is the photoelectron speed. The polar and azimuthal angles specifying the direction of the photoelectron are defined in Fig. 18.2. One should pay particular notice to the Z^5 and

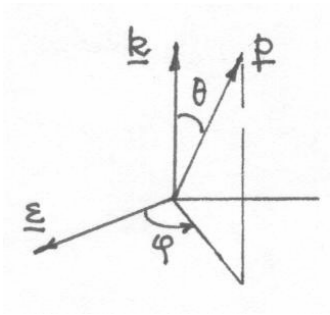

Fig. 18.2. Spherical coordinates defining the photoelectron direction of emission relative to the incoming photon wave vector and its polarization vector.

$(\hbar\omega)^{-7/2}$ variation. As for the angular dependence, the numerator in (18.4) suggests an origin in $(\underline{p}\cdot\underline{\varepsilon})^2$, while the denominator suggests $\underline{p}\cdot\underline{k}$. Integration of (18.4) gives the total cross section

$$\sigma_\tau = \int d\Omega \frac{d\sigma_\tau}{d\Omega} = 4\sqrt{2}\sigma^o \frac{Z^5}{(137)^4}\left(\frac{m_e c^2}{\hbar\omega}\right)^{7/2} \qquad (18.5)$$

where one has ignored the angular dependence in the denominator and has multiplied the result by a factor of 2 to account for 2 electrons in the K-shell [Heitler, p. 207].

In practice it has been found that the charge and energy dependence behave more like

$$\sigma_\tau \propto Z^n/(\hbar\omega)^3 \qquad (18.6)$$

with n varying from 4 to 4.6 as $\hbar\omega$ varies from ~ 0.1 to 3 Mev, and with the energy exponent decreasing from 3 to 1 when $\hbar\omega \geq m_e c^2$. The qualitative behavior of the photoelectric cross section is illustrated in the figures below.

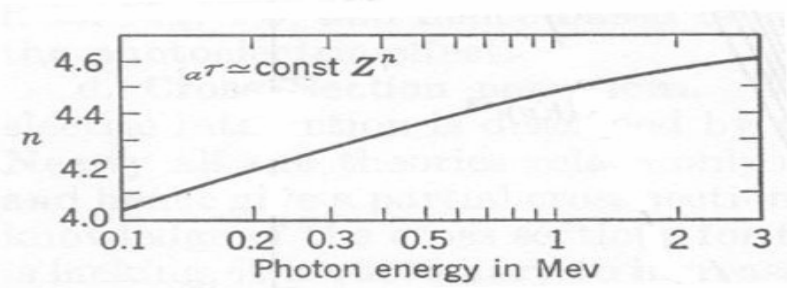

Fig. 18.3. Variation with energy of incident phton of the exponent n of Z in the total cross section for photoelectric effect. (from Evans)

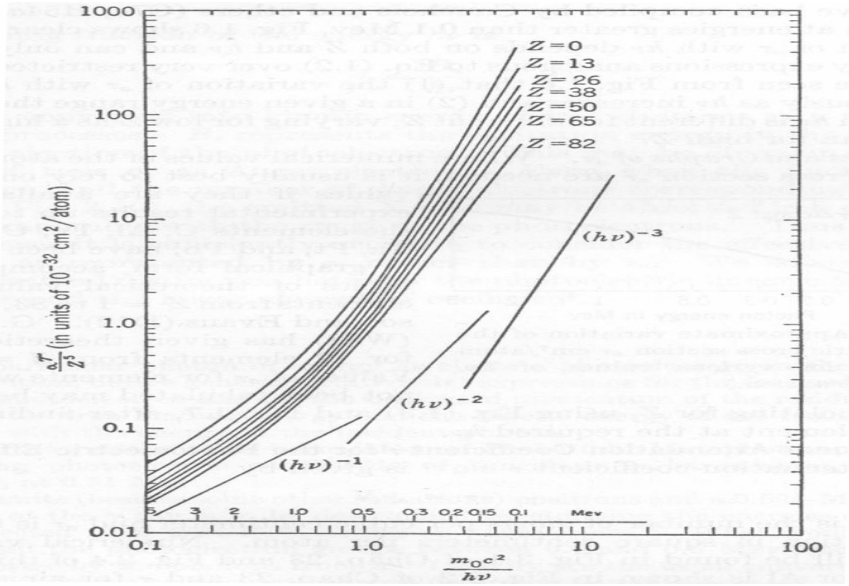

Fig. 18.4. Photoelectric cross sections showing approximate inverse power-law behavior which varies with the energy of the incident photon. (from Evans)

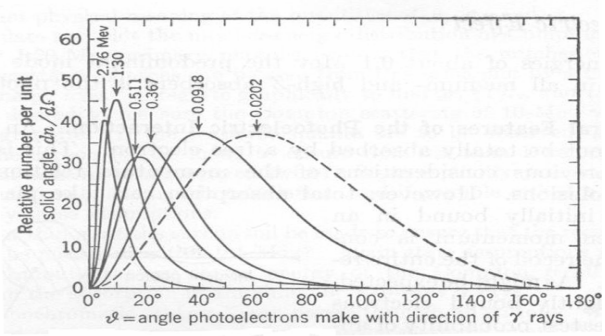

Fig. 18.5. Angular distribution of photoelectrons for various incident photon energies. The peak moves toward forward direction as the energy increases, a behavior which can be qualitatively obtained from the θ-dependence in Eq. (18.4). (from Meyerhof)

Edge Absorption

As the photon energy increases the cross section σ_κ can show discontinuous jumps which are known as *edges*. These correspond to the onset of additional contributions when the energy is sufficient to eject an inner shell electron. The effect is more pronounced in the high-Z material. See Fig. 18.13 below.

Pair Production

In this process, which can occur only when the energy of the incident γ exceeds 1.02 Mev, the photon is absorbed in the vicinity of the nucleus, a positron-electron pair is produced, and the atom is left in an excited state, as indicated in Fig. 18.6. The

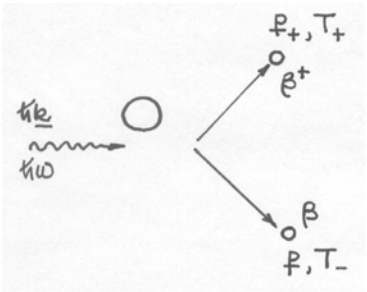

Fig. 18.6. Kinematics of pair production.

conservation equations are therefore

$$\hbar \underline{k} = \underline{p}_+ + \underline{p}_- \tag{18.7}$$

$$\hbar\omega = \left(T_+ \_ m_e c^2\right) + \left(T_- + m_e c^2\right) \tag{18.8}$$

One can show that these conditions cannot be satisfied simulataneously, thus the presence of an atomic nucleus is required. Since the nucleus takes up some momentum, it also takes up some energy in the form of recoil.

The existence of positron is a consequence of the Dirac's relativistic theory of the electron which allows for negative energy states,

$$E = \pm\left(c^2 p^2 + {m_e}^2 c^4\right)^{1/2} \tag{18.9}$$

One assumes that all the negative states are filled; these represent a "sea" of electrons which are generally not observable because no transitions into these states can occur due to the Exclusion Principle. When one of the electrons makes a transition to a positive energy level, it leaves a "hole" (positron) which behaves likes an electron but with a *positive* charge. This is illustrated in Fig. 18.7. In other words, holes in the

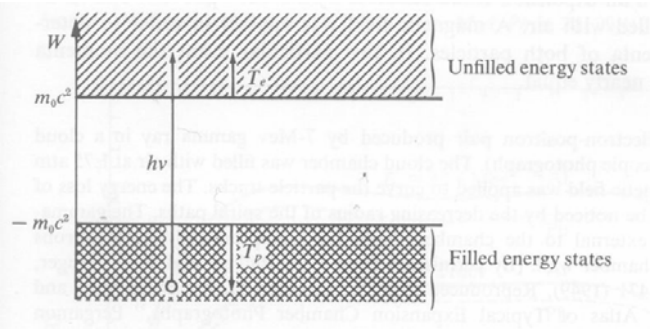

Fig. 18.7. Creation of a positron as a "hole" as in the filled (negative) energy states and an electron as a particle in the unfilled energy state. (from Meyerhof)

negative energy states have positive charge, whereas an electrons in the positive energy states have negative charge. The "hole" is unstable in that it will recombine with an electron when it loses most of its kinetic energy (thermalized). This recombination probess is called pair annihilation. It usually produces two γ (annihilation radiation), each of energy 0.511 Mev, emitted back-to-back. A positron and an electron can form an atom called the positronium. It's life time is ~ 10^{-7} to 10_{-9} sec depending on the relative spin orientation, the shorter lifetime corresponding to antiparallel orientation.

Pair production is intimately related to the process of Bremsstrahlung in which an electron undergoes a transition from one positive energy state to another while a photon is emitted. One can in fact take over directly the theory of Bremsstrahlung for the transition probability with the incident particle being a photon instead of an electron and using the appropriate density of states for the emission of the positron-electron pair [Heitler, Sec. 26]. For the positron the energy differential cross section is

$$\frac{d\sigma_\kappa}{dT_+} = 4\sigma_o Z^2 \frac{T_+^2 + T_-^2 - \frac{2}{3}T_+T_-}{(\hbar\omega)^3}\left[\ell n\left(\frac{2T_+T_-}{\hbar\omega m_e c^2}\right) - \frac{1}{2}\right] \qquad (18.10)$$

where $\sigma_o = r_e^2/137$ = 5.8 x 10^{-4} barns. This result holds under the conditions of Born approximation, which is a high-energy condition ($Ze^2/\hbar v_\pm << 1$), and no screening, which requires $2T_+T_-/\hbar\omega m_e c^2 << 137/Z^{1/3}$. By screening we mean the partial reduction of the nuclear charge by the potential of the inner-shell electrons. As a result of the Born approximation, the cross section is symmetric in T_+ and T-. Screening effects will lead to a lower cross section.

To see the energy distribution we rewrite (18.10) as

$$\frac{d\sigma_\kappa}{dT_+} = \frac{\sigma_o Z^2}{\hbar\omega - 2m_e c^2} P \qquad (18.11)$$

where the dimensionless factor P is a rather complicated function of $\hbar\omega$ and Z; its behavior is depicted in Fig. 18.8. We see the cross section increases with increasing

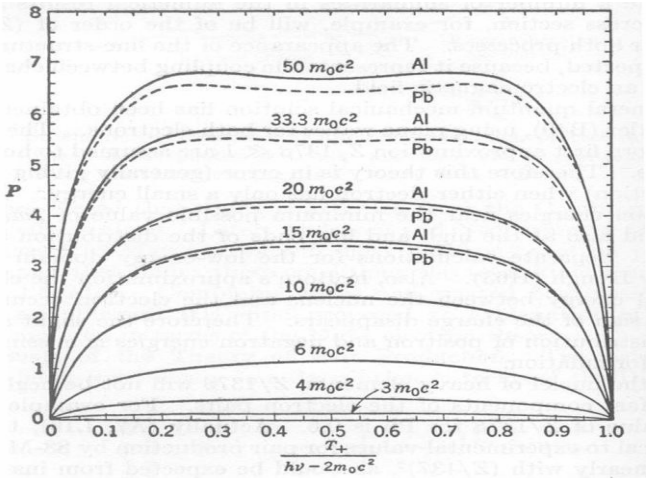

Fig. 18.8. Calculated energy distribution of positron emitted in pair production, as expressed in Eq.(18.11), with correction for screening (dashed curves) for photon energies above $10m_ec^2$. (from Evans)

energy of the incident photon. Since the value is slightly for Al than for Pb, it means the cross section varies with Z somewhat weaker than Z^2. At lower energies the cross section favors equal distribution of energy between the positron and the electron, while at high energies a slight tendency toward unequal distribution could be noted. Intuitively we expect the energy distribution to be biased toward more energy for the positron than for the electron simply because of Coulomb effects, repulsion of the positron and attraction of the electron by the nucleus.

The total cross section for pair production is obtained by integrating (18.11). Analytical integration is possible only for extremely relativistic cases [Evans, p. 705],

$$\sigma_\kappa = \int dT_+ \left(\frac{d\sigma_\kappa}{dT_+}\right) = \sigma_o Z^2 \left[\frac{28}{9}\ell n\left(\frac{2\hbar\omega}{m_ec^2}\right) - \frac{218}{27}\right], \quad \text{no screening} \qquad (18.12)$$

$$= \sigma_o Z^2 \left[\frac{28}{9}\ell n\left(\frac{183}{Z^{1/3}}\right) - \frac{2}{27}\right], \quad \text{complete screening} \qquad (18.13)$$

Moreover, (18.12) and (18.13) are valid only for $m_e c^2 << \hbar\omega << 137 m_e c^2 Z^{-1/2}$ and $\hbar\omega >> 137 m_e c^2 Z^{-1/2}$ respectively. The behavior of this cross section is shown in Fig. 18.9, along with the cross section for Compton scattering. Notice that screening leads to a saturation effect (energy independent), but it is insignificant below $\hbar\omega$ ~ 10 Mev

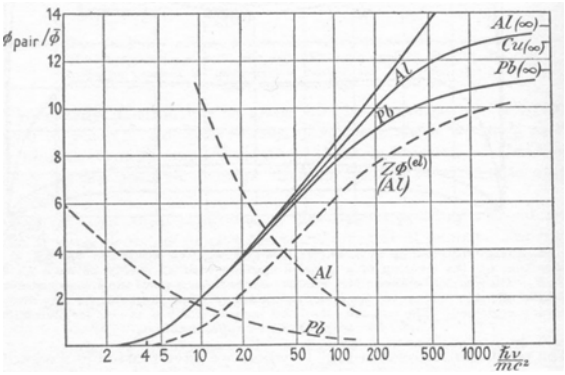

Fig. 18.9. Energy variation of pair production cross section in units of $\sigma_o Z^2$.

Mass Attenuation Coefficients

As we mentioned before, the total linear attenuation coefficient μ for γ-interaction will be taken to be the sum of contributions from Compton scattering, photoelectric effect, and production, with $\mu = N\sigma$, where N is the number of atoms per cm3. Since $N = N_o \rho / A$, where N_o is Avogardro's number and ρ the mass density of the absorber, it is again useful to express the interaction in terms of the *mass attenuation coefficient* μ / ρ, which is essentially independent of the density and physical state of the absorber (recall our observation in the case of charged particle interactions that Z/A is approximately constant for all elements). Thus we write

$$\mu = \mu_C + \mu_\tau + \mu_\kappa \tag{18.14}$$

$$\mu_C / \rho = (N_o / A) Z \sigma_C, \quad \sigma_C \sim 1/\hbar\omega \qquad \text{per electron} \tag{18.15}$$

$$\mu_\tau / \rho = (N_o / A)\sigma_\tau , \qquad \sigma_\tau \sim Z^5 / (\hbar\omega)^{7/2} \qquad \text{per atom} \qquad (18.16)$$

$$\mu_\kappa / \rho = (N_o / A)\sigma_\kappa , \qquad \sigma_\kappa \sim Z^2 \ell n(2\hbar\omega / m_e c^2) \quad \text{per atom} \qquad (18.17)$$

It should be quite clear by now that the three processes we have studied are not equally important for a given region of Z and $\hbar\omega$. Generally speaking, photoelectric effect is important at low energies and high Z, Compton scattering is important at intermediate energies (~ 1 – 5 Mev) and all Z, and pair production becomes at higher energies and high Z. This is illustrated in Fig. 18.10.

We also show several mass attenuation coefficients in Figs. 18.11 – 18.13. One should make note of the magnitude of the attenuation coefficients, their energy dependence, and the contribution associated with each process. In comparing theory with experiment the agreement is good to about 3 % for all elements at $\hbar\omega < 10 m_e c^2$. At higher energies disagreement sets in at high Z (can reach ~ 10% for pb), which is due to the use Born approximation in calculating σ_κ. If one corrects for this, then agreement to within ~ 1% is obtained out to energies ~ 600 $m_e c^2$.

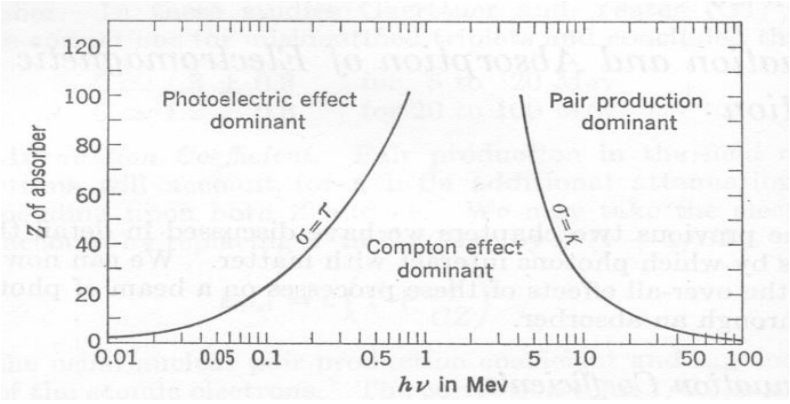

Fig. 18.10. Regions where one of the three γ-interactions dominates over the other two. (from Evans)

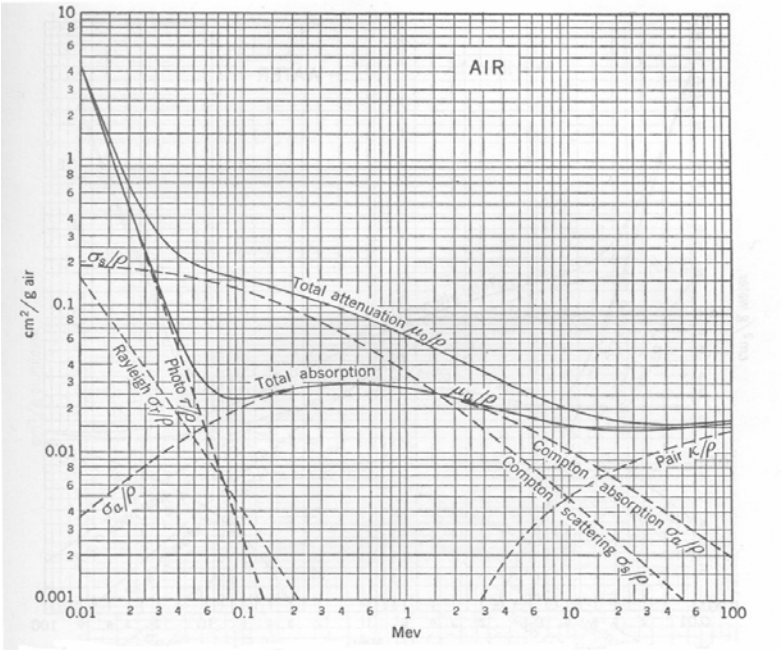

Fig. 18.11. Mass attenuation coefficient for photons in air computed from tables of atomic cross sections. (from Evans)

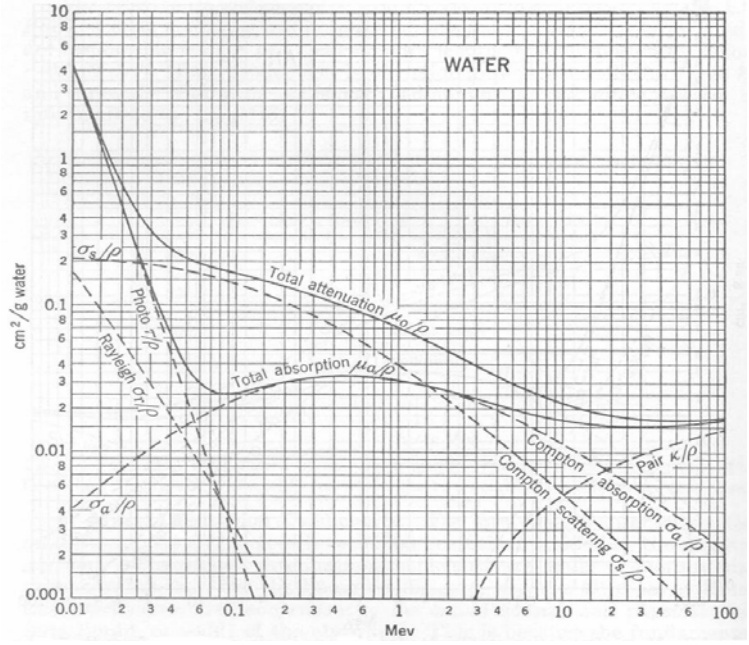

Fig. 18.12. Mass attenuation coefficients for photons in water. (from Evans)

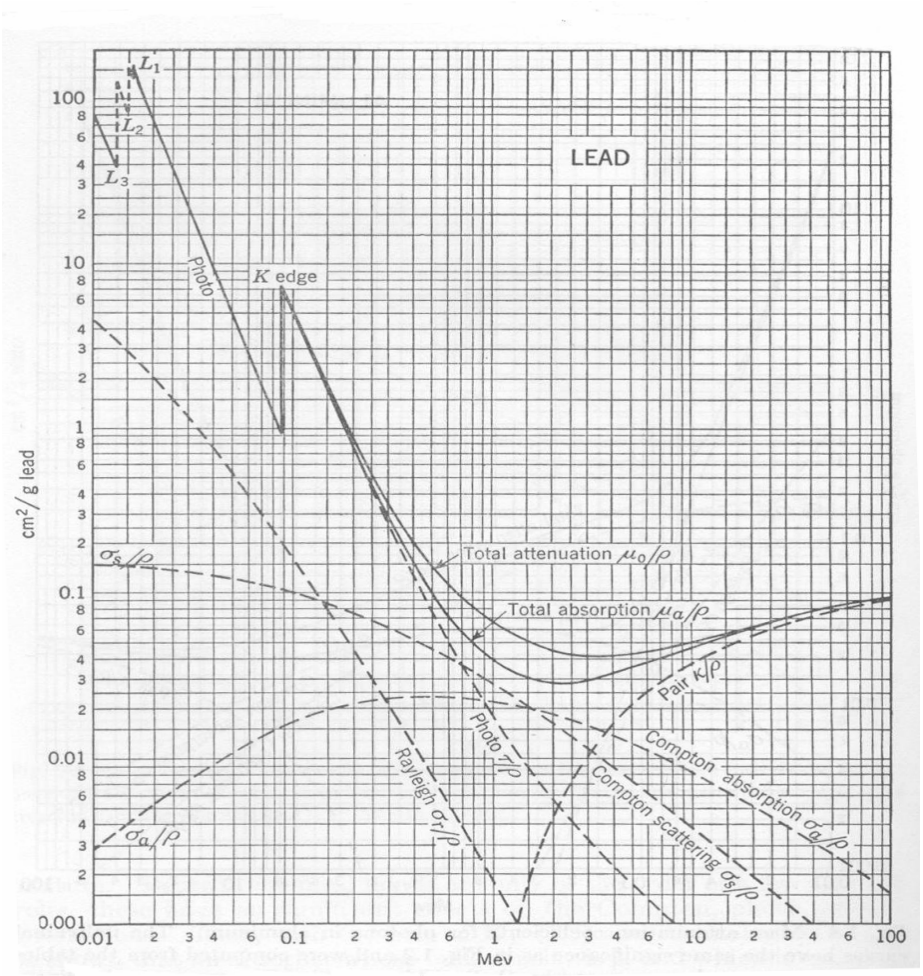

Fig. 18.13. Mass attenuation coefficients for photons in Pb. (from Evans)

22.101 Applied Nuclear Physics (Fall 2004)

Lecture 22 (12/1/04)

Detection of Nuclear Radiation: Pulse Height Spectra

References:

W. E. Meyerhof, *Elements of Nuclear Physics* (McGraw-Hill, New York, 1967), Sec.3-6.

We have just concluded the study of radiation interaction with matter in which the basic mechanisms of charged particle, neutron and gamma interactions were discussed separately. A topic which makes use of all this information is the general problem of detection of nuclear radiation detection. Although this subject properly belongs to a course dealing with experimental aspects applied nuclear physics, it is nevertheless appropriate to make contact with it at this point in the course. There are two reasons for this. First, radiation detection is a central part of the foundational knowledge for all students in the department of Nuclear Engineering (soon to be renamed Nuclear Science and Engineering). Even though we cannot do justice to it in view of the limited time remaining in the syllabus, it is worthwhile to make some contact with it, however briefly. Secondly, an analysis of the features observed experimentally in pulse-height spectra of gamma radiation is timely given what we have just learned about the γ-interaction processes of Compton scattering, photoelectric effect and pair production.

We first remark that regardless of the type of nuclear radiation, the interactions taking place in a material medium invariably result in ionization and excitation which then can be detected. Heavy charged particles and electrons produce ion pairs in ionization chambers, or light emission (excitation of atoms) in scintillation counters, or electron-hole pairs in semiconductor detectors. Neutrons collide with protons which recoil and produce ionization or excitation. In the case of gammas, all 3 processes we have just discussed give rise to energetic electrons which in turn cause ionization or excitation. Thus the basic mechanisms of nuclear radiation detection involve measuring the ionization or excitation occurring in the detector in a way that one can deduce the energy of the incoming radiation. A useful summary of the different types of detectors and methods of detection is given in the following table [from Meyerhof, p. 107].

Table 3-1 Common nuclear detectors

Particle	*Detector*	*Method of detection*	*Remarks*
Heavy charged particles; electrons	Ionization chamber & proportional counter	Total no. of ion pairs determined by collecting charged partners of one sign, e.g. electrons.	Can be used to determine T_0 if particle stops in chamber.†
	Semiconductor detector	Ionization produces electron-hole pairs. Total charge is collected.	Used to determine T_0.
	Geiger counter	Ionization initiates brief discharge.	Good for intensity determination only.
	Cloud chamber or photographic emulsion	Path made visible by ionization causing droplet condensation or developable grains.	Can be used to determine T_0 from range. Type of particle can be recognized from droplet or grain count along path.
	Scintillation detector	Uses light produced in excitation of atoms.	T_0 proportional to light produced.
Neutrons	Any of the above using proton recoils from thin organic lining or nuclear reactions with appropriate filling gas	Ionization by recoiling protons.	T_0 from end point of recoil distribution.
		Ionization by reaction products.	Some reactions can be used to determine T_0.
	Organic scintillator and photomultiplier	Using light produced in excitation of atom by recoiling protons.	T_0 from end point of recoil distribution.
			The above methods for neutrons require $T_0 > 0.1$ Mev.
Gamma rays	Geiger counter	Electrons released in wall of counter ionize gas and initiate discharge.	Good for intensity determination only.
	NaI scintillation detector	Light produced in ionization and excitation by electrons released in the three interaction processes.	T_e proportional to light produced; $h\nu$ inferred from electron energy distributions.
	Semiconductor detector	Electrons produced create electron-hole pairs. Total charge is collected.	$h\nu$ inferred from electron energy distributions.

† The initial kinetic energy of the particle is called T_0.

We now focus on detection of γ radiation. We are concerned with the measurement of two γ rays, at energies 1.37 Mev and 2.75 Mev, emitted from radioactive Na^{24}. The measurements are in the form of pulse-height spectra, number of counts per channel in a multichannel analyzer plotted against the pulse height. Fig. 19.1 shows the results measured by using a Na-I scintillation detector. The spectra consist of two sets of features, one for each incident γ. By a set we mean a photopeak at the incident energy, a Compton edge at an energy approximately 0.25 Mev ($m_e c^2/2$) below the incident energy, and two so-called *escape* peaks denoted as P1 and P2. The escape peaks refer to pair production processes where either one or both annihilation photons

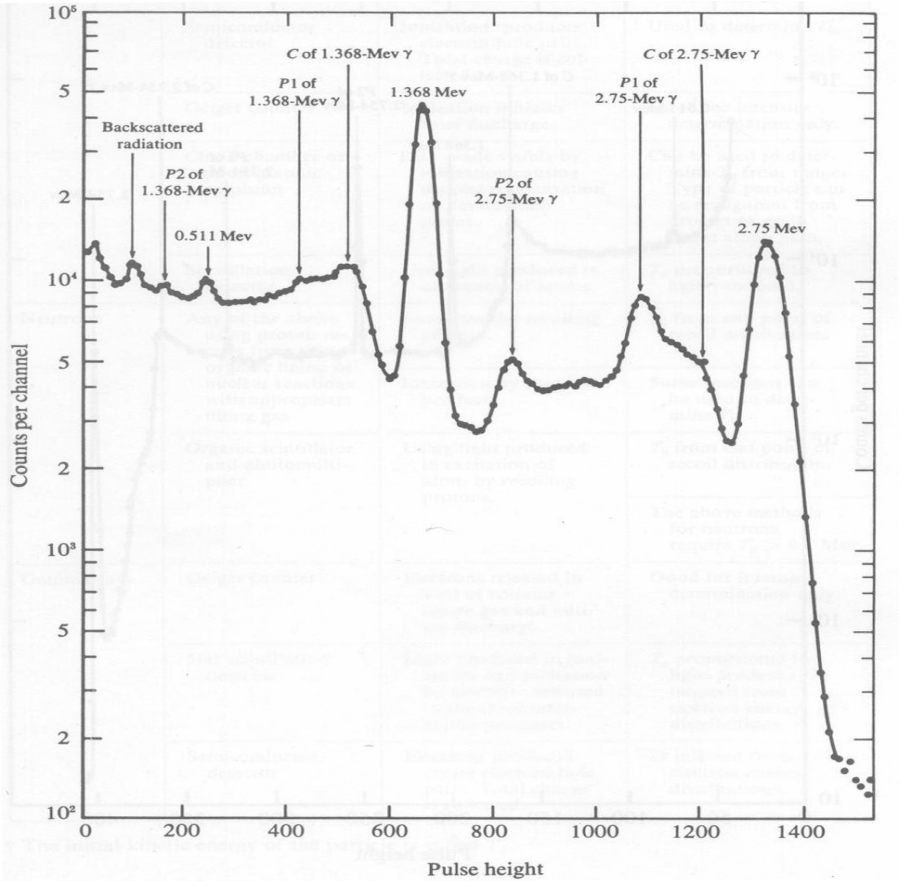

Fig. 19.1. Pulse-height spectra of 1.37 Mev and 2.75 Mev γ obtained using a Na-I detector. (from Meyerhof)

leave the counter. Thus, P1 should be 0.511 Mev below the incident energy and P2 should be 0.511 Mev below P1. The other features that can be seen in Fig. 19.1 are a peak at 0.511 Mev, clearly to be identified as the annihilation photon, a backscattered peak associated with Compton scattering at $\theta = \pi$ which should be positioned at $m_e c^2/2$, and finally an unidentified peak which we can assigned to x-rays emitted from excited atoms.

One can notice in Fig. 19.1 that the various peaks are quite broad. This is a feature of scintillation detector, namely, relatively poor energy resolution. In contrast, a semiconductor detector, such Li-drifted Ge, would have much better energy resolution, as can be seen in Fig. 19.2. In addition to the sharper lines, one should notice that the peaks measured using the semiconductor detector have *different* relative intensities compared the peaks measured by using a scintillation detector. In particular, looking at the relative intensities of P1 and P2, we see that P1 > P2 in Fig. 19.1, whereas P2 > P1 in Fig. 19.2.

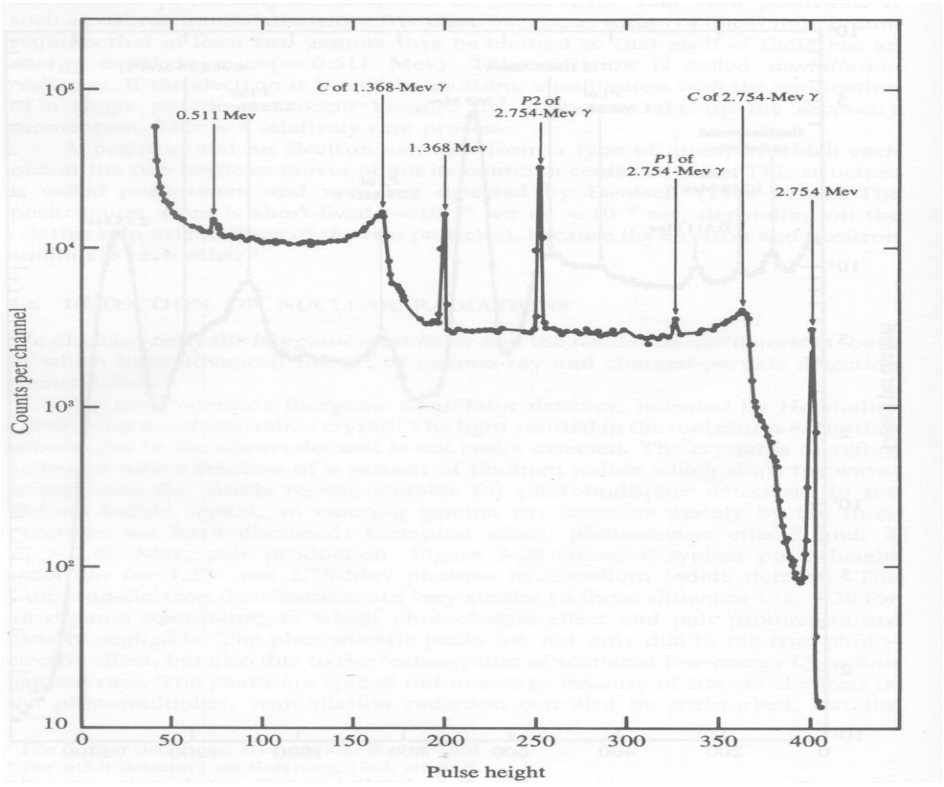

Fig. 19.2. Same as Fig. 19.1 a semiconductor detector is used. (from Meyerhof)

This difference can be explained by noting that the scintillation detector is physically larger than the semiconductor detector, in this case the former is a cylinder 7.6 cm in diameter and 7.6 cm in length, whereas the latter is 1.9 cm in diameter and 0.5 cm in height. Thus one can expect that the probability that a photon will escape from the detector can be quite different in these two cases.

To follow up on this idea, let us define P as the probability of escape. In a one-dimensional situation $P \sim e^{-\mu x}$, where μ is the linear attenuation coefficient and x is the dimension of the detector. Now the probability that one of the two annihilation gammas will escape is P1 = 2P(1-P), the factor of 2 coming from either gamma can escape. For both gammas to escape the probability is $P2=P^2$. So we see that whether P1 is larger or smaller than P2 depends on the magnitude of P. If P is small, P1 > P2, but if P is close to unity, then P2 > P1. For the two detectors in question, it is to be expected that P is larger for the semiconductor detector. Without putting in actual numbers we can infer from an inspection of Figs 19.1 and 19.2 that P is small enough in the case of the scintillation detector for P1 to be larger than P2, and also P is close enough to unity in the case of the semiconductor detector for P2 to be larger than P1.

22.101 Applied Nuclear Physics (Fall 2004)

Lecture 22 (12/1/04)

Nuclear Decays

References:

W. E. Meyerhof, *Elements of Nuclear Physics* (McGraw-Hill, New York, 1967), Chap 4.

A nucleus in an excited state is unstable because it can always undergo a transition (decay) to a lower-energy state of the *same nucleus*. Such a transition will be accompanied by the emission of gamma radiation. A nucleus in either an excited or ground state also can undergo a transition to a lower-energy state of *another nucleus*. This decay is accomplished by the emission of a particle such as an alpha, electron or positron, with or without subsequent gamma emission. A nucleus which undergoes a transition *spontaneously*, that is, without being supplied with additional energy as in bombardment, is said to be radioactive. It is found experimentally that naturally occurring radioactive nuclides emit one or more of the three types of radiations, $\alpha-$particles, $\beta-$particles, and $\gamma-$rays. Measurements of the energy of the nuclear radiation provide the most direct information of the energy-level structure of nuclides. One of the most extensive compilations of radioisotope data and detailed nuclear level diagrams is the *Table of Isotopes*, edited by Lederer, Hollander and Perlman.

In this chapter we will supplement our previous discussions of beta decay and radioactive decay by briefly examining the study of decay constants, selection rules, and some aspects of $\alpha-$, $\beta-$, and $\gamma-$decay energetics.

Alpha Decay

Most radioactive substances are $\alpha-$emitters. Most nuclides with A > 150 are unstable against $\alpha-$decay. On the other hand, $\alpha-$decay is very likely for light nuclides. The decay constant decreases exponentially with decreasing Q-value, here called the decay energy, $\lambda_\alpha \sim \exp(-c/v)$, where c is a constant and v the speed of the

α – particle, $v \propto \sqrt{Q_\alpha}$. The momentum and energy conservation equations are quite straightforward in this case (see Fig. 20.1)

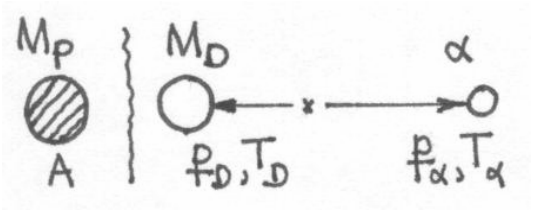

Fig. 20.1. Particle emission and nuclear recoil in α - decay .

$$\underline{p}_D + \underline{p}_\alpha = 0 \tag{20.1}$$

$$M_P c^2 = (M_D c^2 + T_D) + (M_\alpha c^2 + T_\alpha) \tag{20.2}$$

Both kinetic energies are small enough that non-relativistic energy-momentum relations may be used,

$$T_D = p_D^2 / 2M_D = p_\alpha^2 / 2M_D = (M_\alpha / M_D) T_\alpha \tag{20.3}$$

Treating the decay as a reaction the corresponding Q-value becomes

$$\begin{aligned} Q_\alpha &= [M_P - (M_D + M_\alpha)]c^2 \\ &= T_D + T_\alpha \\ &= \frac{M_D + M_\alpha}{M_D} T_\alpha \approx \frac{A}{A-4} T_\alpha \end{aligned} \tag{20.4}$$

which shows that the kinetic energy of the α -particle is always less than Q_α. Since Q_α > 0 (T_α is necessarily positive), it follows that α -decay is an exothermic process. The various energies can be displayed in an energy-level diagram shown in Fig. 20.2. One

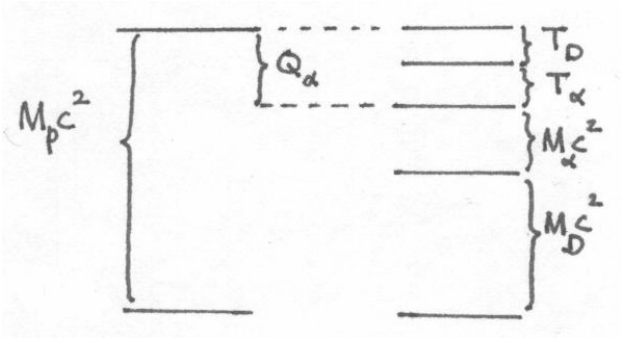

Fig. 20.2. Energy-level diagram for α-decay.

can see at a glance how the rest masses and the kinetic energies combine to ensure energy conservation. We will see later that energy-level diagrams are also useful in depicting collision-induced nuclear reactions. The separation energy S_α is the work necessary to separate an α-particle from the nucleus,

$$S_\alpha = \left[M(A-4,Z-2) + M_\alpha - M(A,Z)\right]c^2$$

$$= B(A,Z) - B(A-4,Z-2) - B(4,2) = -Q_\alpha \qquad (20.5)$$

One can use the semi-empirical mass formula to determine whether a nucleus is stable against α-decay. One finds $Q_\alpha > 0$ for A > 150. Eq.(20.5) also shows that when the daughter nucleus is magic, B(A-4,Z-2) is large, and Q_α is large. Conversely, Q_α is small when the parent nucleus is magic.

Estimating α-decay Constant

An estimate of the decay constant can be made by treating the decay as a barrier penetration problem, an approach proposed by Gamow (1928) and also by Gurney and Condon (1928). One assumes that the α-particle already exists inside the daughter nucleus and it is confined by the Coulomb potential, as indicated in Fig. 20.3. The decay constant is then the probability per unit time that the particle can tunnel through the potential,

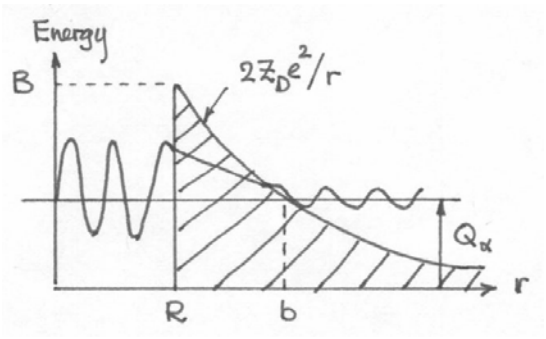

Fig. 20.3. Tunneling of an $\alpha-$particle through a nuclear Coulomb barrier.

$$\lambda_\alpha \sim \left(\frac{v}{R}\right)P \tag{20.6}$$

where v is the relative speed of the α and the daughter nucleus, R is the radius of the daughter nucleus, and P the transmission coefficient. Recall from our study of barrier penetration (cf. Chap 5, eq. (5.20)) that the transmission coefficient can be written in the form

$$P \sim e^{-\gamma} \tag{20.7}$$

$$\gamma = \frac{2}{\hbar}\int_{r_1}^{r_2} dr\left(2m[V(r)-E]\right)^{1/2}$$

$$= \frac{2}{\hbar}\int_{R}^{b} dr\left[2\mu\left(\frac{2Z_De^2}{r}-Q_\alpha\right)\right]^{1/2} \tag{20.8}$$

with $\mu = M_\alpha M_D/(M_\alpha + M_D)$. The integral can be evaluated,

$$\gamma = \frac{8Z_De^2}{\hbar v}\left[\cos^{-1}\sqrt{y} - \sqrt{y}(1-y)^{1/2}\right] \tag{20.9}$$

where y = R/b = Q_α/B, B = $2Z_D e^2/R$, $Q_\alpha = \mu v^2/2 = 2Z_D e^2/b$. Typically B is a few tens or more Mev, while Q_α ~ a few Mev, one can therefore invoke the thick barrier approximation, in which case b >> R (or Q_α << B), and y << 1. Then

$$\cos^{-1}\sqrt{y} \sim \frac{\pi}{2} - \sqrt{y} - \frac{1}{6}y^{3/2} - \ldots \tag{20.10}$$

the square bracket in (20.9) becomes

$$[\ ] \sim \frac{\pi}{2} - 2\sqrt{y} + O(y^{3/2}) \tag{20.11}$$

and

$$\gamma \approx \frac{4\pi Z_D e^2}{\hbar v} - \frac{16 Z_D e^2}{\hbar v}\left(\frac{R}{b}\right)^{1/2} \tag{20.12}$$

So the expression for the decay constant becomes

$$\lambda_\alpha \approx \frac{v}{R}\exp\left[-\frac{4\pi Z_D e^2}{\hbar v} + \frac{8}{\hbar}\left(Z_D e^2 \mu R\right)^{1/2}\right] \tag{20.13}$$

where μ is the reduced mass. This result has a simple interpretation - the prefactor represents the attempt frequency for the existing α-particle to tunnel through the nuclear barrier, and the exponential is the transmission probability Since Gamow was the first to study this problem, the exponent is sometimes known as the Gamow factor G.

To illustrate the application of (20.13) we consider estimating the decay constant of the 4.2 Mev α-particle emitted by U^{238}. Ignoring the small recoil effects, we can write

$$T_\alpha \sim \frac{1}{2}\mu v^2 \rightarrow v \sim 1.4 \text{ x } 10^9 \text{ cm/s}, \quad \mu \sim M_\alpha$$

$$R \sim 1.4\ (234)^{1/3} \text{ x } 10^{-13} \sim 8.6 \text{ x } 10^{-13} \text{ cm}$$

$$-\frac{4\pi Z_D e^2}{\hbar v} = -173, \qquad \frac{8}{\hbar}\left(Z_D e^2 \mu R\right)^{1/2} = 83$$

Thus

$$P = e^{-90} \sim 10^{-39} \tag{20.14}$$

As a result our estimate is

$$\lambda_\alpha \sim 1.7x10^{-18}\ \text{s}^{-1}, \quad \text{or}\ \ t_{1/2} \sim 1.3 \times 10^{10}\ \text{yrs}$$

The experimental half-life is ~ 0.45 x 10^{10} yrs. Considering our estimate is very rough, the agreement is rather remarkable. In general one should not expect to predict λ_α to be better than the correct order of magnitude (say a factor of 5 to 10). Notice that in our example, B ~ 30 Mev and Q_α = 4.2 Mev. Also b = RB/Q_α = 61 x 10^{-13} cm. So the thick barrier approximation, B >> Q_α or b >> R, is well justified.

The theoretical expression for the decay constant provides a basis for an empirical relation between the half-life and the decay energy. Since $t_{1/2} = 0.693/\alpha$, we have from (20.13)

$$\ell n(t_{1/2}) = \ell n\left(0.693R/v\right) + 4\pi Z_D e^2/\hbar v - \frac{8}{\hbar}\left(Z_D e^2 \mu R\right)^{1/2} \tag{20.15}$$

We note R ~$A^{1/3}$ ~ $Z_D^{1/3}$, so the last term varies with ZD like $Z_D^{2/3}$. Also, in the second trerm v $\propto$ $\sqrt{Q_\alpha}$. Therefore (20.15) suggests the following relation,

$$\log(t_{1/2}) = a + \frac{b}{\sqrt{Q_\alpha}} \tag{20.16}$$

with a and b being parameters depending only on Z_D. A relation of this form is known as the Geiger-Nuttall rule.

We conclude our brief consideration of α-decay at this point. For further discussions the student should consult Meyerhof (Chap 4) and Evans (Chap 16).

Beta Decay

Beta decay is considered to be a weak interaction since the interaction potential is ~ 10^{-6} that of nuclear interactions, generally regarded as strong. Electromagnetic and gravitational interactions are intermediate in this sense. β-decay is the most common type of radioactive decay, all nuclides not lying in the "valley of stability" are unstable against this transition. The positrons or electrons emitted in β-decay have a continuous energy distribution, as illustrated in Fig. 20.4 for the decay of Cu^{64},

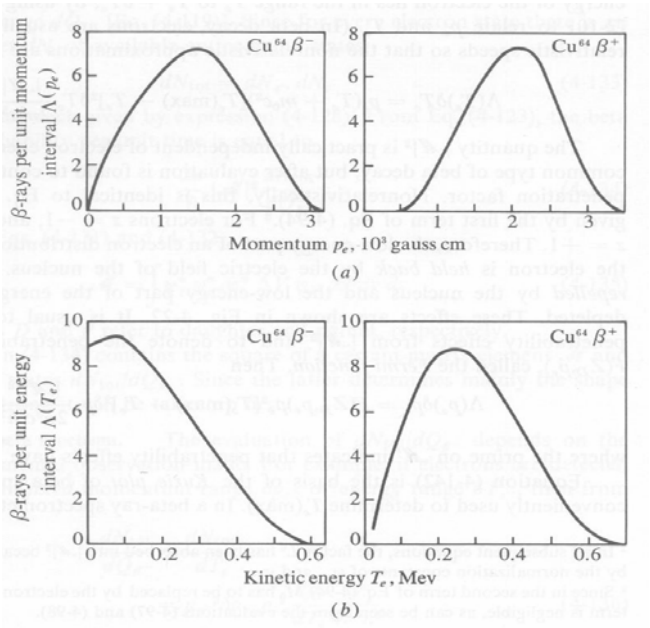

Fig. 20.4. Momentum (a) and energy (b) distributions of beta decay in Cu^{64}. (from Meyerhof)

$$_{29}Cu^{64} \rightarrow {}_{30}Zn^{64} + \beta + \bar{\nu}\,, \qquad T_{-}(\text{max}) = 0.57 \text{ Mev}$$

$$\rightarrow {}_{28}Ni^{64} + \beta^{+} + \nu\,, \qquad T_{+}(\text{max}) = 0.66 \text{ Mev}$$

The values of $T_{\pm}(\max)$ are characteristic of the particular radionuclide; they can be considered as signatures..

If we assume that in β-decay we have only a parent nucleus, a daughter nucleus, and a β-particle, then we would find that the conservations of energy, linear and angular moemnta cannot be all satisfied. It was then proposed by Pauli (1933) that particles, called neutrino ν and antineutrino $\bar{\nu}$, also can be emitted in β-decay. The neutrino particle has the properties of zero charge, zero (or nearly zero) mass, and intrinsic angular momentum (spin) of $\hbar/2$. The detection of the neutrino is unusually difficult because it has a very long mean-free path. Its existence was confirmed by Reines and Cowan (1953) using the *inverse* β-decay reaction induced by a neutrino, $p + \bar{\nu} \rightarrow n + \beta^-$. The emission of a neutrino (or antineutrino) in the β-decay process makes it possible to satisfy the energy conservation condition with a continuous distribution of the kinetic energy of the emitted β-particle. Also, linear and angular momenta are now conserved.

The energetics of β-decay can be summarized as

$$\underline{p}_D + \underline{p}_\beta + \underline{p}_{\bar{\nu}} = 0 \tag{20.17}$$

$$M_P c^2 = M_D c^2 + T_\beta + T_{\bar{\nu}} \qquad \text{electron decay} \tag{20.18}$$

$$M_P c^2 = M_D c^2 + T_{\beta^+} + T_\nu + 2m_e c^2 \qquad \text{positron decay} \tag{20.19}$$

where the extra rest mass term in positron decay has been discussed previously in Chap 11 (cf. Eq. (11.9)). Recall also that electron capture (EC0 is a competing process with β-decay, requiring only the condition $M_P(Z) > M_D(Z-1)$. Fig. 20.4 shows how the energetics can be expressed in the form of energy-level diagrams.

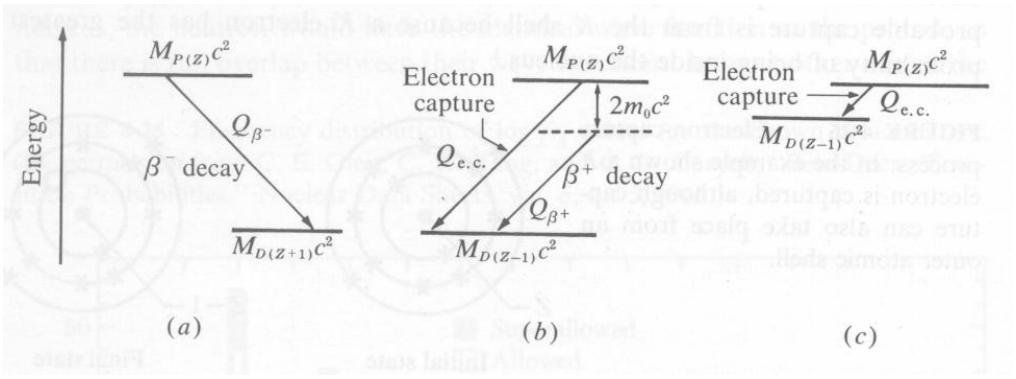

Fig. 20.5. Energetics of β – decay processes. (from Meyerhof)

Typical decay schemes for β-emitters are shown in Fig. 20.6. For each nuclear level there is an assignment of spin and parity. This information is essential for determining whether a transition is allowed according to certain selection rules, as we will discuss below.

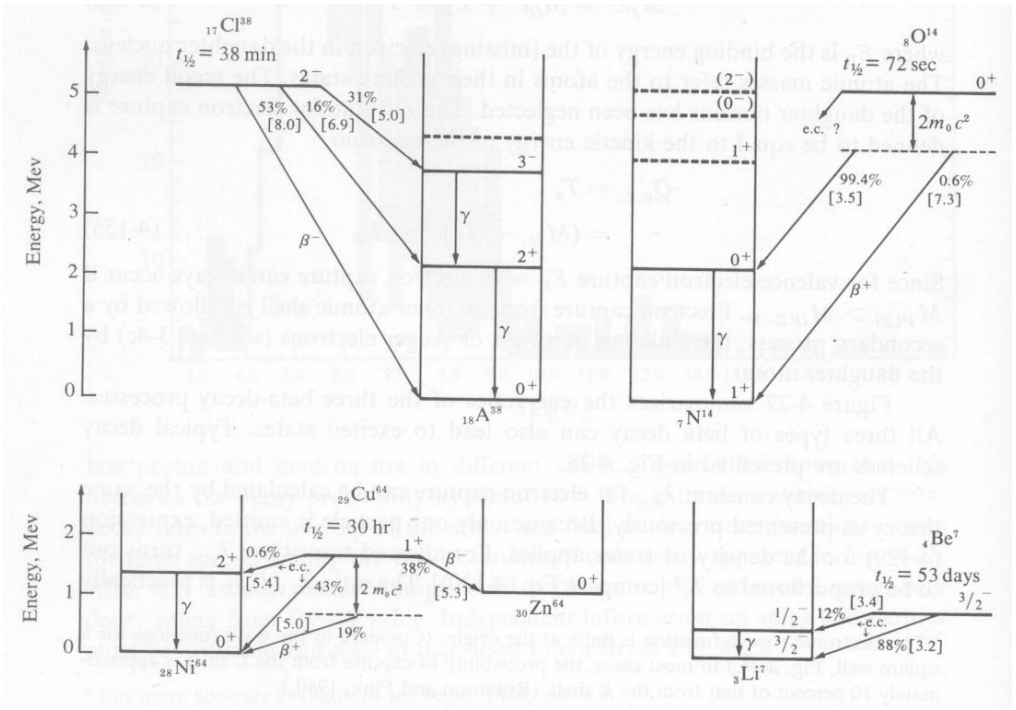

Fig. 20.5. Energy-level diagrams depicting nuclear transitions involving beta decay. (from Meyerhof)

Experimental half-lives of β-decay lied in a wide range, from 10^{-3} sec to 10^{16} yrs. Generally, $\lambda_\beta \sim Q_\beta^5$. The decay process cannot be explained classically. The theory of β-decay was developed by Fermi (1934) in analogy with the quantum theory of electromagnetic decay. For a discussion of the elements of this theory one should consult Meyerhof and references therein. We will be content to show one aspect of the theory which concerns the statistical factor describing the momentum and energy distributions of the emitted β particle. Fig. 20.5 shows the nuclear coulomb effects on the momentum distribution in β-decay in Ca (Z = 20). One can see an enhancement of the β^--decay and a suppression of β^+-decay at low momenta. Coulomb effects on the energy distribution are even more pronounced.

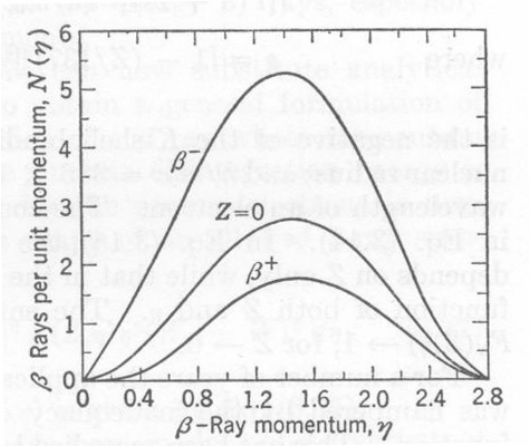

Fig. 20.5. Momentum distributions of β-decay in Ca.

Selection Rules for Beta Decay

Besides energy and linear momentum conservation, a nuclear transition must also satisfy angular momentum and parity conservation. This gives rise to selection rules which specify whether a particular transition between initial and final states, both with specified spin and parity, is allowed, and if allowed what mode of decay is most likely. We will work out the selection rules governing $\beta-$ and γ-decay. For the former conservation of angular momentum and parity are generally expressed as

$$\underline{I}_P = \underline{I}_D + \underline{L}_\beta + \underline{S}_\beta \tag{20.17}$$

$$\pi_P = \pi_D (-1)^{L_\beta} \tag{20.18}$$

where L_β is the orbital angular momentum and S_β the intrinsic spin of the electron-antineutrino system. The magnitude of angular momentum vector can take integral values, 0, 1, 2, …, whereas the latter can take on values of 0 and 1 which would correspond the antiparallel and parallel coupling of the electron and neutrino spins. These two orientations will be called *Fermi* and *Gamow-Teller* respectively in what follows.

In applying the conservation conditions, one finds the lowest value of L_β that will satify (20.17) for which there is a corresponding value of S_β that is compatible with (20.18). This then identifies the allowed transition that is most likely, other allowed transitions with higher values of L_β will be significantly less likely. This is because the decay constant is governed by the square of a transition matrix element, which in term can be written as a series of contributions, one for each L_β (recall the discussion of partial wave expansion in cross section calculation, Appendix B),

$$\lambda_\beta \propto |M|^2 = |M(L_\beta = 0)|^2 + |M(L_\beta = 1)|^2 + |M(L_\beta = 2)|^2 + ... \tag{20.19}$$

Transitions with L_β = 0, 1, 2, … are called *allowed, first-borbidden, second-forbidden,*…respectively. … The magnitude decrease of the square of the matrix element from one order to the next higher order is at least two orders of magnitude. For this reason one generally is interested only in the first allowed transition.

To illustrate how the selection rules are determined, we consider the transition

$${}_2He^6(0^+) \rightarrow {}_3Li^6(1^+)$$

To find the combination of L_β and S_β we note first that parity conservation requires L_β to be even. Then we see that L_β = 0 plus S_β = 1 would satisfy both (20.17) and (20.18). Thus the most likely transition is *allowed, G-T*. Following this line of argument, one can readily arrive at the following assignments.

$$_8O^{14}(0^+)\rightarrow{}_7N^{14}(0^+) \qquad \textit{allowed, F}$$

$$_on^1(1/2^+)\rightarrow{}_1H^1(1/2^+) \qquad \textit{allowed, G-T and F}$$

$$_{17}C\ell^{38}(2^-)\rightarrow{}_{18}A^{38}(2^+) \qquad \textit{first-borbidden, GT and F}$$

$$_4Be^{10}(3^+)\rightarrow{}_5B^{10}(0^+) \qquad \textit{second-forbidden, GT}$$

Parity Non-conservation

The presence of neutrino in β-decay leads to a certain type of non-conservation of parity. It is known that neutrinos have instrinsic spin antiparallel to their velocity, whereas the spin of antineutrino is parallel to their velocity (keeping in mind that ν and $\bar{\nu}$ are *different* particles). Consider the mirror experiment where a neutrino is moving toward the mirror from the left, Fig. 20.6. Applying the inversion symmetry operation

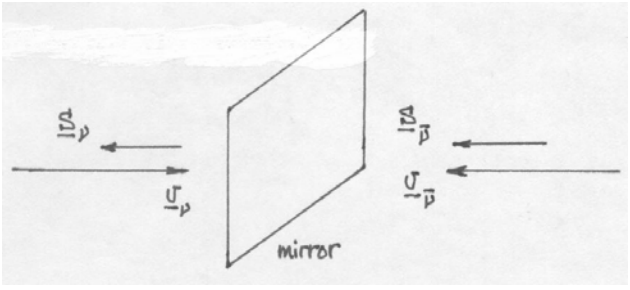

Fig. 20.6. Mirror reflection demonstrating parity non-sonserving property of neutrino. (from Meyerhof)

($x \to -x$), the velocity reverses direction, while the angular momentum (spin) does not. Thus, on the other side of the mirror we have an image of a particle moving from the right, but its spin is now parallel to the velocity so it has to be an antineutrino instead of a neutrino. This means that the property of ν and $\bar{\nu}$, namely definite spin direction relative to the velocity, is not compatible with parity conservation (symmetry under inversion).

For further discussions of beta decay we again refer the student to Meyerhof and the references therein.

Gamma Decay

An excited nucleus can always decay to a lower energy state by γ-emission or a competing process called internal conversion. In the latter the excess nuclear energy is given directly to an atomic electron which is ejected with a certain kinetic energy. In general, complicated rearrangements of nucleons occur during γ-decay.

The energetics of γ-decay is rather straightforward. As shown in Fig. 20. 7 a γ is emitted while the nucleus recoils.

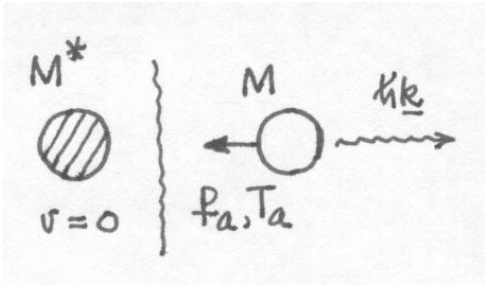

Fig. 20.7. Schematics of γ-decay

$$\hbar \underline{k} + \underline{p}_a = 0 \qquad (20.20)$$

$$M^* c^2 = Mc^2 + E_\gamma + T_a \qquad (20.20)$$

The recoil energy is usually quite small,

$$T_a = p_a^2 / 2M = \hbar^2 k^2 / 2M = E_\gamma^2 / 2Mc^2 \tag{20.21}$$

Typically, E_γ ~ 2 Mev, so if A ~ 50, then Ta ~ 40 ev. This is generally negligible.

Decay Constants and Selection Rules

Nuclear excited states have half-lives for γ-emission ranging from 10-16 sec to > 100 years. A rough estimate of λ_γ can be made using semi-classical ideas. From Maxewell's equations one finds that an accelerated point charge e radiates electromagnetic radiation at a rate given by the Lamor formula (cf. Jackson, *Classical Electrodynamics*, Chap 17),

$$\frac{dE}{dt} = \frac{2}{3}\frac{e^2 a^2}{c^3} \tag{20.22}$$

where a is the acceleration of the charge. Suppose the radiating charge has a motion like the simple oscillator,

$$x(t) = x_o \cos \omega t \tag{20.23}$$

where we take $x_o^2 + y_o^2 + z_o^2 = R^2$, R being the radius of the nucleus. From (20.23) we have

$$a(t) = R\omega^2 \cos \omega t \tag{20.24}$$

To get an average rate of energy radiation, we average (20.22) over a large number of oscillation cycles,

$$\left(\frac{dE}{dt}\right)_{avg} = \frac{2}{3}\frac{R^2\omega^4 e^2}{c^3}\left(\cos^2 \omega t\right)_{avg} \approx \frac{R^2\omega^4 e^2}{3c^3} \tag{20.25}$$

Now we assume that each photon is emitted during a mean time interval τ. Then,

$$\left(\frac{dE}{dt}\right)_{avg} = \frac{\hbar\omega}{\tau} \tag{20.26}$$

Equating this with (20.25) gives

$$\lambda_\gamma \approx \frac{e^2 R^2 E_\gamma^3}{3\hbar^4 c^3} \tag{20.27}$$

If we apply this result to de-excitation of an atom by electromagnetic emission, we would take R ~ 10-8 cm and E_γ ~ 1 ev, in which case (20.27) gives

$$\lambda_\gamma \sim 10^6 \text{ sec}^{-1}, \quad \text{or} \quad t_{1/2} \sim 7 \text{ x } 10^{-7} \text{ sec}$$

On the other hand, if we apply (20.27) to nuclear decay by taking R ~ 5 x 10^{-13} cm, and E_γ ~ 1 Mev, we would obtain

$$\lambda_\gamma \sim 10^{15} \text{ sec-1}, \quad \text{or} \quad t_{1/2} \sim 3 \text{ x } 10^{-16} \text{ sec}$$

These result only indicate typical orders of magnitude. What Eq.(20.27) does not explain is the wide range of values of the half-lives that have been observed.

Turning to the question of selection rules for γ-decay, we again write down the conservation of angular momenta and parity in a form similar to (20.17) and (20.18),

$$\underline{I}_i = \underline{I}_f + \underline{L}_\gamma \tag{20.28}$$

$$\pi_i = \pi_f \pi_\gamma \tag{20.29}$$

Notice that in contrast to (20.27) the orbital and spin angular momenta are both represented by $\underline{L}_\gamma$ (which plays the role of the *total* angular momentum). Since the photon has spin $\hbar$ [for a discussion of photon angular momentum, see A. S. Davydov, *Quantum Mechanics* (1965(, pp. 306 and 578], the possible values of L_γ are 1 (corresponding to the case of zero orbital angular momentum), 2, 3, …For the parity conservation the parity of the photon of course depends on the value of L_γ. There are now two possibilities because we are considering photon emission as the process of electromagnetic multipole radiation, in which case one can have either electric or magnetic multipole radiation,

$$\pi_\gamma = (-1)^{L_\gamma} \qquad \text{electric multipole}$$

$$-(-1)^{L_\gamma} \qquad \text{magnetic multipole}$$

Thus we can set up the following table,

Radiation	Designation	Value of L_γ	π_γ
electric dipole	E1	1	-1
magnetic dipole	M1	1	+1
electric quadrupole	E2	2	+1
magnetic quadrupole	M2	2	-1
electric octupole	E3	3	-1
etc.			

Similar to the case of β-decay, the decay constant can be expressed as a sum of contributions from each multipole [cf. Blatt and Weisskopf, *Theoretical Nuclear Physics*, p. 627],

$$\lambda_\gamma = \lambda_\gamma(E1) + \lambda_\gamma(M1) + \lambda_\gamma(E2) + \ldots \qquad (20.30)$$

provided each contribution is allowed by the selection rules. Once a contribution is allowed, one generally does not bother with the higher-order terms because they are much smaller in magnitude. Take, for example, a transition between an initial state with spin and parity of 2^+ and a final state of 0^+. This transition requires the photon parity to be positive, which means that for an electric multipole radiation L_γ would have to be even, and for a magnetic radiation it has to be odd. In view of the initial and final spins, we see that angular momentum conservation (20.28) requires L_γ to be at least 2. Thus, the most likely mode of γ-decay for this transition is E2, although M3 is also allowed. A few other examples are:

$1^+ \to 0^+$	M1
$\frac{1}{2}^- \to \frac{1}{2}^+$	E1
$\frac{9}{2}^+ \to \frac{1}{2}^-$	M4
$0^+ \to 0^+$	no γ-decay allowed

We conclude this discussion of nuclear decays by the remark that internal conversion (IC) is a competing process with γ-decay. The atomic electron ejected has a kinetic energy given by (ignoring nuclear recoil)

$$T_e = E_i - E_f - E_B \tag{20.31}$$

where $E_i - E_f$ is the energy of de-excitation, and E_B is the binding energy of the atomic electron. If we denote by λ_e the decay constant for internal conversion, then the total decay constant for de-excitation is

$$\lambda = \lambda_\gamma + \lambda_e \tag{20.32}$$

22.101 Applied Nuclear Physics (Fall 2004)

Lecture 23 (12/3/04)

Nuclear Reactions: Energetics and Compound Nucleus

References:

W. E. Meyerhof, *Elements of Nuclear Physics* (McGraw-Hill, New York, 1967), Chap 5.

Among the many models of nuclear reactions there are two opposing basic models which we have encountered. These are (i) the compound nucleus model proposed by Bohr (1936) in which the incident particle interacts strongly with the entire target nucleus, and the decay of the resulting compound nucleus is independent of the mode of formation, and (ii) the independent particle model in which the incident particle interacts with the nucleus through an effective averaged potential. A well-known example of the former is the liquid drop model, and examples of the latter are a model proposed by Bethe (1940), the nuclear shell model with spin-orbit coupling (cf. Chap 9), and a model with a complex potential, known as the optical model, proposed by Feshbach, Porter and Weisskopf (1949). Each model describes well some aspects of what we now know about nuclear structure and reactions, and not so well some of the other aspects. Since we have already examined the nuclear shell model is some detail, we will focus in the brief discussion here on the compound nucleus model. As we will see, this approach is well suited for describing reactions which show single resonance behavior, a sharp peak in the every variation of the cross section. In contrast, the optical model, which we will not discuss in this course, is good for gross behavior of the cross section (in the sense of averaging over an energy interval).

Energetics

Before discussing the compound nucleus model we first summarize the energetics of nuclear reactions. We recall the Q-equation introduced in the study of neutron interactions (cf. Chap 15) for a general reaction depicted in Fig. 21.1,

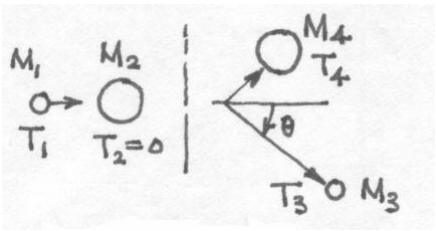

Fig. 21.1. A generic two-body nuclear reaction with target nucleus at rest.

$$Q = T_3\left(1+\frac{M_3}{M_4}\right) - T_1\left(1-\frac{M_1}{M_4}\right) - \frac{2}{M_4}\left(M_1 M_3 T_1 T_3\right)^{1/2}\cos\theta \qquad (21.1)$$

Since $Q = T_3 + T_4 - T_1$, the reaction can take place only if M_3 and M_4 emerge with positive kinetic energies (all kinetic energies are LCS unless specified otherwise),

$$T_3 + T_4 \geq 0, \quad \text{or} \quad Q + T_1 \geq 0 \qquad (21.2)$$

We will see that this condition, although quite reasonable from an intuitive standpoint, is necessary but not sufficient for the reaction to occur.

We have previously emphasized in the discussion of neutron interaction that a fraction of the kinetic energy brought in by the incident particle M_1 goes into setting the center-of-mass into motion and is therefore not available for reaction. To see what is the energy available for reaction we can look into the kinetic energies of the reacting particles in CMCS. First, the kinetic energy of the center-of-mass, in the case where the target nucleus is at rest, is

$$T_o = \frac{1}{2}(M_1 + M_2)v_o^2 \qquad (21.3)$$

where the center-of-mass speed is $v_o = \left[M_1/(M_1+M_2)\right]v_1$, v_1 being the speed of the incident particle. The kinetic energy available for reaction is the kinetic energy of the

incident particle T_1 minus the kinetic energy of the center-of-mass, which we denote as T_i,

$$T_i = T_1 - T_o = \frac{M_2}{M_1 + M_2} T_1$$

$$= \frac{1}{2} M_1 V_1^2 + \frac{1}{2} M_2 v_o^2 \qquad (21.4)$$

The second line in (21.4) shows that T_i is also the sum of the kinetic energies of particles 1 and 2 in CMCS (we follow the same notation of using capital letters to denote velocity in CMCS). In addition to the kinetic energy available for reaction, there is also the rest-mass energy available for reaction, as represented by the Q-value. Thus the total energy available for reaction is the sum of Ti and Q. A necessary and sufficient condition for reaction is therefore

$$E_{avail} = Q + T_i \geq 0 \qquad (21.5)$$

We can rewrite (21.5) as

$$T_1 \geq -Q \frac{M_1 + M_2}{M_2} \qquad (21.6)$$

If $Q > 0$, (21.6) is always satisfied which is expected since the reaction is exothermic. For $Q < 0$, (21.6) shows that the threshold energy, the minimum value of the incident particle kinetic energy for reaction, is greater than the rest-mass deficit. The reason for needing more energy than the rest-mass deficit, of course, is that some energy is needed to put into the center-of-mass.

At threshold, $Q + T_i = 0$. So M_3 and M_4 both move in LCS with speed v_o (V_3 and $V_4 = 0$). At this condition the total kinetic energies of the reaction products is

$$(T_3 + T_4)_{thres} = \frac{1}{2}(M_3 + M_4)v_o^2 \tag{21.7}$$

Since we have $M_3V_3 = M_4V_4$ from momentum conservation, we can say in general

$$Q + T_i = \frac{1}{2}M_3V_3^2 + \frac{1}{2}\frac{(M_3V_3)^2}{M_4} \tag{21.8}$$

With Q and T_1 given, we can find V_3 from (21.8) but not the direction of $\underline{V_3}$. It turns out that for T_1 just above threshold of an endothermic reaction, an interesting situation exists where at a certain scattering angle in LCS one can have two different kinetic energies in LCS, which violates the one-to-one correspondence between scattering angle and outgoing energy. How can this be? The answer is that the one-to-one correspondence that we have spoken of in the past applies *strictly only* to the relation between the kinetic energy T_3 and the scattering angle in CMCS (and not with the scattering angle in LCS). Fig. 21.2 shows how this special situation, which corresponds to the double-valued solution to the Q-equation, can arise.

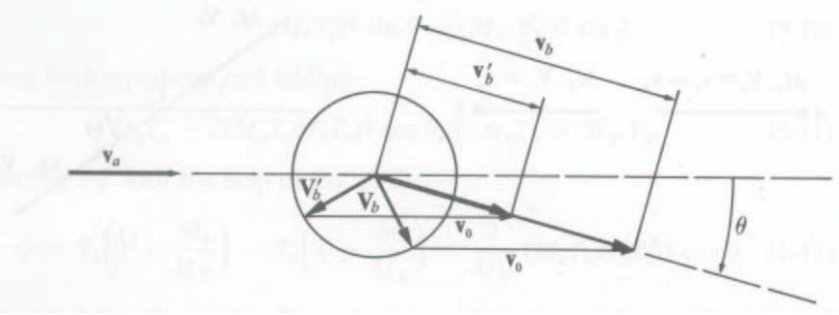

Fig. 21.2. A special condition where a particle can be emitted with two different kinetic energies at the same angle (in LCS only).

Energy-Level Diagrams for Nuclear Reactions

We have seen in the previous chapter how the various energies involved in nuclear decay can be conveniently displayed in an energy-level diagram. The same argument can be applied to nuclear reactions. Fig. 21.3 shows the energies involved in an

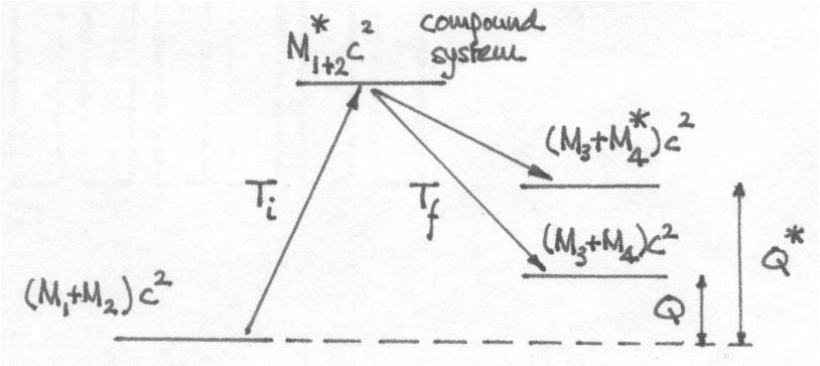

Fig. 21.3. Energy-level diagram for an endothermic reaction.

endothermic reaction. In this case the reaction can end up in two different states, depending on whether the product nucleus M_4 is in the ground state or in an excited state (*). T_f denotes the kinetic energy of the reaction products in CMCS, which one can write as

$$T_f = Q + T_i$$

$$= \frac{1}{2}M_3V_3^2 + \frac{1}{2}M_4V_4^2 \qquad (21.9)$$

Since both T_i and T_f can be considered kinetic energies in CMCS, one can say that the kinetic energies appearing in energy-level diagram should be in CMCS.

Compound Nucleus Reactions

The concept of compound nucleus model for nuclear reactions is depicted in Fig. 21.4. The idea is that an incident particle reacts with the target nucleus in two ways, a scattering that takes place at the surface of the nucleus which is, properly speaking, not a reaction, and a reaction that takes place after the incident particle has entered into the nucleus. The former is what we have been studying as elastic scattering, it is also known

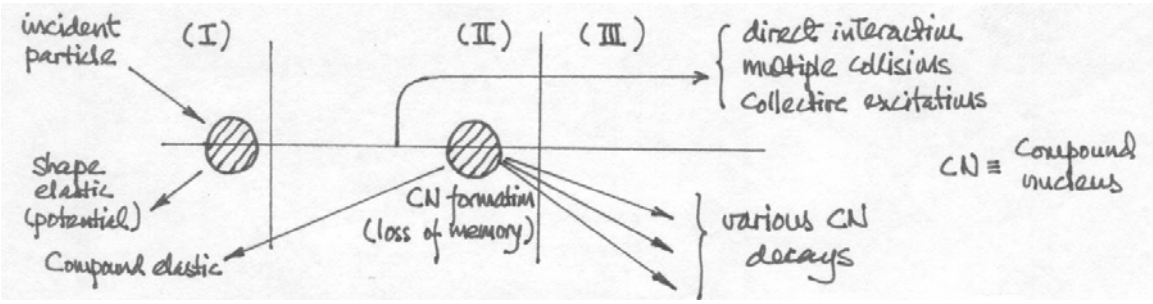

Fig. 21.4. Compound nucleus model of nuclear reaction – formation of compound nucleus (CN) and its subsequent decay are assumed to be decoupled.

shape elastic or potential scattering. This part is always present, we will leave it aside in the present discussion. The interaction which takes place after the particle has penetrated into the target nucleus can be considered an absorption process, leading to the formation of a compound nucleus (this need not be the only process possible, the others can be direct interaction, multiple collisions, and collective excitations). This is the part that we will now consider briefly.

In neutron reactions the formation of compound nucleus (CN) is quite likely at incident energies of ~ 0.1 – 1 Mev. Physically this corresponds to a large reflection coefficient in the inside edge of the potential well. Once CN is formed it is assumed that it will decay in a manner that is independent of the mode in which it was formed (complete loss of memory). This is the basic assumption of the model because it then allows the formation and decay to be treated as two separate processes. The approximation can be expressed by writing the interaction as a two-stage reaction,

$$a + X \rightarrow C^* \rightarrow b + Y$$

the asterisk indicating that the CN is in an excited state. The first arrow denotes the formation stage and the second the decay stage. For this reaction the cross section $\sigma(a,b)$ may be written as

$$\sigma(a,b) = \sigma_C(T_i)P_b(E) \qquad (21.10)$$

where $\sigma_C(T_i)$ is the cross section for the CN formation at kinetic energy T_i, which is the available kinetic energy for reaction as discussed above, and $P_b(E)$ is the probability that the CN at energy level E will decay by emission of particle b. It is understood that σ_C and P_b can be evaluated separately since the formation and decay processes are assumed to be decoupled. The energy-level diagram for this reaction is shown in Fig. 21.5 for an endothermic reaction (Q < 0). Notice that E is the CN excitation and it is measured

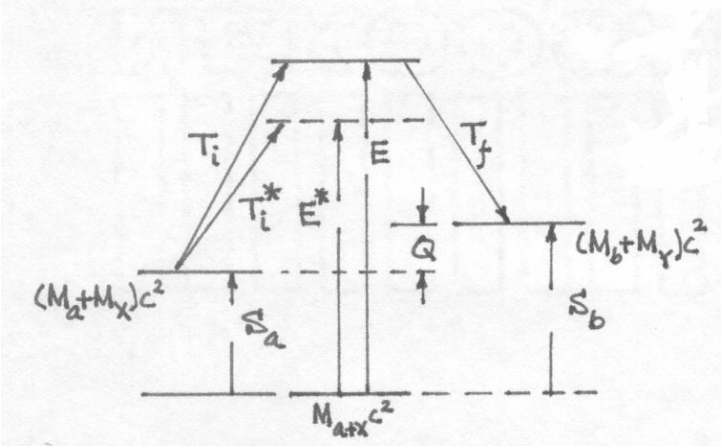

Fig. 21.5. Energy-level diagram for the reaction a + X $\rightarrow$ b + Y via CN formation and decay.

relative to the rest-mass energy of the nucleus (a+X). If this nucleus should have an excited state (a virtual level) at E* which is close to E, then one can have resonance condition. If the incoming particle a should have a kinetic energy such that the kinetic available for reaction has the value T_i*, then the CN excitation energy matches an excited level of nucleus (a+X), E = E*. Therefore the CN formation cross section $\sigma_C(T_i)$ will show a peak in its variation with T_i, an indication of a resonance reaction.

The condition for a reaction resonance is essentially a relation between the incoming kinetic energy and the rest-mass energies of the reactants. Fig. 21.5 shows that this relation can be stated as Ti = Ti*, or

$$(M_a + M_X)c^2 + T_i^* = M_{a+X}c^2 + E^* \qquad (21.11)$$

Each virtual level E* has a certain energy width, denoted as Γ, which corresponds to a finite lifetime of the state (level), $\tau = \hbar/\Gamma$. The smaller the width means the longer the lifetime of the level.

The cross section for CN formation has to be calculated quantum mechanically [see, for example, Burcham, *Nuclear Physics*, p. 532, or for a complete treatment Blatt and Weisskopf, *Theoretical Nuclear Physics*, pp. 398]. One finds

$$\sigma_C(T_i) = \pi\lambda\!\!\!^{-2} g_J \frac{\Gamma_a \Gamma}{\left(T_i - T_i^*\right)^2 + \Gamma^2/4} \qquad (21.12)$$

where $g_J = \dfrac{2J+1}{(2I_a+1)(2I_X+1)}$ and $\underline{J} = \underline{I}_a + \underline{I}_X + \underline{L}_a$. In this expression $\lambda\!\!\!^{-}$ is the reduced wavelength (wavelength/2π) of particle a in CMCS, $\underline{J}$ is the total angular momentum, the sum of the spins of particles a and X and the orbital angular momentum associated with particle a (recall particle X is stationary), Γ_a is the energy width (partial width) for the incoming channel a+X, and Γ (without any index) is the total decay width, the sum of all partial widths. (The idea here is that CN formation can result from a number of channels, each with its own partial width. In our case the channel is reaction with particle a with partial width Γ_a.). Given our relation (21.11) we can also regard the CN formation cross section to be a function of the excitation energy E, in which case $\sigma_C(E)$ is given by (21.12) with $(E - E^*)^2$ replacing the factor $\left(T_i - T_i^*\right)^2$ in the denominator.

To complete the cross section expression (21.10) we need to specify the probability for the decay of the compound nucleus. This is a matter that involves the excitation energy E and the decay channel where particle b is emitted. Treating this process like radioactive decay, we can say

$$P_b(E) = \Gamma_b(E)/\Gamma(E) \tag{21.13}$$

where $\Gamma(E) = \Gamma_a(E) + \Gamma_b(E)$ + width of any other decay channel allowed by the energetics and selective rules. Typically one includes a radiation partial width Γ_γ since gamma emission is usually an allowed process. Combining (21.12) and (21.13) we have the cross section for a resonance reaction. In neutron reaction theory the result is generally known as the Breit-Wigner formula for a single resonance. There are two cross sections of interest to us, one for neutron absorption and another for neutron elastic scattering,

$$\sigma(n,\gamma) = \pi\lambda\!\!\!^{-2} g_J \frac{\Gamma_n \Gamma_\gamma}{\left(T_i - T_i^*\right)^2 + \Gamma^2/4} \tag{21.14}$$

$$\sigma(n,n) = 4\pi a^2 + \pi\lambda\!\!\!^{-2} g_J \frac{\Gamma_n^2}{\left(T_i - T_i^*\right)^2 + \Gamma^2/4} + 4\pi\lambda\!\!\!^{-} g_J a\Gamma_n \frac{\left(T_i - T_i^*\right)}{\left(T_i - T_i^*\right)^2 + \Gamma^2/4} \tag{21.15}$$

In $\sigma(n,n)$ the first term is the potential scattering contribution, what we had previously called the s-wave part of elastic scattering, with a being the scattering length. The second term is the compound elastic scattering contribution. The last term represents the interference between potential scattering and resonant scattering. Notice the interference is *destructive* at energy below the resonance and *constructive* above the resonance. In Fig. 21.6 we show schematically the energy behavior of the absorption cross section in the form of a resonance peak. Below the peak the cross section varies like 1/v as can be deduced from (21.14) by noting the energy dependence of the various factors, along with $\Gamma_n \sim \sqrt{T}$, and $\Gamma_\gamma \sim$ constant. Notice also the full width at half maximum is governed by the total decay width Γ. Fig. 21.7 shows a well-known absorption peak in Cd which is widely used as an absorber of low-energy neutrons. One can see the resonance behavior in both the total cross section, which is dominated by absorption, and the elastic scattering cross section.

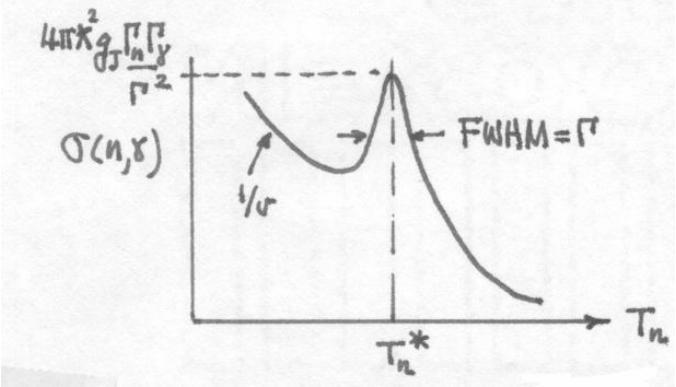

Fig. 21.6. Schematic of Breit-Wigner resonance behavior for neutron absorption.

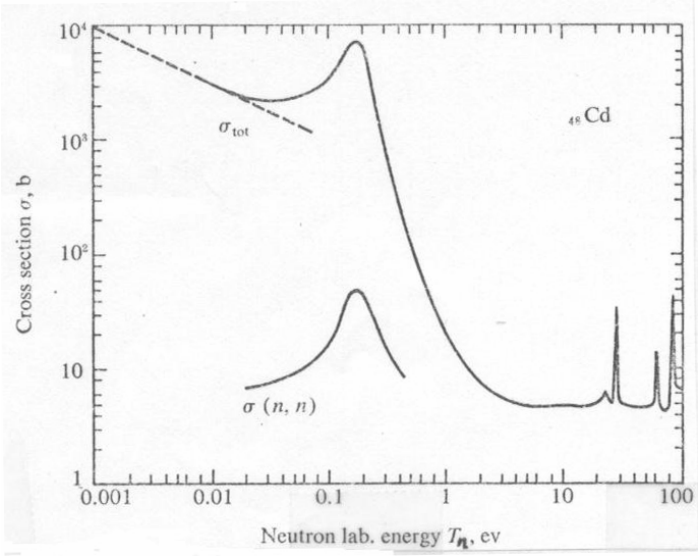

Fig. 21.7. Total and elastic neutron scattering cross sections of Cd showing a resonant absorption peak and a resonant scattering peak, respectively.

We conclude our brief discussion of compound nucleus reactions by noting an interesting feature in the elastic scattering cross section associated with the interference effect between potential scattering and resonance scattering. This is the destructive effect of interference in the energy region just below the resonance and the constructive effect just above the resonance. Fig. 21.8 shows this behavior schematically, and Fig. 21.9 shows that such effects are indeed observed. Admittedly this is generally not so obvious, so the present example is carefully chosen and should not be taken as being typical.

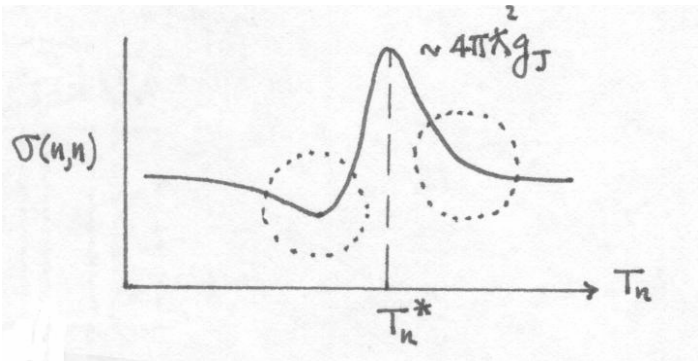

Fig. 21.8. Interference effects in elastic neutron scattering, below and above the resonance.

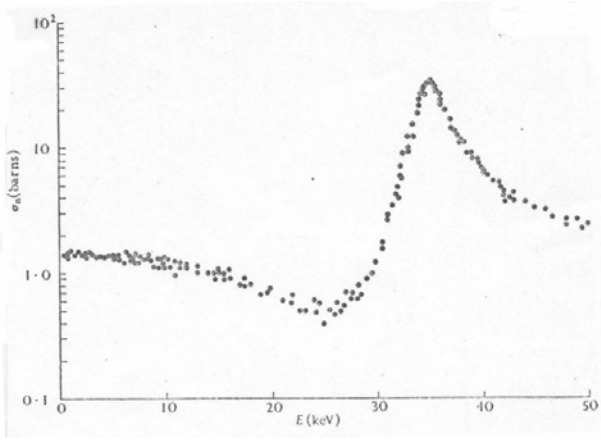

Fig. 21.9. Experimental scattering cross section of Al27 showing the interference effects between potential and resonance scattering, and an asymptotically constant value (potential scattering) sufficiently far away from the resonance. (from Lynn)

22.101 Applied Nuclear Physics (Fall 2004)

Problem Set No. 1 **Due: Sept. 15, 2004**

Problem 1

(i) A thermal neutron in a reactor is a neutron with kinetic energy equal to k_BT, where k_B is the Boltzmann's constant and T is the temperature of the reactor. Explain briefly the physical basis of this statement. Taking T to be the room temperature, 20C, calculate the energy of the thermal neutron (in units of ev), and then find it speed v (in cm/sec) and the corresponding de Broglie wavelength λ (in A). Compare these values with the energy, speed, and interatomic distance of the atoms in the reactor. What is the significance of comparing the neutron wavelength with typical atomic separations in a solid?

(ii) Consider a 2 Kev x-ray, calculate the frequency and wavelength of this photon. What would be the point of comparing the x-ray wavelength with that of the thermal neutron? If we have an electron whose wavelength is equal to that of the thermal neutron, what energy would it have?

(iii) The classical radius of the electron, defined as $e^2 / m_e c^2$, with e being the electron charge, m_e the electron rest mass, and c the speed of light, has the value of 2.818 x 10^{-13} cm. Use this fact to calculate the Coulomb repulsion energy between two protons at a distance of 1 F. On the basis of this result what can you conclude about the energy that is holding together a nucleus of several protons and neutrons?

Problem 2

Write a paragraph or two (no more than two pages) summarizing the major information contained in the Chart of Nuclides that is beyond the Periodic Table. Include a diagram or two showing how the information is labeled in the Chart.

Problem 3

Consider the absorption of a thermal neutron by a hydrogen atom to form a deuteron, with a gamma ray given off as a result. Find the energy of this gamma ray assuming that the kinetic energies of the neutron, the hydrogen, and the deuteron are all negligible. Why is the deuteron considered to be in a bound state (is the deuteron stable)? What is the energy of this bound state?

22.101 Applied Nuclear Physics

(Fall 2004)

Problem Set No. 2 **Due: Sept. 22, 2004**

Problem 1

(a) Starting with the time-dependent Schrödinger wave equation, derive an equation for the probability density $P(\underline{r},t) = \Psi^{+}(\underline{r},t)\Psi(\underline{r},t)$ in the standard form of the continuity equation, and in this way obtain the expression for the particle current which is quoted in Lec2, Eq. (2.24).

(b) Apply (2.24) to a plane wave, $\exp[i\underline{k}\cdot\underline{r}]$, where $\underline{k}$ is the wave vector, then give a physical interpretation of your result. How does the current differ from the flux which is defined as the particle number density times the particle speed (as in a beam of particles of a given flux)?

Problem 2

Solve the 1D time-independent Schrödinger wave equation for a particle in a square well by applying the BC for **an infinite well**. Sketch and discuss the first three eigenvalues and eigenfunctions, and then indicate in your sketch how the solutions are affected if the well were instead *very steep but not infinite*.

Problem 3

(a) Write down the time-independent Schrödinger wave equation of a system of two particles, mass m_1 and m_2, interacting through a central potential V(r), where r is the separation distance between the two particles, $r = |\underline{r}_1 - \underline{r}_2|$. Introduce the center-of-mass $\underline{R} = [m_1\underline{r}_1/(m_1+m_2) + m_2\underline{r}_2/(m_1+m_2)]$ and relative $\underline{r} = \underline{r}_1 - \underline{r}_2$ coordinates and show that the wave equation for two particles naturally separates into two equations, one for the center-of-mass coordinate and another for the relative coordinate. Discuss what is interesting about each equation. What do your results say about the reduction of a 2-body collision problem into an effective one-body problem of a particle moving in a potential field?

(b) Carry out the same reduction for the Newton's equation.of motion for the system of two colliding particles. [**Note**: *This part is for extra credit.*]

22.101 Applied Nuclear Physics

(Fall 2004)

Problem Set No. 3 **Due: Sept. 29, 2004**

Problem 1

Derive the ℓ=0 (s-wave) radial wave equation from the time-independent Schrödinger wave equation for a particle in a spherical well of width r_o and depth V_o. Solve this equation for the ground state wave function and the corresponding bound-state energy. Sketch and discuss briefly your results and then indicate what changes would occur if the well were to become *very steep and very narrow*.

Problem 2

In classical mechanics a particle incident upon a potential with range r_o at an impact parameter b would be scattered if $b < r_o$, but if b were greater than r_o then there would be no interaction. Use this simple picture to show that in the scattering of a neutron at low energy, by which we mean $kr_o << 1$, with $E = \hbar^2 k^2 / 2m$, *only the s-wave interaction is important*. Take r_o = 1.5 F, what is the range of neutron energy where this approximation is valid?

Problem 3

Consider the one-dimensional problem of a particle of mass m and energy E incident upon a potential barrier of height V_o and width L (V_o >E) going from left to right. Derive the following expression for the transmission coefficient

$$T = \left[1 + \frac{V_o^2}{4E(V_o - E)} \sinh^2 \kappa L \right]^{-1}$$

where $\kappa = \sqrt{2m(V_o - E)} / \hbar$. Sketch the variation of T with κL. What physical interpretation can you give for the dimensionless quantity κL? For nuclear physics problems which is the more realistic limit between thin barrier and thick barrier (why)?

22.101 Applied Nuclear Physics

(Fall 2004)

Problem Set No. 4 **Due: Oct. 6, 2004**

Problem 1

(a) Using a sketch explain the physical meaning of the angular differential neutron scattering cross section $\sigma(\theta) \equiv d\sigma / d\Omega$.

(b) Let $P(\underline{\Omega})$ be the probability distribution defined as

$P(\underline{\Omega})d\Omega$ = probability that the scattered neutron goes in the direction $d\Omega$ about $\underline{\Omega}$

How would you express $\sigma(\theta)$ in terms of $P(\underline{\Omega})$?

(c) If you were told that the scattering distribution is spherically symmetric, what would you write for $\sigma(\theta)$?

Problem 2

Derive the expression for the angular differential scattering cross section $\sigma(\theta)$ for s-wave scattering, then obtain the expression for the scattering cross section σ.

Problem 3

Calculate the neutron scattering cross section of C^{12} for thermal neutrons. Assume a potential well with depth V_o = 36 Mev and range $r_o = 1.4 \times A^{1/3}$ F and consider only the s-wave contribution. Compare your result with the experimental value (σ = 5 barns) and discuss any significance.

22.101 Applied Nuclear Physics

(Fall 2004)

Problem Set No. 5 **Due: Oct. 25, 2004**

Problem 1

(a) Sketch the energy levels of nucleons as given by two central force potentials, an infinite spherical well and a parabolic well (see Fig. 9.5). Explain the spectroscopic notation used in labeling each level, and how is degeneracy of each level determined. What is the significance of these results concerning the stability of nuclei?

(b) Sketch the energy levels of nucleons given by a shell-model potential with spin-orbit coupling (see Fig. 9.6), and explain the notation. What new features do you get with this model compared to the two models in part (a)?

Problem 2

Explain the operation of angular momentum addition in general, where one adds two angular momentum operators, $\underline{L}$ and $\underline{S}$, to form a total angular momentum operator $\underline{j}$, $\underline{j} = \underline{L} + \underline{S}$. Apply your explanation to the particular case where $\underline{L}$ and $\underline{S}$ are the orbital and spin angular momentum operators of a nucleon respectively.

Problem 3

On the basis of the single-particle shell model with spin-orbit coupling (Fig. 9.6), predict the ground-state spin and parity of the following nuclides:

$$Li^{6},\ N^{14},\ Mn^{55},\ Nb^{93},\ Xe^{131},\ Au^{197},\ Pb^{207},\ Bi^{209}$$

Compare your results with experimental data (e.g., Nuclide Chart); in the case of any discrepancy between your predictions and experiments, give an explanation.

22.101 Applied Nuclear Physics

(Fall 2004)

Problem Set No. 6 **Due: Nov. 1, 2004**

Problem 1

Use the semiempirical mass formula to calculate the mass of $C1^2$ and Bi^{209}. Tabulate the individual percentage contribution to the average binding energy per nucleon from the volume, surface, Coulomb, asymmetry, and pairing terms. Compare your mass and B/A results with experimental values from the Nuclide Chart.

Problem 2

Use the semi-empirical mass formula to determine which isobars with A = 140 should be stable. Indicate the various modes of decay and the predicted stable isotope. Compare your results with experimental data.

Problem 3

(a) You are given the series disintegration $A \rightarrow B \rightarrow C \rightarrow D$ (stable), with decay constants $\lambda_A, \lambda_B, \lambda_C$ respectively. Find the number of atoms of B, C, and D collected in a time t if the activity of A is held constant. (This is the approximation for a very long-lived source).

(b) Tellurium is bombarded by deuterons in a cyclotron, the reaction being

$$Te^{130}(d, p)Te^{131} \rightarrow I^{131} \rightarrow Xe^{131} \text{ (stable)}$$

with both decays being β^-, and the half lives are 30 hours and 8 days respectively. The bombardment conditions are such that the (d,p) reaction is equivalent to a source strength of 2 mCi. Find

(i) the initial rate of I^{131} production, in μCi per hour,

(ii) the number of Xe^{131} atoms produced during a single 6-hour bombaqrdment,

(iii) the total number of Xe^{131} atoms obtained eventually if the target were allowed to stand undisturbed for several months following a 6-hour bombardment.

22.101 Applied Nuclear Physics

(Fall 2004)

Problem Set No. 7 **Due: Nov. 8, 2004**

Problem 1

Give a derivation of the Rutherford scattering cross section

$$\frac{d\sigma}{d\Omega} = \frac{1}{4}\left(\frac{zZe^2}{mv^2}\right)\frac{1}{\sin^4(\theta/2)}$$

Define all the quantities. State the physical meaning of this formula and its significance regarding charged particle interactions with matter. (Note: You are expected to consult a reference book for this problem. You should cite your reference and give enough details in your derivation to demonstrate that you have worked through all the steps.)

Problem 2

The range-energy relationship for protons in air at 1 atm. and 15^o C is given in Fig. 3.9 of Meyerhof as well as in Lec14. From this curve deduce the energy loss (in Mev cm^2/gm) curve for the same energy range. Compare your result with Fig. 13.2 in the Lecture Notes as well as analyze your result using the Bethe formula.

Problem 3

Estimate the contributions to the stopping power due to ionization and to radiation for the passage of electrons with energy E in aluminum. Consider E = 0.1, 0.5, 1, 2, and 4 Mev. Express your results in both Mev/mm and Mev cm^2/gm, and compare your values with those given in the Lec14. Discuss the significance of your results and the comparison.

22.101 Applied Nuclear Physics

(Fall 2004)

Problem Set No. 8 **Due: Nov. 24, 2004**

Problem 1

(a) Show that the conservation of kinetic energy and linear momentum during an elastic collision requires that in the CMCS the speed of each particle is the same before and after the collision.

(b) Does the relative speed of particle 1 with respect to particle 2 change during an elastic collision, (1) in the CMCS and (2) in LCS?

Problem 2

Consider the problem of neutron elastic scattering in the notation as used in class.

(a) Find an expression for E_4 involving E_1 and angle γ (the angle between the recoil direction of M_4 and the x-axis). Is there a one-to-one relation between E_4 and γ?

(b) Eliminate γ in favor of θ_c in your result in (a), then use the fact that the scattering is isotropic in CMCS to find the distribution $P(E_4)$, the probability per unit energy that the recoil nucleus will have energy E_4.

(c) How would you obtain $P(E_4)$ directly from the result for $F(E' \rightarrow E)$ derived in class? How general is your relation between P and F?

Problem 3

Verify the relation between the angular differential cross sections for neutron elastic scattering in LCS and CMCS, $\sigma(\theta)$ and $\sigma(\theta_c)$, as discussed in class. Use this relation to discuss the behavior of $\bar{\mu}$ and $\bar{\mu}_c$, where $\mu = \cos\theta$?

22.101 Applied Nuclear Physics

(Fall 2004)

Problem Set No. 9 **Due: Dec. 6, 2004**

Problem 1

Consider Compton scattering of a photon. Derive the four expressions stated in the Lecture Notes for (i) the Compton shift, (ii) energy of the scattered photon, (iii) energy of the recoiling electron, and (iv) the relation between the angles of the scattered photon and the recoiling electron.

Problem 2

Calculate the energy distribution of Compton electrons for an incident photon of energy 1.20 Mev. Give your results as the energy differential cross section, $d\sigma / dT$, in units of 10^{-25} cm^2/Mev, at electron energies 0.25, 0.5, 0.75, 0.9 and 0.99 Mev. Make a sketch of $d\sigma / dT$ and compare with the corresponding figure in the Lecture Notes.

Problem 3

A sodium iodide detector in the shape of a 7 cm cube is bombarded by a beam of 2.8 Mev gamma radiation normal to one face of the cube.

(a) What fraction of the gamma radiation is detected?

(b) What fraction of the detected gamma appears in the photo peak, the Compton distribution, and the pair peaks, assuming no re-absorption of Compton gamma or annihilation quanta?

(c) Make a rough estimate of the relative fraction of pair events that appear in the full-energy (photo) peak, in the one-escape peak, and in the two-escape peak. Compare your result with the figure given in the Lecture Notes.

(Note: The attenuation coefficients that you will need can be found in Evans, Chap. 25, Sec.1. For 0.51 Mev photons, $\mu =$ 0.33 cm^{-1}. For 2.8 Mev photons, $\mu =$ 0.135 cm^{-1}, $\mu_\tau =$ 2.5 x 10^{-3} cm^{-1}, $\mu_C =$ 0.113 cm^{-1}, $\mu_\kappa =$ 0.020 cm^{-1}.)

22.101 Applied Nuclear Physics (Fall 2004)

Appendix A: Concepts of Cross Sections

It is instructive to review the physical meaning of a cross section σ, which is a measure of the probability of a reaction. Imagine a beam of neutrons incident on a thin sample of thickness Δx covering an area A on the sample. See Fig. A.1. The intensity of the beam hitting the area A is I neutrons per second. The incident flux is therefore I/A.

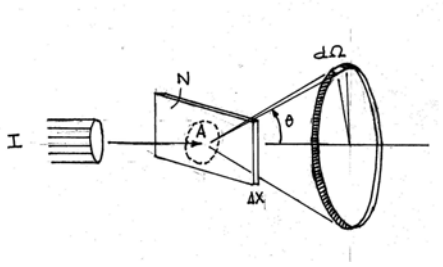

Fig. A.1. Schematic of an incident beam striking a thin target with a particle emitted into a cone subtending an angle θ relative to the direction of incidence, the 'scattering' angle. The element of solid angle $d\Omega$ is a small piece of the cone (see also Fig. A.2).

If the nuclear density of the sample is N nuclei/cm^3, then the no. nuclei exposed is $NA\,\Delta x$ (assuming no shaowing effects, i.e., the nuclei do not cover each other with respect to the incoming neutrons). We now write down the probability for a collision-induced reaction as

$$\{\text{reaction probability}\} = \Theta / I = \left(\frac{NA\Delta x}{A} \right) \bullet \sigma \qquad \text{(A.1)}$$

where Θ is the no. reactions occurring per sec. Notice that σ simply enters or appears in the definition of reaction probability as **a proportionality constant**, with no further justification. Sometimes this simple fact is overlooked by the students. There are other ways to introduce or motivate the meaning of the cross section; they are essentially all equivalent when you think about the physical situation of a beam of particles colliding with a target of atoms. Rewriting (A.1) we get

σ = {reaction probability} / {no. exposed per unit area}

$$= \frac{\Theta}{IN\Delta x} = \frac{1}{I}\left[\frac{\Theta}{N\Delta x}\right]_{\Delta x \to 0} \qquad \text{(A.2)}$$

Moreover, we define $\Sigma = N\sigma$, which is called the macroscopic cross section. Then (A.2) becomes

$$\Sigma \Delta x = \frac{\Theta}{I}, \qquad \text{(A.3)}$$

or $\mathbf{\Sigma \equiv}$ {probability per unit path for small path that a reaction will occur} (A.4)

Both the *microscopic cross section* σ, which has the dimension of an area (unit of σ is the **barn** which is 10^{-24} cm^2 as already noted above) , and its counterpart, the *macroscopic cross section* Σ, which has the dimension of reciprocal length, are fundamental to our study of neutron interactions. Notice that this discussion can be applied to any radiation or particle, there is nothing that is specific to neutrons.

We can readily extend the present discussion to an **angular differential** cross section $d\sigma / d\Omega$. Now we imagine counting the reactions per second in an angular cone subtended at angle θ with respect to the direction of incidence (incoming particles), as shown in Fig. A.1. Let $d\Omega$ be the element of solid angle, which is the small area through which the unit vector $\underline{\Omega}$ passes through (see Fig. A.2). Thus, $d\Omega = \sin\theta d\theta d\varphi$.

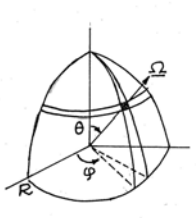

Fig. A.2. The unit vector $\underline{\Omega}$ in spherical coordinates, with θ and φ being the polar and azimuthal angles respectively (R would be unity if the vector ends on the sphere).

We can write

$$\frac{1}{I}\left(\frac{d\Theta}{d\Omega}\right) = N\Delta x\left(\frac{d\sigma}{d\Omega}\right) \qquad \text{(A.5)}$$

Notice that again $d\sigma/d\Omega$ appears as a proportionality constant between the reaction rate per unit solid angle and a product of two simple factors specifying the interacting system - the incient flux and the no, nuclei exposed (or the no, nuclei available for reaction).

Note the condition $\int d\Omega(d\sigma/d\Omega) = \sigma$, which makes it clear why $d\sigma/d\Omega$ is called the *angular differential cross section*.

Another extension is to consider the incoming particles to have energy E and the particles after reaction to have energy in dE' about E'. One can define in a similar way as above an *energy differential cross section,* $d\sigma/dE'$, which is a measure of the probability of an incoming with incoming energy E will have as a result of the reaction outgoing energy E'. Both $d\sigma/d\Omega$ and $d\sigma/dE'$ are distribution functions, the former is a distribution in the variable $\underline{\Omega}$, the solid angle, whereas the latter is a distribution in E', the energy after scattering. Their dimensions are barns per steradian and barns per unit energy, respectively.

Combining the two extensions above from cross section to differential cross sections, we can further extend to a *double differential cross section* $d^2\sigma/d\Omega dE'$, which is a quantity that has been studied extensively in thermal neutron scattering. This cross section contains the most fundamental information about the structure and dynamics of the scattering sample. While $d^2\sigma/d\Omega dE'$ is a distribution in two variables, the solid angle and the energy after scattering, it is not a distribution in E, the energy before scattering.

In 22.106 we will be concerned with all three types of cross sections, σ , the two differential cross sections., and the double differential cross section for neutrons, whereas the double differential cross section is beyond the scope of 22.101.

There are many important applications which are based on neutron interactions with nuclei in various media. We are interested in both the cross sections and the use of these cross sections in various ways. In diffraction and spectroscopy we use neutrons to probe the structure and dynamics of the samples being measured. In cancer therapy we use neutrons to preferentially kill the cancerous cells. Both involve a *single collision* event between the neutron and a nucleus, for which a knowledge of the cross section is all that required so long as the neutron is concerned. In contrast, for reactor and other nuclear applications one is interested in the effects of *a sequence of collisions or multiple collisions*, in which case knowing only the cross section is not sufficient. One needs to follow the neutrons as they undergo many collisions in the media of interest. This then requires the study of **neutron transport** - *the distribution of neutrons in configuration space, direction of travel, and energy*. In 22.106 we will treat transport in two ways, theoretical discussion and direct simulation using the Monte Carlo method, and the general purpose code MCNP (Monte Carlo Neutron and Photon).

22.101 Applied Nuclear Physics (Fall 2004)

Appendix B: Cross Section Calculation - Method of Phase Shift

---

References --

P. Roman, *Advanced Quantum Theory* (Addison-Wesley, Reading, 1965), Chap 3.

A. Foderaro, *The Elements of Neutron Interaction Theory* (MIT Press, 1971), Chap 4.

We will study a method of analyzing potential scattering; it is called the method of partial waves or the method of phase shifts. This is the quantum mechanical description of the two-body collision process. In the center-of-mass coordinate system the problem is to describe the motion of an effective particle with mass μ, the reduced mass, moving in a central potential V(r), where r is the separation distance between the two colliding particles. We will solve the *Schrödinger* wave equation for the spatial distribution of this effective particle, and extract from this solution the information needed to determine the angular differential cross section $\sigma(\theta)$. For a discussion of the concepts of cross sections, see Appendix A.

The Scattering Amplitude $f(\theta)$

In treating the potential scattering problem quantum mechanically the standard approach is to do it in two steps, first to define the cross section $\sigma(\theta)$ in terms of the scattering amplitude $f(\theta)$, and then to calculate $f(\theta)$ by solving the *Schrödinger* equation. For the first step we visualize the scattering process as an incoming beam impinging on a potential field V(r) centered at the origin (CMCS), as shown in Fig. B.1. The incident beam is represented by a traveling plane wave,

$$\Psi_{in} = be^{i(\underline{k}\cdot\underline{r}-\omega t)} \qquad \text{(B.1)}$$

where b is a coefficient determined by the normalization condition, and the wave vector $\underline{k} = k\hat{\underline{z}}$ is directed along the z-axis (direction of incidence). The magnitude of k is set by the energy of the effective particle $E = \hbar^2 k^2 / 2\mu = \hbar\omega$ (the relative energy of the colliding

particles). For the scattered wave which results from the interaction in the region of the potential V(r), we will write it in the form of an outgoing spherical wave,

$$\Psi_{sc} = f(\theta) b \frac{e^{i(kr-\omega t)}}{r} \tag{B.2}$$

where $f(\theta)$, which has the dimension of length, denotes the amplitude of scattering in a direction indicated by the polar angle θ relative to the direction of incidence (see Fig. B.1). It is clear that by representing the scattered wave in the form of (B.2) our intention is to work in spherical coordinates.

Once we have expressions for the incident and scattered waves, the corresponding current (or flux) can be obtained from the relation

$$\underline{J} = \frac{\hbar}{2\mu i}\left[\Psi^*(\underline{\nabla}\Psi) - \Psi(\underline{\nabla}\Psi^*)\right] \tag{B.3}$$

The incident current is $J_{in} = v|b|^2$, where $v = \hbar k / \mu$ is the speed of the effective particle.

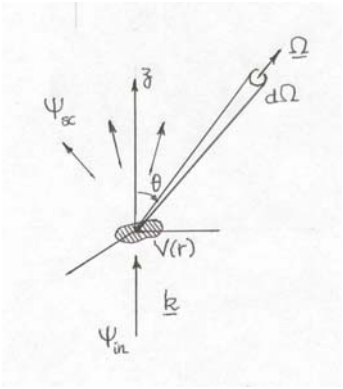

Fig.B.1. Scattering of an incoming plane wave by a potential field V(r), resulting in spherical outgoing wave. The scattered current crossing an element of surface area $d\Omega$ about the direction $\underline{\Omega}$ is used to define the angular differential cross section $d\sigma / d\Omega \equiv \sigma(\theta)$, where the scattering angle θ is the angle between the direction of incidence and direction of scattering.

For the number of particles per sec scattered through an element of surface area $d\Omega$ about the direction $\underline{\Omega}$ on a unit sphere, we have

$$\underline{J} \cdot \underline{\Omega} d\Omega = v \left| f(\theta) \right|^2 d\Omega \tag{B.4}$$

The angular differential cross section for scattering through $d\Omega$ about $\underline{\Omega}$ is therefore (see Appendix A),

$$\sigma(\theta) = \frac{\underline{J} \cdot \underline{\Omega}}{J_{in}} = \left| f(\theta) \right|^2 \tag{B.5}$$

This is the fundamental expression relating the scattering amplitude to the cross section; it has an analog in the analysis of potential scattering in classical mechanics.

Method of Partial Waves

To calculate $f(\theta)$ from the *Schrödinger* wave equation we note that since this is not a time-dependent problem, we can look for a separable solution in space and time, $\Psi(\underline{r}, t) = \psi(\underline{r})\tau(t)$, with $\tau(t) = \exp(-itE/\hbar)$. The *Schrödinger* equation to be solved then is of the form

$$\left(-\frac{\hbar^2}{2\mu} \nabla^2 + V(r) \right) \psi(\underline{r}) = E\psi(\underline{r}) \tag{B.6}$$

For two-body scattering through a central potential, this is the wave equation for an effective particle with mass equal to the reduced mass, $\mu = m_1 m_2 / (m_1 + m_2)$, and energy E equal to the sum of the kinetic energies of the two particles in CMCS, or equivalently $E = \mu v^2 / 2$, with v being the relative speed. The reduction of the two-body problem to the effective one-body problem (B.6) is a useful exercise, although quite standard. For

those in need of a review, a discussion of the reduction in classical as well as quantum mechanics is given at the end of this Appendix.

As is well known, there are two kinds of solutions to (B.6), bound-state solutions for E < 0 and scattering solutions for E > 0. We are concerned with the latter situation. In view of (B.2) and Fig. B.1, it is conventional to look for a particular solution to (B.6), subject to the boundary condition

$$\psi_k(\underline{r}) \rightarrow_{r>>r_o} e^{ikz} + f(\theta)\frac{e^{ikr}}{r} \tag{B.7}$$

where r_o is the range of force, V(r) = 0 for r > r_o. The subscript k is a reminder that the entire analysis is carried out at constant k, or at fixed incoming energy $E = \hbar^2 k^2 / 2\mu$. It also means that $f(\theta)$ depends on E, although this is commonly not indicated explicitly. For simplicity of notation, we will suppress this subscript henceforth.

According to (B.7) at distances far away from the region of the scattering potential, the wave function is a superposition of an incident plane wave and a *spherical outgoing* scattered wave. In the far-away region, the wave equation is therefore that of a free particle since V(r) = 0. The free-particle solution to is what we want to match up with (B.7). The form of the solution that is most convenient for this purpose is the expansion of $\psi(\underline{r})$ into a set of partial waves. Since we are considering central potentials, interactions which are spherically symmetric, or V depends only on the separation distance (magnitude of $\underline{r}$) of the two colliding particles, the natural coordinate system in which to find the solution is spherical coordinates, $\underline{r} \rightarrow (r, \theta, \varphi)$. The azimuthal angle φ is an ignorable coordinate in this case, as the wave function depends only on r and θ. The partial wave expansion is

$$\psi(r,\theta) = \sum_{\ell=0}^{\infty} R_\ell(r) P_\ell(\cos\theta) \tag{B.8}$$

where $P_\ell(\cos\theta)$ is the Legendre polynomial of order ℓ. Each term in the sum is a partial wave of a definite orbital angular momentum, with ℓ being the quantum number. The set of functions $\{P_\ell(x)\}$ is known to be orthogonal and complete on the interval (-1, 1). Some of the properties of $P_\ell(x)$ are:

$$\int_{-1}^{1} dx P_\ell(x) P_{\ell'}(x) = \frac{2}{2\ell+1}\delta_{\ell\ell'}$$

$$P_\ell(1) = 1,\ P_\ell(-1) = (-1)^\ell \qquad \text{(B.9)}$$

$$P_0(x) = 1,\ P_1(x) = x\ \ P_2(x) = (3x^2-1)/2\ \ P_3(x) = (5x^3-3x)/2$$

Inserting (B.8) into (B.6), and making a change of the dependent variable (to put the 3D problem into 1D form), $u_\ell(r) = rR_\ell(r)$, we obtain

$$\left(\frac{d^2}{dr^2} + k^2 - \frac{2\mu}{\hbar^2}V(r) - \frac{\ell(\ell+1)}{r^2}\right)u_\ell(r) = 0\,, \quad \text{r} < \text{r}_\text{o} \qquad \text{(B.10)}$$

This result is called the radial wave equation for rather obvious reasons; it is a one-dimensional equation whose solution determines the scattering process in three dimensions, made possible by the properties of the central potential V(r). Unless V(r) has a special form that admits analytic solutions, it is often more effective to integrate (B.10) numerically. However, we will not be concerned with such calculations since our interest is not to solve the most general scattering problem.

Eq.(B.10) describes the wave function in the region of the interaction, $r < r_o$, where V(r) = 0, $r > r_o$. Its solution clearly depends on the form of V(r). On the other hand, outside of the interaction region, $r > r_o$, Eq.(B.10) reduces to the radial wave equation for a free particle. Since this equation is universal in that it applies to all scattering problems where the interaction potential has a finite range r_o, it is worthwhile

to discuss a particular form of its solution. Writing Eq.(B.10) for the exterior region this time, we have

$$\left(\frac{d^2}{dr^2}+k^2-\frac{\ell(\ell+1)}{r^2}\right)u_\ell(r)=0 \tag{B.11}$$

which is in the standard form of a second-order differential equation whose general solutions are spherical Bessel functions. Thus,

$$u_\ell(r)=B_\ell r j_\ell(kr)+C_\ell r n_\ell(kr) \tag{B.12}$$

where B_ℓ and C_ℓ are integration constants, to be determined by boundary conditions, and j_ℓ and n_ℓ are spherical Bessel and Neumann functions respectively. The latter are tabulated functions; for our purposes it is sufficient to note the following properties.

$$j_o(x)=\sin x/x, \qquad n_o(x)=-\cos x/x$$

$$j_1(x)=\frac{\sin x}{x}-\frac{\cos x}{x}, \qquad n_1(x)=-\frac{\cos x}{x^2}-\frac{\sin x}{x}$$

$$j_\ell(x)\to_{x\to 0}\frac{x^\ell}{1\cdot 3\cdot 5...(2\ell+1)} \qquad n_\ell(x)\to_{x\to 0}\frac{1\cdot 3\cdot 5...(2\ell-1)}{x^{\ell+1}} \tag{B.13}$$

$$j_\ell(x)\to_{x>>1}\frac{1}{x}\sin(x-\ell\pi/2) \qquad n_\ell(x)\to_{x>>1}-\frac{1}{x}\cos(x-\ell\pi/2)$$

The Phase Shift δ

Using the asymptotic expressions for j_ℓ and n_ℓ we rewrite the general solution (B.12) as

$$u_\ell(r) \to_{kr>>1} (B_\ell / k)\sin(kr - \ell\pi/2) - (C_\ell / k)\cos(kr - \ell\pi/2)$$

$$= (a_\ell / k)\sin[kr - (\ell\pi/2) + \delta_\ell] \qquad \text{(B.14)}$$

The second step in (B.14) deserves special attention. Notice that we have replaced the two integration constant B and C by two other constants, a and δ, the latter being introduced as a *phase shift*. The significance of the phase shift will be apparent as we proceed further in discussing how one can calculate the angular differential cross section through (B.5). In Fig. B.2 below we give a simple physical explanation of how the sign of the phase shift depends on whether the interaction is attractive (positive phase shift) or repulsive (negative phase shift).

Combining (B.14) with (B.8) we have the partial-wave expansion of the wave function in the asymptotic region,

$$\psi(r,\theta) \to_{kr>>1} \sum_\ell a_\ell \frac{\sin[kr - (\ell\pi/2) + \delta_\ell]}{kr} P_\ell(\cos\theta) \qquad \text{(B.15)}$$

This is the left-hand side of (B.7). Our intent is to match this with the right-hand side of (B.7), also expanded in partial waves, and thereby relate the scattering amplitude to the phase shift. Both terms on the right-hand side are seen to depend on the scattering angle θ. Since the scattering amplitude is still unknown, we can simply expand it in terms of partial waves,

$$f(\theta) = \sum_\ell f_\ell P_\ell(\cos\theta) \qquad \text{(B.16)}$$

where the coefficients f_ℓ are the quantities to be determined in the present cross section calculation. The other term in (B.7) is the incident plane wave. It can be written as

$$e^{ikr\cos\theta} = \sum_{\ell} i^{\ell}(2\ell+1)\, j_{\ell}(kr) P_{\ell}(\cos\theta)$$

$$\rightarrow_{kr>>1} \sum_{\ell} i^{\ell}(2\ell+1)\frac{\sin(kr-\ell\pi/2)}{kr} P_{\ell}(\cos\theta) \qquad \text{(B.17)}$$

Inserting both (B.16) and (B.17) into the right-hand side of (B.7), we see that terms on both sides are proportional to either exp(ikr) or exp(-ikr). If (B.7) is to hold in general, the coefficients of each exponential have to be equal. This gives

$$f_{\ell} = \frac{1}{2ik}(-i)^{\ell}[a_{\ell}e^{i\delta_{\ell}} - i^{\ell}(2\ell+1)] \qquad \text{(B.18)}$$

$$a_{\ell} = i^{\ell}(2\ell+1)e^{i\delta_{\ell}} \qquad \text{(B.19)}$$

Eq.(B.18) is the desired relation between the ℓ-th component of the scattering amplitude and the ℓ-th order phase shift. Combining it with (B.16), we have the scattering amplitude expressed as a sum of partial-wave components

$$f(\theta) = (1/k)\sum_{\ell=0}^{\infty}(2\ell+1)e^{i\delta_{\ell}}\sin\delta_{\ell} P_{\ell}(\cos\theta) \qquad \text{(B.20)}$$

This expression, more than any other, shows why the present method of calculating the cross section is called the method of partial waves. Now the angular differential cross section, (B.5), becomes

$$\sigma(\theta) = \lambda\!\!\!^{-2}\left|\sum_{\ell=0}^{\infty}(2\ell+1)e^{i\delta_{\ell}}\sin\delta_{\ell} P_{\ell}(\cos\theta)\right|^2 \qquad \text{(B.21)}$$

where $\lambda\!\!\!^{-} = 1/k$ is the reduced wavelength. Correspondingly, the total cross section is

$$\sigma = \int d\Omega \sigma(\theta) = 4\pi \lambda\!\!\!^{-2} \sum_{\ell=0}^{\infty} (2\ell + 1) \sin^2 \delta_\ell \qquad \text{(B.22)}$$

Eqs.(B.21) and (B.22) are very well known results in the quantum theory of potential scattering. They are quite general in that there are no restrictions on the incident energy. Since we are mostly interested in calculating neutron cross sections in the low-energy regime ($kr_o << 1$), it is only necessary to take the leading term in the partial-wave sum.

The $\ell = 0$ term in the partial-wave expansion is called the s-wave. One can make a simple semiclassical argument to show that at a given incident energy $E = \hbar^2 k^2 / 2\mu$, only those partial waves with $\ell < kr_o$ make significant contributions to the scattering. If it happens that furthermore $kr_o << 1$, then only the $\ell = 0$ term matters. In this argument one considers an incoming particle incident on a potential at an impact parameter b. The angular momentum in this interaction is $\hbar\ell$ = pb, where $p = \hbar k$ is the linear momentum of the particle. Now one argues that there is appreciable interaction only when $b < r_o$, the range of interaction; in other words, only the ℓ values satisfying $b = \ell/k < r_o$ will have significant contriubution to the scattering. The condition for a partial wave to contribute is therefore $\ell < kr_o$

S-wave scattering

We have seen that if kr_o is appreciably less than unity, then only the $\ell = 0$ term contributes in (B.21) and (B.22). What does this mean for neutron scattering at energies around $k_BT \sim 0.025$ eV? Suppose we take a typical value for r_o at $\sim 2 \times 10^{-12}$ cm, then we find that for thermal neutrons $kr_o \sim 10^{-5}$. So one is safely under the condition of low-energy scattering, $kr_o << 1$, in which case only the s-wave contribution to the cross section needs to be considered. The differential and total scattering cross sections become

$$\sigma(\theta) = \lambda\!\!\!^{-2} \sin^2 \delta_o(k) \qquad \text{(B.23)}$$

$$\sigma = 4\pi \lambda\!\!\!^{-2} \sin^2 \delta_o(k) \qquad \text{(B.24)}$$

It is important to notice that s-wave scattering is spherically symmetric in that $\sigma(\theta)$ is manifestly independent of the scattering angle (this comes from the property $P_o(x) = 1$). One should also keep in mind that while this is so in CMCS, it is not true in LCS. In both (B.23) and (B.24) we have indicated that s-wave phase shift δ_o depends on the incoming energy E. From (B.18) we see that $f_o = (e^{i\delta_o} \sin\delta_o)/k$. Since the cross section must be finite at low energies, as k $\to 0$ f_o has to remain finite, or $\delta_o(k) \to 0$. Thus we can set

$$\lim_{k\to 0}[e^{i\delta_o(k)} \sin\delta_o(k)] = \delta_o(k) = -ak \qquad \text{(B.25)}$$

where the constant a is called the scattering length. Thus for low-energy scattering, the differential and total cross sections depend only on knowing the scattering length of the target nucleus,

$$\sigma(\theta) = a^2 \qquad \text{(B.26)}$$

$$\sigma = 4\pi a^2 \qquad \text{(B.27)}$$

We will see in the next lecture on neutron-proton scattering that the large scattering cross section of hydrogen arises because the scattering length depends on the relative orientation of the neturon and proton spins.

Physical significance of sign of scattering length

One can ask about the physical meaning of the scattering length a. Although the sign of a does not affect the magnitude of the cross sections, it carries information about the scattering potential. This is readily seen from the geometric significance of a. Fig. 4.2 shows two sine waves, one is the reference wave $\sin kr$ which has not had any

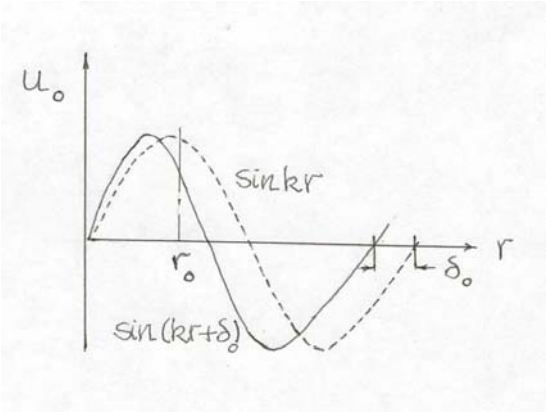

Fig. 4.2. Comparison of unscattered and scattered waves showing a phase shift δ_o in the asymptotic region as a result of the scattering.

interaction (unscattered) and the other one is the wave $\sin(kr + \delta_o)$ which has suffered a phase shift by virtue of the scattering. The entire effect of the scattering is seen to be represented by the phase shift δ_o, or equivalently the scattering length through (B.25). Thus in s-wave scattering the angular differential and total scattering cross sections depend only on knowing the scattering length a. The scattered wave, written in the form of $u_o \sim \sin k(r-a)$, suggests a simple but revealing geometric construction. In the vicinity of the potential, we can take kr_o to be small (this is agin the condition of low-energy scattering), so that $u_o \sim k(r-a)$, in which case a becomes the distance at which the wave function extrapolates to zero from its value and slope at $r = r_o$. There are two ways in which this extrapolation can take place, depending on the value of kr_o. As shown in Fig. B.3, when $kr_o > \pi/2$, the wave function has reached more than a quarter of its wavelength at $r = r_o$. So its slope is downward and the extrapolation gives a distance a which is positive. If on the other hand, $kr_o < \pi/2$, then the extrapolation gives a distance a which is negative. The significance is that $a > 0$ means the potential is such that it can have a bound state, whereas $a < 0$ means that the potential can only give rise to a virtual state.

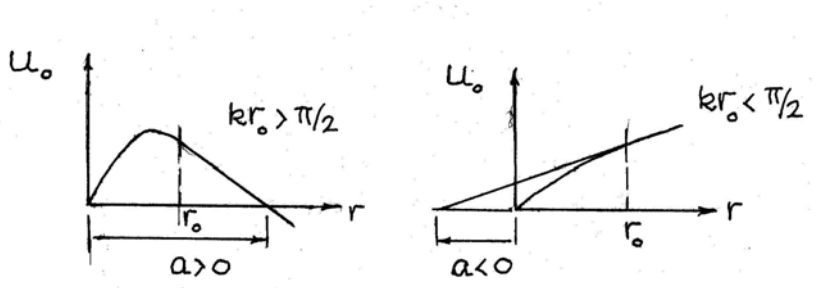

Fig. B.3. Geometric interpretation of positive and negative scattering lengths as the distance of extrapolation of the wave function at the interface between interior and exterior solutions, for potentials which can have a bound state and which can only virtual state respectively.

Reduction of two-body collision to an effective one-body problem

We conclude this Appendix with a supplemental discussion on how the problem of two-body collision through a central force is reduced, in both classical and quantum mechanics, to the problem of scattering of an effective one particle by a potential field V(r) [Meyerhof, pp. 21]. By central force we mean the interaction potential is only a function of the separation distance between the colliding particles. We will first go through the argument in classical mechanics. The equation describing the motion of particle 1 moving under the influence of particle 2 is the Newton's equation of motion,

$$m_1 \ddot{\underline{r}}_1 = \underline{F}_{12} \tag{B.28}$$

where $\underline{r}_1$ is the position of particle 1 and $\underline{F}_{12}$ is the force on particle 1 exerted by particle 2. Similarly, the motion of motion for particle 2 is

$$m_2 \ddot{\underline{r}}_2 = \underline{F}_{21} = -\underline{F}_{12} \tag{B.29}$$

where we have noted that the force exerted on particle 2 by particle 1 is exactly the opposite of $\underline{F}_{12}$. Now we transform from laboratory coordinate system to the center-of-mass coordinate system by defining the center-of-mass and relative positions,

$$\underline{r}_c = \frac{m_1 \underline{r}_1 + m_2 \underline{r}_2}{m_1 + m_2}, \qquad \underline{r} = \underline{r}_1 - \underline{r}_2 \tag{B.30}$$

Solving for $\underline{r}_1$ and $\underline{r}_2$ we have

$$\underline{r}_1 = \underline{r}_c + \frac{m_2}{m_1 + m_2}\underline{r}, \qquad \underline{r}_2 = \underline{r}_c - \frac{m_1}{m_1 + m_2}\underline{r} \tag{B.31}$$

We can add and subtract (B.28) and (B.29) to obtain equations of motion for $\underline{r}_c$ and $\underline{r}$. One finds

$$(m_1 + m_2)\ddot{\underline{r}}_c = 0 \tag{B.32}$$

$$\mu \ddot{\underline{r}} = \underline{F}_{12} = -dV(r)/d\underline{r} \tag{B.33}$$

with $\mu = m_1 m_2 /(m_1 + m_2)$ being the reduced mass. Thus the center-of-mass moves in a straight-line trajectory like a free particle, while the relative position satisfies the equation of an effective particle with mass μ moving under the force generated by the potential V(r). Eq.(B.33) is the desired result of our reduction. It is manifestly the one-body problem of an effective particle scattered by a potential field. Far from the interaction field the particle has the kinetic energy $E = \mu(\dot{\underline{r}})^2/2$

The quantum mechanical analogue of this reduction proceeds from the *Schrödinger* equation for the system of two particles,

$$\left(-\frac{\hbar^2}{2m_1}\nabla_1^2 - \frac{\hbar^2}{2m_2}\nabla_2^2 + V(|\underline{r}_1 - \underline{r}_2|)\right)\Psi(\underline{r}_1, \underline{r}_2) = (E_1 + E_2)\Psi(\underline{r}_1, \underline{r}_2) \tag{B.34}$$

Transforming the Laplacian operator ∇^2 from operating on $(\underline{r}_1, \underline{r}_2)$ to operating on $(\underline{r}_c, \underline{r})$, we find

$$\left(-\frac{\hbar^2}{2(m_1+m_2)}\nabla_c^2-\frac{\hbar^2}{2\mu}\nabla^2+V(r)\right)\Psi(\underline{r}_c,\underline{r})=(E_c+E)\Psi(\underline{r}_c,\underline{r}) \tag{B.35}$$

Since the Hamiltonian is now a sum of two parts, each involving either the center-of-mass position or the relative position, the problem is separable. Anticipating this, we have also divided the total energy, previously the sum of the kinetic energies of the two particles, into a sum of center-of-mass and relative energies. Therefore we can write the wave function as a product, $\Psi(\underline{r}_c,\underline{r})=\psi_c(\underline{r}_c)\psi(\underline{r})$ so that (B.35) reduces to two separate problems,

$$-\frac{\hbar^2}{2(m_1+m_2)}\nabla_c^2\psi_c(\underline{r}_c)=E_c\psi_c(\underline{r}_c) \tag{B.36}$$

$$\left(-\frac{\hbar^2}{2\mu}\nabla^2+V(r)\right)\psi(\underline{r})=E\psi(\underline{r}) \tag{B.37}$$

It is clear that (B.36) and (B.37) are the quantum mechanical analogues of (B.32) and (B.33). The problem of interest is to solve either (B.33) or (B.37). As we have been discussing in this Appendix we are concerned with the solution of (B.37).

Sample questions for Quiz 1, 22.101 (Fall 2004)

Following questions were taken from quizzes given in previous years by S. Yip. They are meant to give you an idea of the kind of questions (what was expected from the class in previous times) that have been asked in the past. Percentage credit is indicated for each question, total for the 90-min Quiz (closed book) is 100%.

You will have to decide for yourself what connections, if any, there may be between these questions and the Quiz 1 that will be conducted on Oct. 13, 2004.

Problem 1 (25%)

Consider a beam of particles, each of mass m and having kinetic energy E, incident from the left upon a square barrier of height V_o and width L, with $E < V_o$. Inside the barrier the wave function is of the form

$$\psi(x) = ae^{\kappa x} + be^{-\kappa x}$$

where you are given the result

$$\frac{a}{b} = \frac{1 + ik/\kappa}{1 - ik/\kappa} e^{-2\kappa L}$$

with $\hbar^2 k^2 / 2m = E$ and $\hbar^2 \kappa^2 / 2m = V_o - E$.

(15%) (a) Using the information given on $\psi(x)$ inside the barrier, derive an approximate expression for the transmission coefficient T for the case of thick barriers, $\kappa L >> 1$.

(10%) (b) Sketch qualitatively the absolute square of the wave function $|\psi(x)|^2$ everywhere and indicate the spatial dependence of $|\psi(x)|^2$ wherever it is known. Does $|\psi(x)|^2$ vanish at any point?

Problem 2 (35% total)

Consider the scattering of low-energy neutrons by a nucleus which acts like an impenetrable sphere of radius R.

(20%) (a) Solve the radial wave equation to obtain the phase shift δ_o.

(10%) (b) Given that the angular differentil scattering cross section for s-waves is $(d\sigma / d\Omega)_o = (1/k^2)\sin^2 \delta_o(k)$, use your result from (a) to find the total scattering cross

section σ_o. Suppose we apply this calculation to n-p scattering and use for R the radius of the deuteron, $R = \hbar\sqrt{m_n E_B}$, where m_n is the neutron mass and E_B is the ground state energy of the deuteron. Find R in unit of F (1 F = 10^{-13} cm), and σ_o in barns.

(5%) (c) Does your result agree with the experimental value of neutron scattering cross section of hydrogen? If not, explain the reason for the discrepancy.

Problem 3 (25%)

(a) Calculate the phase shift δ_o for s-wave scattering of a particle of mass m and incident energy E by a potential barrier V(r) = V_o, r < r_o, and V(r) = 0, r > r_o, with E < V_o.

(b) Simplify your result by going to the limit of low-energy scattering. Examine the total scattering cross section $\sigma = (4\pi \sin^2 \delta_o) / k^2$ in this limit. Sketch σ as a function of $k_o r_o$, where $k_o^2 = 2mV_o / \hbar^2$ and indicate the value of σ in the infinite barrier limit, $k_o r_o \to \infty$.

Problem 4 (25%)

Consider a one-dimensional wave equation with the potential

$$V(x) = \begin{cases} -V_o & -L_1 \le x \le L_1 \quad \text{(region 1)} \\ V_1 & -L_2 \le x \le -L_1, \quad L_1 \le x \le L_2 \quad \text{(region 2)} \\ 0 & \text{otherwise} \quad \text{(region 3)} \end{cases}$$

(a) Find the x-dependence of the wave function in each of the 3 regions for E < 0

(b) What are the boundary conditions to be applied at the interface? (You are asked to state the boundary conditions, but not to apply them.)

Problem 5 (20%)

A particle of mass m is just barely bound by a one-dimensional potential well of width L. Find the value of the depth V_o.

Problem 6 (25%)

Suppose you are given the result for the transmission coefficient T for the barrier penetration problem, one-dimensional barrier of height V_o extending from x=0 to x=L,

$$T = \left[1 + \frac{V_o^2}{4E(V_o - E)} \sinh^2 KL \right]^{-1}$$

where $K^2 = 2m(V_o - E)/\hbar^2$ is positive ($E < V_o$).

(a) From the expression given deduce T for the case $E > V_o$ without solving the wave equation again.
(b) Deduce T for the case of a square well potential from the result for a square barrier.

Sample questions for Quiz 2, 22.101 (Fall 2004)

Following questions were taken from quizzes given in previous years by S. Yip. They are meant to give you an idea of the kind of questions (what was expected from the class in previous times) that have been asked in the past. Percentage credit is indicated for each question based on 100% for a 90-min Quiz (closed book). Problem numbering means nothing here.

You will have to decide for yourself what connections, if any, there may be between these questions and the Quiz 2 that will be conducted on Nov. 10, 2004.

Problem 1 (20%)

The reaction, ${}^3H + {}^1H \rightarrow {}^3_2He + n$, has a Q-value of -0.764 Mev. Tritium ${}^3H$ also undergoes β^- decay with end-point energy of 0.0185 Mev. Find the difference between the neutron and hydrogen mass in Mev. Draw an energy level diagram showing the levels involved in the reaction and the β^- decay, then indicate in your diagram the proton separation energy S_p, the Q-value, and the end-point energy T_{max}.

Problem 2 (35%)

(a) (10%) Among the energy levels of a central force potential is a level labeled 1d. Suppose we now add a spin-orbit interaction term to the Hamiltonian such as in the shell model. Using the spectroscopic notation, label the new levels that evolve from this 1d level. Specify how many nucleons can go into each of the new levels, and explicitly write out the quantum numbers specifying the wave function of each nucleon.

(b) (7%) In an odd-odd nucleus the last neutron and proton go into a $1d_{3/2}$ and a $1g_{9/2}$ level respectively. Use the shell model to predict the spin and parity of this nucleus.

(c) (8%) A beta decay occurs between initial state (3^-) and final state (3^+), while a gamma decay occurs between (2^-) and (4^+) . What is the dominant mode of decay in each case?

(d) (10%) The binding energy per nucleon of ${}^6_3Li$ is about 5.3 Mev while that of ${}^4_2He$ is 7.1 Mev. Does this mean that the former is unstable against $\alpha-$decay? Explain. (Note: The binding energy of the deuteron ${}^2H$ is 2.25 Mev.)

Problem 3 (20%)

In the derivation of the Bethe-Bloch formula for the energy loss per unit path length of a charged particle (ze) moving with speed v, it was shown that an atomic electron in the medium would gain an amount of kinetic energy

$$T = \frac{p_e^2}{2m} = \frac{2(ze)^2}{mv^2 b^2}$$

where m is the electron mass and b the impact parameter. Suppose one can ignore the binding energy of the atomic electrons so that each electron is ejected, find the number of electrons per unit path length with kinetic energy in dT about T. (Hint: Think of the number of electrons in a collision cylinder, with radius b, thickness db, and length Δ x.)

Problem 4 (15%)

Sketch the energy variations of the stopping power (energy loss per unit path) of both electrons and protons in lead (in the same figure). Discuss all the features of these two curves that you know.

Problem 5 (20%)

On the basis of the Bethe-Bloch formula, the stopping power of a material for incident electrons (with kinetic energy T_e) can be related to that for incident alpha particles (with kinetic energy T_α). Denoting the two by $-(dT/dx)_e$ and $-(dT/dx)_\alpha$ respectively, sketch the two curves on the same graph to show how knowing one allows you to find the other.

Problem 6 (15%)

At time t = 0 you are given an atom that can decay through either of two channels, a and b, with known decay constants λ_a and λ_b. Find the probability that it will decay by channel a during the time interval between t_1 and t_2, with t_1 and t_2 arbitrary. Interpret your result.

Problem 7 (40%)

Discuss briefly the significance of each of the following. Give a definition whenever it is appropriate. (If you use the same notation as the Lecture Notes, you may assyme the symbols are already defined in the Notes.)

(a) The asymmetry term in the empirical mass formula.
(b) Mass parabolas for isobars for even A (give a sketch).
(c) Mass or energy requirements for electron capture.
(d) Secular equilibrium in radioactive decay.
(e) Bragg curve for charged particles (give sketch).
(f) Bethe formula for stopping power and its relativistic corrections.
(g) Charge and mass dependence of bremstrahlung intensity.
(h) Mass absorption coefficient for charged particles.

Sample questions for Quiz 3, 22.101 (Fall 2004)

Following questions were taken from quizzes given in previous years by S. Yip. They are meant to give you an idea of the kind of questions (what was expected from the class in previous times) that have been asked in the past. Percentage credit is indicated for each question based on 100% for a 90-min Quiz (closed book). Problem numbering means nothing here.

You will have to decide for yourself what connections, if any, there may be between these questions and the Quiz 3 that will be conducted on Dec. 8, 2004.

Problem 1 (20%)

Define concisely what is Compton scattering. Derive the relation between incident gamma energy $\hbar\omega$ and scattered gamma energy $\hbar\omega'$ for Compton scattering which also involves the scattering angle θ. What is the similarity (and difference) between this relation and the corresponding relation involving incident and scattered energies in neutron elastic scattering?

Problem 2 (30%)

Consider the measurement of monoenergetic gammas (energy $\hbar\omega$) in a scintillation detector whose size is small compared to the mean free path of the secondary gammas produced by interactions of the incident (primary) gammas in the detector.

(10%) (a) Sketch the pulse-height spectrum of low-energy gammas, say $\hbar\omega$ < 500 kev. Explain briefly the important characteristics of this spectrum in terms of the different interactions that can take place.

(10%) (b) Repeat (a) for higher-energy gammas, $\hbar\omega$ > 2 Mev.

(10%) (c) What other peaks can appear in the pulse-height spectrum if the detector were not small? Give a sketch and explain briefly.

Problem 3 (30%)

(15%) (a) You are told the reaction $^{13}C(d,p)^{14}C$ has a resonance at a deuteron energy E_d (LCS), and following this, ^{14}C undergoes $\beta-$ decay to ^{14}N. Draw the energy level diagram for this situation in which you show explicitly how the following energies can be calculated in terms of known masses and E_d: (1) kinetic energy available for reaction T_o, (2) Q value for the reaction, (3) deuteron separation energy, (4) proton separation energy, and (5) Q_β.

(15%) (b) On the basis of (a), predict whether or not the reaction $^{11}B(\alpha,n)^{14}N$ will have a resonance, and if so, at what energy of the α particle this will occur. (Since you are not

given numerical values, you should leave your answer in terms of defined quantities such as masses and various energies.)

Problem 4 (20%)

Sketch the energy variation of an observed resonance in (a) neutron elastic scattering (resonance scattering in the presence of potential scattering), and (b) neutron inelastic scattering. Comment on the characteristic features in the cross sections, especially the low-energy behavior below the resonance. What is the connection between the energy at which the observed cross sections show a peak and the energy of the nuclear level associated with the resonance? (You may assume it is the same level in both cases.)

Problem 5 (20%)

Sketch of the peaks that one would observe in the pulse-height spectra of a small detector in the presence of a 2-Mev gamma ray source, including any radiation from the background. For each peak identify the radiation interaction process that gives rise to it and indicate the energy at which this peak would appear.

Problem 6 (25%)

Consider the compound nucleus reaction of inelastic scattering of neutrons at energy T_1 (LCS) by a nucleus ${}_{Z}^{A}X$.

(a) Draw the energy level diagram showing the different energies that one can use to describe this reaction (including the Q value).

(b) Write down the corresponding Breit-Wigner cross section in terms of some of the energies shown in (a). Define all the parameters appearing in your expression.

Problem 7 (10%)

Consider the reaction $a + b \rightarrow c + d$, where Q is nonzero and particle b is stationary. What can you say about the magnitude and direction of the velocity of the center-of-mass before and after the reaction?

Problem 8 (20%)

The decay scheme of ${}^{80}Br$ is shown below. Classify the various decay modes and estimate all the decay constants that you can.

(energy level diagram shown separately – not available for the sample)

Problem 9 (15%)

At time t = 0 you are given an atom that can decay through either of two channels, a and b, with known decay constants λ_a and λ_b. Find the probability that it will decay by channel a during the time interval between t_1 and t_2, with t_1 and t_2 arbitrary. Interpret your result.

Problem 10 (20% total)

Consider a beam of collimated, monoenergetic neutrons (energy E) incident upon a thin target (density N atoms per cc) of area A and thickness Δx at a rate of I neutrons/sec. Assume the cross sectional area of the beam is greater than A. An energy sensitive detector subtended at an angle θ with respect to the incident beam direction is set up to measure the number of neutrons per second scattered into a small solid angle $d\Omega$ about the direction Ω and into a small energy interval dE' about E'. Let this number be denoted by Π.

(a) (15%) Define the double (energy and angular) differential scattering cross section $d^2\sigma / d\Omega dE'$ in terms of the physical situation described above such that you relate this cross section to the scattering rate Π and any other quantity in the problem. (You may find it helpful to draw a diagram of the specified arrangement.)

(b) (5%) How is $d^2\sigma / d\Omega dE'$ related to the angular and energy differential cross sections, $d\sigma / d\Omega$ and $d\sigma / dE'$, respectively (no need to define the latter, assume they are known)?

Problem 11 (25%)

In neutron elastic scattering by hydrogen where the target nucleus is assumed to be at rest, the ratio of final to initial neutron energy is E'/E = (1/2)(1 + cos θ_c), where θ_c is the scattering angle in CMCS. Suppose you are told the angular distribution of the scattered neutrons is proportional to cos θ_c for $0 \le \theta_c \le \pi/2$ and is zero for all other values of θ_c. Find the corresponding energy distribution $F(E \to E')$. Sketch your result and discuss how it is different from the case of isotropic angular distribution.

Problem 12 (20% total)

Give a brief and concise answer to each of the following.

(a) (7%) What is the physical picture of the model used to estimate the decay constant in alpha decay (give sketch). Why does the model give an upper limit for the decay constant?.

(b) (4%) What is electron capture and with what process does it compete?

(c) (4%) What is internal conversion and with what process does it compete?

(d) (5%) Give a sketch of the variation of the neutron cross section of C in the energy region below 0.1 Mev and explain the features.

22.101 Applied Nuclear Physics
Fall 2004

QUIZ No. 1 (closed book) **October 13, 2004**

Problem 1 (10%)

Suppose you do not know the gamma ray energy that is given off when the proton absorbs a neutron, but you have the Chart of Nuclides. How would you go about determining the energy of the gamma (state the steps but do not do the math)? Can you also find out the cross section value for this reaction?

Problem 2 (25%)

In a one-dimensional system with a square well potential, depth V_o and range r_o, is it possible to have at least one bound state no matter what the values of V_o and r_o? What happens in three dimensions with a spherical well potential, depth V_o and range r_o? In each case, explain your answer with a sketch of the wave function. [Note: you should answer this question without going through any derivation.]

Problem 3 (25%)

Consider the reflection of a particle with mass m and energy E incident from the left upon a 1D potential barrier, $V(x) = V_o$, $x > 0$, and $V(x) = 0$, $x < 0$. Find the reflection coefficient R for $E > V_o$. Investigate the limit of $E \to V_o$.

Problem 4 (40%)

Consider the scattering of a particle of mass m and incident kinetic energy E by a spherical well potential, depth V_o and range r_o. You are given the following information. The s-wave scattering cross section is $\sigma_o = (4\pi / k^2)\sin^2 \delta_o(k)$, where $\delta_o(k)$ is an energy-dependent phase shift. In the case of low-energy scattering, i.e., kro << 1, $\delta_o(k)$ is given by

$$\tan \delta_o(k) \sim \left(k / K \cot Kr_o\right)(1 - Kr_o \cot Kr_o) \qquad (*)$$

where $\hbar^2 K^2 / 2m = V_o$, and $\hbar^2 k^2 / 2m = E$.

(a) (8%) Define the scattering length *a* and express σ_o in terms of *a*.

(b) (20%) Find *a* from eq.(*) [hint: you can take $\delta_o(k)$ to be small.]. Discuss (and give a sketch) the behavior of σ_o as a function of Kr_o. Do you see a connection between the behavior of σ_o and the calculation of bound states in a deep spherical well potential?

(c) (12%) What changes do you expect if the scattering is by a spherical barrier of height V_o with the same range (give a sketch)?

22.101 Applied Nuclear Physics
Fall 2004

QUIZ No. 2 (closed book) **November 10, 2004**

Problem 1 (10%)

Explain briefly what is the reason for introducing the total momentum, $\underline{j} = \underline{L} + \underline{S}$, in the Nuclear Shell model. How does this affect the labeling of the states?

Problem 2 (15%)

Since the binding energy per nucleon (B/A) of ${}_2He^4$, at 7.07 Mev, is higher than that of ${}_3Li^6$, at 5.33 Mev, it may appear that the former is more stable than the latter and therefore Li^6 should spontaneously undergo α-decay,

$$ {}_3Li^6 \rightarrow {}_2He^4 + {}_1H^2 $$

where the B/A of ${}_1H^2$ is 1.11 Mev. Determine whether this is indeed the case.

Problem 3 (15%)

The basic idea underlying the C^{14} dating method is that radioactive C^{14} is produced continuously in the atmosphere by cosmic rays and finds its way into living plants and animals by carbon exchange. When the plant or animal dies the exchange process stops. How would you use this idea to determine the age of an antique wooden chair (when the tree was cut), that is, what activity would you measure and how would you interpret the data? Give a sketch of your method. (Note: The equilibrium concentration of C^{14} in the air is a known constant. C^{14} undergoes β-decay to N^{14} which is stable.)

Problem 4 (20%)

In analyzing the energy loss per unit path length of a charged particle (ze) moving with speed v, an atomic electron in the medium located at an impact parameter b will gain an amount of kinetic energy equal to

$$ T = \frac{2(ze^2)^2}{mv^2b^2} $$

from collision with the charged particle, where m is the electron mass. Suppose you are told to ignore the binding energy of the atomic electrons, so that all the electron in a collision cylinder of radius b, thickness db, and length Δ x are ejected. Find the number of electrons per unit path length ejected with kinetic energy in dT about T. (Hint: Think of this number as a distribution.)

(continue to next page)

Problem 5 (40% total, 8% each)

Give a short and concise answer to each of the following questions.

(a) Derive using a sketch the asymmetry term in the empirical mass formula.

(b) Explain what is β^+-decay, then state and justify the energy condition for this process.

(c) Sketch schematically the curve for the stopping power of a heavy charged particle in a high-Z medium in the energy range, zero to three times its rest mass energy. Label all the characteristic energies that you know, and explain what physical processes are represented in the curve.

(d) Show that the range of an α-particle and a proton, both having the same initial speed, will be approximately the same.

(e) Is *bremsstrahlung* an elastic or inelastic process (explain)? Why is this process more important for electron than for proton in problems of interest to the class.

22.101 Applied Nuclear Physics
Fall 2004

QUIZ No. 3 (closed book) **December 8, 2004**

Problem 1 (20%)

In neutron radiation damage studies an incident neutron with energy E collides with an atom in the crystal lattice, called the primary knock-on atom (PKA), causing it to recoil and displace a number of other atoms in the solid.

(a) (8%) Calculate the average recoil energy of the PKA (mass A). State all assumptions involved in your calculation.

(b) (12%) Let the number of atoms displaced by a PKA with energy T be denoted by $\nu(T)$ which behaves as follows

$$\nu(T) = 0 \qquad \text{for} \quad 0 < T < E_d$$

$$= T/2E_d \qquad E_d < T < L_c$$

where E_d is the energy to displace an atom, and L_c is the energy above which all the energy loss is by electronic excitation. Find the average number of atoms displaced as a function of E in the range, $0 < E < L_c$. Call this quantity N_E. (Note: Neither ν nor N_E are distributions.)

Problem 2 (15%)

When a beam of photons with wavelength 0.7 A is scattered by carbon at various scattering angles, the observed spectra behave in a way as sketched schematically. What is the process responsible for the peak at 0.7 A? What is the process responsible for the other peak in the spectrum? Comment on the variation with scattering angle of the two peaks.

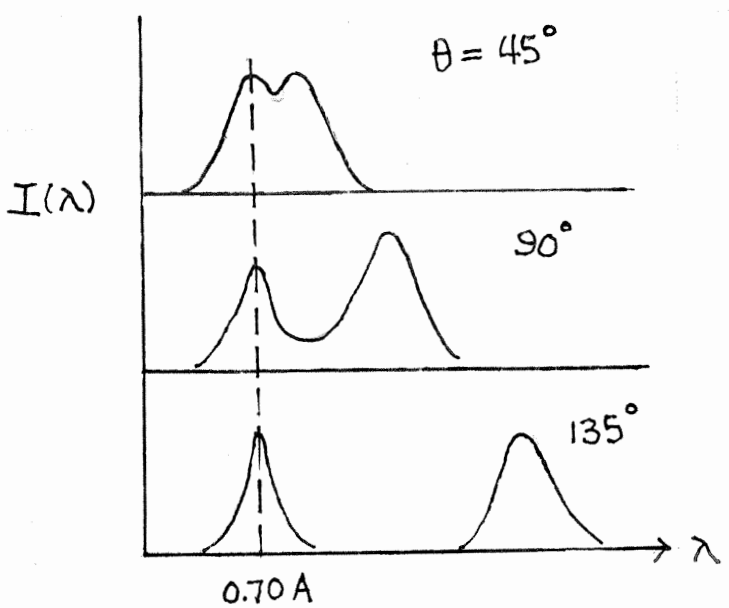

Problem 3 (20%)

For the energy-level diagram shown below, identify all the transitions that can take place. For each transition determine the decay mode and the decay energy (Q-value).

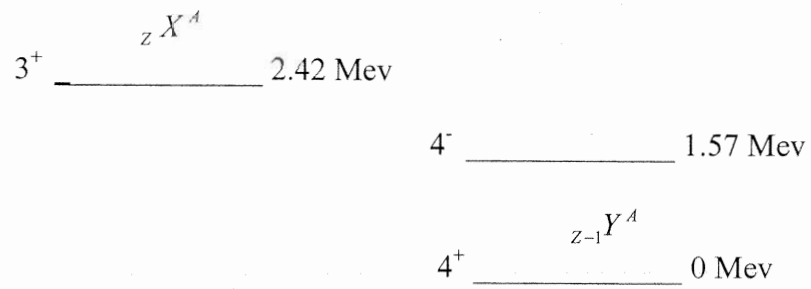

Problem 4 (15%)

Consider neutron inelastic scattering at incident energy T_1 (LCS) where the reaction can be written as

$$n+{}_{z}X^{A} \rightarrow ({}_{Z}X^{A+1})^{*} \rightarrow n'+({}_{Z}X^{A})^{*}$$

Is the Q-value positive or negative? Draw the energy-level diagram depicting the kinetic and rest-mass energies involved in the reaction, and show how the kinetic energies are related to T_1 and any other energies in the problem. You may assume target nucleus is at rest.

Problem 5 (30% total, 6% each)

Give a short and concise answer to each of the following questions

(a) Suppose you are detecting a γ-ray at energy $\hbar\omega = 2$ Mev using a large scintillation detector. Sketch the energy distribution that you would observe, indicating both the origin and position (the energy on a linear energy scale) of each peak.

(b) Sketch (as quantitatively as you can) the mass attenuation of lead for γ-rays with energy from 0.01 Mev to 100 Mev, showing the individual contributions from the various processes of interaction.

(c) Sketch the model used for calculating the decay constant for α -decay (no calculation), and explain the energies and distances in your sketch.

(d) Sketch the distributions of neutron energies for neutron elastic scattering at energy E by target nuclei with mass A in a medium at temperature T, for E/k_BT = 0.1, 1, and 4.

(e) Sketch the total cross section of water for neutron energies from 0.001 ev to 10 ev. Explain the meaning of free-atom and bound-atom cross sections and indicate where they would appear in your sketch.